UNIVERSITY OF TECHNOLOGY SYDNEY

Systemic Administration of a Connexin43 Mimetic Peptide: A Treatment Option for Spinal Cord Injury

A thesis submitted in fulfilment of the requirements for the degree of Doctor of Philosophy

Yilin Mao

2017

School of Life Sciences
Faculty of Science
University of Technology Sydney

Certificate of Original Authorship

I certify that the work in this thesis has not previously been submitted for a degree nor has it been submitted as part of requirements for a degree except as part of the collaborative doctoral degree and/or fully acknowledged within the text.

I also certify that the thesis has been written by me. Any help that I have received in my research work and the preparation of the thesis itself has been acknowledged. In addition, I certify that all information sources and literature used are indicated in the thesis.

This research is supported by an Australian Government Research Training Program Scholarship.

Signature of Student:

Date: 20/05/2017

Acknowledgements

First of all, I would like to express my appreciation to my principle supervisor, Dr. Catherine Gorrie, for your guidance, patience, expertise, intelligence, encouragement and dedication inspiring me. I cherish the liveliest feeling of sincere gratitude for you, not only in academics but also personality. Without your endless direction and instruction in the past four years, I would not have made so much achievement today.

I also wish to thank my co-supervisors, Dr. Hui Chen and Dr. Gila Moalem-Taylor, for your continuous advice and support during my PhD training. Your invaluable mentoring has made my research life so much easier.

To my wise and patient collaborators from the University of Auckland, Dr. Simon O'Carroll, Prof. Louise Nicholson and Prof. Colin Green, thank you for providing professional comments on my research project and manuscripts.

Thank you to all other smart people working for this project: Tara Nguyen, being the research assistant, for your indispensable help in the animal surgeries, post-operative care, euthanasia, locomotion assessments, histology staining and immunohistochemistry; Ryan Tonkin, for providing assistance in the animal surgeries, post-operative care, pain hypersensitivity assessments, western blot and multiplex ELISA; and Justin Lees, for your generous aid in multiplex ELISA.

I want to express my sincere appreciation to the staff in University of Technology Sydney Ernst Facility for taking care of experimental animals, Microbial Imaging Facility for providing the fluorescent microscopies and associated softwares, and Proteomics Core Facility for assistance mass spectrometry and electrophoresis imaging.

I would like to acknowledge all funding organisations, Australian Government, Australasian Spinal Cord Injury Network, CatWalk Spinal Cord Injury Research Trust New Zealand and University of Technology Sydney, for providing me the financial support in the form of research grants, scholarships, travel funds for conferences and in-kind support.

I also want to acknowledge Elite Editing for editing my PhD thesis, in accordance with Standards D and E of the Australian Standards for Editing Practice, and Perry Kwong for proofreading my PhD thesis.

Special thanks to Jeremy Chan, for giving me suggestions in not only laboratory works but, more importantly, personal life.

To all other members at Neural Injury Research Unit - Thomas C, Katheryn, Theresa, Alison, Arjun, Razia, Thomas H and Claire – thank you for your help and kindness during the experimental works in our compact laboratory.

To Coco Kuang, my soul mate, thank you for your accompany during my darkest age of PhD candidature, enduring my frustration and disappointment from the experiments, as well as bringing me to greet the promising dawn.

To Wilson, Jin, Jiaxin, Fiona, Kimmy, Kim, Mashiry and all my great friends around the world, thank you for giving me so many good memories and always helping me escape from the blue periods.

To my lovely family, dad and mum, I want to thank you for your unconditional love and support all the time.

Table of Contents

List of Figures

List of Tables

Abbreviation

3Rs:	Replacement, Reduction and Refinement
ACEC:	Animal Care and Ethics Committee
AMPA:	a-amino-3-hydroxy-5-methyl-4-isoxazole propionic acid
ANOVA:	Analysis of Variance
AS-ODN:	Antisense oligodeoxynucleotide
ATP:	Adenosine triphosphate
BBB:	Basso, Beattie and Bresnahan
BSB:	Blood spinal cord barrier
CNS:	Central nervous system
FITC:	Fluorescein isothiocyanate
FL:	Front limb
GABA:	γ-aminobutyric acid
GFAP:	Glial fibrillary acidic protein
H&E:	Haematoxylin and Eosin
HL:	Hind limb
HREC:	Human Research Ethics Committee
IHC:	Immunohistochemistry
MASCIS:	Multicentre Animal Spinal Cord Injury Study
MP:	Methylprednisolone
mRNA:	Messenger ribonucleic acid
MS:	Mass spectrometry
NASCIS:	National Acute Spinal Cord Injury Studies
NeuN:	Neuronal nuclei
NGS:	Normal goat serum
NMDA:	N-methyl-D-aspartate
OSP:	Oligodendrocyte Specific Protein
P5:	Peptide5
PBG:	Phosphate buffer with 5% normal goat serum
PFA:	Paraformaldehyde
ROS:	Reactive oxygen species
SCI:	Spinal cord injury

SDS:	Sodium dodecyl sulphate
SEM:	Standard error of the mean
SP:	Scrambled peptide
TBS:	Tris-buffered saline
UNSW:	University of New South Wales
UTS:	University of Technology Sydney

Publications Arising from PhD Research

MAO, Y., TONKIN, R.S., NGUYEN, T., O'CARROLL, S.J., NICHOLSON, L.F., GREEN, C.R., MOALEM-TAYLOR, G. and GORRIE, C.A., 2017. Systemic Administration of Connexin43 Mimetic Peptide Improves Functional Recovery after Traumatic Spinal Cord Injury in Adult Rats. *Journal of Neurotrauma* 33, 707-719.

TONKIN, R. S., **MAO, Y.,** O'CARROLL, S. J., NICHOLSON, L. F., GREEN, C. R., GORRIE, C. A. & MOALEM-TAYLOR, G. 2014. Gap junction proteins and their role in spinal cord injury. *Frontiers in Molecular Neuroscience* 7.

Other Publications during PhD Candidature

SUTHERLAND, T.C., MATHEWS, K.J., **MAO, Y.,** NGUYEN, T. & GORRIE, C.A. 2017. Differences in the cellular response to acute spinal cord injury between developing and mature rats highlights the potential significance of the inflammatory response. *Frontiers in Cellular Neuroscience* 10, 310.

CHEN, H., Chan, Y.L., NGUYEN, L.T., **MAO, Y.,** de ROSA, A., Beh, I.T., CHEE, C., OLIVER, B., HEROK, G., SAAD, S. & GORRIE, C., 2016. Moderate traumatic brain injury is linked to acute behaviour deficits and long term mitochondrial alterations. *Clinical and Experimental Pharmacology and Physiology* 43, 1107-1114.

MAO, Y., NGUYEN, T., SUTHERLAND, T. & GORRIE, C. A. 2016. Endogenous neural progenitor cells in the repair of the injured spinal cord. *Neural Regeneration Research*, 11, 1075-1076.

MAO, Y., MATHEWS, K. & GORRIE, C. A. 2016. Temporal response of endogenous neural progenitor cells following injury to the adult rat spinal cord. *Frontiers in Cellular Neuroscience* 10.

Conference Proceedings Arising from PhD Research

MAO, Y., TONKIN, R. S., NGUYEN, T., O'CARROLL, S. J., NICHOLSON, L. F., GREEN, C. R., MOALEM-TAYLOR, G. & GORRIE, C. A., 2017. Systemic administration of a Connexin43 mimetic peptide is neuroprotective and improves functional recovery after spinal cord injury in rats. *BNA 2017 Festival of Neuroscience*, Birmingham, UK: British Neuroscience Association.

MAO, Y., TONKIN, R. S., NGUYEN, T., O'CARROLL, S. J., NICHOLSON, L. F., GREEN, C. R., MOALEM-TAYLOR, G. & GORRIE, C. A., 2016. Systemic administration of a Connexin43 mimetic peptide in rats improves functional recovery after spinal cord injury. *Australasian Neuroscience Society Annual Conference*, Hobart, TAS: Australasian Neuroscience Society.

GORRIE, C. A., **MAO, Y.,** TONKIN, R. S., NGUYEN, T., O'CARROLL, S. J., NICHOLSON, L. F., GREEN, C. R. & MOALEM-TAYLOR, G. 2016. Modulation of Connexin43 hemichannels following mild spinal cord injury. *Australasian Neuroscience Society Annual Conference*, Hobart, TAS: Australasian Neuroscience Society.

MAO, Y., TONKIN, R. S., NGUYEN, T., O'CARROLL, S. J., NICHOLSON, L. F., GREEN, C. R., MOALEM-TAYLOR, G. & GORRIE, C. A., 2016. Systemic delivery of a Connexin43 hemichannel blocking mimetic peptide improves functional recovery following spinal cord injury in rats. *Neuroscience 2016*, San Diego, California: Society for Neuroscience.

MAO, Y., TONKIN, R. S., NGUYEN, T., O'CARROLL, S. J., NICHOLSON, L. F., GREEN, C. R., MOALEM-TAYLOR, G. & GORRIE, C. A., 2015. Systemic delivery of a Connexin43 mimetic peptide in rats improves hindlimb locomotor function following spinal cord injury. *New Horizons Combined Health Science Conference,* Sydney, NSW: NSW Health Government.

MAO, Y., TONKIN, R. S., NGUYEN, T., O'CARROLL, S. J., NICHOLSON, L. F., GREEN, C. R., MOALEM-TAYLOR, G. & GORRIE, C. A., 2015. Systemic delivery of a connexin43 hemichannel blocking mimetic peptide in rats improves hindlimb locomotor function following spinal cord injury. *Inter-university Neuroscience and Mental Health Conference.* Sydney, NSW: Brain Sciences UNSW.

MAO, Y., TONKIN, R. S., NGUYEN, T., O'CARROLL, S. J., NICHOLSON, L. F., GREEN, C. R., MOALEM-TAYLOR, G. & GORRIE, C. A., 2015. Systemic delivery of a mimetic peptide against connexin43 gap junction protein in rats following spinal cord injury. *Australasian Neuroscience Society Annual Conference.* Cairns, QLD: Australasian Neuroscience Society.

Awards and Scholarships

UTS Faculty of Science HDR Student Conference Fund	2017
Australasian Spinal Cord Injury Network Travel Grants	2016/2017
UTS Vice-Chancellor's Postgraduate Research Student Conference Fund	2016 & 2017
Australian Government Research Training Program Scholarship	2015-2017
UTS Doctoral Scholarship	2015-2017
UTS President Scholarship	2014-2015
UTS International Research Scholarship	2014-2015
UTS Science Dean's Merit List Award	2014

Abstract

Spinal cord injury (SCI) is a major cause of morbidity, and leads to significant physical, emotional and financial burdens for individuals and their families. There is no known cure to date and current treatment options are limited. A cascade of secondary tissue damage starts within minutes to hours of an initial traumatic SCI, worsening the cellular and functional recovery. The time course of secondary damage does, however, offer a potential window of opportunity for intervention. It may be possible to administer new therapeutics during this early period, to prevent the extensive spread of damage to adjacent healthy tissue.

Over the past two decades, regulation of Connexin43 hemichannels has provided a novel avenue of research into limiting the secondary damage of SCI. Peptide5, a Connexin43 mimetic peptide, is a promising candidate that shows efficacy in blocking Connexin43 hemichannels, thus preventing the propagation of neurotoxic molecules from the injured cells to the nearby intact tissue in a number of neural injury models. Peptide5, in particular, has been shown to reduce secondary tissue damage and to improve functional recovery when delivered directly to the site of SCI. However, direct application of peptides to a spinal cord lesion is likely to be impractical in a clinical setting, and might result in delays to the initiation of treatment. Therefore, the current research project aims to demonstrate that the systemic administration of Peptide5 is a clinically relevant treatment option for traumatic SCI by (1) optimising the systemic administration protocol of Peptide5; (2) investigating the cellular and function improvements in SCI rats from the Peptide5 systemic administration; and (3) examining the safety profile of Peptide5 systemic administration protocol.

Mass spectrometry and electrophoresis were used to determine the *in vitro* degradation curves in normal rat and human sera. A rat model of contusive SCI was then employed to optimise the dosing regimen and investigate the efficacy of Peptide5 in limiting secondary tissue damage and improving functional recovery. The lesion size was assessed on Haematoxylin and Eosin stained histological sections, and fluorescent immunohistochemistry was utilised to examine the Connexin43 protein and hemichannels, as well as cellular responses. The behavioural improvements were evaluated from motor (open field and error ladder tests) and sensory (mechanical pain hypersensitivity) functions. Fluorescent-labelled Peptide5 was delivered to the SCI and normal rats systemically in order to determine the *in vivo* distribution.

It was found that the *in vitro* half-life of Peptide5 was 2 hours in normal rat serum and that the most effective dosing regimen was three injections of Peptide5 at 0 (10 mg/kg), 2 (5 mg/kg) and 4 (2.5 mg/kg) hours post-injury. Compared with controls, Peptide5 treated rats showed significant improvements in hind limb locomotor function and mechanical pain hypersensitivity. Peptide5 treatment led to a reduction in Connexin43 protein level, hemichannel opening, lesion size, astrogliosis, macrophage and/or microglial activation, and neuronal cell death. There was no evidence to suggest that Peptide5 had any adverse systemic effects in normal and SCI animals, or influenced other connexins in the spinal tissue.

The current research project demonstrated that systemic administration of Peptide5 is a feasible, neuroprotective and safe treatment option for ameliorating secondary damage and improving functional recovery in a contusive SCI model of rats. These findings provide strong support for the clinical use of Peptide5 in the near future.

Chapter 1

General Introduction

Traumatic spinal cord injury (SCI) is a destructive neurological disorder, with lifelong detrimental consequences on individuals' quality of living, as well as a drastic impact on society. It is defined by the United States Centres for Disease Control and Prevention as 'the occurrence of an acute, traumatic lesion of neural elements in the spinal canal (spinal cord and cauda equina) resulting in temporary or permanent sensory deficit, motor deficit, or bladder/bowel dysfunction' (Thurman, 1995). SCI patients typically present with sensory, motor and autonomic deficits below the level of the lesion. At present, there are no fully restorative treatments for SCI; however, various molecular, cellular and rehabilitative therapies approaching clinical trials have led to a limited degree of functional recovery. This chapter explores the current understandings of SCI, the present clinical approaches for SCI and the recent research in SCI repair via modulation of gap junction hemichannels. The application of a mimetic peptide for regulating Connexin43, a gap junction hemichannel protein, is discussed as a novel SCI treatment for limiting lesion spread, inflammatory reaction and scarring, and improving functional recovery.

1.1 Epidemiology of spinal cord injury

Occurring at any age, SCI has profound effects on individuals and societies. The global prevalence is reported to be between 236 and 1009 per million individuals with an incident rate of between 10 and 83 new patients per million population per year (Cripps et al., 2011, Wyndaele and Wyndaele, 2006). In Australia, there is a conservative estimate of 10,000 people living with SCI, with 300 to 400 new cases reported each year (Norton, 2010). The majority of Australians with SCI experienced traumatic events, accounting for 79% of total SCI cases. The leading causes of traumatic SCI in Australia include motor vehicle accidents (46%), falls (28%) and sporting activities (9%) (Norton,

2010). Non-traumatic SCI cases arise mainly from tumours, infection and disc herniation (McDonald and Sadowsky, 2002). The current study focuses on traumatic SCI.

People with SCI can have a range of symptoms, including sensory and motor deficits, chronic pain, bladder or bowel dysfunction, autonomic dysreflexia and sexual dysfunction (Norenberg et al., 2004). According to the level at which SCI occurs, there may be a corresponding degree of sensory and/or motor deficit below the injury site (Figure 1.1). The impairment at cervical segments usually results in tetraplegia (quadriplegia), while the lesion at the thoracic, lumbar and sacral segments accounts for paraplegia (Norton, 2010). Worldwide, one-third of people with SCI admitted to spinal units are reported to be tetraplegic (Wyndaele and Wyndaele, 2006); this proportion increases to 53% in Australia (Norton, 2010). According to Anderson (2004), tetraplegic SCI patients consider arm or hand function to be the first priority affecting their quality of life and life expectancy. As a result of the catastrophic effects of SCI, fully functional recovery is the most desired outcome of therapeutic approaches.

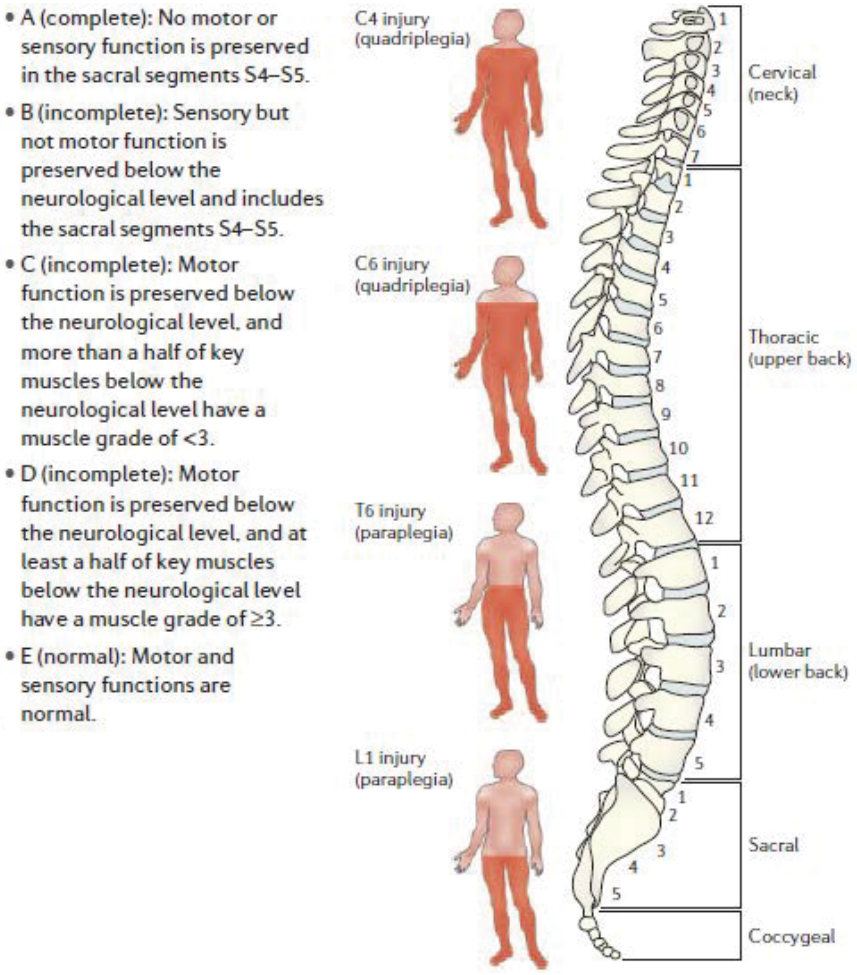

Figure 1.1 The severity of SCI measured by neurological level of injury and extent of injury.
The extent of injury (complete or incomplete) is categorised by the American Spinal Cord Injury Association Impairment Scale (left). The neurological level of injury (tetraplegia/quadriplegia or paraplegia) is determined by the anatomical location of injury (right). Adapted from Thuret et al. (2006).

Apart from the level of neurological injury (tetraplegia or paraplegia), the severity of SCI is also measured by the extent of injury (complete or incomplete). The American Spinal Cord Injury Association Impairment Scale classifies traumatic SCI into grades A–E, based on the neurological responses (sensations and control) of various parts of the body (Figure 1.1). Grade A (complete injury) represents the most severely damaged spinal cord, while Grade E (normal) reflects full neurological function (Steeves et al., 2006). It has been suggested in multiple studies that people with complete SCI,

(between 35% and 50% of SCI cases in Australia and the world respectively (Wyndaele and Wyndaele, 2006, Norton, 2010)), have a significantly higher mortality rate than incompletely injured people (Yeo et al., 1998, Frankel et al., 1998, DeVivo et al., 1987). Up to 20% of Grade A individuals recover to Grade B or C 1 year after SCI (Fawcett et al., 2007). This may be suggestive of limited spontaneous recovery, or may be due to the subjective classification of completeness of SCI.

Apart from the 20% of individuals who recovered from Grade A to B or C, SCI usually leads to permanent functional mobility-related disabilities, which impact daily living activities, working skills, sexual function and fertility (Kirshblum et al., 2007). This further results in employment crisis, educational difficulty, psychological illness, family issues and discrimination (Wandell, 2010). Most tetraplegic patients cannot live independently (Kirshblum et al., 2004). Consequently, the influence of SCI can be an economic burden on individuals, healthcare systems and communities, with respect to the considerable costs associated with nursing care and loss of income. The annual care and health cost for SCI population is estimated to be AU$500 million in Australia (Norton, 2010), and in the United States, US$9.7 billion (Kruse et al., 1998). The reduced domestic productivity is considered the major social impact of SCI, as it typically affects adults of working age (Priebe et al., 2007). Accordingly, functional recovery aiming to minimise disabilities should be considered an essential criterion in SCI treatment so as to maximise patients' benefits and to reduce the profound socio-economic impact in the short and long term.

1.2 Pathophysiology of spinal cord injury

To develop effective therapeutic interventions, it is crucial to understand the pathophysiological mechanisms behind SCI. The progression of SCI involves a biphasic process: primary injury and secondary injury (Fleming et al., 2006). Initially, the primary injury caused by the neurological trauma is restricted to the lesion site within hours to days (Kwon et al., 2004). Within weeks, the acute neurological insult in the primary injury initiates a cascade of other events, known as the secondary injury, which cause progressive post-traumatic damage to the spinal tissue resulting in permanent neurological deficits (Schmidt and Leach, 2003, Baptiste and Fehlings, 2007). In response to SCI, astrocytes, one of the most abundant glial cells in the central nervous system (CNS), become reactive and proliferative near the lesion, to form an astroglial scar (astrogliosis) (Brambilla et al., 2005, Gwak et al., 2012). Meanwhile, the natural inflammatory responses are caused by the disruption of blood spinal cord barrier (BSB) in the lesion area, leading to prolonged inflammation and incomplete healing (Popovich et al., 1997, Kigerl et al., 2009, Sharma, 2011).

1.2.1 Primary injury

The primary injury is caused by the initial mechanical impact and/or persisting compression from the dislocated vertebra, fractured vertebral fragments, disc material and ligamentous structures of the spinal cord (Tator, 1995). The mechanical forces, including compression, contusion, laceration, distraction and shear, primarily damage the central grey matter, causing a massive necrosis of neural cells (neurons, astrocytes and oligodendrocytes) and endothelial cells (Scheff et al., 2003, Dumont et al., 2001, Mautes et al., 2000b). As a consequence of the death of endothelial cells in blood vessels, the spinal cord undergoes pathological changes, such as haemorrhage,

ischaemia and oedema, resulting in the disturbance of oxygen and nutrient supply in the lesion and surrounding area (Jones et al., 2003a, Maier and Schwab, 2006). Further, demyelination of axon occurs in the lesion area, due to the damage of the myelin membrane on axons, leading to the deposition of the myelin inhibitors, such as Nogo-A, oligodendrocytes-myelin glycoprotein and myelin-associated glycoprotein, at the injury site (Su et al., 2007, Maier and Schwab, 2006). In turn, inhibitory factors restrict any possible axonal regeneration (Freund et al., 2007, Wang et al., 2006, Fitch and Silver, 2008).

SCI also immediately causes the disruption of BSB, a highly selective permeability barrier regulating the passage of molecules between the peripheral blood and CNS (Maikos and Shreiber, 2007, Sharma, 2011). The BSB plays a vital role in limiting the infiltration of inflammatory cells and the leakage of plasma fluid (Muldoon et al., 2013, Mautes et al., 2000b). Resulting from the breakdown of BSB, the sudden invasion of inflammatory cells from the damaged blood vessels drastically alters the quiescent inflammatory regulation in the spinal cord (Trivedi et al., 2006). In addition to the dysregulation of inflammatory responses, fibrinogen, a blood-clotting protein, from the efflux of plasma fluid accumulates in the extracellular space of the spinal cord. It has been reported that the fibrinogen activates the epidermal growth factor receptors, thus suppressing neurite outgrowth and axonal regeneration (Schachtrup et al., 2007, Mautes et al., 2000a, Li et al., 2011). The initial disruption of BSB is a critical event in the secondary injury.

1.2.2 Secondary injury

Following the initial damage to the spinal cord, the secondary injury starts from the extension of progressive ischaemia to the surrounding white matter, resulting in further neuronal and axonal necrosis (Tator and Koyanagi, 1997, Kanno et al., 2011). Ruptured blood vessels, microcirculatory impairment and injured cells and axons cause further loss of neighbouring intact neurons, oligodendrocytes and axons (Maier and Schwab, 2006). Consequently, the intact axons start to demyelinate, and the necrotic oligodendrocytes release growth inhibitory molecules, neurite outgrowth inhibitors and myelin-associated glycoprotein preventing neural self-regeneration (Laabs et al., 2005).

The hypoxic condition induced by the primary injury leads to a massive release of glutamate from necrotic neural cells into the extracellular space (Park et al., 2004, Bernards and Akers, 2006, Choi, 1994, Leem et al., 2010, Lepore et al., 2011). More importantly, the abnormally high level of extracellular glutamate, released from the impaired membrane of neurons and axons, overexcites neighbouring neurons to increase the intracellular concentration of calcium and sodium ions, and the extracellular concentration of potassium ions (Matute et al., 1997, Uberti et al., 2002). Therefore, these abnormal electrolytic shifts give rise to the functional failure of neural circuits, resulting in additional demyelination of axons and apoptosis of neurons and oligodendrocytes (Ankarcrona et al., 1995, Nguyen and McQuillen, 2010). This event is known as excitotoxicity.

The excitotoxicity, along with the hypoxia after the primary injury, induces an abundance of free radicals, such as superoxide and hydroxyl (Basu et al., 2001, Gwak et al., 2012). The free radicals play a vital role in normal cellular metabolism; however, the excessive number of free radicals in the secondary injury cannot be catabolised by diverse enzymes, such as superoxide dismutase and catalase (Grabitz et al., 1990,

Honegger et al., 1989, Bains and Hall, 2012, Jia et al., 2012). A consequence of this is the peroxidation of membrane lipid and the formation of aldehyde products, disturbing crucial metabolic enzymes such as Na^+/K^+-ATPase (Ditor et al., 2004, Li et al., 2001), as well as glucose transporters (Nagamatsu et al., 1993). Thus, the energy metabolism in mitochondria is disrupted, resulting in apoptosis of neural cells (Lewen et al., 2000, Liu et al., 2011, Zhang et al., 2013).

1.2.3 Astroglial scar formation

Within hours of the injury, the formation of an astroglial scar in the CNS is induced after the mechanical destruction of neural cells (Chan, 2008). As shown in Figure 1.2, the astrogliosis is initiated by the invasion of extrinsic macrophages (the monocytes infiltrated from peripheral blood) and intrinsic microglia (the resident macrophages in the CNS) to the lesion site for scavenging myelin debris, and then a fluid-filled cyst containing a large number of macrophages forms from 2 weeks post-injury (Maier and Schwab, 2006). A large number of astrocytes line the cyst as a dense glial boundary to form a scar (Fleming et al., 2006), and numerous reactive astrocytes (characterised by cellular hypertrophy) in proliferation around the scar (astrogliosis) (Cizkova et al., 2009, Horky et al., 2006, Horner et al., 2000, Brambilla et al., 2005), while the peripheral neural cells continue to die (Sun et al., 2010). Faulty remyelination proceeds in this aggressive environment, leading to failure of neural regeneration (Lane et al., 2007). Finally, a dense network comprised of astrocytes, macrophages, microglia and fibroblasts, combined with neuroinhibitory molecules, including chondroitin sulphate proteoglycans and Nogo-A, forms in the lesion area, creating a physical and chemical barrier that prevents neural and axonal regeneration (Sharma et al., 2012, Fawcett, 2006, Fitch and Silver, 2008, Karimi-Abdolrezaee and Billakanti, 2012, Wang et al., 2011).

However, other studies suggest a beneficial and protective function of the astroglial scar (Faulkner et al., 2004, White et al., 2010, Sofroniew and Vinters, 2010). It acts as a neuroprotective boundary restricting inflammation and limiting the progression of lesion expansion (Faulkner et al., 2004, Sofroniew and Vinters, 2010). This boundary is essential for preserving motor function, protecting neurons and oligodendrocytes, and wound healing, even though the mechanism is unclear (Faulkner et al., 2004, White et al., 2010, Rolls et al., 2009, Hu et al., 2010). Indeed, the role of astrogliosis remains controversial in response to SCI.

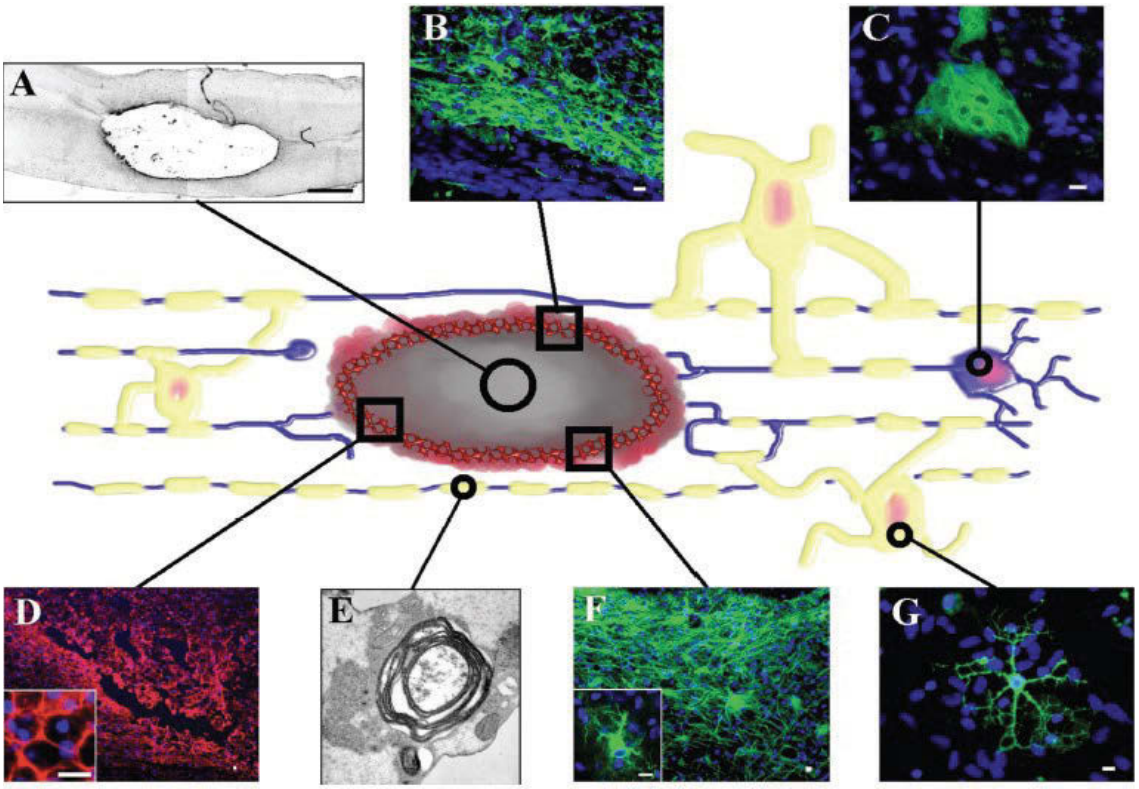

Figure 1.2 The formation of astroglial scar following spinal cord injury in humans. The formation of an astroglial scar around the injured site leads to an impaired repair process after SCI. A cyst (A) forms at the lesion site of spinal cord 2 weeks post-injury. The abundance of astrocytes expressing glial fibrillary acidic protein (B) is the main characteristic of an astroglial scar. The motor neurons (C) close to the lesion site consecutively undergo apoptosis, a cell death programme. There are large numbers of macrophages (D) in the fluid-filled cyst, as a sign of inflammation reaction and continual scavenging of necrotic cells and debris. Restricted axonal sprouting and remyelination occurs near the glial scar, but the extremely aggressive microenvironment is most likely to result in faulty myelination (E). There are high numbers of proliferating astrocytes and oligodendrocytes predominantly presenting Nestin (F), an intermediate filament protein, surrounding the astroglial scar. The oligodendrocytes (G) in white matter continuously die. Scale bars = 1 mm (A) and 10 μm (B to G). Adapted from Becker et al. (2003).

1.2.4 Inflammatory cells

Following the initial trauma to the spinal cord, the breakdown of BSB initiates the natural inflammatory response to the injury. Inflammatory cells, first neutrophils (within hours after injury) and later T-lymphocytes and monocytes (delayed for days), invades the lesion site and surrounding parenchyma to sterilise the injured tissue and phagocytise cellular debris and infectious agents (Popovich et al., 1997, Marracci et al., 2002, Crocker et al., 2006, Beck et al., 2010, Shechter et al., 2013). Although the diverse inflammatory responses following SCI have been extensively explored, the role of inflammatory cells following SCI is still disputed. Both beneficial and harmful effects of inflammatory cells are described and probably depend on different factors, including timing, cytokines, duration and magnitude. A rat model used in the proposed study illustrates the sequence of inflammatory cell responses to SCI in humans (Figure 1.3). However, the timeframes of the series of events differ between rats and humans.

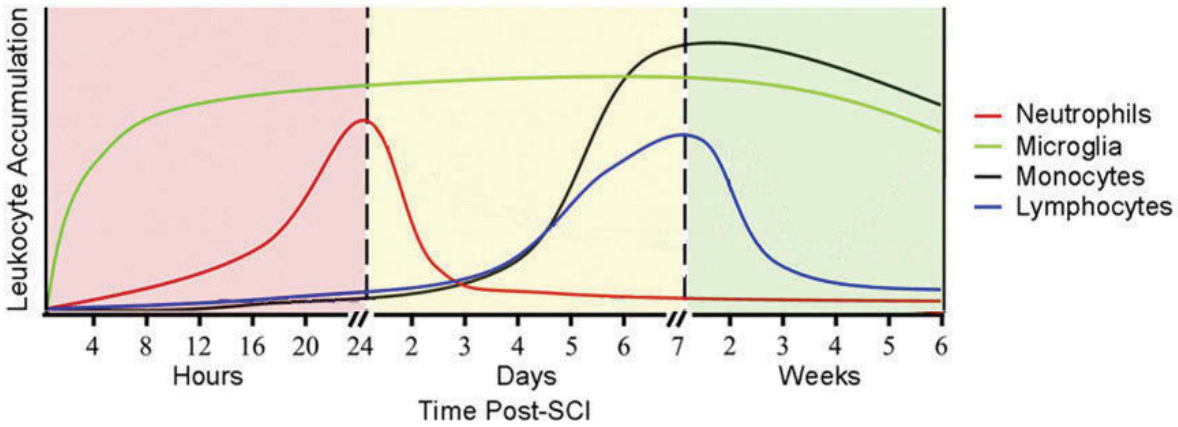

Figure 1.3 Temporal response of inflammatory cells in spinal cord injury rats. Neutrophils initiate infiltration into the injured spinal cord within 6 hours post-SCI as a sign of acute inflammation, and then attenuate after the maximum response at 24 hours post-injury. The number of activated microglia rapidly reaches a relatively high level in the first 8 hours post-SCI, and maintains the same level until the slight drop from 2 weeks post-injury. The recruitment of monocytes into the injured spinal cord is observed within 24 hours post-SCI. The number of recruited monocytes peaks at 1 week after injury and then slowly declines. Lymphocytes accumulate at the injured spinal cord peaking at 7 days following SCI. Adapted from Donnelly and Popovich (2008).

1.2.4.1 Activation of resident microglia

Microglia are the resident macrophages in the CNS, and are distributed throughout the brain and spinal cord (Watanabe et al., 1999). Their primary function is to protect the CNS by engulfing myelin debris and invading micro-organisms, a process known as phagocytosis (Andjelkovic et al., 1998, Gehrmann et al., 1995). Microglia also present antigens to T lymphocytes (Flaris et al., 1993). As the immune cells in the CNS, microglia are particularly sensitive to any pathological changes. Following SCI, the resident microglia are first activated as demonstrated by the hypertrophic cell bodies and retracted processes, as early as 4 hours post-injury (Trivedi et al., 2006, Dibaj et al., 2010, Gwak et al., 2012). The peak of microglia occurs between 1 and 5 weeks post-injury (Watanabe et al., 1999, Streit, 2001, Gwak et al., 2012). At the early stage, the activated microglia are believed to cause neuronal and glial toxicity, as well as neutrophil infiltration by releasing pro-inflammatory cytokines, such as tumour necrosis factor-α (TNF-α), Interleukin (IL)-1ß and IL-6 (Flaris et al., 1993, Yang et al., 2004a). These pro-inflammatory cytokines rapidly accumulate to the maximum level within 8 hours post-injury, indicating the magnitude of pro-inflammatory response (Pineau and Lacroix, 2007, Detloff et al., 2008, Hains and Waxman, 2006). The sustained elevation of pro-inflammatory cytokines further enhances vascular permeability (Schnell et al., 1999), leukocyte infiltration (Lacroix et al., 2002), neuronal and axonal degeneration (Lacroix et al., 2002, Okada et al., 2004, Shamash et al., 2002) and the expression of synaptic α-amino-3-hydroxy-5-methyl-4-isoxazole propionic acid (AMPA) and γ-aminobutyric acid (GABA) receptors, rendering neurons more susceptible to excitotoxicity (Beattie et al., 2002, Stellwagen et al., 2005). At the later stage, microglia are shown to secrete growth factors such as glial cell line-derived neurotrophic factor and brain-derived neurotrophic factor, which may help neuronal survival (Hashimoto et al., 2005, Stirling et al., 2013, Dougherty et al., 2000).

1.2.4.2 Penetration of circulating neutrophils

Within 6 hours of injury, circulating neutrophils invade the lesion site and surrounding parenchyma, as a consequence of the breakdown of BSB and the increase in vascular permeability following SCI (Popovich et al., 1997, Campbell et al., 2002). After injury, neutrophils sanitise the damaged tissue by phagocytising infectious agents and cellular debris (Popovich et al., 1997, Saiwai et al., 2010). In contrast, other studies suggest that neutrophils also function by enlarging the lesion and destroying neural cells by releasing reactive oxygen species (ROS) (Campbell et al., 2002, Jones, 2005, Kubota et al., 2012). Activated neutrophils can also produce neurotoxic enzymes (e.g., phospholipase A2), extracellular matrix-degrading enzymes (e.g., matrix metalloproteinases), arachidonic acid and eicosanoids, contributing to the secondary injury (Liu et al., 2006, Fleming et al., 2006, Wells et al., 2003b, Yong et al., 2001). Arachidonic acid and eicosanoids are able to promote cyclooxygenase and free radical synthesis, as well as enhance vascular permeability and leukocyte influx (Kwon et al., 2005, Araki et al., 2001, Manabe et al., 2004). Moreover, matrix metalloproteinase-9, produced by neutrophils, facilitates diapedesis of inflammatory cells and thus further expands the inflammatory response (Tjoa et al., 2003, Kigerl et al., 2006, Taoka et al., 1997, Izumi et al., 2011, de Rivero Vaccari et al., 2012, Mautes et al., 2000b), so they appear to contribute to further enlargement of the lesion size.

1.2.4.3 Recruitment of blood-borne monocytes

The recruitment of blood-borne monocytes generally occurs within 48 hours of injury (Popovich et al., 1997). The recruited monocytes reach a maximum number at 2 weeks post-injury, then slowly attenuate (Popovich et al., 1997), although they can possibly last for 180 days or longer (Beck et al., 2010). They immediately differentiate into activated macrophages in response to cytokine, chemokines and extracellular metabolites in the lesion area of the spinal cord (Crocker et al., 2006, Shechter et al., 2013).

Conventionally, the activated macrophages are thought to be detrimental to neural cells, as they release pro-inflammatory cytokines and neurotoxins, such as nitric oxide (Petersen et al., 1990, Popovich et al., 1997, Bartholdi and Schwab, 1997). Recent studies suggest that there are two main subclasses of activated macrophages: inflammatory and resident macrophages (Kigerl et al., 2009, Sroga et al., 2003, Shechter et al., 2009). Inflammatory macrophages infiltrate the spinal cord between 12 hours and 4 days post-injury, and become dendritic cells (Naik et al., 2006, Sroga et al., 2003). They present the cellular and myelin debris to T lymphocytes for clearance in the pro-inflammatory phase (Mabon et al., 2000, Naik et al., 2006, Pineau et al., 2010). However, the fate, number and function of inflammatory macrophages in SCI remain elusive. Resident macrophages produce pro-inflammatory cytokines and neurotoxins in immediate response to interferon-γ (IFN-γ) and lipopolysaccharide in the injured tissue (Prüss et al., 2011). In most non-CNS tissues, resident macrophages cease secreting pro-inflammatory cytokines, and transform into alternative activated macrophages (M2) in the presence of IL-4 or IL-13, and glucocorticoid hormones in the anti-inflammatory phase (Mantovani et al., 2007, Shechter et al., 2013). M2 functions to dampen inflammation and promote healing and angiogenesis by expressing IL-10, IL-12 and

mannose receptors (David and Kroner, 2011, Stirling et al., 2013). However, the resident macrophages in the injured spinal cord fail to transform into M2 (Nahrendorf et al., 2007, Guerrero et al., 2012, Jiang et al., 2012, Sato et al., 2012). This suggests that the pro-inflammatory phase of inflammation for scavenging is prolonged and fails to transit to the anti-inflammatory phase for healing (Kigerl et al. 2006, Yang et al. 2004) . The fate and functional roles of both inflammatory and resident macrophages in SCI remain unclear due to the lack of characteristic markers for identification (Sroga et al., 2003). However, the polarisation of macrophages may be more complex *in vivo*, as the subclasses of macrophages are interchangeable and more diverse in phenotypes and genotypes in the injured spinal cord (Mantovani et al., 2004, Pelegrin and Surprenant, 2009, Sato et al., 2012).

1.2.4.4 Infiltration of lymphocytes

The infiltration of lymphocytes into the injured spinal cord has been reported as early as 48 hours post-SCI, and the number of lymphocytes peaks at 7 days post-injury, in parallel with the influx of peripheral monocytes (Jones et al., 2002). Lymphocytes play a vital role in immune defence and protection, though their significance following SCI remains unknown. Most lymphocytes become activated by reacting with the major histocompatibility complex from antigen-presenting cells, such as activated macrophages, microglia and dendritic cells. Activated lymphocytes proliferate and produce cytokines and antibodies (via B lymphocytes), which are responsible for amplifying the inflammatory response and enhancing phagocytosis by macrophages (Jones et al., 2005). This autoimmune response enhances the microglia function to neuronal and glial toxicity, and further contributes to secondary injury (Blight, 1994, Fee et al., 2003). The activated T lymphocytes are currently thought to confer protective

autoimmunity. The active or passive immunisation of myelin proteins stimulates the expression of neuroprotective cytokines by the activated T lymphocytes, to limit secondary neurodegeneration (Friedmann et al., 2001, Schwartz and Kipnis, 2002, Ishii et al., 2012). However, the activated T lymphocytes have been shown to impair neurological improvement in other studies (Butovsky et al., 2001, Hauben et al., 2000, Kipnis et al., 2001, Wu et al., 2012). In particular, athymic rats have demonstrated augmented functional recovery in locomotion and depressed microglia/macrophage response following transection SCI (Potas et al., 2006). Further investigation is required to understand the importance of activated lymphocytes in the injured spinal cord.

Whether or not the responses of inflammatory cells after SCI are beneficial or detrimental has long been argued, and depends on numerous factors, such as microenvironments and timing. In other tissues, inflammation usually transitions from the pro-inflammatory phase, which clears foreign substances and/or damaged tissue, to the anti-inflammatory phase, which suppresses immune responses and promotes healing (Yang et al. 2004) . However, the transition of inflammatory phases in the spinal cord is dysregulated because of the disruption of the BSB, leading to prolonged inflammation and deficient healing (Kigerl et al., 2009).

1.2.5 Neurotoxic molecules

Glutamate is an important excitatory neurotransmitter, and is normally removed from the synaptic cleft, mainly by astrocytes in the mammalian CNS (Rothstein et al., 1996, Shibata et al., 1997). After SCI, the glutamate clearance process is impaired resulting in the elevation of extracellular glutamate in white matter to the neurotoxic level (Azbill et al., 1997, Wells et al., 1994, Liu et al., 1999, Hermann et al., 2001). A consequence of this is neuronal cell death via continued activation of N-methyl-D-aspartate (NMDA) and AMPA receptors, known as excitotoxicity (Agrawal and Fehlings, 1997, Park et al., 2004, Ferguson et al., 2008, Besancon et al., 2008). High levels of glutamate bind to NMDA receptors to induce an uncontrolled influx of calcium ions as calcium waves into neurons. The overload of calcium ions activates calpain and mitochondrial oxidative phosphorylation, ultimately leading to apoptosis (Hermann et al., 2001, Faulkner et al., 2004, Gaviria et al., 2000, Caccamo et al., 2004). The prolonged activation of AMPA receptors caused by excess glutamate induces a superfluous influx of sodium ions into neurons. The overload of sodium ions results in osmotic imbalance and cellular swelling, further leading to necrosis (Caccamo et al., 2004, Park et al., 2004, Xu et al., 2004, Ferguson et al., 2008).

ROS are highly reactive ions and free radicals containing oxygen molecules. They play a critical role in normal cellular metabolism and immune responses, including neutrophil signalling (Honegger et al., 1989, Fialkow et al., 2007, Dugan et al., 1995). In the healthy spinal cord, they are reduced in number by several enzymes such as catalase and superoxide dismutase, in order to maintain a sustainable amount (Vaziri et al., 2004, Shaw et al., 1997). Following SCI, the excitotoxicity together with neutrophil penetration produce a large amount of ROS, which cannot be cleared up by enzymes (Basu et al., 2001, Luo et al., 2002). The excess of ROS causes aldehyde product

formation and membrane lipid peroxidation, resulting in the dysfunction of many metabolic enzymes such as glucose transporters and Na^+/K^+-ATPase (Li and Stys, 2001, Nagamatsu et al., 1993). This consequently leads to a disturbance of the energy metabolism in mitochondria and then the initiation of apoptosis in neural cells (Bao et al., 2005, Teng et al., 2004).

1.2.6 Gap junctional communication

Gap junctions are specialised intercellular connections that form direct channels and facilitate the passage of various ions and small cytoplasmic molecules (< 1000 daltons) between two adjacent cells in a multitude of animals (Goodenough et al., 1996, Kang et al., 2008). They are found in all mammalian tissues, excluding erythrocytes, thrombocytes, spermatids and skeletal muscles (Goodenough et al., 1996). In vertebrates, a gap junction consists of two hemichannels (connexons) inserted in the cell membrane, which connect across the intercellular space (Figure 1.4A). Each hemichannel is composed of six oligomerised connexin proteins, which can be expressed as either homomeric (same connexins in a connexon) or heteromeric (different connexins in a connexon) hemichannels. Connexin hemichannels from adjacent cells are able to dock with each other to form either homotypic (two identical connexons) or heterotypic (different connexons) gap junction channels. At a structural level, connexins spanning the plasma membrane contain four transmembrane domains, a cytoplasmic loop and two extracellular loops, which have three cysteine chains for docking opposite hemichannels, along with amino- and carboxyl-terminals, which act as phosphorylation sites for regulation (Figure 1.4B). A conformational change induced by phosphorylation of connexins is suggested to control the gating of hemichannels, in

order to regulate the transmission of ions and small molecules (Solan and Lampe, 2005, Moreno, 2005).

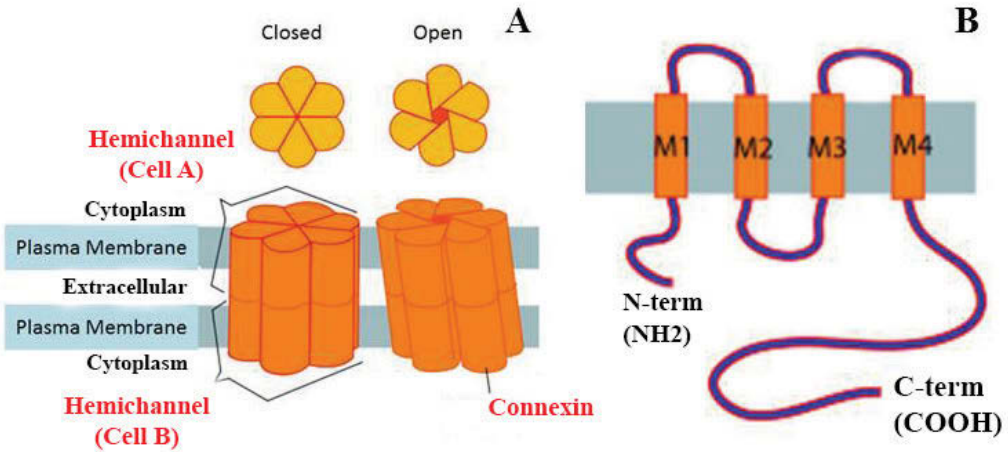

Figure 1.4 Illustration of gap junction (A) and connexin (B) structures in vertebrates.
(A) A gap junction is composed of two hemichannels or connexons, one in each of the apposed cell membranes. Each hemichannel is made of six connexin proteins. The gating mechanism of hemichannels controlled by a conformational change is induced by phosphorylation of connexins. (B) A connexin contains four transmembrane domains (M), a cytoplasmic loop (CL) and two extracellular loops (E), along with amino- and carboxyl- terminals (N-term and C-term respectively). Adapted from Hill (2013).

A varied range of connexin proteins are expressed in neurons, astrocytes and oligodendrocytes in the adult CNS. In neurons, Connexin36 is the major connexin protein in mediating electrical synapses (Bautista et al., 2014, Meyer et al., 2014). Connexin30 and Connexin43 are abundantly expressed in astrocytes (Stehberg et al., 2012, Lee et al., 2005), while Connexin 29, Connexin32 and Connexin47 are localised to oligodendrocytes and abaxonal membranes of myelinated fibres (Kamasawa et al., 2005, Li et al., 2004, Kleopa et al., 2004). Studies examining the distribution of connexins in the spinal cord indicate that connexin gap junctions undergo cell-to-cell coupling between neurons, adjacent astrocytes and astrocytes/oligodendrocytes. The

homotypic junctions between neurons contain Connexin36 (Gibson et al., 2005, Hormuzdi et al., 2004, Rash et al., 2000) and the homotypic junction between astrocytes include Connexin30 and Connexin43 (Lee et al., 2005, Orthmann-Murphy et al., 2008). The heterotypic gap junctions between astrocytes and oligodendrocyes are composed of Connexin43 - Connexin47 and Connexin30 - Connexin32 (Orthmann-Murphy et al., 2008, Kamasawa et al., 2005, Nagy and Rash, 2003). The current study focuses on Connexin43 which is the most abundant gap junctional protein in the human CNS (mainly expressed in astrocytes) (Lee et al., 2005). It is also found in various cell types, such as cardiomyocytes and endothelial cells (Chang et al., 2013, Rottlaender et al., 2010, Ishikawa et al., 2012, Márquez-Rosado et al., 2012).

In pathological conditions, it is well documented that the gap junction-mediated communication is involved in secondary necrotic and apoptotic cell death. Gap junctions intercellularly transmit neurotoxins including glutamate, nitric oxide, lactate, arachidonate, ammonia, ROS and calcium waves from the initial injured cells to the adjacent healthy cells, a process known as the bystander effect (Lin et al., 1998, Theriault et al., 1997, Scemes et al., 2000). The opening of uncoupled hemichannels alters the permeability of cell membrane to release those neurotoxins and calcium waves to extracellular space, which are then received by surrounding intact cells (Thompson et al., 2006, Ye et al., 2003, Orellana et al., 2011a, Davidson et al., 2015, Decrock et al., 2015). Various mechanisms of action have been suggested and debated for gap junction-mediated cell death, such as glutamate release (Ye et al., 2003, Parpura et al., 2004), metabolic stress (Ramachandran et al., 2007, Contreras et al., 2002), adenosine triphosphate (ATP) efflux (Stout et al., 2002, Kang et al., 2008, Bennett et al., 2012) and ionic dysregulation (Cotrina et al., 1998, Thompson et al., 2006).

Following traumatic injury to the CNS, there is increasing evidence that the expression of gap junction protein Connexin43 is elevated in astrocytes. Theriault et al. (1997) observed for the first time that the increase of astrocytic Connexin43 within grey and white matter at 1 day post-injury reaches a maximum at 3 days in rat spinal cords. These results were then replicated by Lee et al. (2005), who demonstrated elevated astrocytic Connexin43 messenger ribonucleic acid (mRNA) and protein levels as early as 4 hours post-injury in a transection SCI model. The increased expression of Connexin43 is found to be significant until 4 weeks (Lee et al., 2005). However, this appears to be inconsistent with Theriault et al. (1997), who claim the absence of Connexin43 staining at 7 days post-SCI. This controversy may arise because various anti-Connexin43 antibodies in the two studies failed to recognise the masked epitopes in astrocytic Connexin43, which are caused by the proliferation of astrocytes in response to injury. Similarly, an upregulation of Connexin43 in astrocytes is shown between 24 and 72 hours following traumatic brain injury; however, the astrocytic Connexin43 is recorded to be initially down-regulated in the hippocampus 6 hours post-injury, which has not been previously reported (Ohsumi et al., 2006). This upregulation of astrocytic Connexin43 plays a vital role in propagating neurotoxins and calcium waves extensively through Connexin43 gap junctions and hemichannels in the astroglial network, contributing to the secondary cell death (De Vuyst et al., 2007, Ye et al., 2003, Orellana et al., 2010, Davidson et al., 2015, Decrock et al., 2015). The increase in Connexin43 protein level has also been implied in other pathological conditions, such as cardiac infarct/ischaemia (Hawat et al., 2012, Kuhlmann et al., 2006, Hesketh et al., 2010), retinal ischaemia (Chen et al., 2015, Danesh-Meyer et al., 2012, Kerr et al., 2010) and diabetic skin wounds (Pollok et al., 2011, Wang et al., 2007, Becker et al., 2012).

1.3 Present clinical approaches for spinal cord injury

Although the understanding of SCI has improved in the past decades, there is still no treatment that will successfully repair and regenerate spinal cord tissue. Clinically, pharmacologic treatment, surgical procedures, multisystem medical management and functional rehabilitation have evolved to be the current treatment options for SCI. Although there is no consensus on the benefits of current treatments, they show improved functional outcomes to a certain extent in some SCI cases (Hagg and Oudega, 2006, Lynch and Popovic, 2008).

1.3.1 Methylprednisolone to limit secondary injury

Methylprednisolone (MP), as the only United States Food and Drug Administration approved drug for SCI, is a synthetic glucocorticosteroid identified in the early 1980s as a powerful lipid peroxidation inhibitor (Hall and Braughler, 1981). High doses of MP were considered as 'gold standard' for acute SCI treatment between the 1990s and 2000s (Bracken et al., 1990, Hurlbert, 2000, Short et al., 2000). MP is used to maintain the BSB, enhance spinal cord blood flow, inhibit endorphin release and limit the inflammatory response to reduce haemorrhage, and suppress immune responses (Taoka et al., 2001, Mu et al., 2000, Tator, 1998). These pre-clinical findings led to the initiation of the National Acute Spinal Cord Injury Studies (NASCIS), a multicentre, randomised, and double blind clinical trial. The NASCIS I trial included 330 patients and failed to show any significant improvement in neurological recovery and motor and/or sensory functions at either 6 weeks or 6 months post-injury (Bracken et al., 1984). The follow-up animal studies revealed that the MP dose used in NASCIS I was not sufficient to be neuroprotective (Braughler and Hall, 1984). Thus, the NASCIS II trial was initiated to evaluate the efficacy of using a dose of 30 mg/kg in 487 patients.

The authors reported that a high dose of MP intravenously administrated within 8 hours of injury was associated with a significant improvement of motor and sensory functions at 6 months (Bracken et al., 1990). However, the result of NASCIS II has not been accepted universally, because several methodological, statistical and scientific issues were criticised (Hanigan and Anderson, 1992, Coleman et al., 2000, Short et al., 2000). The most prominent deficit in NASCIS II was revealed to be lack of functional outcome measurements to assess whether the statistically significant improvements associated with MP were clinically relevant. This criticism led to the initiation of NASCIS III involving 499 individuals with additional functional outcome measurement. Bracken and his colleagues observed improvements in motor capabilities at 6 weeks and 6 months after injury but found they were not statistically significant at 1 year (Bracken et al., 1998, Bracken et al., 1997). However, the complications caused by MP, including hypoxia, ischaemia, pulmonary embolism, bronchopneumonia, wound infections, sepsis, gastrointestinal haemorrhage and myopathy, were also observed in most SCI cases (O'Connor et al., 2003, Apuzzo, 2002, Evaniew et al., 2015).

All three NASCIS trials failed to distinguish any significant differences in neurological recovery between the groups receiving placebo and different MP treatments (Bracken et al., 1984, Bracken and Holford, 1993, Bracken et al., 1998). Recent studies suggest that the administration of MP at NASCIS dosage after acute SCI has been reported to have no significant effect on functional recovery in terms of long-term locomotion performance (Pereira et al., 2009, Evaniew et al., 2016), and neurological recovery based on histological studies (Hurlbert et al., 2013, Pandya et al., 2010). MP is no longer recommended as the 'gold standard' for acute SCI treatment (Evaniew et al., 2016, Evaniew et al., 2015).

1.3.2 Surgical stabilisation and decompression

Surgical treatment for traumatic SCI involving vertebral stabilisation and decompression of neural tissue has been shown to improve functional recovery and minimise secondary injury in animal models (McKinley et al., 2004, Dimar et al., 1999, Carlson et al., 1997, Rabinowitz et al., 2008, Shields et al., 2005). The optimal timing for surgical intervention has been the subject of considerable debate, and early surgical intervention (within 24 hours of injury) has demonstrated a neuroprotective effect (Fehlings et al., 2012, Furlan et al., 2011, Hadley et al., 2010). However, no conclusive data was able to demonstrate that surgery is a valid practice option for improving neurological recovery, because of the absence of evidence from randomised and controlled clinical trials (Rahimi-Movaghar et al., 2009), and because the risks of surgical procedures, such as haemorrhage and infection, are marked at a high level (McKinley et al., 2004).

1.3.3 Multisystem medical management

Multisystem medical management plays a critical role in the acute treatment of patients with traumatic SCI, as isolated and multiple organ failures are frequently associated with injury to the spinal cord (Hadley et al., 2010). Patients with SCI are usually at a high risk of systemic inflammation precipitating organ damage (Stein et al., 2010). The potential cardiovascular and respiratory compromise in the injury at the cervical and upper thoracic spine can cause high mortality, and is a vital concern of physicians (Furlan and Fehlings, 2008, Berney et al., 2011). Medical complications caused by SCI are generally focused on: airway and respiratory management, management of cardiovascular complications, venous thromboembolism, nutrition and glucose control and infection management(Becker et al., 2003) (Table 1.1). While these immediate

medical interventions are critical for the continued health of a sufferer, and can possibly provide a platform for restoration of spinal neural pathways, they do not offer long-term spinal cord repair for functional recovery.

Table 1.1 Medical management for people with spinal cord injury (Becker et al., 2003).

Complication	Surgical Management	Rehabilitative Management
Cardiovascular: Hemodynamic instability Autonomic dysfunction Thromboembolism	Spinal stabilisation: Internal instrumentation, external orthoses	Management of chronic haemodynamic issues, Autonomic dysreflexia
Respiratory dysfunction: Respiratory failure Atelectasis Pneumonia Vent-dependent care	Tracheostomy	Preventive respiratory care, Respiratory conditioning programme
Gastrointestinal: Ileus Impaction, constipation Gastric/duodenal ulcers Reflux disease Cholelithiasis		Establish predictable bowel continence programme, Preventive gastrointestinal care
Urological: Urinary tract infection Hydronephrosis Cycto/nephrolithiasis	Urinary system augmentation, diversion procedures, penile implants, lithotripsy, sphincterotomy	Establish bladder continence program, Preventive genitourinary care, sexual dysfunction programmes
Dermatological: Pressure ulcers	Pressure ulcer repair	Establish skin integrity program, Prevention/management of pressure ulcers
Musculoskeletal: Osteoporosis Heterotopic ossification Fractures Overuse syndromes Acute and chronic pain	Delayed neurologic/spine complications: syringomyelia, focal nerve entrapments, central pain, spasticity, spinal instability, implantation of intrathecal drug delivery systems	Prevention of musculoskeletal complications: contractures, spasticity, postural abnormalities, skeletal deformities, long-term maintenance of intrathecal drug therapy

1.3.4 Functional rehabilitation

It is a critical aim of the health care and research communities to optimise the recovery of individuals after SCI, aiming towards high personal independency and good quality of life with little socio-economic burden. The functional rehabilitation strategy has evolved from compensation for weakened or lost functions to neural control of motor functions (Somers, 2001). The procurement of functional skills, appropriate behaviours and suitable equipment facilitates individuals' return to performance of ordinary roles and duties in family and society (Somers, 2001). Bladder and bowel control and improved upper extremity function are high priorities for tetraplegic SCI patients, whereas bladder/bowel control and sexual function are desired by paraplegic SCI patients (Anderson, 2004). Electrical stimulation (Granat et al., 1993) and passive bicycle training (Phadke et al., 2009) have shown to improve cardiovascular function and muscle tone, with a certain level of functional recovery on mobility. The task-specific functional training physiotherapy combined with manual or robotic bodyweight-supported treadmill training has also shown an improvement in the regaining of ambulatory function in individuals with incomplete SCI (Dobkin et al., 2006). To date, these options present the most effective rehabilitative care for SCI, and some people with SCI have regained a certain degree of function with continued use, depending on the severity of their injury (Lynch and Popovic, 2008). However, functional rehabilitation is very modestly effective, and should be used as a secondary treatment for SCI.

The effectiveness of existing clinical approaches to SCI is still limited in the short term, and deeply controversial as there is no consensus on substantial restoration. Long-term functional outcomes have not been improved significantly, despite a distinct

improvement in the mortality rate observed in the first year post-SCI (DeVivo, 2007). Therefore, it is critical to develop novel approaches to reduce the effects of injury and improve functional recovery over the long term.

1.4 Current research on Connexin43 for spinal cord injury repair

The lack of effective treatment options for restoring neurological function following SCI has led to a great demand for novel approaches for neuroprotection at the acute phase and neuroregeneration at the chronic phase. Various innovative strategies have been successfully developed in animal models. There are four aspects of experimental strategies in SCI research:

1) Cellular replacement including activation of endogenous neural progenitor cells (Mao et al., 2016, Ke et al., 2006, Sabelström et al., 2013, Cawsey et al., 2015, Mothe and Tator, 2005) and transplantation of exogenous stem cells (Tetzlaff et al., 2011), such as neural progenitor/stem cells (Jin et al., 2016, Mothe et al., 2013, Okano et al., 2003, Karimi-Abdolrezaee et al., 2006), embryonic stem cells (McDonald et al., 1999, Sharp et al., 2010), olfactory escheating cells (Gorrie et al., 2010, Féron et al., 2005, Tabakow et al., 2013), mesenchymal stem cells (Watanabe et al., 2015, Nakajima et al., 2012, Čížková et al., 2006) and adipose-derived stem cells (Ryu et al., 2009, Arboleda et al., 2011);

2) Inflammatory modulation including regulation of anti-inflammatory and pro-inflammatory responses (Beck et al., 2010, Mukaino et al., 2010, Fenn et al., 2014, Liu et al., 2013, Cox et al., 2015, Popovich, 2000, Bracken et al., 1998, Grossman et al., 2014, Streit et al., 1998, Wells et al., 2003a);

3) Microenvironment conditioning including elimination of neuroinhibitory molecules (Petrosyan et al., 2013, Wilems et al., 2015, Zhao et al., 2013) and promotion of neurotrophic factors (Nakajima et al., 2014, Gransee et al., 2015, Tom et al., 2013)

4) Tissue engineering of scaffolds providing biomechanical support and guidance for nerve regrowth (Zeng et al., 2011, McCreedy et al., 2014, Kubinová et al., 2015, Gao et al., 2013, Teng et al., 2002, Stokols and Tuszynski, 2006).

The period of secondary injury following SCI offers an exciting window of opportunity for acute intervention. There is a great need to develop new treatments that can be used in this early period, before the extensive spread of lesions to adjacent healthy tissue. Modulation of Connexin43 hemichannels provides a novel platform for acute intervention, aimed at limiting secondary tissue damage and ameliorating behavioural function deficits. As most evidence suggests, both protein and mRNA levels of Connexin43 are increased following the traumatic CNS injury (Theriault et al., 1997, Lee et al., 2005, Ohsumi et al., 2006, Lin et al., 1998). A wide range of methods have been used to reduce Connexin43 protein expression in astrocytes to investigate the neuroprotective functions. They are genetic deletion of Connexin43, gap junction inhibitors, Connexin43 antisense oligodeoxynucleotides (AS-ODN) and Connexin43 mimetic peptides as reviewed in Tonkin et al., 2015.

1.4.1 Genetic deletion of Connexin43

Homozygous knockout of the Connexin43 gene leads to malfunction of the pulmonary outflow tract, so the Connexin43-knockout mammals cannot survive beyond the

neonatal period (De Maio et al., 2002, Reaume et al., 1995). Instead, Frantseva et al. (2002a) used hippocampal organotypic slice cultures from 7-day old rats in a weight-drop model of traumatic brain injury, to investigate the effects of genetic deletion of Connexin43. A significant decrease in neocortical cell death was found in slices from homozygous Connexin43-knockout mice at 24 hours following the impact, compared with heterozygous and wild-type littermates, suggesting that a complete loss of Connexin43 is beneficial to neural cell survival after traumatic brain injury. However, the functions of Connexin43 gap junctions and hemichannels were partly reserved, as the permanent deletion of the Connexin43 gene permitted the altered expression of other connexin genes, such as Connexin30, to compensate astrocytic gap junction functions (Koulakoff et al., 2008). Indeed, the attenuated functions of Connexin43 gap junctions and hemichannels are implicated with neuroprotection by limiting secondary cell death after traumatic injury to the CNS.

1.4.2 Gap junction inhibitors

Genetic deletion of Connexin43 is limited to experimental approaches, and not suitable for translation as a pioneer experimental approach. Transient gap junction blockade models were investigated as an alternative. Frantseva et al. (2002a) repeated the experiment with a different approach, where wild-type slices were incubated with global gap junction blockers, carbenoxolone or octanol, up to 2 hours after traumatic brain injury. This led to a significant decrease in pyramidal cell death with improved synaptic function, measured over 72 hours. Carbenoxolone is a glycyrrhetinic acid derivative with a steroid-like structure and traditionally used to treat gastric ulcers (Doll et al., 1965). It has been suggested to reversibly decouple and ‘squeeze’ gap junctions closed (Rozental et al., 2001, Roh et al., 2010, Gigout et al., 2006, Figiel et al., 2007). A recent

study employed a rat model of hemisection SCI to examine the effects of intrathecal injection of carbenoxolone (Roh et al., 2010). The acute administration of carbenoxolone up to 5 days post-injury attenuated the induction of neuropathic pain and the astrogliosis at the lesion edge, but did not improve the hind limb locomotor function. This is possibly because the open unpaired hemichannels release neurotoxins such as ATP, glutamate and nitric oxide into the extracellular space, thereby invading the surrounding intact neural cells, even though these global blockers have a limited degree of regulation on the integrated gap junctions. The global inhibitors non-specifically block all types of gap junctions, affecting physiological functions such as electrolyte homeostasis, thermoregulation and angiogenesis (Hong et al., 2009, Betageri and Rogers, 1987, Connors, 2012). While the global gap junction blockers have confining or questionable control of lesion spread and astrogliosis following traumatic CNS injury, other tissues containing connexin gap junctions are also adversely affected. Thus, it is important to develop a transient connexin blockade in the lesion area, and AS-ODN is a possible approach being studied.

1.4.3 Connexin43 antisense oligodeoxynucleotides

The specific transient connexin blockade can be executed by Connexin43 AS-ODNs with the advantage of not only their specificity to Connexin43, but also the transient restriction of Connexin43 gap junctional communication to allow for quick recovery for normal astrocytic homeostasis (Green et al., 2001). The Connexin43 AS-ODNs are short chain nucleotides designed to temporarily knock down the expression of the Connexin43 gene by binding to its mRNA, blocking translation and thus Connexin43 production (Moore and Burt, 1994). The protective effect of AS-ODNs from secondary cell death is induced by depressing the upregulation of Connexin43 (Cronin et al., 2008,

Cronin et al., 2006). The limited formation of Connexin43 gap junctions and hemichannels in astrocytes restricts the propagation of death signals to neighbouring healthy cells and extracellular space respectively, and the surrounding intact tissue is preserved (Green et al., 2001). Due to a short half-life of about 20 minutes, AS-ODNs have been incorporated into a Pluronic gel delivery system to assist penetration into cells and provide sustained release (Green et al., 2001).

A neuroprotective effect of Connexin43 AS-ODNs has been shown following traumatic CNS injury. Cronin et al. (2008) examined the neuroprotective function of Connexin43 AS-ODNs in two *in vivo* models of SCI (partial transection and compression). Within 24 hours of a partial transection injury, spinal cords treated with Connexin43 AS-ODNs appeared less swollen, inflamed or disrupted than the controls. In both models, Connexin43 AS-ODNs demonstrated an ability to reduce the elevation of Connexin43 and reactive astrocyte levels, depress inflammatory response assessed by neutrophils and activated microglia and decrease leakage from damaged vasculature. In the compression model, the hind limb locomotor performance of the Connexin43 AS-ODNs-treated rats was consistently better than that of the control groups at 1 month following injury. A recent study demonstrated the neural protective function of Connexin43 AS-ODNs in a rat model of traumatic brain injury (Wu et al., 2013). The animals treated with Connexin43 AS-ODNs intraventricularly showed a reduced expression of Connexin43, decreased water content and less proliferative astrocytes in brains at 6, 24 and 48 hours after trauma.

The regulation of Connexin43 by AS-ODNs is shown to not only protect neural cells after traumatic CNS injury but improve wound healing in many tissues, including cornea (Grupcheva et al., 2012, Ratkay-Traub et al., 2001, Cursiefen et al., 2009), skin (Coutinho et al., 2003, Qiu et al., 2003, Becker et al., 2012, Chang et al., 2015), cardiac

muscle (Yasui et al., 2000), smooth muscle (Yeh et al., 1997, Liao and Duling, 2000) and vascular endothelium (Ormonde et al., 2012, Yeh et al., 2000, Kwak et al., 2001). Similar to the traumatic injury in CNS, the upregulation of Connexin43 was observed at the wound edge of chronic wounds, which is detrimental for wound healing (Coutinho et al., 2003, Wang et al., 2007). By modulating the expression of Connexin43 gap junctions and hemichannels via the same proposed mechanism of action as in the CNS, the AS-ODNs were shown to dampen inflammatory responses and decrease wound spread, resulting in reduced swelling and scarring to accelerate healing (Mori et al., 2006, Qiu et al., 2003, Coutinho et al., 2005). Significantly, the topical gel of Connexin43 AS-ODNs (Nexagon®) has been commercialised and is currently in clinical trials with CoDa Therapeutics, Inc (Table 1.2).

Table 1.2 Summary of clinical trials for Nexagon®

Identifier	Condition	Phase	Enrolled Subjects	Start Date	End Date	Status
NCT00736593	Skin wounds	I	43	Sep 2008	Apr 2009	Completed
NCT00820196	Venous leg ulcers	II	98	Mar 2009	May 2010	Completed
NCT00820703	Diabetic foot ulcer	I/II	24	Apr 2009	Dec 2009	Terminated (Business reasons)
NCT00821561	Persistent epithelial defect	II	90	Mar 2009	Mar 2010	Withdrawn (Business reasons)
NCT01165450	Persistent corneal epithelial defects	II	2	Nov 2011	Feb 2014	Terminated (Drug supply cease)
NCT01199588	Venous leg ulcers	II	300	Mar 2011	Mar 2013	Completed
NCT01490879	Diabetic foot ulcers	II	168	Jul 2012	Apr 2014	Completed
NCT00654550	Corneal re-epithelialisation	I	24	Apr 2008	Dec 2008	Completed

This approach, which relies on the topical application of Pluronic gel containing Connexin43 AS-ODNs to the lesion surface, has been demonstrated to reduce lesion spread in traumatic injuries and improve locomotor function following traumatic CNS injury in animal models. However, the administration of Connexin43 AS-ODNs is not a practical option for the emergency prescription of SCI, as the delivery of Connexin43 AS-ODNs topical gel directly to the injured human spinal cord surface necessitates a highly invasive surgery immediately after injury. The surgery might postpone the application of Connexin43 AS-ODNs topical gel onto the lesion surface, which is required to regulate the Connexin43 expression, and thus the Connexin43 gap junctional communication within hours after SCI. In reality, spinal surgery is usually given less priority than other surgeries for vital organs following a traumatic event such as a motor vehicle accident, leading to a further delay in the administration of Connexin43 AS-ODNs topical gel. Additionally, the spinal surgery not only involves risky procedures that easily damage injured spinal cords further, but prevents the healing process by creating an open wound. The difficulties of delivering Connexin43 AS-ODNs in a topical gel directly to the surface of the spinal cord necessitate an alternative approach for people with SCI.

1.4.4 Connexin43 mimetic peptides

The Connexin43 gap junction and hemichannel communication can also be altered with the use of mimetic peptides. These are short peptide sequences designed against the extracellular loops of the Connexin43 proteins. They have been shown to interfere with the interactions of the extracellular loops by binding to recognition sites on Connexin43 hemichannels, leading to impairment of hemichannel docking (Berthoud et al., 2000, Boitano and Evans, 2000, Martin et al., 2005). Connexin43 mimetic peptides may also

induce a conformational change in hemichannels to maintain the closure of the unpaired hemichannels (Berthoud et al., 2000, Chaytor et al., 1997). Both gap junctions and hemichannels are independently regulated by each other by connexin mimetic peptides, with short incubation times or low concentration restricting hemichannel opening and docking without affecting the communication of existing gap junctions, whereas long incubation times or high concentration prevents gap junction and hemichannel communication (Leybaert et al., 2003, O'Carroll et al., 2008, Yoon et al., 2010, Abudara et al., 2014). Limiting Connexin43 hemichannel opening and docking prevents the efflux of neurotoxins to extracellular space and surrounding intact cells, providing a targeted pathway to restrict the secondary injury immediately following SCI.

A series of Connexin43 mimetic peptides have been designed against the two extracellular loops of Connexin43 protein, and one of these, referred to as Peptide5 (sequence VDCFLSRPETK) against the extracellular loop 2 of Connexin43, shows particular efficacy in regulating the communication of Connexin43 gap junctions and hemichannels (O'Carroll et al., 2008). Initially, *in vitro* experiments showed that concentrations of Peptide5 below 100 μM were specifically able to regulate Connexin43 hemichannel communication, reducing cell-to-cell dye transfer and calcium dye uptake (O'Carroll et al., 2008). O'Carroll et al. (2008) also demonstrated that low doses of Peptide5 down-regulated the Connexin43 expression in *ex vivo* spinal cord segments, resulting in less swelling, decreased astrogliosis and improved neuronal survival. Afterwards, a weight-drop contusion model of SCI in rats was employed to evaluate the *in vivo* effects of Peptide5, which was delivered to the lesion by an intrathecal catheter attached to an osmotic pump for up to 24 hours post-injury (O'Carroll et al., 2013). In the acute phase, a decrease in Connexin43 protein was seen with Peptide5 treatment, in contrast to an increase in Connexin43 phosphorylation, which leads to hemichannel

closure (Plotkin et al., 2002, Faigle et al., 2008). The levels of pro-inflammatory cytokines TNF-α and IL-1ß were observed to be reduced in the Peptide5 treatment group at 8 hours post-injury, demonstrating a dampened inflammatory response. In terms of chronic effects, the Peptide5 treated rats had reduced lesion size, astrogliosis and activated microglia compared with the controls, as well as increased neuronal survival at 6 weeks after SCI. Additionally, there were improvements in hind limb locomotor function seen in the Peptide5 treatment group in comparison with controls when assessed over 6 weeks. These results reveal that application of Peptide5 effectively reduces secondary tissue damage following SCI and improves functional outcomes, indicating the clinical potential of Peptide5 in the treatment of SCI sufferers.

Peptide5 could feasibly be administered systemically to reach the injury sites, where the capillary bed is compromised in the injured spinal cords, thus offering a practical therapeutic approach for people with SCI. A recent study has shown that the intravenous injections of mimetic peptides permeate the lesion site of spinal cords (Han et al., 2010). However, the exact mechanisms of Peptide5 still remain unclear and the possible actions are (1) internalisation and degradation of the Connexin43 proteins; (2) indirect action of Peptide5 in mediating the reponse to injury; and (3) conformational change of Connexin43 hemichannels (Berthoud et al., 2000, Chaytor et al., 1997, O'Carroll et al., 2008). The current evidence most likely suggests the possibility of conformational change, in association with the elevated level of phosphorylated Connexin43 (O'Carroll et al., 2013). The most recent study revealed that Peptide5 acts on the extracellular loop 2 of Connexin43 (Kim et al., 2017). It also demonstrated that Peptide5 sequence specificity is essential for the Connexin43 hemichannel blocking, and the SRPTEKT motif is central to the Peptide5 mechanism (Kim et al., 2017). The application of connexin mimetic peptides has been widely explored in dampening

immune responses (Matsue et al., 2006, Oviedo-Orta et al., 2002, Wong et al., 2006), restricting cardiovascular injury (Hawat et al., 2010, Hawat et al., 2012, Ongstad et al., 2013, Wang et al., 2013), limiting ischaemic injury (Glass et al., 2015, Chen et al., 2015, Danesh-Meyer et al., 2012, Davidson et al., 2013a), promoting wound repair (Ongstad et al., 2013, Pollok et al., 2011) and inhibiting osteoclastic differentiation (Ilvesaro et al., 2001).

With rising evidence indicating the neuroprotective function of Peptide5, researchers are now facing the serious issue of transporting mimetic peptides systemically to the lesion site, but not to other intact tissue so as to not disturb normal physiological function of gap junctions and hemichannels, especially in the brain and heart where Connexin43 hemichannels are also located (Li et al., 2001, Márquez-Rosado et al., 2012). To date, no study has investigated the efficacy of systemic delivery of Peptide5 following SCI. Therefore, the current research project will determine the effects of Peptide5 systemic administration using an *in vivo* contusion model of SCI in rats.

1.5 Project overview

The time course of secondary injury after traumatic SCI provides a window of opportunity for acute intervention. At present, there are no successfully restorative treatment options available for SCI use. There is an extensive demand to exploit novel approaches that are used in the early post-injury time period, prior to the wider spread of lesions to surrounding healthy tissue. Previous studies have already shown that intrathecal delivery of Peptide5 can modulate the Connexin43 hemichannels to limit the secondary injury in a rat SCI model (O'Carroll et al., 2013). As Peptide5 has the

potential to be intravenously injected into SCI patients, the systemic administration of Peptide5 offers a promising approach for an immediate non-invasive treatment of SCI.

1.5.1 Hypotheses and aims

The systemic administration of the Connexin43 mimetic peptide, Peptide5, is a feasible, neuroprotective and safe treatment for SCI using a rat model of contusion SCI. The specific aims are:

Aim 1: To optimise the systemic administration protocol of Peptide5 for traumatic SCI by analysing Peptide5 degradation *in vitro* and dose responses *in vivo*, as well as verifying that the Peptide5 is systemically delivered to the lesion area of the spinal cord (Chapter 2).

Aim 2: To investigate the cellular and functional improvements in SCI rats from the Peptide5 systemic administration by comparing lesion size, Connexin43 and phosphorylated Connexin43 levels, astrogliosis formation, inflammatory responses, neuronal cell loss and behavioural functions (hind limb locomotion and mechanical pain hypersensitivity) (Chapter 3).

Aim 3: To examine the safety profile of the Peptide5 systemic administration protocol as a practical treatment option for traumatic SCI by examining the distribution of Peptide5 *in vivo*, Connexin43 hemichannels in the heart and lung tissue, other connexins in the spinal cord and inflammatory responses in plasma (Chapter 4).

A summary of the animal cohorts and tissue samples obtained is provided in Table 1.3.

Table 1.3 Summary of animal cohorts and tissue samples obtained in the current study

Cohort	Condition	Treatment	Survival Time	Sample	Experiment	Chapter
I n = 12 (3 per group) UTS ACEC 2013-742	SCI	Peptide5 x 1 Peptide5 x 2 Peptide5 x 3	24 Hours	Fresh spinal cord at T10	Western blot	2
				Formalin fixed heart and lung	H&E IHC	4 4
	Sham	Saline x 1				
II n = 8 (4 per group) UTS ACEC 2013-742	SCI	Peptide5	8 Hours	PFA fixed spinal cord at T10	H&E IHC	2 2 & 4
				Formalin fixed heart and lung	H&E IHC	4 4
		Scrambled Peptide		Formalin fixed spinal cord at lumbar	IHC	4
III n = 96 (8 per group) UTS ACEC 2013-742	SCI	Peptide5	24 Hours 2 Weeks 6 Weeks	PFA fixed spinal cord at T10	H&E IHC	3 3 & 4
		Scrambled Peptide				
	Sham	Peptide5		Formalin fixed heart and lung	H&E IHC	4 4
		Scrambled Peptide		Plasma	Multiplexes assays	4
IV n = 16 (4 per group) UTS ACEC 2015-515	SCI	FITC-Peptide5	2 Hours 4 Hours	Fresh spinal cord at T10 and cervical, brain, heart, lung, liver, spleen and kidney	Histology	4
	Normal					

FITC: fluorescein isothiocyanate; H&E: Haematoxylin and Eosin stain; IHC: immunohistochemistry;
PFA: paraformaldehyde; SCI: spinal cord injury;
UTS ACEC: University of Technology Sydney Animal Care and Ethics Committee;

Chapter 2

Optimisation of the Peptide5 Systemic Administration Protocol for Traumatic Spinal Cord Injury

2.1 Introduction

Following injury to the spinal cord, expression of Connexin43 protein and mRNA in astrocytes is upregulated, playing an important role in propagating death signals extensively through the glial network (Rami et al., 2001, Theriault et al., 1997, Lin et al., 1998, Lee et al., 2005, O'Carroll et al., 2008). As in the other CNS injuries, Connexin43 hemichannel-mediated transfer and release of death signals destroys local neighbour cells, contributing to lesion spread following SCI (Decrock et al., 2015, Chen et al., 2014a, Davidson et al., 2013b). Our collaborators at the University of Auckland had led the field in developing a unique Connexin43 mimetic peptide, Peptide5, to modulate Connexin43 hemichannels and gap junctions. It is a short peptide consisting of 12 amino acids, which mimic the sequences in the extracellular loop 2 of Connexin43 protein. The active motif (SRPTEKT) in Peptide5 is able to bind to the recognition site (SHVR) in the extracellular loop 2 of Connexin43 protein, to induce a conformational change of Connexin43 hemichannels from an open to a closed state (Leybaert et al., 2003, Berthoud et al., 2000, O'Carroll et al., 2008, Faigle et al., 2008).

Although the exact mechanism of actions remains unclear, Peptide5 via local administration has demonstrated particular efficacies in reducing Connexin43 protein and mRNA levels as well as maintaining the closure of Connexin43 hemichannels within 24 hours of injury in several injury models (O'Carroll et al., 2013, O'Carroll et al., 2008, Chen et al., 2015, Chen et al., 2014b, Danesh-Meyer et al., 2012, Yoon et al., 2010). A previous study in this laboratory has shown that Peptide5 via intrathecal delivery (20 μmol/kg for 1 hour at a rate of 1 μL/min starting 1 hour after injury) was neuroprotective in limiting secondary injury and improving functional recovery in locomotion following contusion SCI in rats (O'Carroll et al., 2013). However, even intrathecal delivery, while possible in humans, will not always be practical in a clinical

setting, and there could be delays before treatment can be initiated. Peptide5 has the potential to be delivered systemically to reach the injury site via the compromised capillary bed (Mautes et al., 2000b), thus providing a practical therapeutic approach without invasive, time-consuming surgical procedures. To date, there is barely any scientific evidence to provide systemic administration protocols of Peptide5 for SCI in rodents or humans.

The current study was proposed to the optimise systemic administration protocol of Peptide5 for traumatic SCI by:

1) analysing Peptide5 degradation in normal rat and human sera to determine the maintenance doses using mass spectrometry (MS) and electrophoresis;
2) comparing the Connexin43 and phosphorylated Connexin43 protein levels in SCI animals receiving different doses of Peptide5, to determine the optimal dosing regimen by using western blot analysis;
3) investigating the systemic route of administration delivering Peptide5 to the lesion area of the spinal cord to regulate the Connexin43 hemichannels by using Haematoxylin and Eosin (H&E) staining and fluorescent immunohistochemistry (IHC).

2.2 Materials and methods

2.2.1 Preparation of peptides

Experimental protocols and procedures involving human samples in the study were approved by the Human Research Ethics Committee (HREC) of the University of New South Wales (UNSW) (UNSW HREC HC16005), in accordance with the National Health and Medical Research Council's National Statement on Ethical Conduct in Human Research (2007). Normal rat serum collected from mixed gender Sprague Dawley rats was purchased from Abcam (ab7488) and separated into three biological triplicates. Normal human sera were collected from five healthy human volunteers at Prince of Wales Hospital, Sydney by colleagues at UNSW. Age and sex information of the sera was not disclosed according to the Ethical Conduct in Human Research. Peptide5 (sequence VDCFLSRPTEKT, Mimotopes) and Peptide5 with a fluorescent tag, fluorescein isothiocyanate (FITC) (sequence FITC-A-VDCFLSRPTEKT, Auspep) were incubated in pre-heated sera at 37 ºC. The loading dose of Peptide5 was established at 10 mg/kg by colleagues at the University of Auckland. The equivalent Peptide5 and FITC-Peptide5 concentrations in normal rat serum was determined as 0.32 mg/ml and 0.45 mg/ml respectively, based on the average body weight of 9-week old experimental rats (250 g) and average plasma volume of adult experimental rats (7.8 ml) (Sharp and LaRegina, 1998). The equivalent FITC-Peptide5 concentration in normal human serum was determined as 0.30 mg/ml based on the average body weight of human adults (70 kg) and the average plasma volume of human adults (3.3 L) (Lamke and Liljedahl, 1976). Samples were then taken every hour for up to 8 hours and stored at -20 ºC until analysis.

2.2.2 Mass spectrometry

Using an Eksigent AS-1 autosampler connected to a Tempo nanoLC system (Eksigent), 10 µl of the Peptide5 sample was filtered to remove the particles larger than 10 kDa and then loaded at 20 µl/min with MS loading solvent (2% (w/v) acetonitrile and 0.2% trifluoroacetic acid (w/v)) onto a C8 trap column (Michrom Biosciences). After washing the trap for 3 minutes, the peptides were washed off at 300 nl/min onto a PicoFrit column (75 m x 150 mm) packed with Magic C18AQ resin (Michrom Biosciences). Peptides were eluted from the column and into the source of a QSTAR Elite hybrid quadrupole time-of-flight mass spectrometer (Applied Biosystems/MDS Sciex) using the following programme: 5-50% (v/v) MS solvent B (98% acetonitrile (w/v) and 0.2% (w/v) formic acid) over 8 minutes, 50-80% (v/v) MS solvent B over 5 minutes, 80% (v/v) MS solvent B for 2 minutes, 85% (v/v) MS solvent B for 3 minutes. The eluting peptides were ionised with a 75 µm ID emitter tip that tapered to 15 µm (New Objective) at 2300V. An Intelligent Data Acquisition experiment was performed, with a mass range of 375-1500 Da continuously scanned for peptides of charge state 2^+ - 5^+ with an intensity of more than 30 counts/s. Selected peptides were fragmented and the product ion fragment masses measured over a mass range of 100-1500 Da. The mass of the precursor peptide was then excluded for 15 seconds.

The data files produced by the QSTAR Elite hybrid quadrupole-time-of-flight mass spectrometer were searched using Mascot Daemon (Walter and Elisa Hall Institute, Version 2.4) and searched against the LudwigNR database comprised of the UniProt, plasmoDB and Ensembl databases (vQ111. 16,818,973 sequences; 5,891,363,821 residues) with the following parameter settings. Fixed modifications: none. Variable modifications: carbamidomethyl, propionamide, oxidised methionine. Enzyme: semi-trypsin. Number of allowed missed cleavages: 3. Peptide mass tolerance: 100 ppm.

MS/MS mass tolerance: 0.2 Da. Charge state: 2+ and 3+. The results of the search were then filtered by including only protein hits with at least one unique peptide (Bold Red) and excluding peptide hits with a p-value greater than 0.05. Peptides identified by Mascot Daemon were further validated by manual inspection of the MS/MS spectra for the peptide to ensure the b- and y-ion series were sufficiently extensive for an accurate identification. Quantitation of the peptide was performed using Analyst® QS (Applied Biosciences, Version 2.0) to determine the area under the curve from Extracted Ion Chromatograms of the relevant mass. These data were further analysed using Microsoft Excel (Version 2010) to plot concentration versus area.

2.2.3 Electrophoresis

Each FITC-Peptide5 sample (0.25 μg/μl for normal rat serum samples and 0.125 μg/μl for normal human serum samples) was prepared with 4 μl loading buffer as well as lysis buffer to make up a total volume of 20 μl. The loading buffer was made of 0.313 M Tris-hydrochloride, 10% (w/v) sodium dodecyl sulphate (SDS) and 50% (w/v) glycerol. The HEPES lysis buffer was made of 20 mM 4-(2-hydroxyethyl)-1-piperazineethanesulfonic acid buffer, pH 7.2, containing 1 mM ethylene glycol tetraacetic acid, 210 mM mannitol, 70 mM sucrose and 1x protease inhibitor cocktail (Roche). A positive control containing 0.25 μg/μl FITC-P5 in saline (0.9% (w/v) sodium chloride) was included in each gel, along with two negative controls containing saline or normal serum. The samples were then each loaded into wells of NuPAGE® 4-12% Bis-Tris gels (Thermo Fisher) and separated at 140V for 45 minutes with NuPAGE® MES SDS running buffer (Thermo Fisher). The gels were imaged in Typhoon FLA 9500 imager (GE Life Science) with LPB filter (laser at 473 nm). The

fluorescent intensity of each sample band at approximately 1.8 kDa was measured in mean grey scale value (GSV) by ImageJ (National Institute of Health, Version 2X). In each gel, the mean GSVs of 0-hour technical triplicates were averaged as a baseline for determining the percentage fluorescent intensity of sample bands at different time points. The degradation curves of Peptide5 in normal rat and human sera were established in Microsoft Excel (Version 2010) to determine maintenance doses.

2.2.4 Animals and general care

All experimental protocols and procedures involving animals used in the study were approved by the Animal Care and Ethics Committee (ACEC) of University of Technology Sydney (UTS) (UTS ACEC 2013-742), in accordance with the guidelines of the National Health and Medical Research Council of Australia. Two animal cohorts were used: Cohort I, 12 female Sprague Dawley rats (7 weeks old, 140 -180 g, Animal Resources Centre, Perth) were used to determine the most effective dosing regimen. They were randomly allocated into four groups: SCI with one dose of Peptide5 (n = 3), SCI with two doses of Peptide5 (n = 3), SCI with three doses of Peptide5 (n = 3) and sham with one dose of saline vehicle (n = 3). In Cohort II, eight female Sprague Dawley rats (7 weeks old, 140 -180 g, Animal Resources Centre, Perth) were used to verify that the intraperitoneal injection delivered Peptide5 to the injury area of spinal cord. They were randomly allocated into two groups: SCI with three doses of Peptide5 (n = 4) and SCI with three doses of control scrambled peptide (SP) (n = 4). All animals were maintained in standard cages with ad-lib water and food on a 12:12 hour light-dark cycle and housed in the Ernst Facility, Faculty of Science, UTS. Daily checks of room temperature, humidity and animal wellbeing were performed. Each animal's weight was

checked at least twice a week. All animals were acclimatised in the Ernst Facility for 2 weeks prior to any procedures.

2.2.5 Surgical procedures

The animals in injury groups were submitted to a laminectomy at the tenth thoracic vertebrae level (T10) and a mild contusion SCI, while the sham animals were subject to T10 laminectomy only. Anaesthesia was induced using 4% (v/v) isoflurane in oxygen (1 L/min) and then maintained at 2% (v/v) isoflurane in oxygen (1 L/min). The anaesthetic (Bupivacaine, 0.5% (w/v), 0.02 ml, s.c.) was injected locally at all surgical sites before incisions were made. Immediately prior to surgery animals were given antibiotics (Cephalozin sodium, 33 mg/kg, s.c.), analgesics (Temgesic, 0.03 mg/kg, s.c.) and supplementary fluid (Hartman's replacement solution, 15 ml/kg, s.c.). Skin and muscle were then incised and retracted through the dorsal midline, in order to perform a T10 laminectomy for exposing the spinal cord. The Multicentre Animal Spinal Cord Injury Study (MASCIS) impactor device (New York University) was used to produce a mild contusion SCI (6.25 mm drop, 10 g weight, 2.5 mm diameter) (Figure 2.1). The surgical data, including compression (mm), compression rate (m/s) and weight-drop velocity (m/s), were recorded by the impactor software. After removing the retracting clips, the surgical wound was closed in layers. The rats were maintained on the heating pad with 5 minutes of oxygen (1 L/min) before revival.

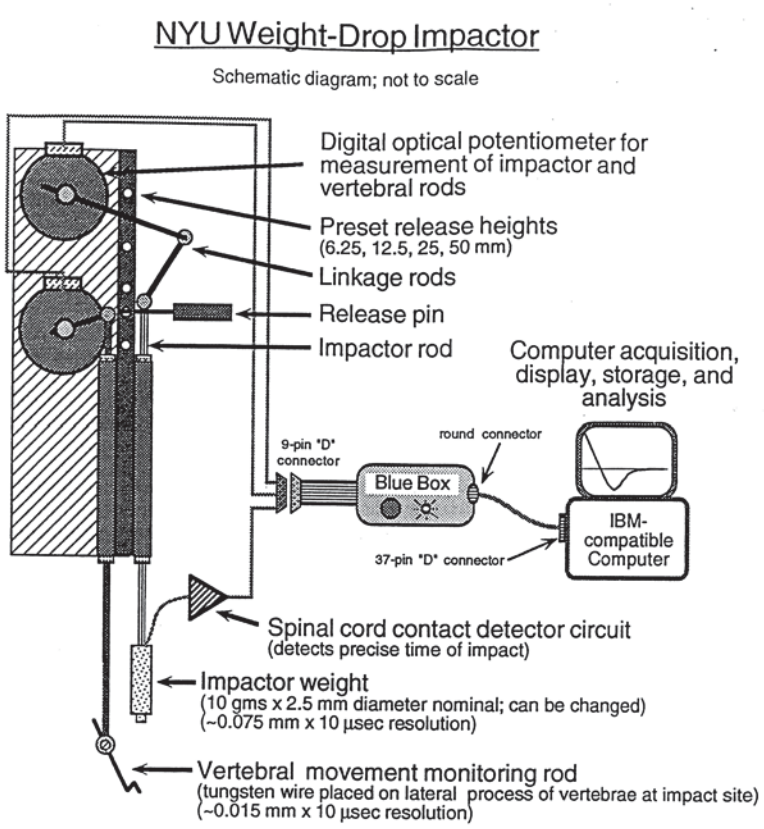

Figure 2.1 Schematic diagram of the Multicentre Animal Spinal Cord Injury Study impactor.
This diagram illustrates the mechanism of the Multicentre Animal Spinal Cord Injury Study impactor, and the relationship between impactor, blue box (sensor) and computer system. Adapted from Operation manual (1993).

2.2.6 Peptide treatment

Peptide5 was designed to match a portion of the extracellular loop 2 of Connexin43 (sequence VDCFLSRPTEKT). Peptide5 and control SP (sequence RFKPSLCTTDEV) were synthesised in solid phase by Mimotopes Pty Ltd., Australia, using Fmoc chemistries on a Protein Technology Symphony instrument, purified by high-performance liquid chromatography with the structure confirmed by MS analysis. In Cohort I, the first dose (10 mg/kg in 0.5 ml saline, i.p.) was administered immediately after surgery, while the second (5 mg/kg in 0.5 ml saline, i.p.) and the third (2.5 mg/kg in 0.5 ml saline, i.p.) doses were delivered at 2 and 4 hours after surgery respectively. The sham animals were intraperitoneally injected with one dose of saline immediately

following surgery (0.9% (w/v) sodium chloride, 0.5 ml) to show the normal levels of Conneixn43 and phosphorylated Connexin43 in the T10 spinal cord. In Cohort II, three doses of Peptide5 or scrambled peptide (10 mg/kg in 0.5 ml saline at 0 hours after injury, 5 mg/kg in 0.5 ml saline at 2 hours after injury, 2.5 mg/kg in 0.5 ml saline at 4 hours after injury) were delivered intraperitoneally.

2.2.7 Post-operative care

Animals were housed individually following surgery. They were kept in a holding room with a controlled temperature (22-25 ºC), humidity and light cycle (12 hr on/12 hr off) and had access to food and water *ad libitum*. Post-operatively, animals were given antibiotics (cephalothin sodium, 0.33 mg/kg, s.c.), analgesic (buprenorphine hydrochloride, 0.03 mg/kg, s.c.) and supplementary fluid (Hartman's replacement solution, 3.8 ml, s.c.) twice daily for 1 day. Bladders were expressed manually twice daily until euthanasia.

2.2.8 Behavioural assessments

To assess the consistency of injury produced in all SCI groups of animals by the MASCIS impactor, hind limb locomotor function was scored at Day 1 following surgery. In Cohort I, all animals were placed in an open field with a diameter of one metre, and the locomotion was recorded in a 2-minute video for each animal. The hind limb locomotor function was rated according to the Basso, Beattie and Bresnahan (BBB) scale (Table 2.1) to assess the degree of locomotor deficit (Basso et al., 1996).

Table 2.1 Basso, Beattie, and Bresnahan locomotor rating scale (Basso et al., 1996).

Score	Description
0	No observable HL movement
1	Slight movement of one or two joints, usually the hip and/or knee
2	Extensive movement of one joint or extensive movement of one joint and slight movement of one other joint
3	Extensive movement of two joints
4	Slight movement of all three joints of the HL
5	Slight movement of two joints and extensive movement of the third
6	Extensive movement of two joints and slight movement of the third
7	Extensive movement of all three joints of the HL
8	Sweeping with no weight support or plantar placement of the paw with no weight support
9	Plantar placement of the paw with weight support in stance only or occasional, frequent, or consistent weight-supported dorsal stepping and no plantar stepping
10	Occasional weight-supported plantar steps; no FL–HL coordination
11	Frequent to consistent weight-supported plantar steps and no FL–HL coordination
12	Frequent to consistent weight-supported plantar steps and occasional FL–HL coordination
13	Frequent to consistent weight-supported plantar steps and frequent FL–HL coordination
14	Consistent weight-supported plantar steps, consistent FL–HL coordination, and predominant paw position during locomotion is rotated when it makes initial contact with the surface as well as just before it is lifted off at the end of stance; or frequent plantar stepping, consistent FL–HL coordination, and occasional dorsal stepping
15	Consistent plantar stepping and consistent FL–HL coordination and no toe clearance or occasional toe clearance during forward limb advancement; predominant paw position is parallel to the body at initial contact
16	Consistent plantar stepping and consistent FL–HL coordination during gait and toe clearance occurs frequently during forward limb advancement; predominant paw position is parallel at initial contact and rotated at lift-off
17	Consistent plantar stepping and consistent FL–HL coordination during gait and toe clearance occurs frequently during forward limb advancement; predominant paw position is parallel at initial contact and lift-off
18	Consistent plantar stepping and consistent FL–HL coordination during gait and toe clearance occurs consistently during forward limb advancement; predominant paw position is parallel at initial contact and rotated at lift-off
19	Consistent plantar stepping and consistent FL–HL coordination during gait, toe clearance occurs consistently during forward limb advancement, predominant paw position is parallel at initial contact and lift-off, and tail is down part or all of the time
20	Consistent plantar stepping and consistent coordinated gait, consistent toe clearance, predominant paw position is parallel at initial contact and lift-off, and trunk instability; tail consistently up
21	Consistent plantar stepping and coordinated gait, consistent toe clearance, predominant paw position is parallel throughout stance, and consistent trunk stability; tail consistently up

FL: front limb; HL: hind limb

2.2.9 Euthanasia

In Cohort I, animals (n = 12) were deeply anaesthetised by an injection of Lethabarb (pentobarbitone sodium, 1 ml/kg, i.p.) at 24 hours following surgery. The abdomen was cut across at the level of diaphragm, and the diaphragm was snipped away from the ribs laterally following the line of rib cages. Animals were then perfused intracardially with saline (0.9% (w/v) sodium chloride) with 0.2% (v/v) heparin. The spinal cords were collected at the injury site and the segment adjacent to the injury area for 1 cm respectively and stored at -80 ºC until western blot analysis. Hearts and lungs were also collected and post-fixed in 10% (w/v) formalin for 3 days and stored in 30% (w/v) sucrose with 1% (w/v) sodium azide for the safety study (Chapter 4).

In Cohort II, at 8 hours (n = 8) after surgery, animals were euthanised as above, and perfused intracardially with 200 ml of 0.2% (v/v) heparinised saline followed by 400 ml of 4% (w/v) paraformaldehyde in 0.1 M phosphate buffer (pH 7.4). Approximately 20 mm of spinal cord centred at T10 was dissected, removed and post-fixed in 4% (w/v) paraformaldehyde overnight and then transferred to 30% (w/v) sucrose with 1% (w/v) sodium azide for cryoprotection. Hearts, lungs and lumbar spinal cords were also collected and post-fixed in 10% (w/v) formalin for 3 days and stored in 30% (w/v) sucrose with 1% (w/v) sodium azide for the safety study (Chapter 4).

2.2.10 Western blot

The following procedures were performed by a collaborator (RT) from UNSW. Spinal cord tissue from Cohort I was homogenised in 250-500 µl ice cold HEPES lysis buffer (20 mM 4-(2-hydroxyethyl)-1-piperazineethanesulfonic acid buffer, pH 7.2, containing 1 mM ethylene glycol tetraacetic acid, 210 mM mannitol, 70 mM sucrose) with 1x protease inhibitor cocktail (Roche). The samples were centrifuged for 2 minutes at 5000

rpm in a microcentrifuge at 4°C to remove cellular debris, and the supernatant was kept. To quantify protein in the sample, protein assay was performed by Bio-Rad Protein Assay Kit according to the manufacturer's instructions. Protein samples (50 μg) were electrophoresed on 6% (w/v) SDS-polyacrylamide gels, and transferred to nitrocellulose membrane. The membrane was then washed with Tris-buffered saline (TBS) and incubated with blocking solution (3% (w/v) skim milk in TBS) for 2 hours at room temperature. After blocking, the membrane was incubated with primary antibody (Rabbit anti-Connexin43, 1/8000, Sigma-Aldrich, Germany and Rabbit anti-phosphorylated Connexin43, 1/1000, Santa Cruz) at 4°C overnight, and then washed with TBS containing 0.1% (v/v) Tween-20, followed by incubation with the secondary antibody (horseradish peroxidase-conjugated goat anti-rabbit IgG, 1:2000, Thermo Fisher) for 2 hours at room temperature. Protein bands were visualised by Lumi-Light chemiluminescence substrate by exposure of the membrane to Amersham Hyperfilm. The MCID image analysis software (InterFocus Imaging, Linton, Cambridge, United Kingdom) was used to quantify the area and density of the protein bands.

2.2.11 Histology

Cryoprotected spinal cords from Cohort II were sectioned horizontally (from the dorsal to ventral side) in a cryostat (Leica CM1950) at 15 μm onto Matsunami Platinum PLC-14 and 2% (w/v) gelatine-coated glass slides, alternately. Sections were mounted in a series of ten so that each section on a slide was at 150 μm intervals. Mayer's H&E staining was performed to assess tissue morphology and to determine the lesion area. Slides were immersed through xylene and decreasingly graded ethanol to distilled water. Sections were stained in Mayer's Haematoxylin (Fronine) for 5 minutes and then blued by Scott's Blue (Fronine) for 1 minute to demonstrate the cell nuclei in blue to purple

colour. Sections were counterstained with alcoholic Eosin (Fronine) for 3 minutes to highlight the cell cytoplasm in pink to orange colour. All slides were dehydrated in increasingly graded ethanol and xylene, and mounted with DPX mountant (Sigma-Aldrich).

2.2.12 Fluorescent immunohistochemistry

All slides were rehydrated in xylene, decreasingly graded ethanol and phosphate buffered saline with Triton X-100 at pH 7.4 (PBST). The slides were incubated in 5% (v/v) normal goat serum (NGS) in PBST for 30 minutes. Primary antibodies were diluted in phosphate buffer with 5% (v/v) normal goat serum (PBG) and incubated overnight at 4 ºC. The primary antibodies used were rabbit anti-Connexin43 (1:2000, Sigma-Aldrich) to show levels of Connexin43 and rabbit anti-phosphorylated Connexin43 (1:100, Santa Cruz). This second antibody recognised Connexin43 phosphorylation on Ser368, which has been shown to change Connexin43 hemichannels from an open to a closed state (O'Carroll et al., 2013, Faigle et al., 2008, Lampe et al., 2000). Slides were then washed in PBST and incubated with correspondent secondary antibodies: goat anti-rabbit Alexa Fluor 488 for anti-Connexin43 (1:200, Thermo Fisher) and goat anti-rabbit Alexa Fluor 568 for anti-phosphorylated Connexin43 (1:200, Thermo Fisher) in PBG for 2 hours at room temperature. All slides were washed with PBST and counterstained by Hoechst (1:5000, Thermo Fisher) for 10 minutes. Primary antibodies were omitted from negative controls. All slides were cover-slipped in fluorescent mounting medium (Dako).

2.2.13 Imaging and quantification

Imaging was carried out using an Olympus BH-2 light microscope with a PixeLINK Pl-A662 camera (H&E staining) or Olympus BX-51 light microscope with an Olympus U-RFL-T fluorescence burner and appropriate filters (fluorescent immunohistochemistry staining) (Table 2.2). The black balance was adjusted at the negative control sections to normalise the mean GSV. H&E stained sections were imaged at low power at 150 μm intervals through the dorsal-ventral plane, and the injury area measured on each section using Image J software (National Institutes of Health, version 2X). The lesion size was then calculated for each spinal cord as an approximate volume, using these measurements.

Spinal cord sections were aligned using the central canal as an anatomical landmark (midline) for immunohistochemistry analysis. High power images were taken adjacent to the lesion and at both 3.5 and 7 mm distal to the lesion centre in both rostral and caudal directions. Image analysis was conducted using ImageJ software (National Institutes of Health, version 2X). Analysis of Connexin43 and phosphorylated Connexin43 was undertaken by measuring the staining intensity, mean GSV, in 10x images of the midline section.

Table 2.2 Summary of filter characteristics for fluorescent imaging.

Filter	Colour	Conjugated Fluoresce
U-MWIG3	Red	Alexa Fluor 568
U-MWIB3	Green	Alexa Fluor 488
U-MNUA2	Blue	Hoechst

2.2.14 Statistical analysis

All data were expressed as mean ± standard error of the mean (SEM). Unpaired t-test or one-way Analysis of Variance (ANOVA) with a Bonferroni *post-hoc* test was used to determine significant differences (PRISM, Version 6.0e, GraphPad). BBB scale is non-parametric, and the BBB scores at day 1 post-injury were analysed by one-way ANOVA for the simple effect to confirm the consistency of injury severity (Scheff et al., 2002). Statistically significant differences were considered at $p < 0.05$. There were no significant differences between rostral and caudal measurements in mean GSV using paired t-test, so the average value of the rostral and caudal measurements for each sample was used for further analysis.

2.3 Results

2.3.1 Degradation curves of Peptide5 *in vitro*

2.3.1.1 Mass spectrometry

Six separate trials were undertaken with slight variation to the methodology. There are significant experimental difficulties in obtaining reproducible and reliable data from the MS. A set of data in the trial run was selected to demonstrate that Peptide5 gradually degraded in normal rat serum *in vitro* (n = 1, Figure 2.2). Even though there was an erratic fluctuation in the breakdown curve, that approximately 75% and 50% of intact Peptide5 remained in rat serum at 2 and 4 hours respectively.

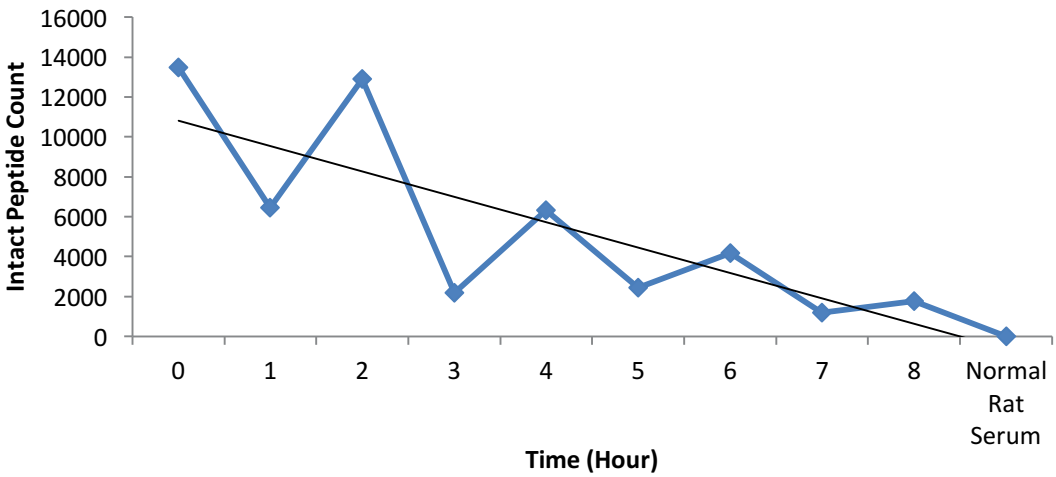

Figure 2.2 Mass spectrometry analysis of Peptide5 degradation in normal rat serum *in vitro*.
A fluctuated curve was generated by the mass spectrometer and the peptide counts were not reproducible (n = 1).

2.3.1.2 Electrophoresis

Following a series of MS-trouble shooting runs without any success, an alternative method, electrophoresis, was used to determine the peptide degradation in serum. Electrophoresis analysis demonstrated the degraded products of FITC-Peptide5 at different time points after incubating in normal rat serum (Figure 2.3A) and normal human serum (Figure 2.3B). In both sera experiments, the fluorescent intensity of top bands (~60 kDa) in all experimental samples was gradually increased over time, and represented the binding of peptide to albumin according to the molecular size. The upper bands (~6 kDa) in the positive controls were considered as FITC-Peptide5 dimer/polymer complex. The bottom bands were FITC-Peptide5 monomers (~2 kDa) and gradually decreased in fluorescent intensity over time. Mean GSVs of FITC-Peptide5 monomers were quantified to establish the degradation curves in normal rat and human sera (Figure 2.3C). In normal rat serum, the concentration of Peptide5 was decreased to 57.25 ± 2.83% at 2 hours and 28.76 ± 1.76% at 4 hours of incubation. However, Peptide5 degraded more slowly in normal human serum and its concentration was reduced to 70.10 ± 5.52% at 2 hours and 55.49 ± 6.97% at 4 hours of incubation. Therefore, the dosing regimen for the systemic administration of Peptide5 was determined as the initial dose (10 mg/kg in 0.5 ml saline, i.p.) immediately following surgery, the second dose (5 mg/kg in 0.5 ml saline, i.p.) at 2 hours after surgery and the third dose (2.5 mg/kg in 0.5 ml saline, i.p.) at 4 hours post-surgery.

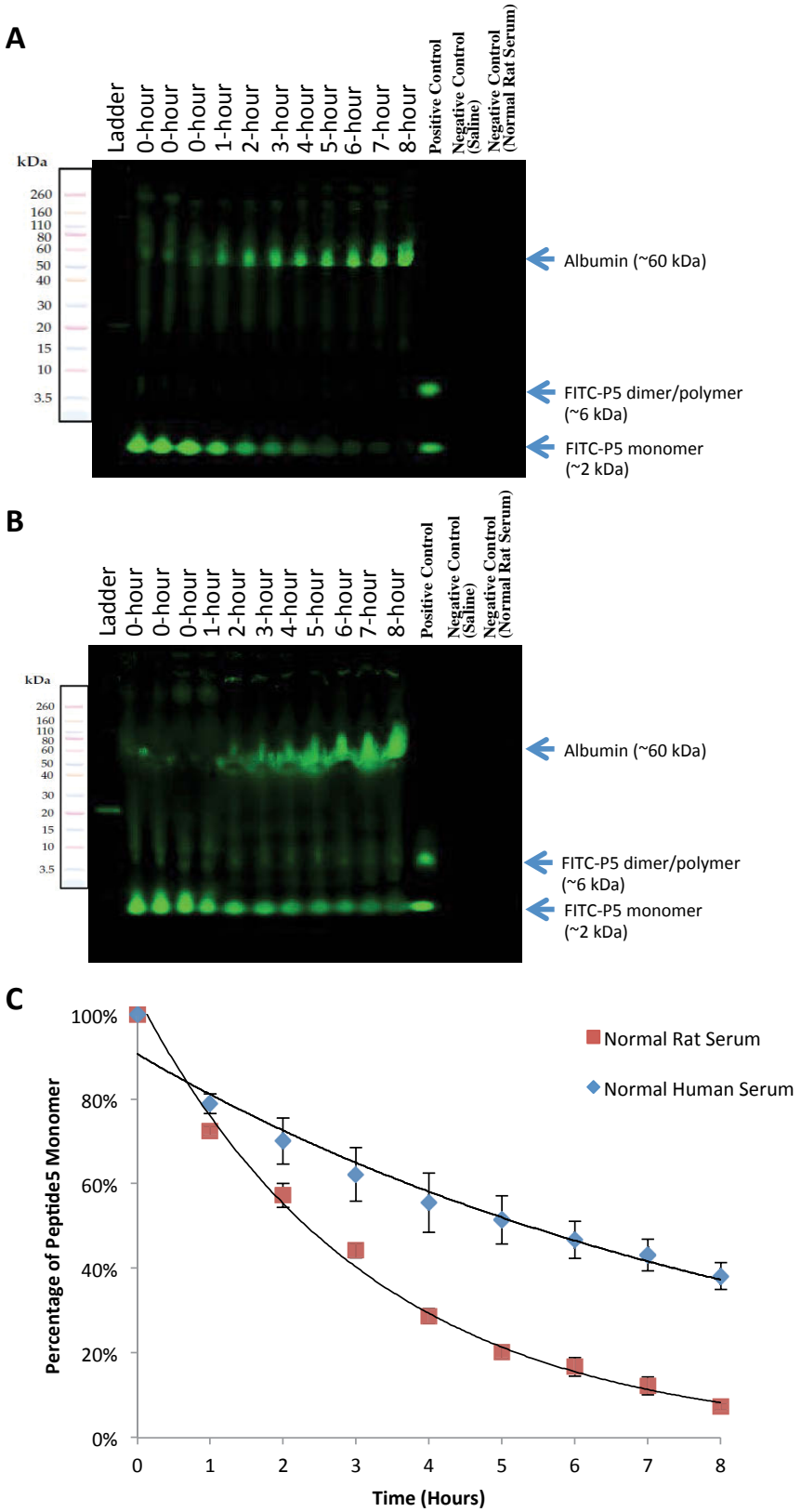

Figure 2.3 Electrophoresis analysis of Peptide5 degradation in normal rat and human sera *in vitro*.

(A) Peptide5 degraded in normal rat serum at different time points. (B) Peptide5 degraded in normal human serum at different time points. (C) Degradation curves of Peptide5 in normal rat and human sera in vitro. (FITC: fluorescein isothiocyanate; P5: Peptide5)

2.3.2 Consistent spinal cord injury in rats

All surgical procedures and intraperitoneal injections were conducted without incident or post-operative complications. None of the rats undergoing sham surgeries showed any indications of SCI. The contusion injury was produced consistently in all SCI groups in both animal models. In Cohort I (24-hour survival), the impactor parameters for the SCI rats in all Peptide5 treatment groups were not significantly different (Figure 2.4). The mean values of weight-drop velocity, compression and compression rate for all SCI groups were 0.341 ± 0.018 m/s, 1.445 ± 0.177 mm and 0.297 ± 0.023 m/s, respectively. There were no statistically significant differences in BBB scores at Day 1 post-injury between all injury groups (Figure 2.5). At Day 1 following surgery, the SCI rats showed immediate loss of locomotor function at a mean BBB score of 2.83 ± 0.29, compared with 21.00 ± 0.00 in the sham animals (one-way ANOVA, $p < 0.001$; Bonferroni *post-hoc* comparisons, ***$p < 0.001$). The impactor parameters for the SCI rats were not significantly different between groups in Cohort II (8-hour survival) (Figure 2.6). The mean values of weight-drop velocity, compression and compression rate were 0.357 ± 0.029 m/s, 1.472 ± 0.260 mm and 0.313 ± 0.029 m/s, respectively.

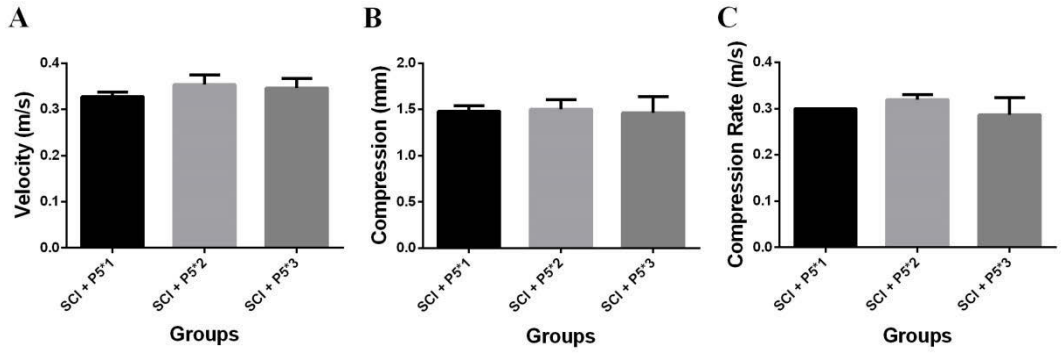

Figure 2.4 Surgical parameters for Cohort I showing the means of (A) weight-drop velocity in m/s, (B) compression in mm and (C) compression rate in m/s with standard error of the mean.
No surgical data obtained from the sham group. There were no statistically significant differences in surgical parameters between the three injury groups (one-way ANOVA, velocity $p > 0.05$; compression $p > 0.05$; compression rate $p > 0.05$). (P5*1: one injection of Peptide5; P5*2: two injections of Peptide5; P5*3: three injections of Peptide5; SCI: spinal cord injury)

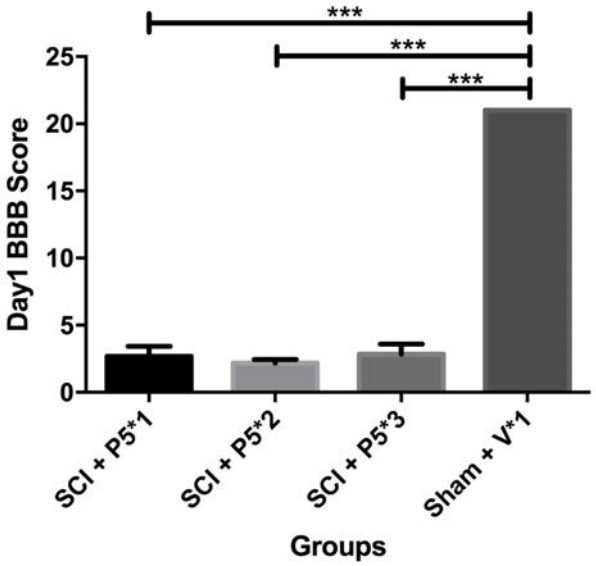

Figure 2.5 Behavioural assessment of hind limb locomotor function for Cohort I.
The Basso-Beattie-Bresnahan (BBB) scores for injury groups were significantly lower than that for sham group (one-way ANOVA, $p < 0.001$; Bonferroni *post-hoc* comparisons, ***$p < 0.001$). There were no statistically significant differences in Day 1 BBB scores between the injury groups (Bonferroni *post-hoc* comparisons, $p > 0.05$). (P5*1: one injection of Peptide5; P5*2: two injections of Peptide5; P5*3: three injections of Peptide5; SCI: spinal cord injury; V*1: one injection of saline vehicle)

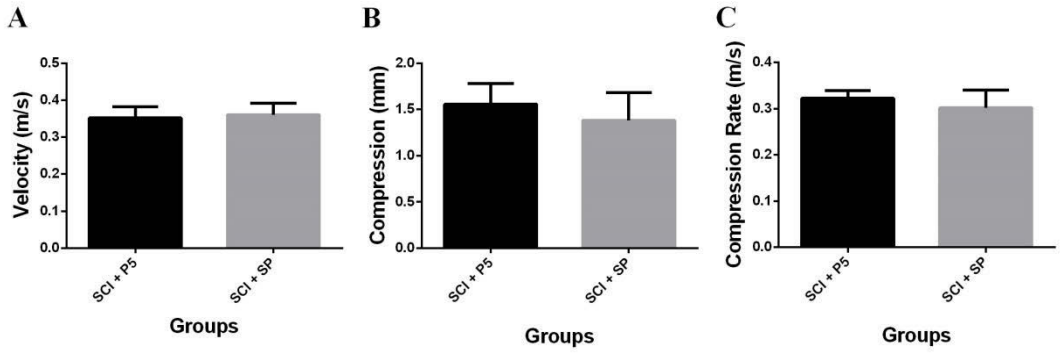

Figure 2.6 Surgical parameters for Cohort II showing the means of (A) weight-drop velocity in m/s, (B) compression in mm and (C) compression rate in m/s with standard error of the mean.
There were no statistically significant differences in surgical parameters between the three injury groups (t-test, velocity $p > 0.05$; compression $p > 0.05$; compression rate $p > 0.05$). (P5: Peptide5; SCI: spinal cord injury; SP: control scrambled peptide)

2.3.3 Dosing responses of Peptide5

In Cohort I, western blot analysis showed the Connexin43 total protein levels at 24 hours following SCI (Figure 2.7A). Connexin43 total protein levels were significantly elevated in the SCI animals receiving one (1.9 fold) or two (1.6 fold) doses of Peptide5 compared with that in the sham rats (one-way ANOVA, $p < 0.05$, Bonferroni *post-hoc* comparisons: one injection $p < 0.01$; two injections $p < 0.05$) (Figure 2.7B). The SCI animals that received three doses of Peptide5 demonstrated a total protein level of Connexin43 close to that in the sham animals. Western blot analysis showed the phosphorylated Connexin43 protein levels at 24 hours following SCI (Figure 2.7C). The differences in phosphorylated Connexin43 protein level between groups were not statistically significant (one-way ANOVA, $p > 0.05$) (Figure 2.7D). The phosphorylated Connexin43 total protein levels seemed to be reduced in the SCI animals receiving one (0.6 fold) or two (0.6 fold) doses of Peptride5 compared with that in the sham rats.

Three injections of Peptide5 appeared to be the most effective dosing regimen to maintain the level of Connexin43 phosphorylation on Ser368 following SCI.

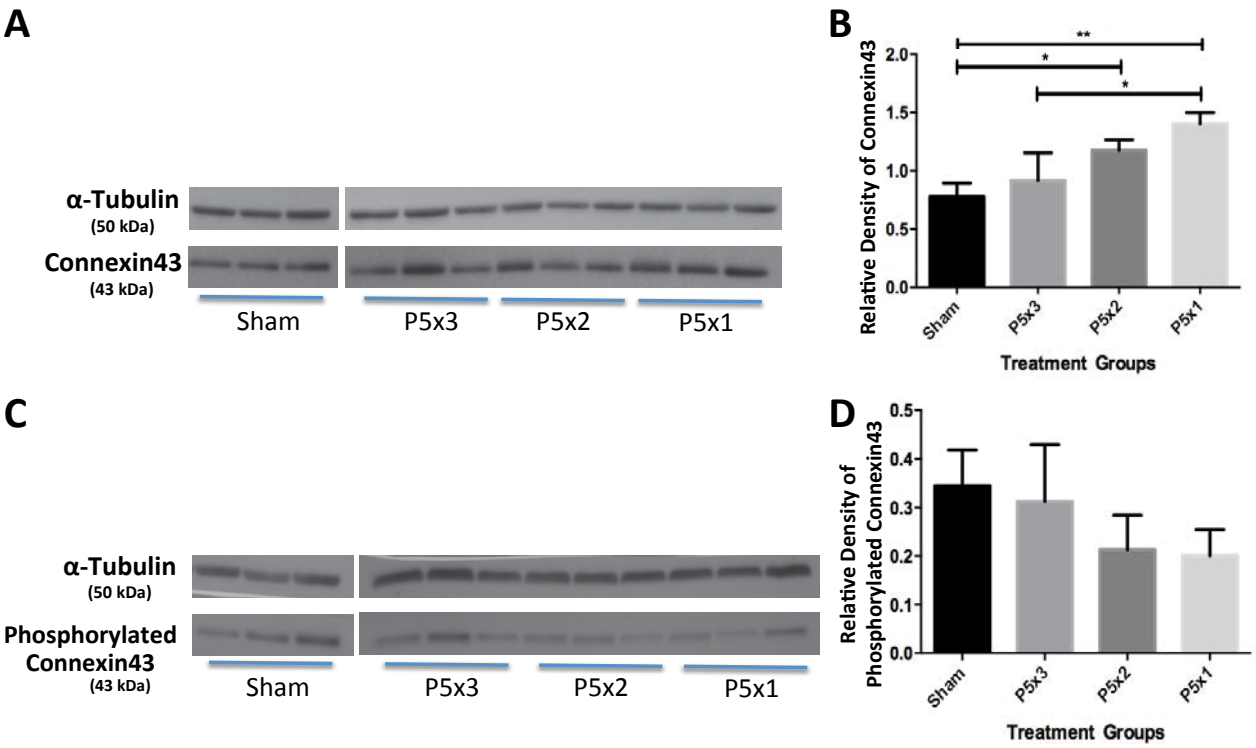

Figure 2.7 Western blot analysis of Connexin43 and phosphorylated Connexin43 protein levels at the injury site 24 hours following surgery.
(A) Western blot analysis showed changes in total Connexin43 protein levels between treatment groups. (B) Treatment with three injections of Peptide5 limited the increase in total Connexin43 protein levels most effectively (one-way ANOVA, $p < 0.05$; Bonferroni *post-hoc* comparisons, *$p < 0.05$, **$p < 0.01$). (C) Western blot analysis showed changes in Connexin43 phosphorylation at residue Ser368. (D) There were no statistically significant differences in phosphorylated Connexin43 protein levels between groups (one-way ANOVA, $p > 0.05$). Treatment with three injections of Peptide5 appeared to maintain the highest level of phosphorylated Connexin43 protein. (P5x1: spinal cord injury with one injection of Peptide5; P5x2: spinal cord injury with two injections of Peptide5; P5x3: spinal cord injury with three injections of Peptide5; Sham: Sham surgery with one injection of saline vehicle)

2.3.4 Systemic delivery of Peptide5 to the lesion

In Cohort II, the contusion injury was observed as haemorrhage, axonal swellings, cells with no nuclei or pyknotic nuclei or areas of cellular debris in the H&E stained longitudinal sections (Figure 2.8 A and B). The lesion volume was significantly smaller in the Peptide5 treated animals (6.28 ± 2.51 mm3) in comparison with the control SP group (9.64 ± 0.66 mm3) at 8 hours after SCI ($p < 0.05$, Figure 2.8 C).

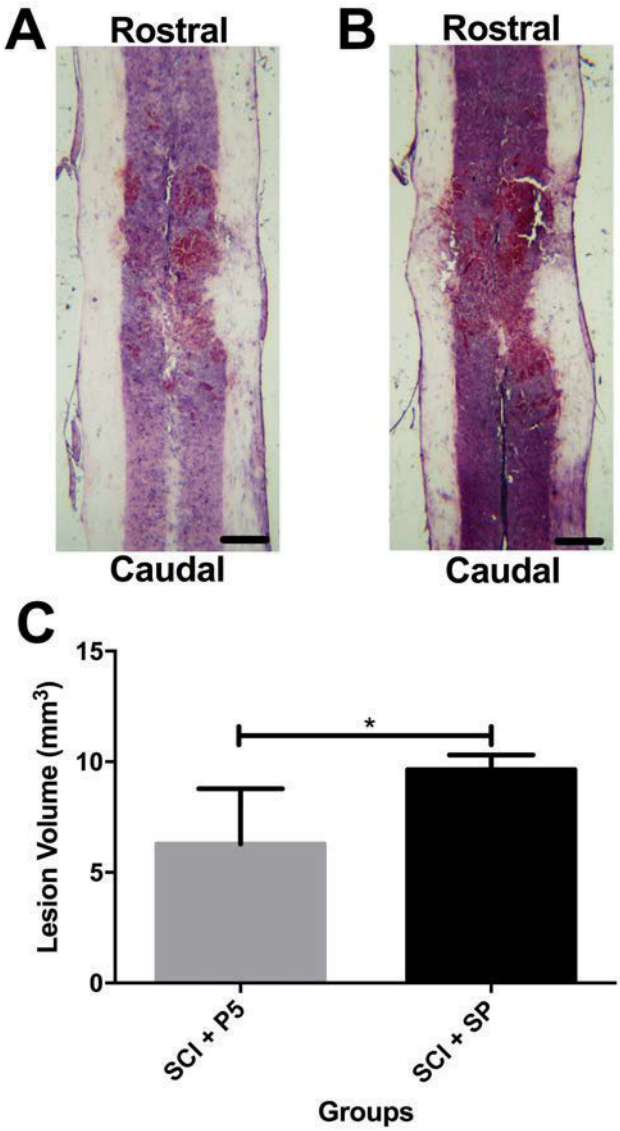

Figure 2.8 Changes in lesion size at 8 hours following spinal cord contusion injury. Mayer's Haematoxylin and Eosin staining showed the lesion area at the midline level of spinal cord in Peptide5 (A) and control scrambled peptide (B) treated animals. Scale bars = 1 mm. (C) Peptide5 reduced the lesion spread at 8 hours post-injury (t-test, *$p < 0.05$). (P5: Peptide5; SCI: spinal cord injury; SP: control scrambled peptide)

In Cohort II, analysis of Connexin43 and phosphorylated Connexin43 (closed hemichannels) protein levels was undertaken at 8 hours post injury using fluorescent immunohistochemistry on midline sections. Connexin43 protein levels, as measured by mean GSV of immunohistochemistry labelling intensity, were lower at the epicentre of the lesion in the Peptide5 treated animals compared with the control scrambled peptide group in both grey (49.51 ± 13.36 vs. 63.35 ± 5.38, $p < 0.01$) and white matter (28.41 ± 10.86 vs. 46.91 ± 5.13, $p < 0.001$) (Figure 2.9). The immunohistochemistry labelling intensity of Connexin43 protein levels was down-regulated by the Peptide5 treatment compared with the control SP group at 3.5 mm (grey matter, 39.74 ± 2.71 vs. 81.16 ± 4.07, $p < 0.001$; white matter, 22.87 ±0.60 vs. 48.77 ± 5.00, $p < 0.001$) and 7 mm (grey matter, 38.15 ± 1.35 vs. 76.29 ± 1.21, $p < 0.001$; white matter, 23.58 ± 1.19 vs. 47.66 ± 1.71, $p < 0.001$) distal to the lesion. In contrast, there was an increase in the level of Connexin43 phosphorylation at 8 hours following injury in the Peptide5 treated animals compared to the animals receiving control scrambled peptide treatment with an increase in overall labelling intensity at the epicentre of the lesion from 30.93 ± 3.41 to 48.61 ± 5.06 in grey matter ($p < 0.001$) and from 15.75 ± 2.56 to 24.90 ± 3.92 in white matter ($p < 0.001$) (Figure 2.10). The increased immunohistochemistry labelling intensity of phosphorylated Connexin43 protein levels was also observed at 3.5 mm (grey matter, 49.82 ± 1.58 vs. 29.60 ± 1.39, $p < 0.001$; white matter, 28.16 ± 1.50 vs. 14.95 ± 1.25, $p < 0.001$) and 7 mm (grey matter, 46.56 ± 0.66 vs. 31.53 ± 2.82, $p < 0.001$; white matter 25.52 ± 1.67 vs. 14.99 ± 0.16, $p < 0.001$) distal to the lesion.

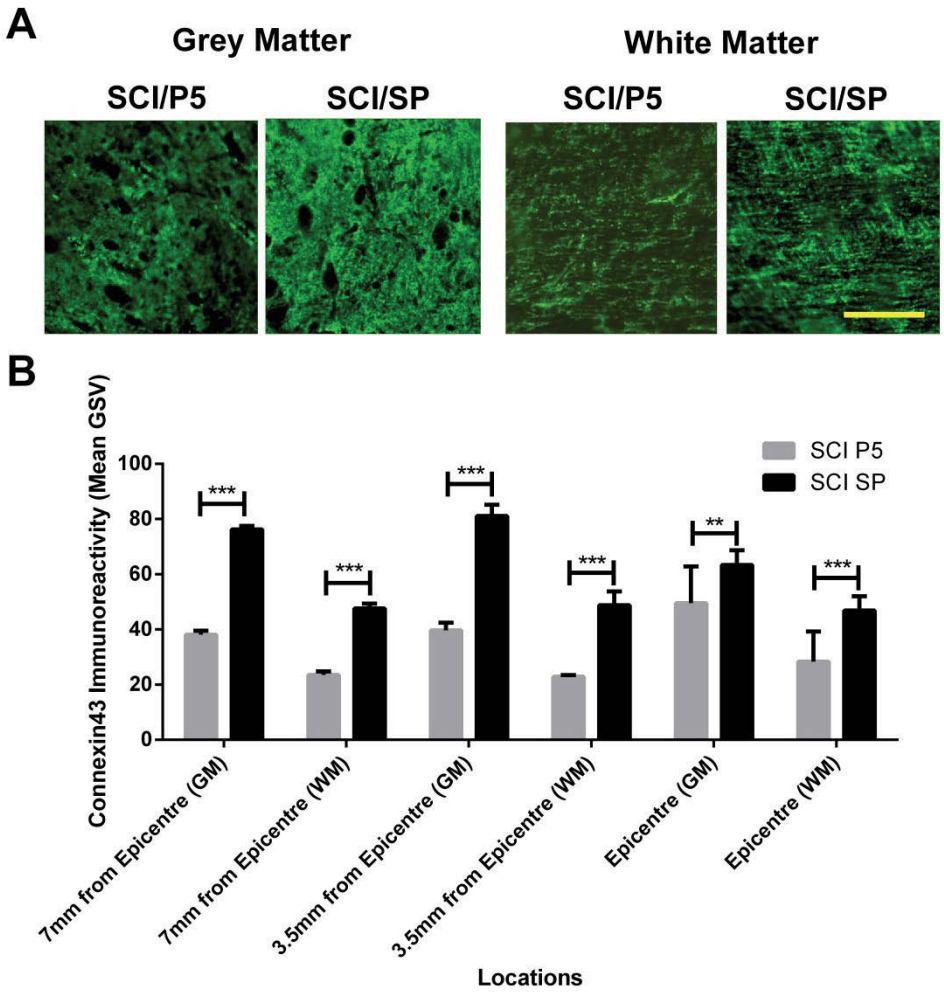

Figure 2.9 Immunohistochemistry staining of Connexin43 at 8 hours following spinal cord injury.

(A) Representative images of fluorescent immunohistochemistry staining showed the changes in Connexin43 (green) level at the epicentre of the lesion in both grey and white matter. Scale bar = 50 μm. (B) Systemic administration of Peptide5 limited the increase in post-injury Connexin43 protein level (t-test, **p < 0.01, ***p < 0.001). (GM: grey matter; GSV: greyscale value; P5: Peptide5; SCI: spinal cord injury; SP: control scrambled peptide; WM: white matter)

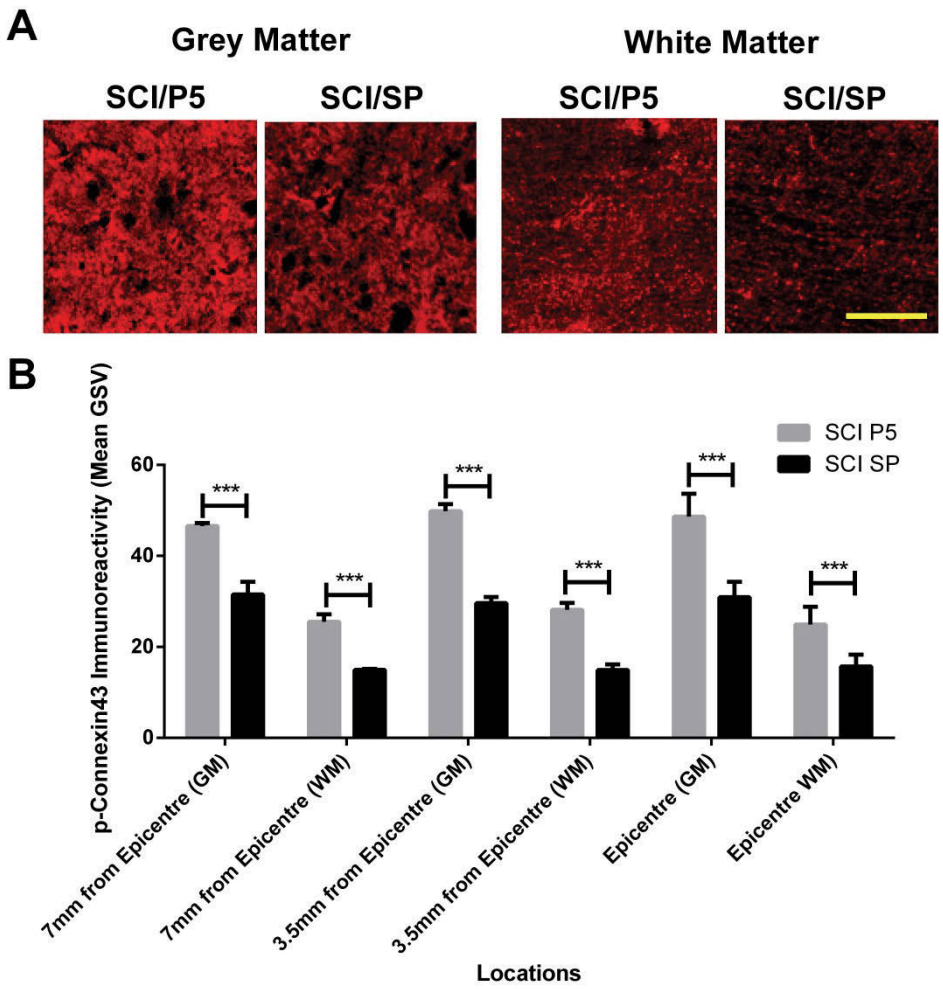

Figure 2.10 Immunohistochemistry staining of phosphorylated Connexin43 at 8 hours following spinal cord injury.

(A) Representative images of fluorescent immunohistochemistry staining showed the changes in phosphorylated Connexin43 (red) level at the epicentre of the lesion in both grey and white matter. Scale bar = 50 μm. (B) Systemic administration of Peptide5 significantly increased phosphorylation of Connexin43 at residue Ser368 (t-test, ***$p < 0.001$). (GM: grey matter; GSV: greyscale value; P5: Peptide5; p-Connexin43: phosphorylated Connexin43; SCI: spinal cord injury; SP: control scrambled peptide; WM: white matter)

2.4 Discussion

To determine the dosing regimen of peptide5 systemic administration, MS was used to identify and quantify the intact Peptide5 incubated in normal rat serum *in vitro*. However, the mass spectrometer was not able to generate reproducible results due to technical difficulties. The same experiment was carried out in another laboratory by the collaborators at the University of Auckland without success. As Peptide5 contains two basic residues (arginine and lysine), different molecules of the peptide manifest either two or three positive charges (Cagney and Emili, 2002, Molina et al., 2007). Combining the intact peptide counts for both charged states, the total quantity of complete Peptide5 fluctuated and was inconclusive (Figure 2.2). Considering the current peptide sequencing algorithms, there are mostly one or two charged ions taken to generate existing models; however, the higher-charge (three or more) spectra have been rarely explored (Marx et al., 2013, Hoopmann and Moritz, 2013, Zhang et al., 2014). The higher-charge spectra were suggested to contribute significantly to prediction of the complete peptide (Chong et al., 2006, Kim et al., 2009, Ning et al., 2007). Therefore, the existing algorithms did not perform well on multi-charge spectra to evaluate and interpret the signal for intact Peptide5 (two or three charged ions). Further investigation should be conducted to model and characterise multi-charge mass spectra using de novo sequencing algorithms, such as greedy best strong tag.

As an alternative pathway, electrophoresis was employed to analyse Peptide5 degradation in normal sera. The fluorescence and molecular size were used to identify and quantify the intact Peptide5 in serum as per protocols described in the literature (Hong and Clayman, 2000, Kosuge et al., 2008, Cleveland et al., 1977, Fling and Gregerson, 1986, Farley et al., 1984, Weidekamm et al., 1973). For the quantification of more than 100 pg mass, the one-dimensional gel electrophoresis did not demonstrate

significant disadvantages in the accuracy of results compared with matrix-assisted lase desorption/ionisation-MS (Mackintosh et al., 2003).

In both rat and human serum samples, the fluorescent bands at 2 kDa in all experimental samples and the positive controls represented Peptide5 monomers (2 kDa). Peptide5 monomers were considered to be biologically active to modulate Connexin43 hemichannels in the injury site (detailed mechanism described in Section 3.4), and thus used for quantification. In saline (positive control), Peptide5 contained a cysteine that bound to another one via disulphide bonds to form a dimer/polymer complex shown at approximately 6 kDa (Muskal et al., 1990). In the presence of disulphide bond oxidoreductases in serum, such as protein disulphide isomerase, thioredoxin and glutaredoxin-1, the Peptide5 dimer/polymer complex became monomers immediately via allosteric cleavage of disulphide bonds (Wiita et al., 2006, Chen et al., 2006, Cook and Hogg, 2013). In the meantime, allosteric disulphide bonds started forming between the cysteine in Peptide5 and albumin in serum (Farrah et al., 2011, Kozlov et al., 2010, Holmgren et al., 2005), as shown in the increased fluorescence of 60 kDa bands over time. The albumin bound peptides in complete and/or fragmentary forms would not be biologically potent in regulating Connexin43 hemichannels because of the altered conformation (Dennis et al., 2002, Rowland and Tozer, 2005), even though its clearance half-life from the renal system was improved (Dennis et al., 2002, Kratz, 2008, Witt et al., 2001). In accordance with the absence of bands less than 2 kDa, it was less likely that the FITC tags disassociated from Peptide5, as a β-alanine was inserted between FITC and Peptide5 to increase the stability from hydrolysis (Kamiya et al., 2009, Soudy et al., 2011).

A limitation of electrophoresis was that the intact Peptide5 and its fragments might not be sufficiently separated because of the small molecular size of Peptide5. However, it

was less likely that the 2 kDa bands contained both intact Peptide5 and fragmented Peptide5 with FITC in the current experiments, since a blurry shallow smear was absent at the bottom of 2 kDa bands. A series of truncated Peptide5 conjugated with FITC combinations resolved in the gel would be necessary to confirm this in the near future.

According to the percentage of intact Peptide5 monomer in normal rat serum, the second dose (maintenance) was determined as half of the initial dose to maintain the optimal concentration of intact Peptide5 *in vivo* (10 mg/kg). The third dose (maintenance) was decided to be one fourth of the initial dose to avoid overdosing. As suggested in previous studies, Connexin43 mimetic peptides have been shown to modulate both Connexin43 hemichannels and gap junctions independently of each other (O'Carroll et al., 2008, Leybaert et al., 2003, Yoon et al., 2010). It was suggested that low concentrations of Peptide5 regulating the hemichannel opening, but not the gap junctional communication, were neuroprotective, while high concentrations interfering with gap junctional communication as well as spatial buffering activity of astrocytes were not beneficial (O'Carroll et al., 2008). In the current study, the dosing regimen was proposed to regulate Connexin43 hemichannels without affecting gap junction communication, to limit the secondary injury in rat spinal cords. As more intact Peptide5 is available in human serum than in rat serum at all time points, the maintenance doses for human studies might be different in percentage concentrations and/or timing. This experiment not only established the dosing regimen of Peptide5 systemic administration for SCI models in rats, but provided the first important step in a transition from rodent models to clinical trials.

An animal experiment (Cohort I) was undertaken to determine whether one, two or three doses of Peptide5 injections were most effective in regulating Connexin43 hemichannels *in vivo*. The contusion model produced in the current study was consistent

with the expected pattern of injury as described in previous studies in this laboratory (O'Carroll et al., 2013, Mao et al., 2016) and several other groups (Horky et al., 2006, Mothe and Tator, 2005, Basso et al., 1996). To reduce the usage of experimental animals, sham animals receiving saline vehicle injections were used as a negative control, while positive control was not included, as the increased level of total Connexin43 protein and the decrease level of phosphorylated Connexin43 at residue Ser368 have been well documented following SCI (O'Carroll et al., 2013, O'Carroll et al., 2008, Lee et al., 2005, Cronin et al., 2008, Theriault et al., 1997). Connexin43 phosphorylation on Ser368 has been shown to change Connexin43 hemichannels from an open to a closed state (O'Carroll et al., 2013, Faigle et al., 2008, Lampe et al., 2000). Three doses of Peptide5 demonstrated the most efficacy in reducing the level of total Connexin43 protein and limiting the opening of Connexin 43 hemichannels and so were used for the subsequent studies, unless otherwise indicated.

Peptide5 via systemic administration (intraperitoneal injection) was able to reach the lesion area and regulate the Connexin43 hemichannels in the spinal cord. The increase in Connexin43 protein level after injury was suppressed with administration of Peptide5, and the phosphorylated Connexin43 protein level (closed hemichannels) was higher in the spinal cords at 8 hours following Peptide5 administration. Substantial evidence indicates an increase in Connexin43 protein following brain ischaemia (Budd and Lipton, 1998, Contreras et al., 2004, Haupt et al., 2007, Davidson et al., 2013b, Frantseva et al., 2002b) and SCI (O'Carroll et al., 2013, O'Carroll et al., 2008, Lee et al., 2005, Cronin et al., 2008, Theriault et al., 1997). Down regulation of Connexin43 or blocking gap junction channels using gap junction blockers has been shown to be beneficial (Cronin et al., 2008, Roh et al., 2010, Frantseva et al., 2002a, Frantseva et al., 2002b). Other studies using gene knockout models have conversely demonstrated an

increase in lesion size, resulting from complete loss of Connexin43 stopping normal gap junctional communication necessary for spatial buffering and neuronal survival at the later stages of recovery (Nakase et al., 2004, Takahashi et al., 2010, Siushansian et al., 2001). In the current study, Peptide5 was used at a concentration known to close Connexin43 hemichannels rather than affect intact gap junctions (O'Carroll et al., 2008). O'Carroll et al. (2008) demonstrated that the concentration of Peptide5 below 100 μM was specifically able to regulate Connexin43 hemichannel communication *in vitro* and reduce Connexin43 expression in *ex vivo* spinal cord segments. Consequently, the lesion size was limited at a very early time point after SCI.

Chapter 3

Investigation of Cellular and Functional Improvement in Spinal Cord Injury Rats from the Peptide5 Systemic Administration

3.1 Introduction

Using an intrathecal catheter and an osmotic pump to deliver Peptide5 directly to the lesion area of the spinal cord in a rat contusion model, the previous study demonstrated the neuroprotective efficacy of Peptide5 (O'Carroll et al., 2013). However, local administration is not always a practical option for human spinal patients as the intrathecal delivery of Peptide5 necessitates an additional invasive procedure immediately after a traumatic event, which in reality might delay the application of Peptide5 within the limited window of opportunity for regulating the pathological Connexin43 hemichannels. Systemic administration is able to deliver proteins and mimetic peptides to the lesion area of the spinal cord (Han et al., 2010). An early study also reported that selective inhibition of unopposed Connexin43 hemichannels by two other Connexin43 mimetic peptides (Gap26 and 27) delivered intravenously protected ischaemic hearts against myocardial infarction in rats (Hawat et al., 2012).

It is feasible for Peptide5 to be delivered to the injury sites systemically where the capillary bed has been compromised in the injured spinal cord, thus offering a practical therapeutic approach for people with SCI. The previous chapter has shown that Peptide5, via systemic administration, is able to regulate the Connexin43 hemichannels at the lesion area of the spinal cord in a rat contusion model and has optimised dosing regimen for use in SCI rats. By using this optimal dosing regimen of Peptide5, the current chapter has focused the investigation on determining whether systemic delivery of Peptide5, rather than local delivery, influences Connexin43 expression and recovery following SCI by:

1) comparing the lesion size on the H&E stained sections, and the levels of Connexin43 protein and Connexin43 phosphorylation at residue Ser368, using fluorescent immunohistochemistry;

2) assessing the cellular improvements, including astrogliosis, macrophage/microglial activation and neuronal survival by using fluorescent immunohistochemistry;
3) determining behavioural improvements, including motor (open field and error ladder tests) and sensory (mechanical pain hypersensitivity) functions.

The current chapter is published (Mao et al., 2017).

3.2 Materials and methods

3.2.1 Animals and general care

All experimental protocols and procedures used in the study were approved by the ACEC of UTS (UTS ACEC 2013-742), in accordance with the guidelines of the National Health and Medical Research Council of Australia. Cohort III consisting of 96 female Sprague Dawley rats (7 weeks old, 140-180 g, Animal Resources Centre, Perth) was used to investigate cellular and functional improvement. All animals were maintained in standard cages with ad-lib water and food on a 12:12 hour light-dark cycle, and housed in the Ernst Facility, Faculty of Science, UTS. Daily checks of room temperature, humidity and animal wellbeing were performed. Each animal's weight was checked at least twice a week. All animals were acclimatised in the Ernst Facility for 1 week and in the behavioural apparatus prior to any surgical procedures. SCI or sham operated animals received the optimal dose and injection regimen as determined in Chapter 2 of Peptide5 or SP control treatment, and recovered for 24 hours (n = 32), 2 weeks (n = 32) or 6 weeks (n = 32).

3.2.2 Surgical procedures

The animals in injury groups were subject to a T10 laminectomy and a mild contusion SCI, while the sham animals received T10 laminectomy surgery, as previously described (Section 2.2.5).

3.2.3 Peptide treatment

Peptide5 (sequence VDCFLSRPTEKT) and SP (RFKPSLCTTDEV) were synthesised in solid phase by Mimotopes Pty Ltd., Australia, using Fmoc chemistries on a Protein Technology Symphony instrument, purified by high-performance liquid chromatography and the structure confirmed by MS analysis. The first dose (10 mg/kg in 0.5 ml saline, i.p.) was administered immediately following surgery, while the second (5 mg/kg in 0.5 ml saline, i.p.) and the third (2.5 mg/kg in 0.5 ml saline, i.p.) doses were delivered at 2 and 4 hours after surgery, respectively.

3.2.4 Post-operative care

Animals were housed individually after surgery for 1 week. They were kept in a holding room with a controlled temperature (22-25 ºC), humidity and light cycle (12 hr on/12 hr off) and had access to food and water *ad libitum*. Post-operatively, animals were given antibiotics (cephalothin sodium, 0.33 mg/kg, s.c.), analgesic (buprenorphine hydrochloride, 0.03 mg/kg, s.c.) and supplementary fluid (Hartman's replacement solution, 3.8 ml, s.c.) twice daily for 3 days. Bladders were voided manually twice daily until the return of spontaneous urination.

3.2.5 Behavioural assessments

3.2.5.1 Locomotor function

Following the surgical procedures, each animal was assessed for functional recovery using an open field and a horizontal ladder testing paradigm. Animals were tested at Days 1, 3, 7, 14, 21, 28, 35 and 42 of the post-operative recovery period. For the open-field test, rats were gently handled and adapted to a molded-plastic circular enclosure

with a smooth, non-slip floor (90 cm diameter; 20 cm wall height). They were allowed to continuously walk in the open field for 3 minutes. For the horizontal ladder test, rats were placed into a horizontal ladder rung walking test apparatus consisted of clear plastic side-walls and metal rungs (3 mm diameter) which were randomly inserted with a minimum distance of 1 cm. They were encouraged to walk back and forth three times in the apparatus. Hind limb locomotor function was assessed using the BBB locomotor rating scale (Table 2.1) for the open-field test (Basso et al., 1996) and by calculating the percentage of foot fault error regardless of the type foot misplacement for the horizontal ladder test (Metz and Whishaw, 2002). All tests were digitally recorded and assessments were conducted by a research assistant (TN) and myself who were blinded to the groups. The scores from the two reviewers had a high correlation ($R^2 = 0.879$) without statistically significant differences (unpaired t-test, $p > 0.05$), so the average scores were used for all further analysis.

3.2.5.2 Pain hypersensitivity

The following procedures were performed by a collaborator (RT) from UNSW. Mechanical pain hypersensitivity tests were conducted a week prior to the surgical injury to determine the baseline level, and then once weekly following surgery, for up to 6 weeks. The rats were placed on an elevated wire mesh platform in individual Perspex cubicles, and were allowed to acclimatise to the mechanical pain hypersensitivity testing apparatus for 40 minutes in a quiet, temperature-controlled room. Mechanical hypersensitivity was measured at-level (injury site) and below-level (hind paws) using a series of calibrated von Frey filaments with incremental stiffness, ranging from 0.02g to 60g. The von Frey filaments were applied serially according to the up-down method, and the 50% withdrawal threshold was calculated, as previously described (Chaplan et

al., 1994). At-level mechanical pain hypersensitivity was tested via application of the von Frey filaments, three times on both the medial and lateral side, approximately 3 cm away from the injury site. Below-level mechanical pain hypersensitivity was tested via application of the von Frey filaments to the plantar surface of both hind paws. Positive pain responses included licking, flinching, vocalisation, and lifting of the leg in the case of below-level mechanical pain hypersensitivity. Responses that occurred independent of the filament were not recorded.

3.2.6 Euthanasia and histology

At 24 hours (n = 32), 2 weeks (n = 32) and 6 weeks (n =32) after surgery, animals were euthanised with Lethobarb (pentobarbitone sodium, 1 ml/kg, i.p.). The abdomen was cut across at the level of the diaphragm, and the diaphragm was snipped away from the ribs, laterally following the line of rib cages. Using a heparin-rinsed syringe, cardiopuncture was then performed to collect 5 ml of blood, and the plasma was extracted by centrifuging the fresh blood at 13k rpm for 5 minutes. Animals were perfused intracardially with 200 ml of 0.2% (v/v) heparinised saline followed by 400 ml of 4% (w/v) paraformaldehyde in 0.1 M phosphate buffer (pH 7.4). Approximately 20 mm of spinal cord centred at T10 was dissected, removed and post-fixed in 4% (w/v) paraformaldehyde overnight and then transferred to 30% (w/v) sucrose with 1% (w/v) sodium azide for cryoprotection. Hearts and lungs were also collected and post-fixed in 10% (w/v) formalin for the safety study (Chapter 4).

Spinal cords were sectioned horizontally (from the dorsal to ventral side) in a cryostat (Leica CM1950) at 15 μm onto Matsunami Platinum PLC-14 and 2% (w/v) gelatine-coated glass slides alternately. Sections were mounted in a series of ten so that each

section on a slide was at 150 μm intervals. Mayer's Haematoxylin and Eosin (H&E) staining was performed to assess tissue morphology and determine the lesion area. Slides were immersed through xylene and decreasingly graded ethanol to distilled water. Sections were stained in Mayer's Haematoxylin (Fronine) for 5 minutes and then blued by Scott's Blue (Fronine) for 1 minute to demonstrate the cell nuclei in blue to purple colour. Sections were counterstained with alcoholic Eosin (Fronine) for 3 minutes to highlight the cell cytoplasm in pink to orange colour. All slides were dehydrated in increasingly graded ethanol and xylene, and mounted with DPX mountant (Sigma-Aldrich).

3.2.7 Fluorescent immunohistochemistry

All slides were rehydrated in xylene, decreasingly graded ethanol and phosphate buffered saline with Triton X-100 at pH 7.4 (PBST). Heat-induced antigen retrieval was conducted in citrate buffer (10 mM citric acid, pH 6.0) for 10 minutes in a pressure cooker for neuronal nuclei (NeuN) staining. The slides were incubated in 5% (v/v) NGS in PBST for 30 minutes. Primary antibodies were diluted in PBG and incubated overnight at 4 ºC (Table 3.1). For the early time points (24 hours), primary antibodies used were rabbit anti-Connexin43 (1:2000, Sigma-Aldrich) to show levels of Connexin43 and rabbit anti-phosphorylated Connexin43 (1:100, Santa Cruz). This second antibody recognised Connexin43 phosphorylation on Ser368 which has been shown to change Connexin43 hemichannels from an open to a closed state (O'Carroll et al., 2013, Faigle et al., 2008, Lampe et al., 2000). For the late time points (2 and 6 weeks), primary antibodies used were rabbit anti-GFAP (1:1000, Dako) to label astrocytes, mouse anti-NeuN (1:1000, Millipore) to label neurons, and a double labelling of mouse anti-CD68 (ED1) (1:2000, AbD Serotec) and rabbit anti-ionised calcium-binding adapter molecule 1 (Iba1) (1:1000, Abcam) to demonstrate activated

macrophages/microglia. The neural cell markers: GFAP for astrocytes, NeuN for neurons and Iba1/ED1 for activated microglia and/or macrophages, were not used at the early time point (24 hours), as the current study focuses on the improvement on these neural cell responses at the secondary phase of SCI (2 and 6 weeks). Slides were then washed in PBST and incubated with secondary antibodies (Table 3.1): goat anti-rabbit Alexa Fluor 488 (1:200, Thermo Fisher), goat anti-rabbit Alexa Fluor 568 (1:200, Thermo Fisher), goat anti-mouse Alexa Fluor 488 (1:200, Thermo Fisher) or goat anti-mouse Alexa Fluor 568 (1:200, Thermo Fisher) in PBG for 2 hours at room temperature. All slides were washed with PBST and counterstained by Hoechst (1:5000, Thermo Fisher) for 10 minutes. The primary antibodies were omitted from negative controls. All slides were cover-slipped in fluorescent mounting medium (Dako).

Table 3.1 Summary of antibody characteristics for immunohistochemistry.

Primary Antibody	Dilution	Source	Secondary Antibody	Dilution
Rabbit anti-Connexin43	1:2000	Sigma-Aldrich	AF488 anti-rabbit	1:200
Rabbit anti-p-Connexin43	1:100	Santa Cruz	AF568 anti-rabbit	1:200
Rabbit anti-GFAP	1:1000	Dako	AF488 anti-rabbit	1:200
Mouse anti-NeuN	1:1000	Millipore	AF488 anti-mouse	1:200
Mouse anti-ED1	1:2000	AbD Serotec	AF568 anti-mouse	1:200
Rabbit anti-Iba1	1:1000	Abcam	AF488 anti-rabbit	1:200

AF: Alexa Fluor; GFAP: Glial fibrillary acidic protein;
Iba1: Ionised calcium-binding adapter molecule 1; NeuN: Neuronal nuclei;
p-Connexin43: Phosphorylated Connexin43

3.2.8 Imaging and quantification

Imaging was conducted using an Olympus BH-2 light microscope with a PixeLINK Pl-A662 camera (H&E staining) or Olympus BX-51 light microscope with an Olympus U-RFL-T fluorescence burner and appropriate filters (immunohistochemistry staining) used previously (Table 2.2). The black balance was adjusted at the negative control sections to normalise the mean GSV. Injury on the H&E stained sections was observed as haemorrhage, axonal swellings, cells with no nuclei or pyknotic nuclei, areas of cellular debris or cavity formation. Sections were imaged at 150 μm intervals through the dorsal-ventral plane and the injury area measured on each section using Image J software. The lesion size was then calculated for each spinal cord as an approximate volume using these measurements.

Spinal cord sections were aligned using the central canal as an anatomical landmark (midline) for immunohistochemistry analysis. Images were taken adjacent to the lesion and at both 3.5 and 7 mm distal to the lesion centre in both rostral and caudal directions.

Image analysis was conducted using ImageJ software (National Institutes of Health, version 2X). Analysis of Connexin43, phosphorylated Connexin43 and astrocytes (astrogliosis) was undertaken by measuring the staining intensity, mean GSV, in 10x images of the midline section. For activated macrophages/microglia quantification, all cells were identified with nuclear Hoechst stain and co-labelled with both ED1 (phagocytic macrophages) and Iba1 (microglia), counted manually in 40x images of midline sections and reported as number of cells/field of view. Neurons were identified using NeuN and counted manually in 40x images of midline sections and in sections at 300 μm dorsal and ventral to the midline and are reported as number of cells/field of view.

3.2.9 Statistical analysis

All data were expressed as mean ± SEM. Unpaired t-test (surgical parameters) or one-way ANOVA with a Bonferroni *post-hoc* test (lesion size and fluorescent immunohistochemistry) was used to determine significant differences (PRISM, Version 6.0e, GraphPad). The BBB scores were analysed by Kruskal-Wallis one-way analysis of variance with a Mann-Whitney *U* test between injury groups at each time point. The rest of behavioural data were analysed by two-way ANOVA with a Bonferroni *post-hoc* test for the simple effects of treatment. Statistically significant differences were considered at $p < 0.05$. The rostral and caudal measurements in mean GSV of immunofluorescence and cell counts were indistinguishable (paired t-test, $p > 0.05$), and thus pooled for further analysis.

3.3 Results

3.3.1 Consistent spinal cord injury in rats

All surgical procedures and intraperitoneal peptide injections were conducted without incident. None of the rats undergoing sham surgery showed any indication of SCI or any post-operative complications. The impactor parameters for the SCI rats in the Peptide5 and control SP groups were not significantly different for impact velocity (0.319 ± 0.027 m/s vs. 0.319 ± 0.027 m/s), compression (1.502 ± 0.182 mm vs. 1.505 ± 0.181 mm) or compression rate (0.28 ± 0.03 m/s vs. 0.28 ± 0.03 m/s) (Table 3.2). At Day 1 following surgery, the SCI rats showed immediate loss of locomotor function at a mean BBB score of 3.47 ± 3.14 compared with 21.00 ± 0.06 in the sham animals ($p < 0.001$). There were no significant differences in Day 1 BBB score of SCI rats between Peptide5 and control SP groups (3.40 ± 3.04 vs 3.44 ± 3.27) (Table 3.2). Bladder function and weight gain returned to normal within a week to 10 days for all rats.

Table 3.2 Consistent contusion spinal cord injury produced in rats.

Measurement	Treatment Group	
	Peptide5	**Scrambled Peptide**
Impact velocity (m/s)	0.319 ± 0.027	0.319 ± 0.027
Compression (mm)	1.502 ± 0.182	1.505 ± 0.181
Compression rate (m/s)	0.28 ± 0.03	0.28 ± 0.03
Day 1 BBB Score	3.40 ± 3.04	3.44 ± 3.27

BBB Score: Basso, Beattie and Bresnahan

3.3.2 Connexin43 and phosphorylated Connexin43

Analysis of Connexin43 protein and phosphorylated Connexin43 protein (closed hemichannels) was undertaken at 24 hours post-injury using fluorescent immunohistochemistry on midline sections. Connexin43 protein levels were measured by mean GSV of immunohistochemistry labelling intensity in both grey and white matter at 3.5 and 7 mm distal to the lesion and the epicentre of the lesion (Figure 3.1). Compared with sham animals, the Connexin43 protein levels increased significantly following the contusion injury in the SP-treated animals at all anatomical locations (grey matter: 7 mm, 17.22 ± 2.67 vs. 24.82 ± 5.58, $p < 0.001$; 3.5 mm, 16.88 ± 2.38 vs. 26.87 ± 4.98, $p < 0.001$; epicentre, 18.25 ± 6.59 vs 26.80 ± 3.47, $p < 0.01$. white matter: 7 mm, 7.81 ± 2.39 vs. 13.17 ± 4.96, $p < 0.01$; 3.5 mm, 8.03 ± 2.21 vs. 13.39 ± 4.67, $p < 0.01$; epicentre: 8.27 ± 3.23 vs. 14.31 ± 5.31, $p < 0.01$). The Peptide5 treatment significantly lowered the Connexin43 protein levels in the injured animals compared with the control SP treatment in the grey matter of the lesion epicentre (20.33 ±1.30 vs. 26.80 ±3.47, $p < 0.05$). Phosphorylated Connexin43 protein levels were measured by mean GSV of immunohistochemistry labelling intensity in both grey and white matter at 3.5 and 7 mm distal to the lesion and the epicentre of the lesion (Figure 3.2). Compared to the sham animals, the phosphorylated Connexin43 protein levels decreased significantly following the contusion injury at all locations (grey matter: 7 mm, 73.67 ± 14.19 vs. 52.77 ± 8.41, $p < 0.01$; 3.5 mm, 73.18 ± 15.42 vs. 53.87 ± 12.62, $p < 0.05$; epicentre: 69.75 ± 19.16 vs. 50.28 ± 12.02, $p < 0.05$. white matter: 7 mm, 44.61 ± 4.20 vs. 37.27 ± 4.56, $p < 0.05$; 3.5 mm, 44.18 ± 5.91 vs. 37.72 ± 5.16, $p < 0.05$; epicentre: 43.89 ± 5.87 vs. 32.76 ± 5.13, $p < 0.05$). The Peptide5 treatment significantly increased the phosphorylated Connexin43 levels in the injured animals compared with the control SP treatment in the white matter at 7 mm distal to the lesion epicentre (44.59 ± 3.23 vs 37.27 ±4.56, $p < 0.05$).

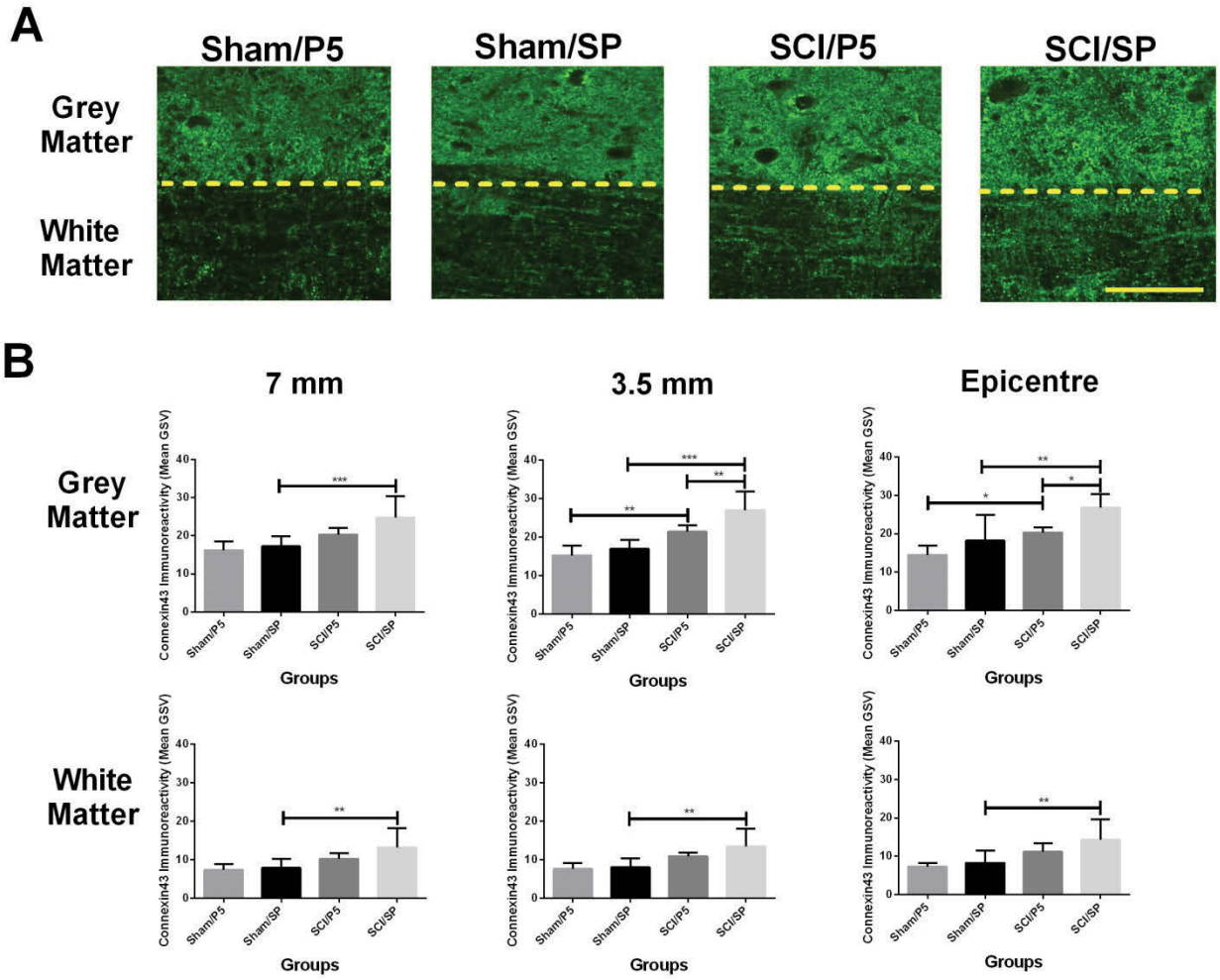

Figure 3.1 Immunohistochemistry staining of Connexin43 at 24 hours following spinal cord injury.

(A) Representative images of fluorescent immunohistochemistry staining showed the Connexin43 (green) at the epicentre of the lesion in both grey and white matter. Scale bar = 50 μm. (B) Following SCI, the levels of Connexin43 immunoreactivity were increased significantly at all locations and the systemic administration of Peptide5 limited the increase in Connexin43 in the grey matter at the lesion epicentre, and 3.5 mm distal to the epicentre of the lesion (one-way ANOVA, $p < 0.01$ at all locations; Bonferroni *post-hoc* comparison, *$p < 0.05$, **$p < 0.01$, ***$p < 0.001$). (GSV: greyscale value; P5: Peptide5; SCI: spinal cord injury; SP: control scrambled peptide)

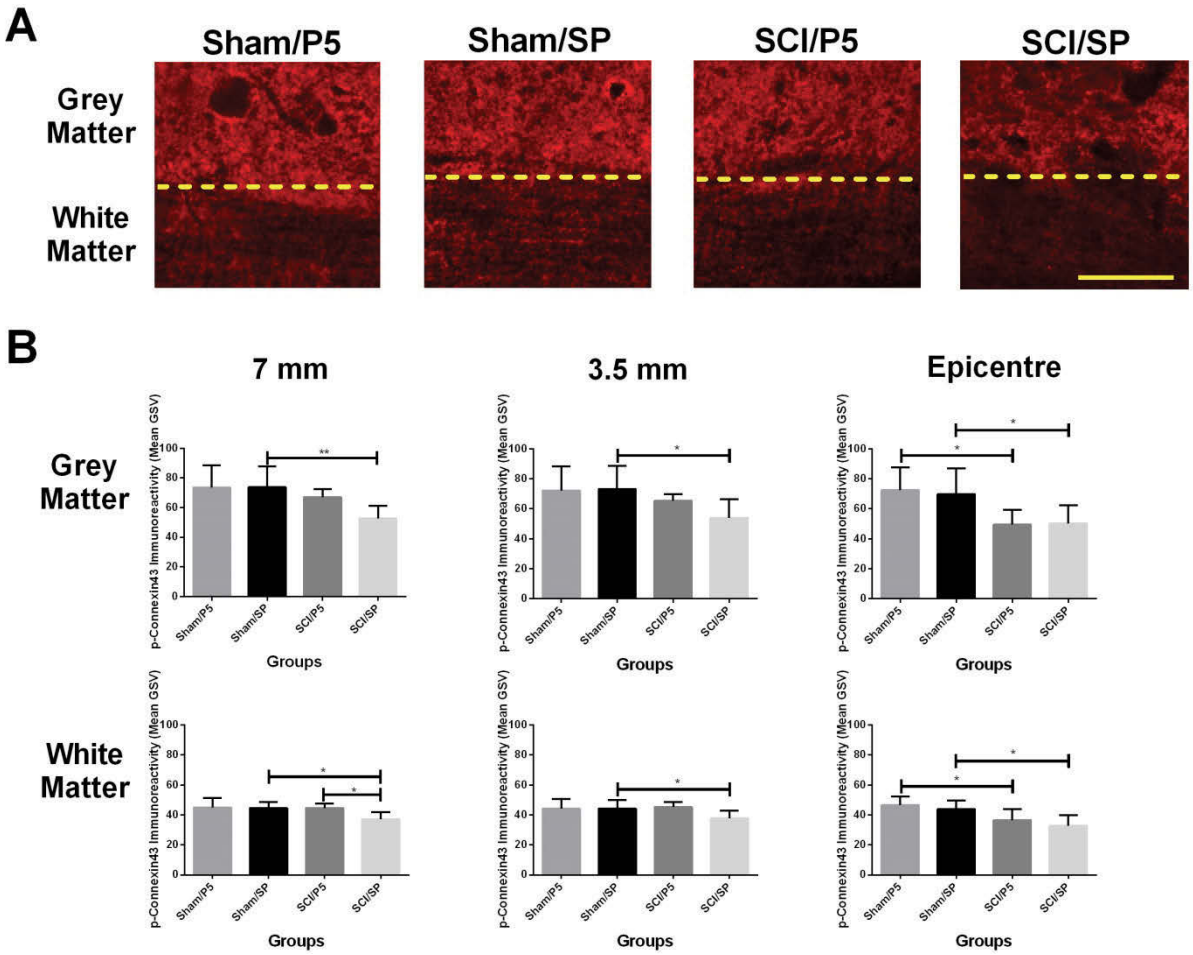

Figure 3.2 Immunohistochemistry staining of phosphorylated Connexin43 at 24 hours following spinal cord injury.

(A) Representative images of fluorescent immunohistochemistry staining showed the changes in phosphorylated Connexin43 (red) level at the epicentre of the lesion in both grey and white matter. Scale bar = 50 μm. (B) Following SCI, the levels of phosphorylated Connexin43 immunoreactivity were reduced significantly at all locations and the systemic administration of Peptide5 maintained phosphorylation of Connexin43 at residue Ser368 in the white matter at 7 mm distal to the epicentre of the lesion (one-way ANOVA, $p < 0.01$ at all locations; Bonferroni *post-hoc* comparison, *$p < 0.05$, **$p < 0.01$). (GSV: greyscale value; P5: Peptide5; p-Connexin43: phosphorylated Connexin43; SCI: spinal cord injury; SP: control scrambled peptide)

3.3.3 Lesion size

There was no histological evidence of any tissue damage in the sham animals at any time points. Longitudinal H&E stained sections including the lesion are shown for 24 hours, 2 and 6 weeks after SCI (Figure 3.3 A, B and C, respectively). For the SCI groups, there was an obvious lesion apparent from 24 hours post-injury, which increased in size and changed in morphology over the 6-week period. At the earlier time points, there was more haemorrhage visible, and over time this changed to include more cell loss and increased cellular debris, before development of a clearly defined central cavity. Lesion size was significantly reduced by the systemic administration of Peptide5 in comparison with the control SP treatment at all time points post-injury (Figure 3.3 D). At 24 hours post-injury, the lesion volume was 14.79 ± 4.51 mm^3 in the control SP group while the Peptide5 treatment was able to limit the lesion size to 8.23 ± 1.66 mm^3 ($p < 0.001$). At 2 weeks post-SCI, the lesion was measured as 6.72 ± 2.49 mm^3 in the SP group, and 2.58 ± 1.78 mm^3 in the Peptide5 group ($p < 0.05$). By 6 weeks post-injury, the lesion was found to be 7.55 ± 3.11 mm^3 in the SP-treated animals, while the lesion in the animals receiving Peptide5 treatment was limited to 3.60 ± 0.60 mm^3 ($p < 0.05$).

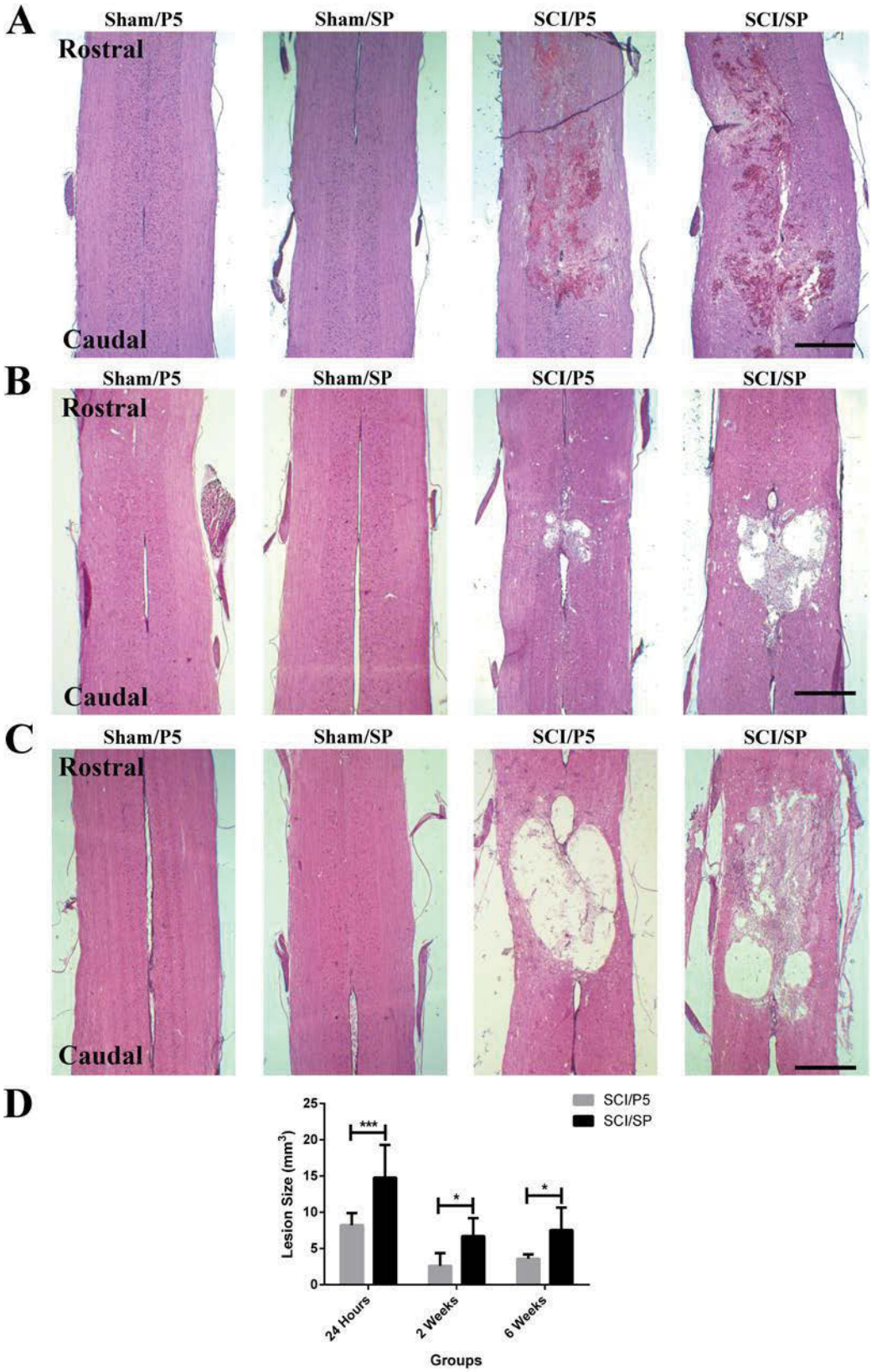

Figure 3.3 Changes in lesion size following spinal cord contusion injury.
Mayer's Haematoxylin and Eosin staining showed the lesion area at the midline level of spinal cord at 24 hours (A), 2 weeks (B) and 6 weeks (C) following injury. Scale bars = 1 mm. (D) The lesion size was reduced by peptide5 treatment at 24 hours, 2 weeks and 6 weeks post-injury (t-test, *$p < 0.05$, ***$p < 0.01$). (P5: Peptide5; SCI: spinal cord injury; SP: scrambled peptide)

3.3.4 Astrogliosis (GFAP immunohistochemistry)

Astrogliosis (astrocyte activation) is known to be a key response following SCI and ultimately results in the formation of a glial scar, starting from approximately one week. GFAP immunohistochemistry on sections at the midline level were used to evaluate the effect of Peptide5 on astrogliosis after SCI (Figure 3.4 A for representative sections at 2 weeks post-surgery). The GFAP staining intensity at 3.5 and 7 mm distal to the lesion and the epicentre of the lesion was quantified in mean GSV for statistical analysis (Figure 3.4 B).

The normal patterns and intensity of astrocyte staining were seen in the sham spinal cords and these measurements were used as the baseline for comparison to injury and treatment. The normal astrocytes exhibited small cell bodies with dense ramification of multiple fine processes. The increase in both astrocyte cell number and GFAP expression was observed in P5/SP treated SCI rats. Statistically significant differences were found in the level of GFAP immunoreactivity at all locations at 2 and 6 weeks post-injury (one-way ANOVA, $p < 0.001$). Following the contusion SCI, the level of GFAP immunofluorescence at the epicentre of the lesion in the control SP animals at 2 and 6 weeks post-injury was increased 2.1 and 3.3 times, respectively, compared with the sham groups (2 weeks, $p < 0.001$; 6 weeks, $p < 0.001$). The Peptide5 treatment resulted in a significantly reduced level of GFAP immunoreactivity compared with SP-treated SCI animals at both post-injury time points (2 weeks, $p < 0.001$; 6 weeks, $p < 0.001$) with levels 1.5 and 2.4 fold decrease compared with that seen in sham animals, respectively. At 3.5 and 7 mm distal to the lesion, the GFAP immunoreactivity was elevated 1.8 and 1.6 times, respectively, compared with the sham groups at 2 weeks following SCI (3.5 mm, $p < 0.001$; 7 mm, $p < 0.001$). The Peptide5 treatment significantly decreased the level of GFAP immunofluorescence to the baseline at both

locations distal to the epicentre compared with SP control treatment ($p < 0.001$). By 6 weeks post-injury, the levels of GFAP immunoreactivity in SCI groups were increased 2.0 and 1.7 times at 3.5 and 7 mm distal to the lesion, respectively, compared with the sham groups (3.5 mm, $p < 0.001$; 7 mm, $p < 0.001$).

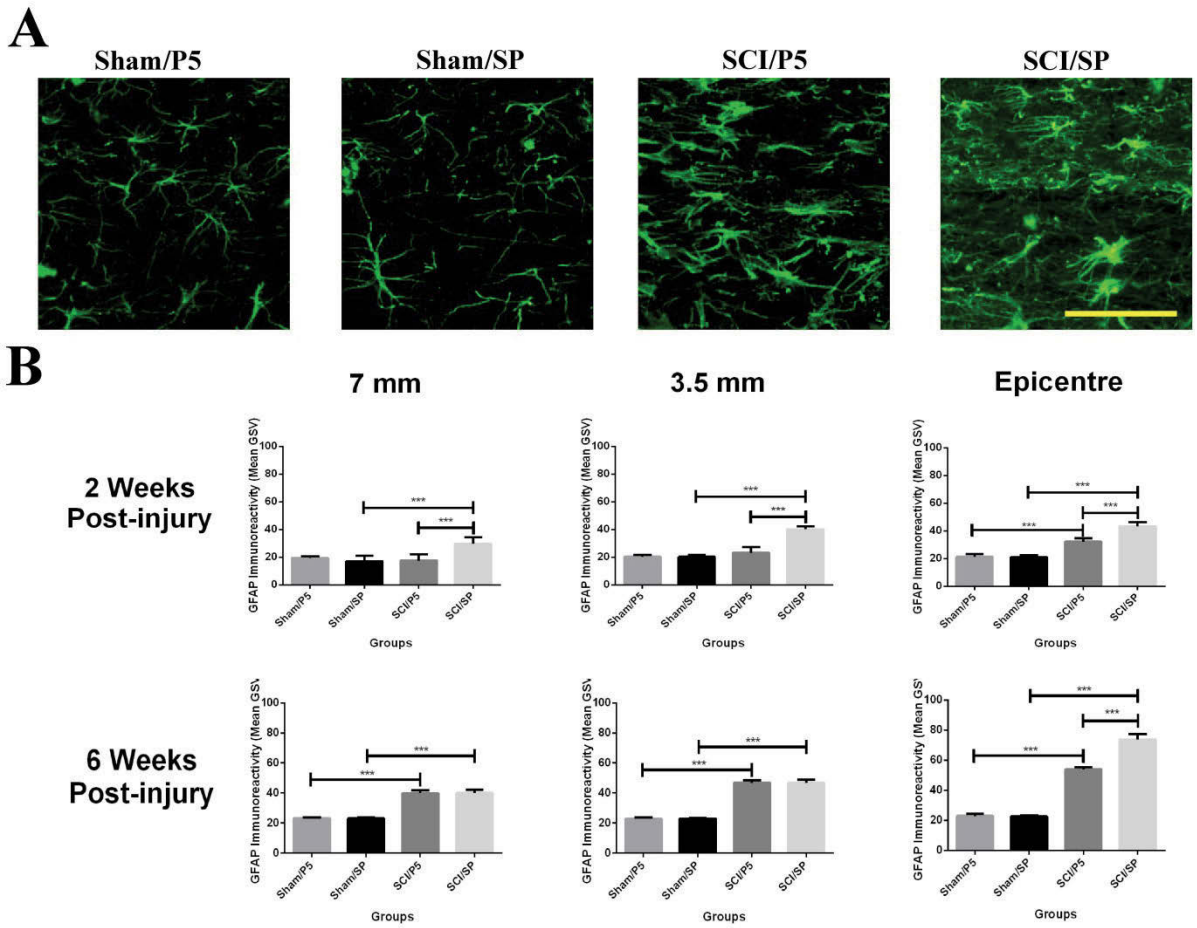

Figure 3.4 Glial fibrillary acidic protein (GFAP) expression following spinal cord contusion injury.
(A) At 2 weeks after spinal cord injury, representative images of GFAP immunofluorescence (green) adjacent to the lesion in sham and injury animals treated with Peptide5 or scrambled peptide. Scale bar = 50 μm. (B) GFAP immunofluorescence intensity was quantified in mean grey scale value at 2 and 6 weeks after injury. Systemic administration of Peptide5 led to a significant reduction in the amount of GFAP protein at the epicentre of the lesion at 2 and 6 weeks post-injury. The GFAP protein level was reduced to normal at 3.5 and 7 mm distal to the lesion at 2 weeks following injury (one-way ANOVA, $p < 0.001$ at all locations and time points; Bonferroni *post-hoc* comparison, ***$p < 0.001$). (GSV: greyscale value; P5: Peptide5; SCI: spinal cord injury; SP: scrambled peptide)

3.3.5 Microglial/macrophage activation (Iba1&ED1 immunohistochemistry)

One of the events that occurs during secondary SCI is the activation of microglial cells and the recruitment and activation of macrophages. These cells are involved in the inflammatory cascades that follow injury, and are generally thought to be detrimental to recovery. Activated microglia and/or macrophages were identified using Hoechst (nuclear staining) and double labelling with Iba1 and ED1 (Figure 3.5 A for representative sections at 2 weeks post-surgery). The activated microglia and/or macrophages were observed in all areas of both grey and white matter, and the quantification of midline sections was conducted at 3.5 and 7 mm distal to the lesion and the epicentre of the lesion (Figure 3.5 B). Negative controls (primary antibodies omitted) showed no auto-fluorescence in macrophages in the spinal tissue, thus it did not affect the quantification. Statistically significant differences were found in the $Iba1^+/ED1^+$ cell numbers at 2 weeks (one-way ANOVA, all three locations, $p < 0.001$) and 6 weeks (one-way ANOVA, all three locations, $p < 0.001$) post-injury. There were no $Iba1^+/ED1^+$ cells in any of the sham surgery spinal cords. At the epicentre of the lesion, the cells double labelled with Iba1 and ED1 appeared in the greatest number. In the SP-treated SCI rats the number of $Iba1^+/ED1^+$ cells increased to 95 ± 18 cells/field of view at 2 weeks and 68 ± 3 cells/field of view at 6 weeks and were significantly lower with Peptide5 treatment at both 2 weeks (20 ± 10 cells/field of view, $p < 0.001$) and at 6 weeks (24 ± 2 cells/field of view, $p < 0.001$). At 3.5 mm distal to the lesion, the number of $Iba1^+/ED1^+$ cells raised to 6 ± 6 cells/field of view at 2 weeks and 15 ± 2 cells/field of view at 6 weeks in the scrambled treated injured animals and were significantly decreased with Peptide5 administration to 1 ± 1 cells/field of view at 2 weeks ($p < 0.001$) and 4 ± 1 cells/field of view at 6 weeks ($p < 0.001$). Similarly, at 7 mm distal to the lesion, the Peptide5 treatment significantly reduced the number of $Iba1^+/ED1^+$ cells to 1 ± 1 cells/field of view at 2 weeks ($p < 0.001$) and 4 ± 1 cells/field

of view at 6 weeks ($p < 0.001$) compared with the control SP treatment in the SCI groups (7 ± 8 cells/field of view at 2 weeks and 17 ± 3 cells/field of view at 6 weeks).

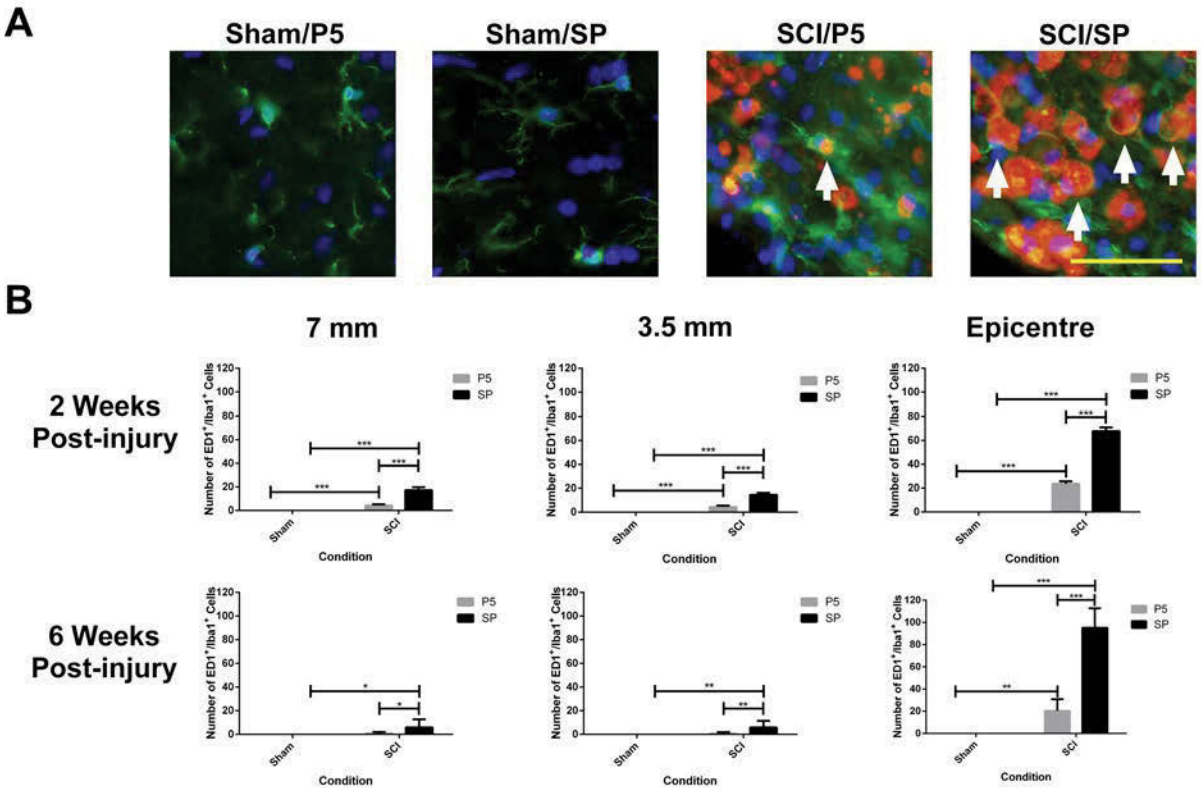

Figure 3.5 Activation of microglia and/or macrophages at the lesion edge following spinal cord contusion injury.
(A) At 2 weeks after spinal cord injury, representative images showing co-localisation of Iba1 (green) and ED1 (red) adjacent to the lesion in sham and injury animals treated with Peptide5 or scrambled peptide. Scale bar = 10 μm. (B) The $Iba1^{+}/ED1^{+}$ microglia and/or macrophages (arrows) were quantified at 2 and 6 weeks after injury. Systemic administration of Peptide5 led to a significant reduction in the number of activated microglia and/or macrophages at the epicentre of the lesion and 3.5 and 7 mm distal to the lesion at both time points (one-way ANOVA $p < 0.001$ at all locations and time points; Bonferroni *post-hoc* comparison, $^{**}p < 0.01$, $^{***}p < 0.001$). (P5: Peptide5; SCI: spinal cord injury; SP: scrambled peptide)

3.3.6 Neuronal survival (NeuN immunohistochemistry)

A significant loss of neuronal cells during the secondary phase of SCI is known to be a consequence of inflammatory responses, including microglial/macrophage activation. As Peptide5 treatment via systemic delivery resulted in a reduced level of activated microglia and/or macrophages in the secondary phase, it was important to determine whether neuronal survival was enhanced using NeuN immunohistochemistry (Figure 3.6 A for representative sections at 2 weeks post-surgery). The surviving neuronal nuclei were identified by NeuN positive staining. There were no surviving neurons observed at the epicentre of the lesion and therefore the quantification of neuronal cells was conducted at 3.5 and 7 mm to the epicentre of the lesion at the dorsal, midline and ventral levels (Figure 3.6 B). Neuronal cell number and distribution was not altered over time in the sham animals, so this was used as a baseline (77 ± 3 cells/field of view at the dorsal level and 36 ± 3 cells/field of view at the midline level) for comparisons at 3.5 and 7 mm to the lesion at two time points. There were statistically significant differences in the neuronal cell numbers at both 3.5 and 7 mm distal to the lesion at 2 weeks (one-way ANOVA, all four locations, $p < 0.001$) and 6 weeks (one-way ANOVA, all three locations, $p < 0.001$) post-injury. The number of motor neurons at ventral horns did not decrease significantly following a mild contusion injury at the dorsal site of the spinal cord. As anticipated, at 7 mm to the lesion of the dorsal level, the number of neurons in the SP treated SCI animals significantly decreased to 28 ± 9 cells/field of view at 2 weeks ($p < 0.001$) and 24 ± 4 cells/field of view by 6 weeks ($p < 0.001$) post-injury. In Peptide5-treated animals this number was retained at 57 ± 4 cells/field of view at 2 weeks ($p < 0.001$) and 51 ± 2 cells/field of view by 6 weeks ($p < 0.001$) post-injury compared with the animals that received SP control treatment. Similarly, at 3.5mm to the lesion of the dorsal level, the Peptide5 treatment was shown to maintain the number of neurons in SCI animals at 53 ± 6 cells/field of view at 2 weeks ($p < 0.001$) and 44 ± 1

cells/field of view by 6 weeks ($p < 0.001$) post-injury compared with the SP- treated SCI rats (28 ± 9 cells/field of view at 2 weeks and 24 ± 4 cells/field of view at 6 weeks). At the midline level, the number of neurons at 7 mm distal to the lesion significantly reduced to 14 ± 2 cells/field of view at 2 weeks ($p < 0.001$) and 11 ± 1 cells/field of view by 6 weeks ($p < 0.001$) post-injury in the SCI animals treated with SP. This number was retained at 31 ± 3 cells/field of view at 2 weeks ($p < 0.001$) and 24 ± 1 cells/field of view by 6 weeks ($p < 0.001$) following SCI in the Peptide5 treated animals. Likewise, at 3.5mm to the lesion of the midline level, the Peptide5 treatment was demonstrated to preserve the number of neurons per field in injured animals at 30 ± 6 cells/field of view at 2 weeks ($p < 0.001$) and 21 ± 2 cells/field of view by 6 weeks ($p < 0.001$) post-injury compared with the SP-treated SCI rats (11 ± 2 cells/field of view at 2 weeks and 9 ± 2 cells/field of view at 6 weeks). Therefore, the Peptide5 treatment via systemic delivery was able to promote neuronal survival during the secondary phase of SCI.

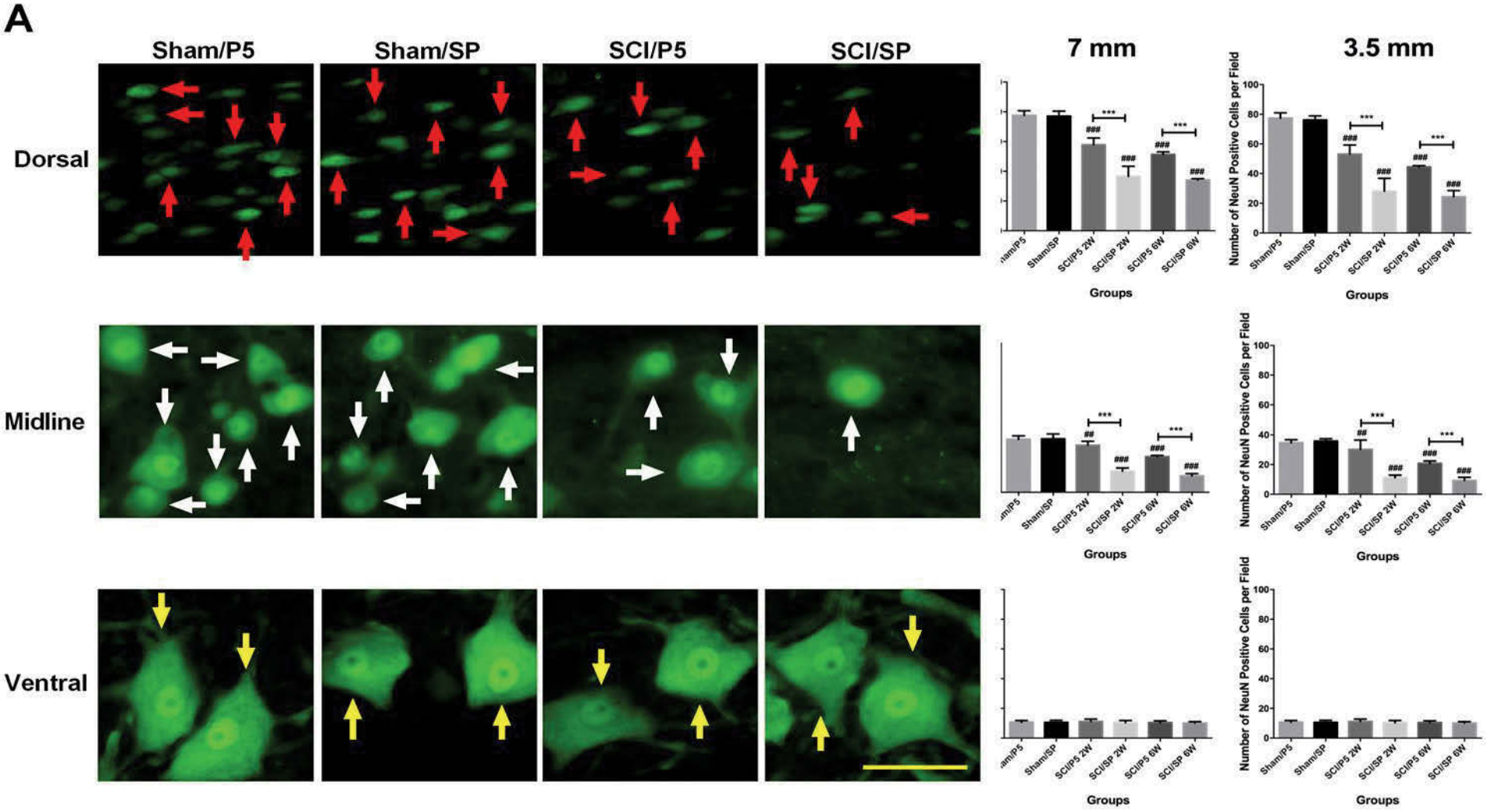

Figure 3.6 Surviving neuronal cells following spinal cord contusion injury.

(A) At 2 weeks following spinal cord injury, representative images of NeuN immunofluorescence (green) 7 mm from the lesion at dorsal (red arrows), midline (white arrows) and ventral (yellow arrows) levels in sham and injury animals treated with Peptide5 or scrambled control peptide. Scale bar = 10 μm. (B) The $NeuN^{+}$ neurons were quantified at 3.5 and 7 mm distal to the lesion at 2 and 6 weeks following injury. Systemic administration of Peptide5 led to a significant increase in the number of spared neurons at 3.5 and 7 mm from the lesion at the dorsal and midline levels (one-way ANOVA, $p < 0.001$ at all locations; Bonferroni *post-hoc* comparison, ***$p < 0.001$, $^{\#\#}p < 0.01$, $^{\#\#\#}p < 0.001$ compared with sham). (P5: Peptide5; SCI: spinal cord injury; SP: scrambled peptide; 2W: 2 weeks after injury; 6W: 6 weeks after injury)

3.3.7 Motor function (Open field and horizontal ladder tests)

Two behavioural assessments, open field and horizontal ladder tests, were used to determine whether Peptide5 treatment led to an improvement in functional recovery. The SCI animals treated with Peptide5 showed a significant improvement in hind limb locomotor function in both tests from Week 3, compared with the injured animals treated with SP

(

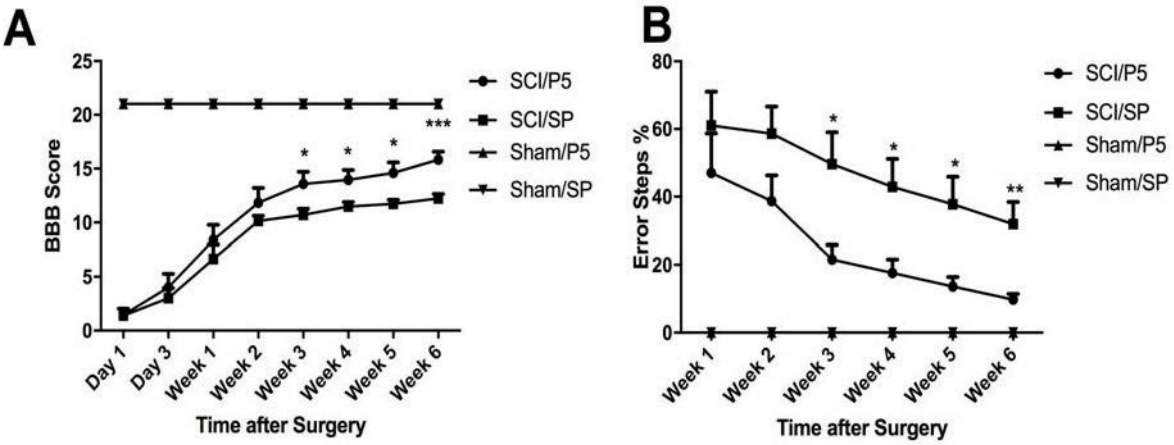

Figure 3.7). There was no deficit in hind limb locomotion in any of the sham animals, regardless of treatment for both behavioural assessments. In the open field test, injury groups displayed improvements in the BBB scores from Day 1 to Week 6 (SCI/ Peptide5, 1.44 ± 0.50 to 15.81 ± 0.76, $p < 0.01$; SCI/SP, 1.00 ± 0.67 to 12.00 ± 0.41, $p < 0.01$) as expected following a mild contusion SCI

(

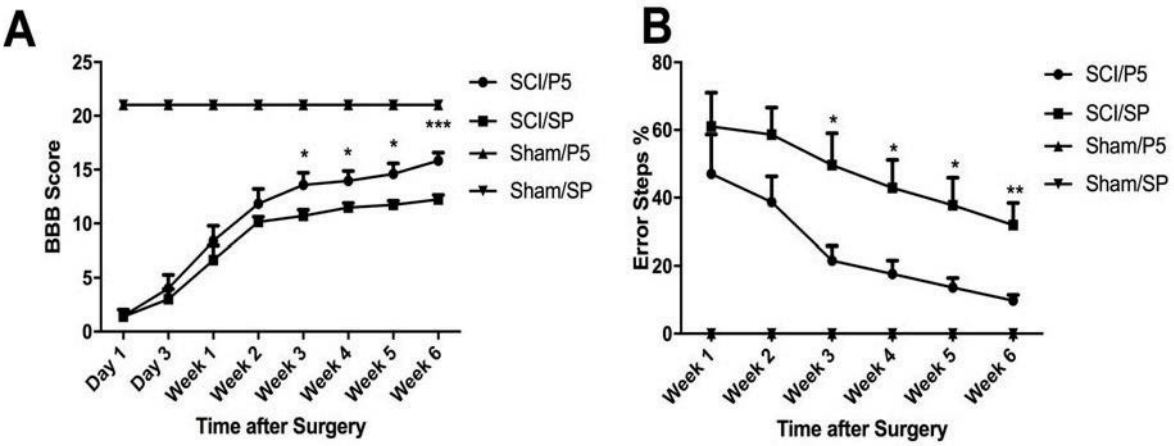

Figure 3.7A), but Peptide5 treated injury animals showed improved hind limb locomotor function when compared with the SCI animals treated with SP with significant differences observed from Week 3 (13.56 ± 1.14 vs. 11.00 ± 0.57, $p < 0.05$) to Week 6 (15.81 ± 0.76 vs. 12.00 ± 0.41, $p < 0.001$) at which the behavioural assessment was ceased. Similar results were obtained with a horizontal ladder test

(

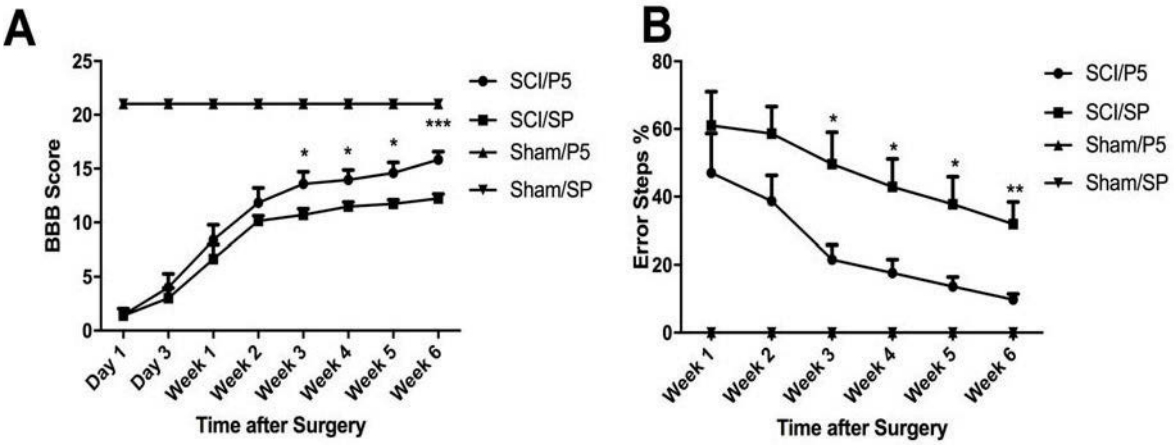

Figure 3.7B). All injury animals with Peptide5 or SP treatments exhibited a reduction in the percentages of error steps from Weeks 1 to 6 (SCI/ Peptide5, 47.20 ± 11.68% to 9.64 ± 1.66%, $p < 0.001$; SCI/SP, 61.09 ± 10.02% to 32.04 ± 6.58%, $p < 0.001$). However, the injury animals treated with Peptide5 displayed fewer hind limb error step

percentages compared with those that received the SP control treatment with significant differences seen from Week 3 (21.65 ± 4.25% vs. 49.72 ± 9.42%, $p < 0.01$) to Week 6 (9.64 ± 1.66% vs. 32.04 ± 6.58%, $p < 0.01$). Differences in the percentages of error steps at Weeks 1 and 2 were seen between Peptide5 and SP-treated injury animals, however these differences were not statistically significant ($p > 0.05$).

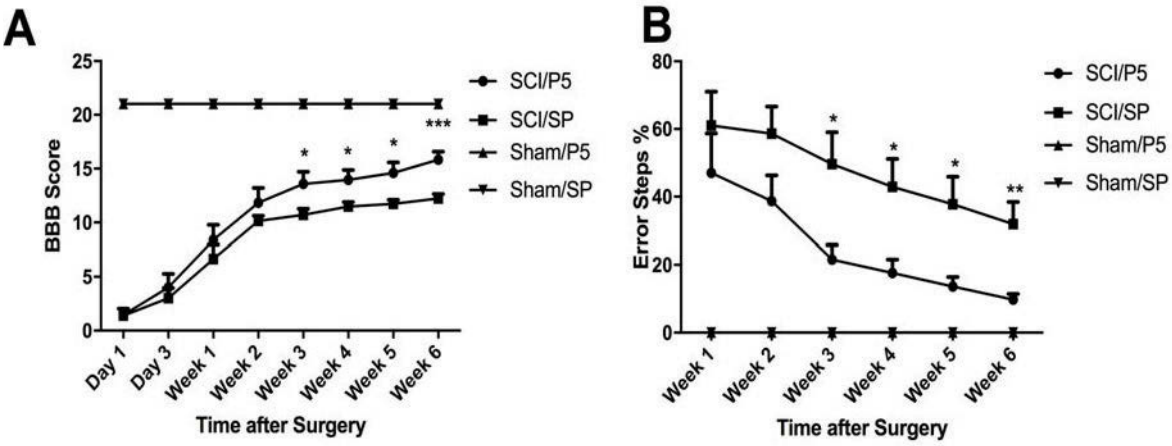

Figure 3.7 Locomotor function assessments following spinal cord injury.
(A) The Basso-Beattie-Bresnahan scores are shown for the Peptide5 treated animals compared with the scrambled peptide treated animals. There were significant differences seen in BBB scores using Kruskal-Wallis one-way analysis of variance at all time points ($p < 0.001$). Peptide5 treated rats showed improvement in BBB scores from Week 3 to Week 6 (*$p < 0.05$, *** $p < 0.001$). (B) The percentage of hind limb error steps is shown for the Peptide5 treated animals compared with the scrambled peptide treated animals. There were significant differences seen in the percentage of errors using two-way ANOVA for both the treatment ($p < 0.001$) and for time ($p < 0.001$). Peptide5 treated rats showed improvement in stepping from Week 3 to Week 6 (*$p < 0.05$, ** $p < 0.01$). (Basso-Beattie-Bresnahan: BBB; P5: Peptide5; SCI: spinal cord injury; SP: scrambled peptide)

3.3.8 Sensory function (Mechanical allodynia)

Spinal astrogliosis is well understood to be a contributor to the development of neuropathic pain states, via the release of small excitatory molecules through opened hemichannels following SCI. As Connexin43 is the primary hemichannel formed in

astrocytes, we investigated whether blockade of these channels using Peptide5 alleviates mechanical pain hypersensitivity following SCI. Spinal cord injured rats developed at-level hypersensitivity demonstrated by reduced withdrawal thresholds after the injury. Compared to SP-treated controls, treatment with Peptide5 significantly improved at-level mechanical pain hypersensitivity with a 41% increase in the withdrawal threshold at Week 1 ($p < 0.01$), and a 27% increase in the withdrawal threshold at Week 6 ($p < 0.05$) following SCI (Figure 3.8A). Below-level mechanical pain hypersensitivity was also measured on the hind paws (Figure 3.8B). However, there was no significant difference in paw withdrawal thresholds between the treatment groups over the 6 weeks ($p > 0.05$) (Figure 3.8B).

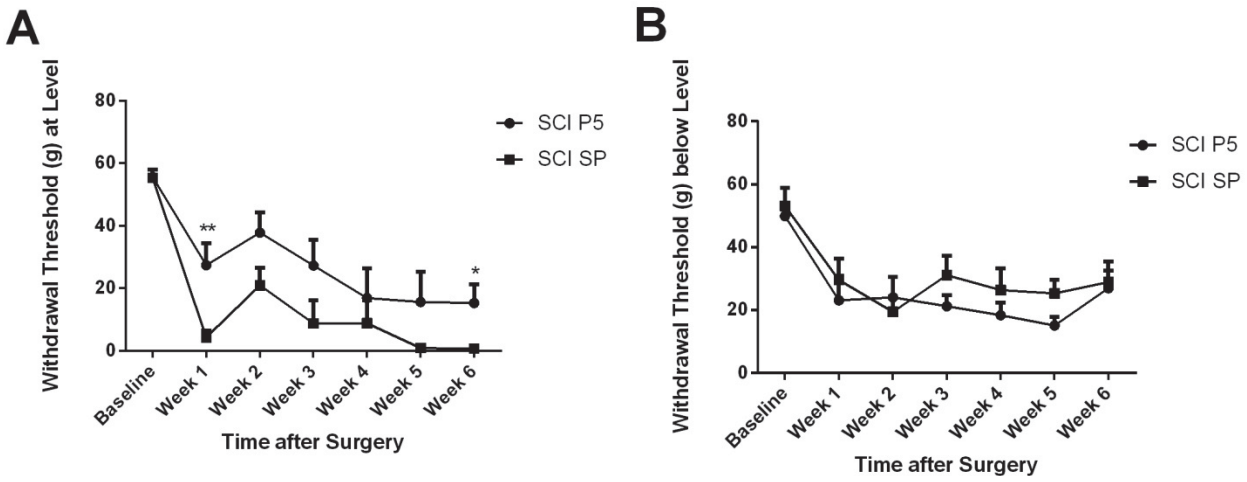

Figure 3.8 Sensory function assessments following spinal cord injury.
(A) Long-term effects of Peptide5 on mechanical pain hypersensitivity following contusion spinal cord injury on at-level mechanical pain hypersensitivity. Mechanical withdrawal thresholds are shown for Peptide5 treated animals (compared to the scrambled peptide treated animals. There were significant differences seen in the mechanical withdrawal thresholds using two-way ANOVA for both the treatment ($p < 0.001$) and for time ($p < 0.001$). Peptide5 treated rats showed improvement at Week 1 and Week 6 (*$p < 0.05$, ** $p < 0.01$). (B) Long-term effects of Peptide5 on mechanical pain hypersensitivity following contusion spinal cord injury on below-level mechanical pain hypersensitivity. There were no significant differences in paw withdrawal thresholds between Peptide5 and scrambled peptide treated animals. (P5: Peptide5; SCI: spinal cord injury; SP: scrambled peptide)

3.4 Discussion

Earlier studies in our laboratory have demonstrated that the local application of Peptide5 at a low concentration within the first 24 hours after traumatic SCI reduces tissue swelling, lesion spread, inflammation, astrogliosis, neuronal cell death and functional deficits in *ex vivo* and *in vivo* models (O'Carroll et al., 2008, O'Carroll et al., 2013). Acute administration of Peptide5 at low doses has also been shown to be neuroprotective in models of retinal and cerebral ischaemia (Davidson et al., 2013a, Davidson et al., 2014, Chen et al., 2015, Danesh-Meyer et al., 2012, Davidson et al., 2012a, Chen et al., 2014b). However, the local administration of Peptide5 is not practical for use in human spinal patients as this would necessitate a highly invasive surgical procedure to expose the injury area or involve another procedure such as inserting an intrathecal catheter. Upregulation of connexin43 has been demonstrated early after SCI (Theriault et al., 1997, Lee et al., 2005, O'Carroll et al., 2013). Therefore, application of Peptide5 should occur within 8 hours, prior to maximal upregulation of Connexin43 protein, to be most effective. Many SCI patients arrive in emergency departments with traumatic co-morbidities or life threatening injuries, and a timely spinal cord procedure is not always possible. If the acute clinical management of a SCI patient includes an open surgery procedure such as decompression or stabilisation there may be an avenue for application of either a Connexin43 AS-ODN in a topical gel (Cronin et al., 2008) or a direct application of Peptide5 (O'Carroll et al., 2013).

Unfortunately, in most cases these procedures do not occur early enough for effective regulation of Connexin43 protein. The most recent study indicates that in Australian and New Zealand between 2010 and 2013 the median time from the accident scene to the decompression surgery was 21 hours, and could be as long as 300 hours (Battistuzzo et al., 2016). Since mimetic peptides have been shown to permeate the lesion site of spinal cords through the disrupted BSB (Han et al., 2010), vascular administration of Peptide5 is a suitable approach for early delivery to the lesion. The finding in the current study regarding the neuroprotective effects of Peptide5 via systemic delivery is in agreement with previous studies using direct peptide administration (O'Carroll et al., 2013, O'Carroll et al., 2008).

As anticipated, Peptide5 transiently suppresses Connexin43 expression and blocks Connexin43 hemichannels, both of which were seen at 8 and 24 hours after SCI. The inhibiting effect of Peptide5 in Connexin43 upregulation has also been reported in an early study using an ex vivo rat model of SCI (O'Carroll et al., 2008). This temporary regulation of Connexin43 and its hemichannels after injury has been reported to be neuroprotective in tissue and behavioural recovery (Cronin et al., 2008, Roh et al., 2010, Frantseva et al., 2002a, Frantseva et al., 2002b). However, the permanent or long-term modulation of Connexin43 hemichannels and/or gap junctions is believed to be detrimental, as the gap junctional communication is essential for spatial buffering and neuronal survival at the later stages of recovery (Nakase et al., 2004, Takahashi et al., 2010, Siushansian et al., 2001). The systemic administration protocol of Peptide5 was determined in Chapter 2 to regulate the Connexin43 expression and hemichannel opening up to 24 hours after SCI. Considering the 2-hour half-life of Peptide5 *in vivo* and the renal excretion, the Connexin43 expression and hemichannels were less regulated by Peptide5 at 24 hours post-injury than the effects at 8 hours post-injury.

Peptide5, via systemic delivery, will be less likely to affect Connexin43 gap junctional communication beyond 24 hours after SCI. In the white matter, Peptide5 reduced Connexin43 expression to the sham level at 24 hours post-injury, however the reduction of Connexin43 expression was not extensive, especially closer to the lesion. This may simply be due to the proximity to the injury which was predominantly in the grey matter. However, this is an area that deserves further attention if the inflammation is sustained, as the robust response of activated microglia and/or macrophages still presenting at 6 weeks post-injury might drive a cycle of Connexin43 hemichannel opening, indicating the therapeutic window may be much longer than currently thought.

Injured spinal cords treated with Peptide5 had smaller lesions, decreased astrogliosis, less inflammatory cell infiltration and activation, and increased neuron survival, all indicating reduced effects of secondary injury and lesion spread. There is increasing evidence that the uncontrolled opening of Connexin43 hemichannels causes the release of neurotoxins and ATP from activated microglia and/or macrophages, thus propagating secondary injury (De Vuyst et al., 2007, Ye et al., 2003, Orellana et al., 2010, Davidson et al., 2015, Decrock et al., 2015). Additionally, many of these neurotoxins including glutamate and ROS have been shown to increase the opening of Connexin43 hemichannels (Ye et al., 2003, Retamal et al., 2006, Perez Velazquez et al., 2006, Thompson et al., 2006, Ramachandran et al., 2007), thus forming a positive feedback loop. The current study shows that blocking Connexin43 hemichannels with Peptide5 halts the amplification of injury and reduces a number of downstream effects that would normally be part of the secondary injury cascade, including astrogliosis.

Normally, astrogliosis will commence in the rat spinal cord from about 3 days after injury and lead to glial scar formation, a major physical and chemical barrier to neural regeneration (Frisén et al., 1995, Kozlova, 2003, Renault-Mihara et al., 2008, Tysseling-

Mattiace et al., 2008, Mao et al., 2016). The physical barrier acts to prevent remyelination and regrowth of axons (Sharma et al., 2012, Fawcett, 2006, Lane et al., 2007), while the chemical barrier adds to the nerve regrowth inhibitory microenvironment by producing a number of molecules, such as chondroitin sulphate proteoglycans, tenascins and bone morphogenetic proteins (Jones et al., 2003b, Barkho et al., 2006, Karimi-Abdolrezaee and Billakanti, 2012, Wang et al., 2011, Mizuno et al., 2008, Fitch and Silver, 2008, Sofroniew, 2009). The reactive astrocytes in astrogliosis are believed to be adverse for neuroregeneration by inhibiting axonal regeneration and oligodendrocyte differentiation from precursor cells, leading to remyelination failure, as well as generating and secreting nitric oxide, a neurotoxin that damages local neural cells contributing to the secondary injury (Hu et al., 2010, Ikeda and Murase, 2004, Wang et al., 2011, Kozlova, 2003, Barnabe-Heider et al., 2010).

Phagocytes found at the lesion area of CNS injury arise from two sources: resident microglia proliferating *in situ* and infiltrating macrophages recruited from the bloodstream. Both become activated and remain for several weeks after injury in response to the pro-inflammatory environment at the site of injury (Hinkerohe et al., 2005, Kreutzberg, 1996, Loane and Byrnes, 2010, Amat et al., 1996). In the current study, the cells expressing $Iba^{+}/ED1^{+}$ were counted as phagocytically activated microglia and/or macrophages (Chiu et al., 2013, Ajami et al., 2011). With the systemic administration of Peptide5, there was a decrease in the number of activated microglia and/or macrophages present in or adjacent to lesions. Studies have shown that activated microglia and/or macrophages are involved in an acute inflammatory response to neurotrauma, such as synthesis and release of cytokines and chemokines (Donnelly and Popovich, 2008, Fitch et al., 1999, Klusman and Schwab, 1997, Yan et al., 2001, Trivedi et al., 2006, Pineau and Lacroix, 2007). These pro-inflammatory cytokines, such

as TNF-α, IL-1ß and IL-6, are believed to cause neuronal and glial toxicity (Flaris et al., 1993, Pineau and Lacroix, 2007, Hausmann, 2003, Yang et al., 2004a, Yang et al., 2005). The activated microglia and/or macrophages have been reported to increase Connexin43 expression and gap junction coupling in response to a trauma in the CNS (Eugenín et al., 2001). The decrease in activated microglia and/or macrophages in Peptide5 treated spinal cords may not only be a downstream consequence of a decrease in astrocytic Connexin43, but may also result from Connexin43 hemichannel closure blocking pro-inflammatory signalling molecule release from the activated microglia and/or macrophages themselves.

The death of neuronal cells following CNS injury is thought to be a consequence of a complex cascade of events involving uncontrolled opening of Connexin43 hemichannels, spread of inflammation and release of neurotoxic molecules (Kang et al., 2008, Ye et al., 2003, Takeuchi et al., 2006). There is growing evidence that a number of neurotoxins are synthesised and released from the activated microglia and/or macrophages in response to injury, including glutamate, nitric oxide, pro-inflammatory cytokines, ATP and prostaglandins (Morita et al., 2007, Takeuchi et al., 2006, Retamal et al., 2007, Yang et al., 2004a, Yang et al., 2005, Huang et al., 2012). These neurotoxic molecules enhance the opening of astrocytic Connexin43 hemichannels, resulting in a further release of neurotoxins from the injured astrocytes (Orellana et al., 2011a, Orellana et al., 2009). Thus, there is a positive feedback loop developed in the lesion area to decrease the neuroprotective functions of astrogliosis, leading to an increase of neuronal cell death via the activation of amyloid-β peptide and pannexin 1 hemichannel pathways (Orellana et al., 2011a, Orellana et al., 2011b).

Behavioural assessments over a 6-week period after injury showed significant improvement in hind limb locomotor ability in the Peptide5 treated animals. Given the

time frame of the current study, it is believed that this represents a reduction in tissue damage, which translates directly to a reduction in the degree of functional deficit seen after injury. By 3 weeks after injury, the Peptide5 treated animals reached an average BBB score of 14, which corresponds with consistent weight-supported plantar steps. This is a significant improvement in rat locomotor function and affords the rat increased mobility and activity compared with a control injury group BBB score of less than 9, where rats have no weight-bearing stepping at all (Basso et al., 1996). Similarly, in the horizontal ladder test, the improvements in locomotor function with the Peptide5 treatment were shown to be distinguishable from the sham-operated rats from 3 weeks post-injury. If the systemic treatment in humans could preserve the function of even one spinal cord segment, then there would be significant preservation of function.

There was no indication that the rats used in the current study experienced increased pain levels. They were treated carefully with analgesics in the post-operative period. The injured rats did exhibit mechanical pain hypersensitivity in response to stimuli. At-level mechanical pain hypersensitivity following SCI has previously been reported to be the most common of neuropathic pain types (41% of subjects), with an early onset and pain described as severe or excruciating (Nashold, 1991, Siddall et al., 2003). The current study demonstrated that Peptide5 treatment was able to alleviate at-level pain hypersensitivity during the early (1 week) and later (6 week) stages of recovery following SCI, confirming the role of connexin hemichannels in the development of neuropathic pain (Lee-Kubli et al., 2016). Treatment with Peptide5 had no effect on paw withdrawal threshold (i.e., below-level mechanical pain hypersensitivity) in response to mechanical stimuli. It is noteworthy that interpretation of spinal-mediated reflex responses may be problematic when assessing below-level SCI pain hypersensitivity due to the development of hyperactive reflex circuitries (Baastrup et al., 2010). Hind

paw stimulation caused increased innate reflex responses in the absence of increased brainstem responses, thus reflecting a spasticity syndrome rather than pain-like behaviour (Baastrup et al., 2010). Additionally, in humans, below-level mechanical pain hypersensitivity is reported to occur months to years following SCI, in contrast to the days or weeks for the development of at-level mechanical pain hypersensitivity (Siddall et al., 2003). Although promising, further studies are required to determine the effects of Peptide5 treatment on the full spectrum of SCI-induced pain behaviours, and the correlation between the reduced tissue damage (lesion size, astrogliosis, inflammatory responses and neuronal cell lost) and the functional improvements (sensory and locomotor functions) by statistical analysis such as Spearman's rank-order correlation for non-parametric data, and Pearson's correlation for parametric data.

Chapter 4

Safety Profile of the Peptide5 Systemic Administration for Traumatic Spinal Cord Injury

4.1 Introduction

Peptide5 has been shown to be effective in regulating Connexin43 hemichannels in the injured spinal cord when delivered systemically (Chapter 3) and locally (O'Carroll et al., 2013). Other studies have also demonstrated that local administration of Peptide5 can regulate Connexin43 hemichannels and/or gap junctions in a number of pathological conditions of the CNS and the peripheral nervous system including retinal ischaemia (Chen et al., 2015, Chen et al., 2014b, Danesh-Meyer et al., 2012), cerebral ischaemia (Davidson et al., 2015, Davidson et al., 2013a, Davidson et al., 2013b), foetal ischaemia (Davidson et al., 2012a) and asphyxia (Davidson et al., 2014). However, the safety profiles of Peptide5 must still be completed.

As previously reported, Connexin43 expression is found in other tissue, such as heart (Van Kempen et al., 1991, Gourdie et al., 1993, Gu et al., 2014), brain (Yamamoto et al., 1990, Nakase et al., 2004, Deng et al., 2014), testis (Steger et al., 1999, Li et al., 2010, Chevallier et al., 2013), skin (Guo et al., 1992, Tada and Hashimoto, 1997, Chang et al., 2015) and bone marrow (Dürig et al., 2000, Zhang et al., 2006, Dorshkind et al., 1993). Connexin43 mimetic peptides have been shown to regulate the Connexin43 hemichannels for protecting ischaemic injury in the heart (Hawat et al., 2010, Hawat et al., 2012) and brain (Davidson et al., 2015, Davidson et al., 2013a, Davidson et al., 2013b). However, it is still unclear whether the Connexin43 hemichannels and/or gap

junctions in the heart and brain are affected by Peptide5 via systemic delivery for treating SCI.

In the spinal cord, there is a wide distribution of connexin gap junctions: astrocyte/astrocyte gap junctions containing Connexin30 and 43, neuron/neuron gap junctions containing Connexin36, and oligodendrocyte/astrocyte gap junctions containing Connexin29, 32 and 47, with the major heterotypic gap channels composed of Connexin43-Connexin47 and Connexin30-Connexin32 (Rash et al., 2001, Rash et al., 1998, Lee et al., 2005, Orthmann-Murphy et al., 2008, Kleopa et al., 2004). Apart from Connexin43, none of these connexins have been reported to be altered following traumatic SCI. It is possible that the expression of these connexins might respond to compensate for the blocked Connexin43 hemichannels following the Peptide5 treatment.

The current study proposed to examine the safety profiles of the Peptide5 systemic administration protocol as a practical treatment option for traumatic SCI by:

1) determining the distribution of Peptide5 *in vivo* following intraperitoneal injection of fluorescently labelled peptide in selected organs of SCI and normal rats;
2) investigating the Connexin43 hemichannels in the heart and lung tissue, and other connexins in the spinal cord by using fluorescence immunohistochemistry;
3) assessing the systemic inflammatory responses by measuring cytokine, chemokine and growth factor levels in plasma.

4.2 Materials and methods

4.2.1 Distribution of Peptide5 *in vivo*

4.2.1.1 Animals and general care

All experimental protocols and procedures used in the study were approved by the ACEC of UTS (UTS ACEC 2015-515), in accordance with the guidelines of the National Health and Medical Research Council of Australia. Cohort IV, consisting of 16 female Sprague Dawley rats (7 weeks old, 140-180 g, Animal Resources Centre, Perth) was used to verify the safety of Peptide5 acute systemic administration. All animals were maintained in standard cages with ad-lib water and food on a 12:12 hour light-dark cycle, and housed in the Ernst Facility, Faculty of Science, UTS. Daily checks of room temperature, humidity and animal wellbeing were performed. Each animal's weight was checked at least twice a week. All animals were acclimatised in the Ernst Facility for one week prior to any procedures. Spinal cord injured or normal control animals (with intact BSB) received FITC-conjugated Peptide5 treatment and recovered for 2 hours (n = 8) or 4 hours (n = 8).

4.2.1.2 Surgical procedures

The animals in injury groups were subject to a T10 laminectomy and a mild contusion SCI as previously described (Section 2.2.5), while the normal animals were not subject to any surgical procedures. A single dose of FITC-Peptide5 (sequence FITC-A-

VDCFLSRPTEKT, Auspep; 3.5 mg in 0.5 ml saline, equivalent to 10 mg/kg of Peptide5) was injected to rats intraperitoneally immediately after surgery.

4.2.1.3 Euthanasia and tissue preparation

At 2 hours (n = 8) and 4 hours (n = 8) after surgery, animals were euthanised with Lethobarb (pentobarbitone sodium, 1 ml/kg, i.p.) as previously described for Cohort I (Chapter 2). Approximately 10 mm of spinal cord centred at T10 and cervical enlargement as well as the major organs (brain, heart, lung, liver, kidney and spleen) were dissected. The fresh tissue specimens were embedded and frozen into Optimal Cutting Temperature compound. Using a cryostat (Leica CM1950), fresh frozen sections were produced at 15 μm onto Matsunami Platinum PLC-14 glass slides. Slides were immersed into water for 5 minutes to remove OCT and then cover-slipped in fluorescent mounting medium (Dako). Imaging was conducted using an Olympus BH-2 light microscope with a PixeLINK Pl-A662 camera (H&E staining) or Olympus BX-51 light microscope with an Olympus U-RFL-T fluorescence burner and the U-MWIB3 filter.

4.2.2 Connexin43 protein in the heart and lung tissue

As the Connexin43 and its hemichannels are also expressed on the cardiomyocytes (Van Kempen et al., 1991, Gourdie et al., 1993, Gu et al., 2014), it was essential to examine any alteration of Connexin43 expression and its hemichannels in the heart following the systemic delivery of Peptide5. The expression of Connexin43 in the lung tissue was examined to investigate any possible effects of Peptide5 on pneumocytes. Therefore, the heart and lung specimens obtained from the previous experiments

(Cohorts I, II and III) were used for detailed histological and immunohistological studies. For each of the studies (heart and lung), there were five groups: sham/saline 24 hours (n = 3), SCI/Peptide5 24 hours (n = 3), SCI/scrambled peptide 24 hours (n = 3), SCI/Peptide5 8 hours (n = 3) and SCI/scrambled peptide 8 hours (n = 3) (Table 4.1).

Table 4.1 Summary of the heart and lung samples used for the Connexin43 study.

Specimen	IHC	Condition	Treatment	Survival Time	Cohort
Heart and Lung n = 15 (3 per group)	Connexin43 p-Connexin43	Sham	Saline	24 Hours	I
		SCI	Peptide5	24 Hours	III
		SCI	SP	24 Hours	III
		SCI	Peptide5	8 Hours	II
		SCI	SP	8 Hours	II

IHC: Immunohistochemistry; p-Connexin43: Phosphorylated Connexin43;
SCI: Spinal cord injury; SP: Scrambled peptide

4.2.2.1 Histology on the heart and lung tissue

Approximately 5 × 5 × 3 mm^3 of heart and lung specimens were placed in plastic cassettes and processed through a routine overnight programme (Table 4.2) in a histology processor (Thermo Shandon Excelsior). Paraffin sections were produced at 5 μm in a microtome (Microm HM325) onto Matsunami Platinum PLC-14 glass slides. The slides were incubated at 55 ºC for 20 minutes. Mayer's H&E staining was performed to assess tissue morphology. Slides were immersed in xylene and decreasingly graded ethanol to distilled water. Sections were stained in Mayer's Haematoxylin (Fronine) for 5 minutes and then blued by Scott's Blue (Fronine) for 1 minute to demonstrate the cell nuclei in blue to purple colour. Sections were counterstained with alcoholic Eosin (Fronine) for 3 minutes to highlight the cell

cytoplasm in pink to orange colour. All slides were dehydrated in increasingly graded ethanol and xylene, and mounted with DPX mountant (Sigma-Aldrich).

Table 4.2 The routine overnight processing programme for histology.

Reagent	Temperature (ºC)	Time (minutes)
Formalin	37	240
Formalin	37	240
70% (v/v) Ethanol	25	120
70% (v/v) Ethanol	25	120
95% (v/v) Ethanol	25	120
95% (v/v) Ethanol	25	60
100% (v/v) Ethanol	25	60
100% (v/v) Ethanol	25	60
Xylene	25	60
Xylene	25	60
Xylene	25	60
Paraffin	62	60
Paraffin	62	30
Paraffin	62	30

4.2.1.2 Immunohistochemistry on the heart and lung tissue

The paraffin sections of heart and lung at 5 μm were used for fluorescent immunohistochemistry staining of Connexin43 and phosphorylated Connexin43, as previously described (Section 2.2.12).

4.2.3 Major connexin proteins in the spinal cord tissue

4.2.3.1 Cellular distribution of major connexins in the spinal cord tissue

A lumbar spinal cord specimen (SCI with Peptide5 treatment at 8 hours post-injury from Cohort II) was selected for histological processing, as described in Section 4.2.2.1. The paraffin sections of lumber spinal cord produced at 5 μm were used for the immunohistochemistry co-labelling of Connexin30 and GFAP, Connexin36 and NeuN, Connexin43 and GFAP, as well as Connexin47 and Oligodendrocyte Specific Protein (OSP), to illustrate the distribution of these connexins. Slides were rehydrated in xylene, decreasingly graded ethanol and PBST. Heat-induced antigen retrieval was carried out in citrate buffer (10 mM citric acid, pH 6.0) for 10 minutes in a pressure cooker for Connexin36/NeuN staining. All sections were incubated in blocking agents for 30 minutes (5% (v/v) NGS in PBST for Connexin30/GFAP, Connexin43/GFAP and Connexi47/OSP; 5% (w/v) skim milk for Connexin36/NeuN). The primary antibodies of rabbit anti-Connexin30 (1:250, Thermo Fisher), rabbit anti-Connexin36 (1:250, Thermo Fisher), rabbit anti-Connexin43 (1:2000, Sigma-Aldrich) or rabbit anti-Connexin47 (1:250, Thermo Fisher) were diluted in PBG and incubated overnight at 4 ºC (Table 4.3). After washing in PBST three times, the slides were incubated with secondary goat anti-rabbit Alexa Fluor 568 antibody (Connexin30, 43 and 47, 1:200, Thermo Fisher) or goat anti-rabbit Alexa Fluor 488 antibody (Connexin36, 1:200, Thermo Fisher) in PBG for 2 hours at room temperature (Table 4.3). After washing in PBST five times, the slides were incubated with primary antibodies of rabbit anti-GFAP (1:1000, Dako), mouse anti-NeuN (1:1000, Millipore) or rabbit anti-OSP (1:3000, Abcam) in PBG overnight at 4 ºC (Table 4.3). Following washing in PBST three times, the slides were incubated with the secondary goat anti-rabbit Alexa Fluor 488 antibody

(GFAP and OSP, 1:200, Thermo Fisher) or goat anti-rabbit Alexa Fluor 568 antibody (NeuN, 1:200, Thermo Fisher) in PBG for 2 hours at room temperature (Table 4.3). Slides were then washed with PBST and counterstained by Hoechst (1:5000, Thermo Fisher) for 10 minutes. Primary antibodies were omitted from negative controls. All slides were cover-slipped in fluorescent mounting medium (Dako).

Table 4.3 Summary of antibody characteristics for immunohistochemistry co-labelling of connexins and neural markers.

Primary Antibody	Dilution	Source	Secondary Antibody	Dilution
Rabbit anti-Connexin30	1:250	Thermo Fisher	AF568 anti-rabbit	1:200
Rabbit anti-GFAP	1:2000	Dako	AF488 anti-rabbit	1:200
Rabbit anti-Connexin36	1:250	Thermo Fisher	AF488 anti-rabbit	1:200
Mouse anti-NeuN	1:1000	Millipore	AF488 anti-mouse	1:200
Rabbit anti-Connexin43	1:2000	Sigma-Aldrich	AF568 anti-rabbit	1:200
Rabbit anti-GFAP	1:2000	Dako	AF488 anti-rabbit	1:200
Rabbit anti-Connexin47	1:250	Thermo Fisher	AF568 anti-rabbit	1:200
Rabbit anti-OSP	1:3000	Abcam	AF488 anti-rabbit	1:200

AF: Alexa Fluor; GFAP: Glial fibrillary acidic protein;
Iba1: Ionised calcium-binding adapter molecule 1; NeuN: Neuronal nuclei

4.2.3.1 Quantification of major connexins in the spinal cord tissue

The frozen sections of T10 spinal cord at 15 μm produced from Cohorts II and III were used for immunohistochemistry staining of Connexin30, 36 and 47, in order to quantify any changes in these connexin proteins (Table 4.4). The staining procedures were described as the fluorescent immunohistochemistry of Connexin 43 in Section 2.2.12 with the anti-Connexin30, 36 and 47 antibodies shown in Table 4.5.

Table 4.4 Summary of the spinal cord samples used for quantification of major connexins.

Specimen	IHC	Condition	Treatment	Survival Time	Cohort
		SCI	Peptide5	8 Hours	II
T10 Spinal cord	Connexin30	SCI	SP	8 Hours	II
n = 24	Connexin36	SCI	Peptide5	24 Hours	III
(4 per group)	Connexin47	SCI	SP	24 Hours	III
		Sham	Peptide5	24 Hours	III
		Sham	SP	24 Hours	III

IHC: Immunohistochemistry; SCI: Spinal cord injury; SP: Scrambled peptide

Table 4.5 Summary of antibody characteristics for immunohistochemistry of major connexins.

Primary Antibody	Dilution	Source	Secondary Antibody	Dilution
Rabbit anti-Connexin30	1:250	Thermo Fisher	AF488 anti-rabbit	1:200
Rabbit anti-Connexin36	1:250	Thermo Fisher	AF488 anti-rabbit	1:200
Rabbit anti-Connexin47	1:250	Thermo Fisher	AF488 anti-rabbit	1:200

AF: Alexa Fluor

4.2.4 Imaging and quantification

Imaging was conducted using an Olympus BH-2 light microscope with a PixeLINK Pl-A662 camera (H&E staining) or Olympus BX-51 light microscope with an Olympus U-RFL-T fluorescence burner and appropriate filters (immunohistochemistry staining) used previously (Table 2.2). The black balance was adjusted at the negative control sections to normalise the mean GSV.

Spinal cord sections were aligned using the central canal as an anatomical landmark (midline) for immunohistochemistry analysis. Images were taken adjacent to the lesion and at both 3.5 and 7 mm distal to the lesion centre in both rostral and caudal directions. Image analysis was conducted using ImageJ software (National Institutes of Health, version 2X). Analysis of fluorescent immunohistochemistry was undertaken by measuring the staining intensity, mean GSV, in 20x images. High power images (100x) were taken from the double labelling of connexins and neural markers for visualising the distribution.

4.2.5 Inflammatory effects in plasma

The plasma samples obtained from the 24-hour post-injury groups in Cohort III (n = 8 per group) were used for a multiplex assay to compare cytokines, chemokines and growth factors (Bio-Rad, Bio-Plex Pro™ Rat Cytokine 23-Plex Assay #L8001V11S5). The analytes were 14 cytokines including IL-1α, IL-1β, IL-2, IL-4, IL-5, IL-6, IL-7, IL-10, IL-12, IL-13, IL-17α, IL-18, interferon gamma (IFNγ) and TNFα; 4 chemokines including chemokine (C-X-C motif) ligand 1 (GRO/KC), monocyte chemoattractant protein 1 (MCP-1), chemokine (C-C motif) ligand 5 (RANTES) and Macrophage inflammatory protein 3α (MIP-3A) and five growth factors including granulocyte-colony stimulating factor (G-CSF), granulocyte-macrophage colony-stimulating factor

(GM-CSF), macrophage colony-stimulating factor (M-CSF) vascular endothelial growth factor (VEGF) and erythropoietin (EPO). The following procedures were performed by collaborators (RT and JL) from UNSW. Plasma samples were diluted 1:4 and analysed in duplicates following the manufacturer's instructions. The plates were pre-wetted with wash buffer (Bio-Rad) and loaded with 1 × beads (Bio-Rad). The wells were rinsed by wash buffer (Bio-Rad) two times and then loaded with blank, standards, or samples for one-hour incubation at room temperature with shaking at 850 rpm. Following washing three times, the detection antibodies were added for 30-minute incubation at room temperature with shaking at 850 rpm. The plates were washed 3 times and incubated in streptavidin-phycoerythrin for 10 minutes at room temperature with shaking at 850 rpm. After washing three times, the analytes were resuspended with assay buffer (Bio-Rad) with shaking at 850 rpm for 30 seconds. The plates were read using the Bio-Plex reader (Bio-Rad), and results were converted to a pg/ml concentration for all of the cytokines tested.

4.2.6 Statistical analysis

All data were expressed as mean ± SEM. Unpaired t-test or one-way ANOVA with a Bonferroni *post-hoc* test was used to determine significant differences (PRISM, Version 6.0e, GraphPad). Statistically significant differences were considered at $p < 0.05$. There were no significant differences between rostral and caudal measurements in mean GSV using paired t-test, therefore the mean of rostral and caudal measurements for each sample was used for further analysis.

4.3 Results

4.3.1 Distribution of Peptide5 *in vivo*

All surgical procedures and intraperitoneal injections of FITC-Peptide5 were conducted without incident. None of the rats showed any indication of complications from the SCI surgery or intraperitoneal injection. FITC-Peptide5 was visualised as green fluorescence in the frozen sections (Figure 4.1). There was no evidence that FITC-Peptide5 was distributed in the cervical enlargement of spinal cord, brain, heart and liver tissue in either normal or SCI animals. FITC-Peptide5 was found in the lung, spleen and kidney (cortex and medulla) tissue in both normal and SCI animals. FITC-Peptide5 presented in the T10 segment of spinal cord in the SCI rats, but not the normal uninjured rats. No autofluorescence was observed in the normal organs without any treatment.

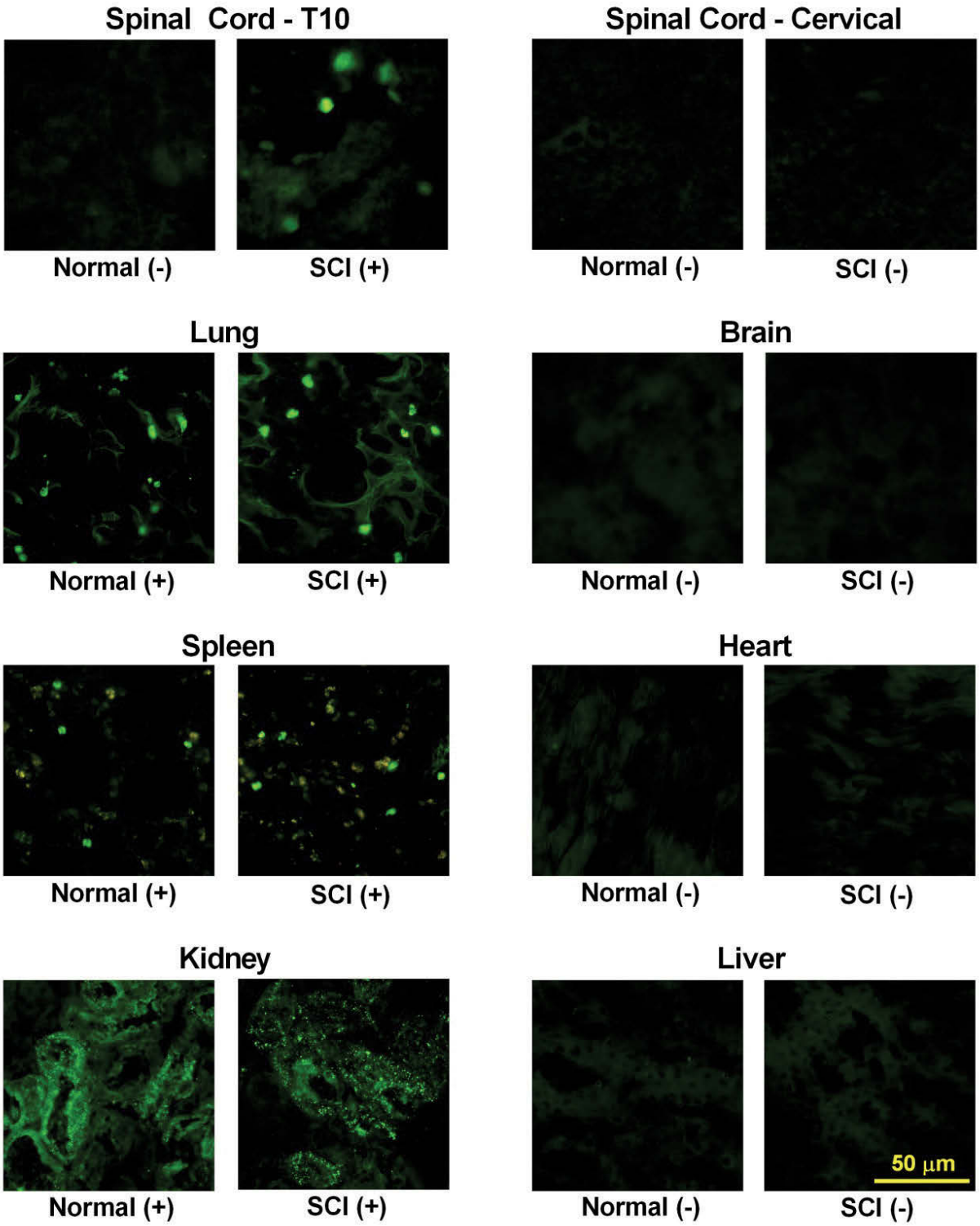

Figure 4.1 Distribution of fluorescein isothiocyanate labelled Peptide5 in normal and spinal cord injury rats.

The fluorescein isothiocyanate (FITC) labelled Peptide5 was shown in green fluorescence. There were no indications of FITC-Peptide5 in the cervical enlargement of spinal cord, brain, heart and liver tissue in either normal or spinal cord injury (SCI) animals. FITC-Peptide5 presented in the lung, spleen and kidney tissue in both normal and SCI animals. At the T10 segment of spinal cord, FITC-Peptide5 was found in the SCI rats, but not the normal rats.

4.3.2 Connexin43 protein in the heart tissue

The heart sections stained by Mayer's H&E showed the histological characters of cardiac muscle: single central nuclei, branching cell shape and striation (Figure 4.2A). There was no evidence to indicate any differences in the histological morphology of heart tissue between groups. Fluorescent immunohistochemistry staining demonstrated the Connexin43 (Figure 4.2B) and phosphorylated Connexin43 at residue Ser368 (Figure 4.2C) proteins in the heart tissue. The immunoreactivity levels of Connexin43 and phosphorylated Connexin43 were measured by mean GSV for statistical analysis. There were no statistically significant differences in the immunohistochemistry labelling intensity of Connexin43 (36.06 ± 9.32) between groups (Figure 4.2D). Similarly, no significant differences were found in the immunohistochemistry staining intensity of Connexin43 phosphorylation at residue Ser368 (18.86 ± 3.73) between groups using two-way ANOVA analysis (Figure 4.2E).

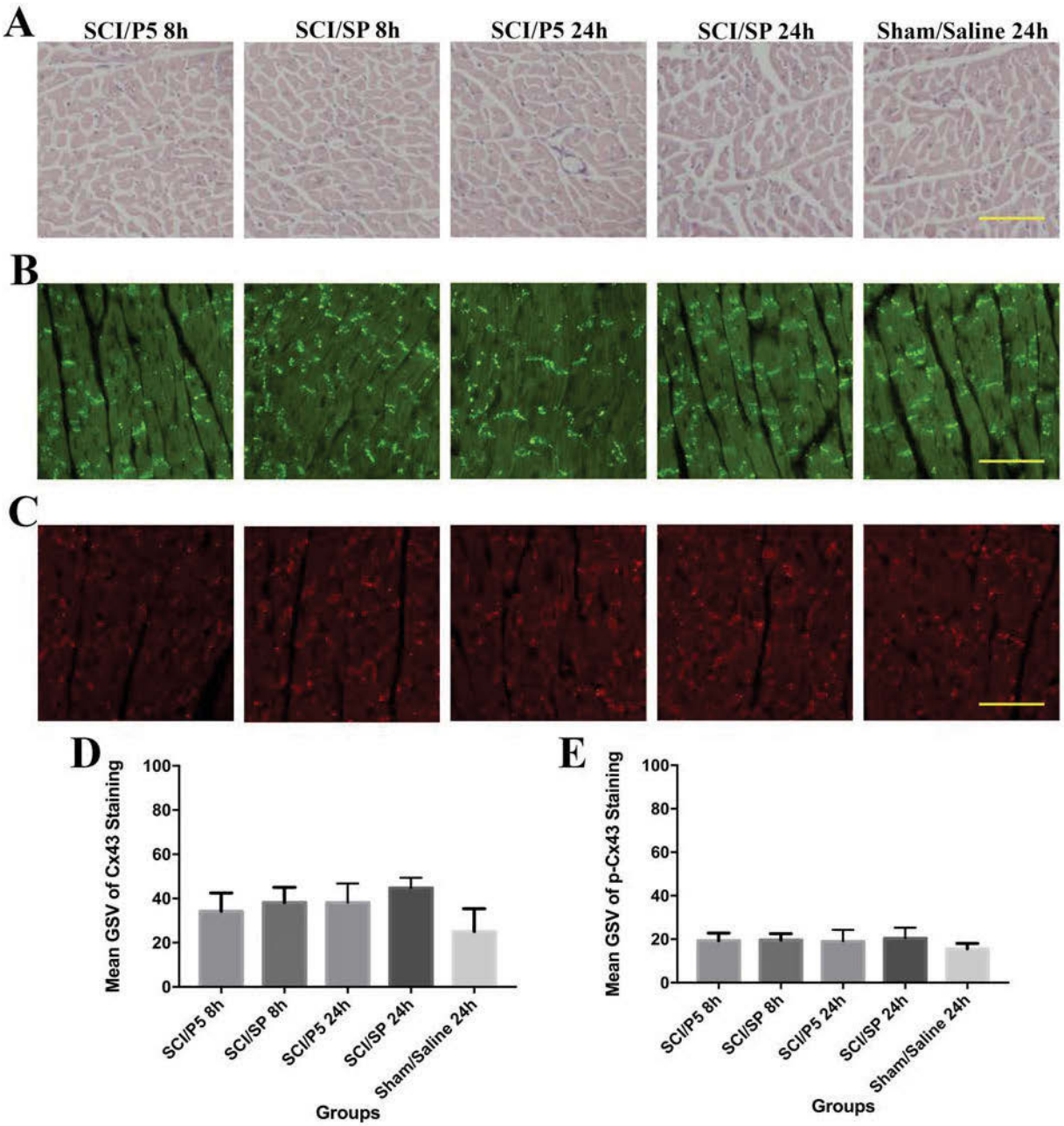

Figure 4.2 Histological morphology and the immunohistochemistry staining of Connexin43 and phosphorylated Connexin43 in the heart tissue.
(A) Mayer's Haematoxylin and Eosin staining showed no differences in the histological morphology of cardiac muscle between groups. Scale bar = 150 μm. (B) Representative images of fluorescent immunohistochemistry staining showed the Connexin43 (green) in the heart tissue. Scale bar = 150 μm. (C) Representative images of fluorescent immunohistochemistry staining showed the Connexin43 phosphorylation at residue Ser368 (red) in the heart tissue. Scale bar = 150 μm. (D) Immunohistochemistry analysis showed no statistically significant differences in the level of Connexin43 immunoreactivity in the heart tissue between groups. (E) Immunohistochemistry analysis showed no statistically significant differences in the level of phosphorylated Connexin43 immunoreactivity in the heart tissue between groups. (GSV: greyscale value; P5: Peptide5; p-Connexin43: phosphorylated Connexin43; SCI: spinal cord injury; SP: control scrambled peptide)

4.3.3 Connexin43 protein in the lung tissue

The lung sections stained by Mayer's H&E staining showed the histological characteristics of alveolar tissue: alveolar wall lined by type 1 pneumocytes (squamous epithelial cells) and type 2 pneumocytes (cuboidal epithelial cells), as well as alveolar macrophages found in the alveolar ducts and sacs (Figure 4.3A). In particular, the thickness of the alveolar wall and the number of erythrocytes were significantly increased compared with that expected in normal rats (Abdelaziz et al., 2016, Gauter-Fleckenstein et al., 2014, van den Brule et al., 2014). The alveolar wall was also partially incomplete in all lung samples. There was no evidence of any differences in the histological morphology of lung tissue between groups. Fluorescent immunohistochemistry staining was not able to detect the Connexin43 protein in the lung tissue (Figure 4.3B), so no further fluorescent immunohistochemistry staining of Connexin43 phosphorylation at residue Ser368 was conducted in the lung tissue.

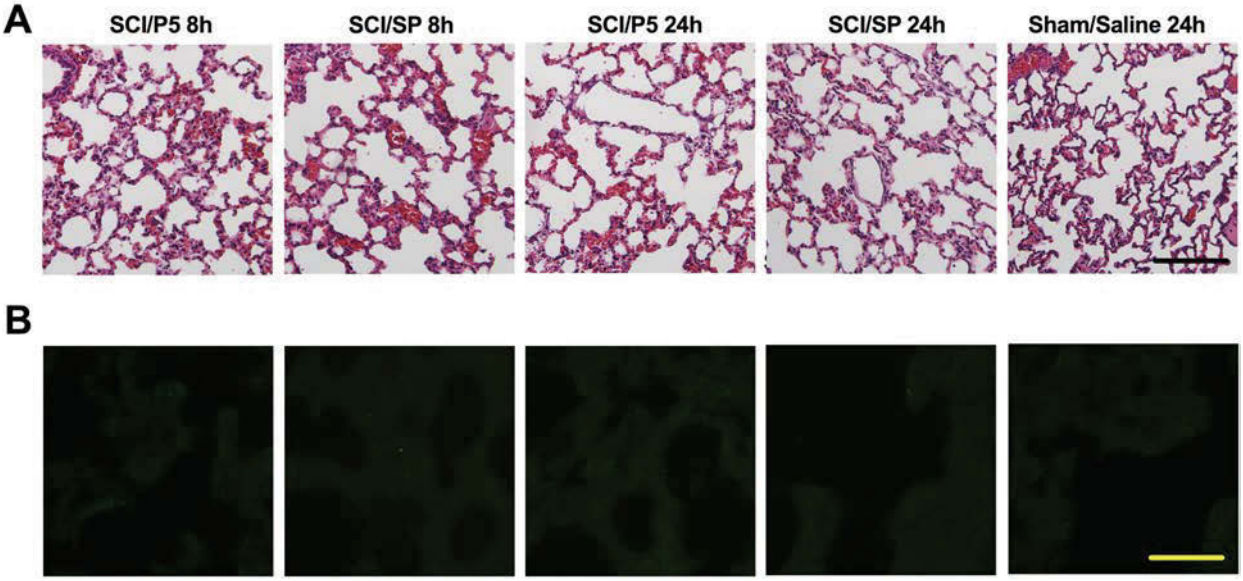

Figure 4.3 Histological morphology and the immunohistochemistry staining of Connexin43 in the lung tissue.
(A) Mayer's Haematoxylin and Eosin staining showed no differences in histological morphology of alveolar tissue between groups. Scale bar = 150 μm. (B) Fluorescent immunohistochemistry staining failed to detect the Connexin43 protein in the lung tissue. Scale bar = 150 μm. (P5: Peptide5; SCI: spinal cord injury; SP: control scrambled peptide)

4.3.4 Major connexin proteins in the spinal cord tissue

The immunohistochemistry co-labelling of Connexin43 and GFAP, Connexin30 and GFAP, Connexin36 and NeuN, as well as Connexin47 and OSP was performed to determine the location of Connexin43, 30, 36 and 47 respectively in the rat spinal cord. The Connexin30 and 43 expression was found to be associated with astrocytes and their processes labelled by GFAP. Neuronal cells labelled by NeuN co-expressed Connexin36 protein in the spinal cord (Figure 4.4). The Connexin47 expression was found to be associated with oligodendrocytes and their processes labelled by OSP. The expression levels of Connexin30, 36 and 47 were then further analysed in the frozen spinal cord sections at 8 and 24 hours following injury.

The protein levels of Connexin30, 36 and 47 were measured by mean GSV of immunohistochemistry labelling intensity in both grey and white matter at 3.5 and 7 mm distal to the lesion centre and the epicentre of the lesion. At all anatomical locations, there were no statistically significant differences in Connexin30 protein levels between groups in both grey (7 mm: 31.28 ± 3.14, 3.5 mm: 30.67 ± 3.08, Epicentre: 35.38 ± 4.27) and white matter (7 mm: 17.19 ± 2.00, 3.5 mm: 17.50 ± 2.43, Epicentre: 17.35 ± 2.69) (Figure 4.5). The expression levels of Connexin36 were not significantly different between groups in both grey (7 mm: 21.26 ± 1.91, 3.5 mm: 21.11 ± 1.99, Epicentre: 21.55 ± 1.88) and white matter (7 mm: 10.82 ± 1.35, 3.5 mm: 11.11 ± 1.45, Epicentre: 11.78 ± 1.11) (Figure 4.6). Similarly, there were no statistically significant differences found in Connexin47 protein levels between groups in both grey (7 mm: 35.56 ± 1.40, 3.5 mm: 35.64 ± 1.70, Epicentre: 35.37 ± 2.13) and white matter (7 mm: 23.52 ± 1.39, 3.5 mm: 23.22 ± 1.26, Epicentre: 22.31 ± 2.72) (Figure 4.7).

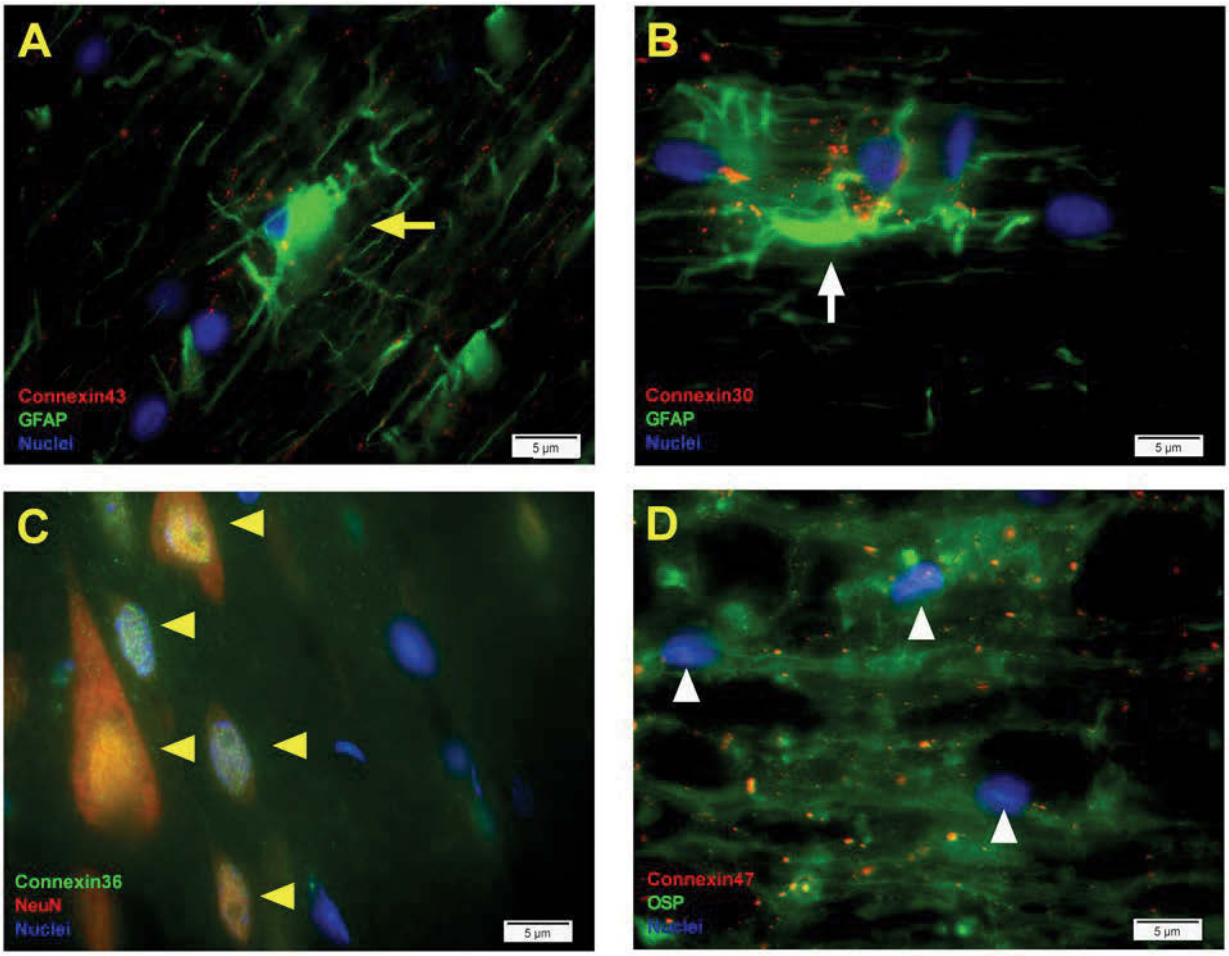

Figure 4.4 Immunohistochemistry co-labelling of major connexin proteins and neural markers at 8 hours following spinal cord injury.
(A) Connexin43 protein (red) was associated with astrocytes (yellow arrow) labelled by glial fibrillary acidic protein (GFAP) (green). (B) Connexin30 protein (red) was associated with astrocytes (white arrow) labelled by GFAP (green). (C) Neurons (yellow arrow heads) labelled by neuronal nuclear antigen (NeuN) (red) was co-labelled with Connexin36 protein (green). (D) Connexin47 protein (red) was associated with oligodendrocytes (white arrow heads) labelled by oligodendrocyte specific protein (OSP) (green). All nuclei were counterstained by Hoechst in blue.

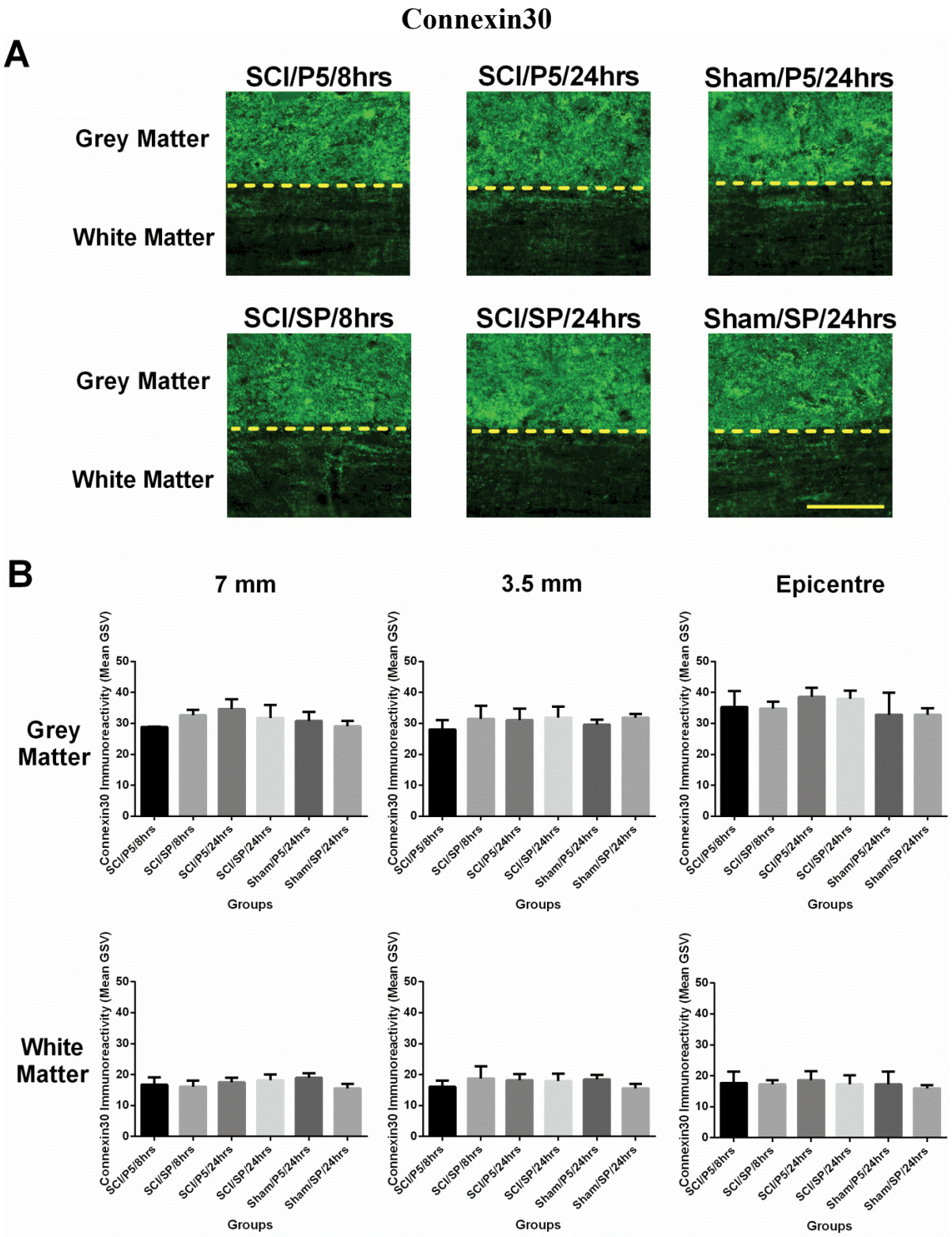

Figure 4.5 Immunohistochemistry staining of Connexin30 in rat spinal cord at 8 and 24 hours following injury.

(A) Representative images of Connexin30 immunofluorescence (green) at the epicentre of the lesion. Scale bar = 40 μm. (B) Immunohistochemistry analysis showed the Connexin30 protein levels in both grey and white matter at 3.5 and 7 mm distal to the lesion centre and the epicentre of the lesion. At all locations, there were no statistically significant differences in the Connexin30 levels between groups. (GSV: greyscale value; P5: Peptide5; SCI: spinal cord injury; SP: control scrambled peptide)

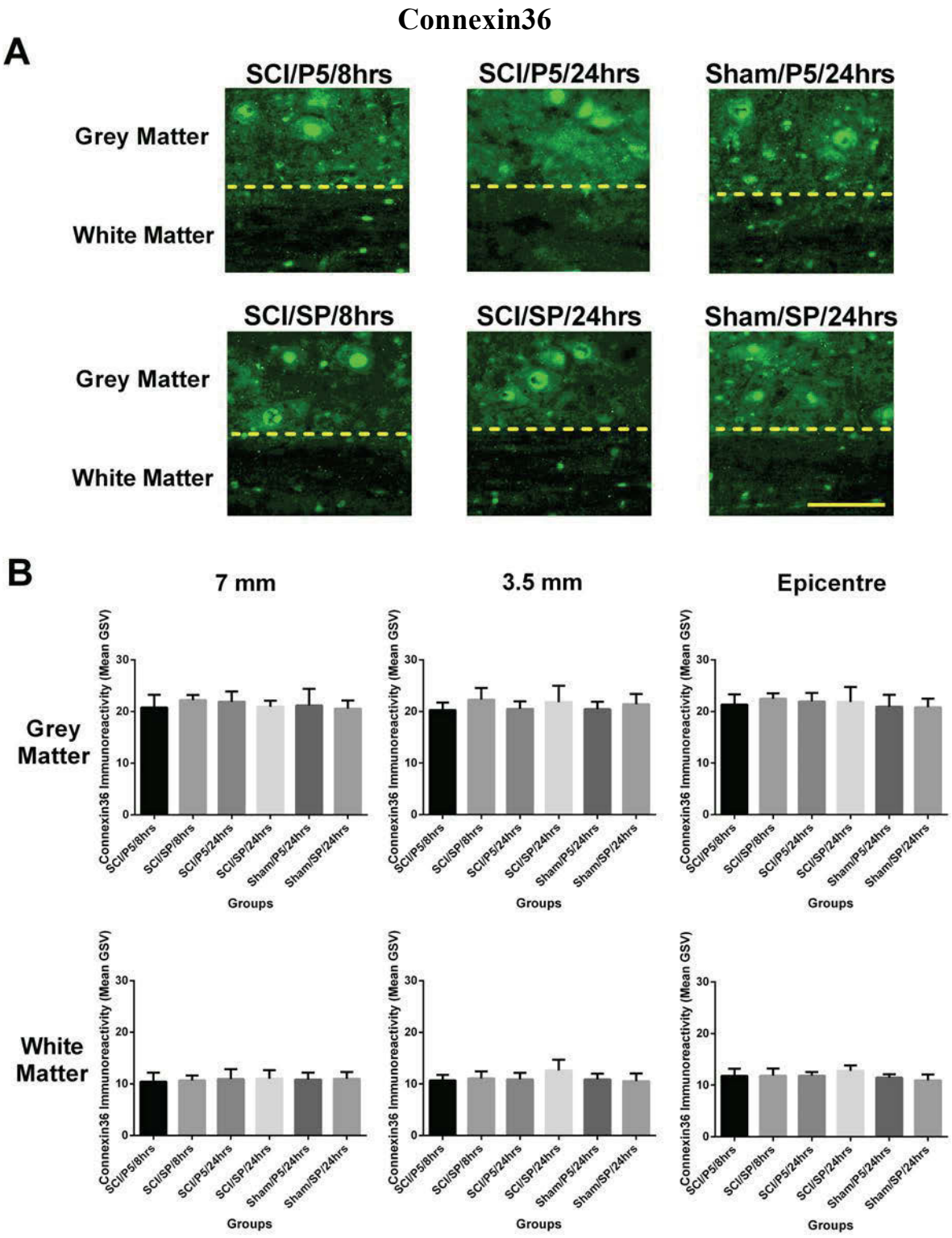

Figure 4.6 Immunohistochemistry staining of Connexin36 in rat spinal cord at 8 and 24 hours following injury.

(A) Representative images of Connexin36 immunofluorescence (green) at the epicentre of the lesion. Scale bar = 40 μm. (B) Immunohistochemistry analysis showed the Connexin36 protein levels in both grey and white matter at 3.5 and 7 mm distal to the lesion centre and the epicentre of the lesion. At all locations, there were no statistically significant differences in the Connexin36 levels between groups. (GSV: greyscale value; P5: Peptide5; SCI: spinal cord injury; SP: control scrambled peptide)

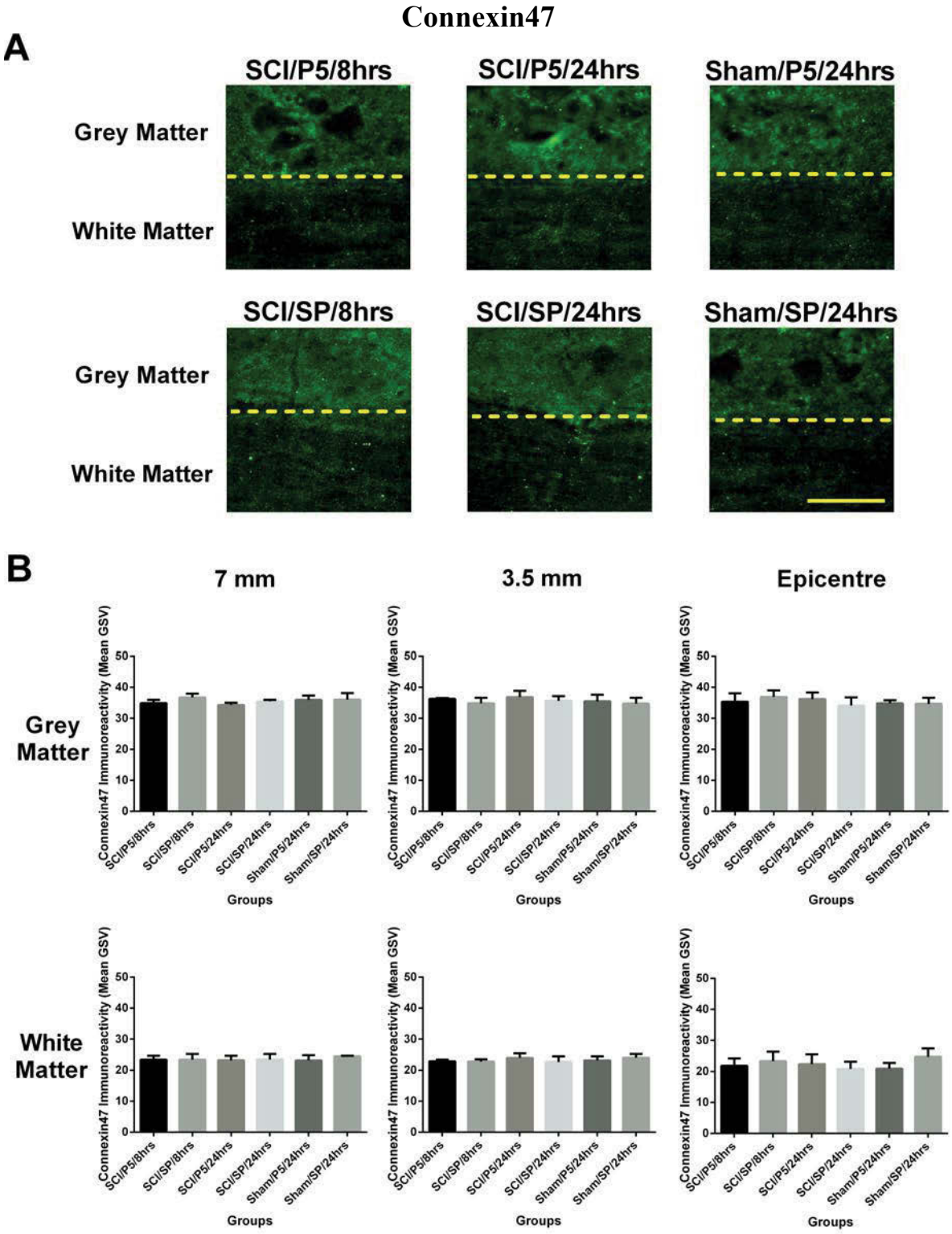

Figure 4.7 Immunohistochemistry staining of Connexin47 in rat spinal cord at 8 and 24 hours following injury.

(A) Representative images of Connexin47 immunofluorescence (green) at the epicentre of the lesion. Scale bar = 40 μm. (B) Immunohistochemistry analysis showed the Connexin47 protein levels in both grey and white matter at 3.5 and 7 mm distal to the lesion centre and the epicentre of the lesion. At all locations, there were no statistically significant differences in the Connexin47 levels between groups. (GSV: greyscale value; P5: Peptide5; SCI: spinal cord injury; SP: control scrambled peptide)

4.3.5 Inflammatory effects in plasma

Following the multiplex assay on the rat plasma, there were nine analytes (IL-5, IL-18, RANTES GRO/KC, MCP-1, MIP-3A, EPO, M-CSF and VEGF) with detectable values (Table 4.6). No significant differences were detected between groups for any of the analytes using one-way ANOVA. The mean concentrations for each of the analytes were 17.39 ± 23.06 pg/ml, 832.83 ± 874.17 pg/ml, 438.88 ± 301.33 pg/ml, 65.40 ± 36.87 pg/ml, 2918.17 ± 1017.62 pg/ml, 110.82 ± 94.26 pg/ml, 910.69 ± 897.56 pg/ml, 285.24 ± 73.39 pg/ml and 28.45 ± 8.34 pg/ml respectively. The rest of analytes were below the detection range.

Table 4.6 Comparison of cytokines, chemokines and growth factors in rat plasma.

Group	Cytokines (pg/ml)		Chemokines (pg/ml)				Growth factors (pg/ml)		
	IL-5	IL-18	RANTES	GROKC	MCP-1	MIP-3A	EPO	M-CSF	VEGF
Sham P5	15.45 ±19.3	665.32 ±410.95	557.39 ±154.04	73.79 ±45.54	3611.07 ±1131.33	77.58 ±55.71	979.24 ±1171.65	293.96 ±78.17	28.46 ±10.98
Sham SP	20.58 ±22.43	1355.64 ±513.35	406.40 ±361.29	66.80 ±26.37	3201.20 ±606.39	76.690 ±55.22	1305.92 ±879.92	296.92 ±67.46	29.64 ±7.72
SCI P5	28.38 ±6.08	736.24 ±434.68	525.46 ±108.66	79.17 ±22.45	2400.42 ±925.75	151.44 ±141.11	688.42 ±667.94	270.78 ±68.64	28.38 ±7.99
SCI SP	15.17 ±33.42	574.12 ±713.69	266.29 ±419.72	41.85 ±42.57	2460.00 ±945.97	137.59 ±89.35	669.20 ±817.03	279.32 ±89.23	27.34 ±7.82

EPO: Erythropoietin; GROKC: Chemokine (C-X-C motif) ligand 1; IL: Interleukin;
MCP-1: Monocyte chemoattractant protein 1; MIP-3A: Macrophage inflammatory protein 3α;
M-CSF: macrophage colony-stimulating factor; P5: Peptide5; SCI: Spinal cord injury;
SP: Scrambled peptide; RANTES: Chemokine (C-C motif) ligand 5;
VEGF: Vascular endothelial growth factor

4.4 Discussion

The data presented here provides an indication of the safety profile of the Peptide5 via acute systemic administration as a treatment option for traumatic SCI. It has been demonstrated that Peptide5 via systemic delivery reaches the lesion area of the spinal cord without entering the non-injured tissue in the CNS of both SCI and normal animals. Additionally, there was no evidence that the acute systemic administration of Peptide5 modulates Connexin43 protein expression or hemichannel closure in the heart and lung tissue of SCI animals. The expression levels of other major connexin proteins including Connexin30 on astrocytes, Connexin36 on neurons and Connexin47 on oligodendrocytes were not altered by the systemic delivery of Peptide5 in the injured and the non-injured spinal cords. Further, there was no evidence that the systemic delivery of Peptide5 affects the levels of cytokines, chemokines and growth factors in the plasma. Together, the findings of this chapter indicate that the acute systemic administration of Peptide5 does not cause any systemic adverse effects in control and SCI animals.

As anticipated, systemic administration can deliver Peptide5 to the lesion area of the spinal cord. Following a traumatic event to the spinal cord, the capillary bed at the lesion area is compromised (Figley et al., 2014, Soubeyrand et al., 2014). This provides an opportunity for Peptide5 leaking from the disrupted blood vessels from the vascular system. The permeability of BSB is significantly increased following traumatic SCI (Bilgen et al., 2002, Popovich et al., 1996, Gordh et al., 2006). Consequently, Peptide5 may infiltrate into the spinal tissue in the case of minor injury with little disruption to the BSB. In the normal physiological condition, the selective permeability of the blood brain and/or spinal cord barrier prevents small molecules (< 10 kDa) from entering the CNS tissue (Habgood et al., 2007, Popovich et al., 1996); as shown in the current study,

the FITC-labelled Peptide5 (~2 kDa) was not detected in the non-injured tissue of the CNS.

Peptide5 is synthesised to mimic the sequence on the extracellular loop 2 of Connexin43 without matching any sequence in any other connexin proteins (Kim et al., 2017). As expected, systemic administration of Peptide5 has been shown to successfully regulate Connexin43 protein expression levels and hemichannel closure in the injured spinal cord (Chapter 2) without affecting the expression levels of Connexin 30, 36 and 47 in the current study. Connexin30, abundantly expressed on astrocytes, is found in astrocyte/astrocyte gap junctions (Rash et al., 2001, Nagy et al., 1999) and has not been reported to be changed in the spinal cord following traumatic injury. In the current study, there was no evidence that the Connexin30 expression levels and patterns altered in response to SCI or Peptide5 treatment, indicating that Connexin30 did not seem to compensate or adapt to the suppression of Connexin43. Even though the expression of Connexin30 and 43 is tightly regulated by neurons (Koulakoff et al., 2008), further studies are required to reveal the interaction and relationship between the two main astrocytic connexins. Connexin36 is the major connexin found in neuron/neuron gap junctions (Rash et al., 2000, Rash et al., 2001, Lee et al., 2005). The current study demonstrated that its expression surrounding the lesion in the spinal cord did not alter in response to traumatic injury as shown by Lee et al. (2005), nor by the Peptide5 treatment. However, Yates et al. (2008) observed a downregulation of Connexin36 protein at the lumber enlargement distant to the injury area at 7 days after a complete T10 transection in rats. The change in Connexin36 protein below the lesion level, in association with decreased electrical coupling, has been suggested to contribute to hyperreflexia and spasticity after SCI (Yates et al., 2008, Yates et al., 2011). The effect of Peptide5 distal to the lesion was not specifically examined in the current study, as the

spinal cord segment at the lumber enlargement was not collected in all animals. Connexin47, localised to oligodendrocytes, is shown to dock with Connexin43 on astrocytes in astrocyte/oligodendrocyte gap junctions (Kamasawa et al., 2005, Li et al., 2004, Kleopa et al., 2004). The alteration of Connexin47 expression has not been reported following a traumatic event on the spinal cord, despite increased expression of Connexin43 on astrocytes. This may suggest that the upregulated Connexin43 following SCI composes the gap junctions between astrocytes rather than astrocyte and oligodendrocyte.

To date, the alteration of Connexin30, 36 and 47 expression has not been studied extensively. Masaki et al. (2012) observed a marked downregulation of Connexin47, as well as two other major connexins on astrocytes (Connexin32 and 43) in Baló's disease (a rare demyelinating disorder of the CNS). However, the mutation of these connexin genes (GJB6 for Connexin30, GJD2 for Connexin36 and GJC2 for Connexin47) has been found in several disorders. Connexin30, in association with Connexin26, is the predominant gap junction protein in the cochlea, and its defects lead to certain forms of hearing impairment (del Castillo et al., 2002, Amorini et al., 2015, Pandey et al., 2016, Teubner et al., 2003, Schütz et al., 2010). The expression of Connexin30 is also found in the upper differentiated epidermal layer of the skin (Di et al., 2001) and a novel mutation of Connexin30, p.N54K, has just been suggested to cause a series of skin anomalies such as pes planus, ichthyosis, cutaneous nodules, and keratoderma, due to the restricted transfer of neurobiotin (Pandey et al., 2016). Connexin36 plays an important role in the coupling of pancreatic beta cells to mediate the expression and release of insulin (Nlend et al., 2012, Serre-Beinier et al., 2009, Cigliola et al., 2013, Lebreton et al., 2015). Recently, its genetic variation has been implicated in the dysfunction of insulin production (Cigliola et al., 2016, Nlend et al., 2012). As

Connexin47 is associated with myelination on oligodendrocytes (Kamasawa et al., 2005), its mutation has been linked to Pelizaeus–Merzbacher-like disease, a delayed myelination disorder characterised by early-onset nystagmus, delayed motor milestones, progressive spasticity, ataxia and diffuse leukodystrophy (Diekmann et al., 2010, Meyer et al., 2011).

There was no evidence of Peptide5 entering the heart tissue, indicating that Peptide5 remains in the vascular system rather than affecting the Connexin43 hemichannels on the cardiomyocytes. This was further confirmed by the immunohistochemistry studies, showing that both Connexin43 protein and phosphorylation (hemichannel closure) levels in the heart tissue did not differ between Peptide5 treatment and controls at both 8 and 24 hours following SCI. Although Peptide5 has been used for other indications, such as retinal ischaemia (Chen et al., 2015, Chen et al., 2014b, Danesh-Meyer et al., 2012), cerebral ischaemia (Davidson et al., 2012b) and an epileptiform lesion model (Yoon et al., 2010), its effect targeting the Connexin43 hemichannels on cardiomyocytes has not been reported. Another Connexin43 mimetic peptide, Gap26 (sequence VCYDKSFPISHVR), is synthesised to modulate Connexin43 hemichannels on cardiomyocytes. It has been shown to protect the intact heart against ischaemia reperfusion injury *ex vivo* (Hawat et al., 2010) and the ischemic heart against myocardial infarction *in vivo* (Hawat et al., 2012). Therefore, it is more likely that Peptide5, via systemic delivery, may also have protective effects in the ischaemic and infarcted heart tissue without adverse impacts on the normal heart tissue.

Peptide5, via systemic delivery, is not expected to enter or affect the lung tissue *in vivo*, as Connexin43 expression has not been reported in pneumocytes (Chang et al., 2013, Rottlaender et al., 2010, Ishikawa et al., 2012, Márquez-Rosado et al., 2012). In the current study, Connexin43 was not detected in the lung sections by the fluorescent

immunohistochemistry staining. The abnormal histological morphology shown by H&E staining (thick and incomplete alveolar wall and increased number of erythrocytes) indicated the lung tissue had not been preserved well for histological studies during the tissue collection. As all the animals were cardiac perfused by heparinised saline and 4% (w/v) paraformaldehyde for rinsing and fixing the spinal cords, the strong flow of liquids might burst the capillary in the lung tissue, leading to a leakage of erythrocytes and Peptide5 into the alveoli, as shown in the FITC-Peptide5 experiment. This can possibly be improved by conducting the intra-tracheal inflation to maintain the alveolar and endothelial structure instead of cardiac perfusion before dissection (Hayatdavoudi et al., 1980). There is no solid evidence that Peptide5, via systemic administration, causes any adverse effect on the lung tissue and function.

FITC-labelled Peptide5 was found in the spleen and kidney tissue as expected. The spleen, a critically important immune organ combining both innate and adaptive immunities, is responsible for capturing and destroying pathogens and foreign bodies, to enable its efficient removal process (Mebius and Kraal, 2005, Cesta, 2006). Peptide5, as a foreign body, was detected by the antigen-presenting cells in the spleen, such as dendritic cells, and subsequently cleared by phagocytes, such as macrophages (Lopes‐Carvalho and Kearney, 2004, van Rooijen, 1990, Eloranta and Alm, 1999). However, Peptide5 could also be filtered through the glomeruli into urine, as the high permeability of the glomerular capillary wall allows the molecules smaller than albumin to pass into the filtrate (Venkatachalam and Rennke, 1978, Lund et al., 2003, Sandoval et al., 2012). Similarly, a few recent studies of tissue distribution observed the accumulation of other pharmaceutical and biological agents in the spleen and their excretion through urine (Jasim et al., 2015, Liang et al., 2013, Cho et al., 2013, Baek et al., 2012, Aubert et al.,

2012). Peptide5 was also likely to be degraded by the immune response in the spleen, and then cleared out via urinary excretion.

Although Connexin43 is expressed by human peripheral blood lymphocytes (Bermudez-Fajardo et al., 2007, Oviedo‐orta et al., 2000), the current study demonstrates that there were no obvious systemic immunomodulatory effects, as measured by cytokine and chemokine profile in plasma, following intraperitoneal injection of Peptide5. Prior to clinical translation further toxicity studies will be required to determine if peptide5 cause any subtler immunomodulatory changes. However, it has been previously shown that IL-1β and TNFα are significantly up regulated in spinal cord itself after injury (O'Carroll et al., 2013), and other reports indicate that VEGF can be either up regulated (Nesic et al., 2010) or down regulated (Herrera et al., 2009) after SCI. This does not appear to translate to significant changes in plasma cytokines, however, at least at the 24 hours post-injury time point.

In the current research project, no evidence has been found of any systemic effects from the vascular injection of Peptide5. Neither the sham animals treated with Peptide5 nor the animals treated with SP showed any evidence of adverse effects in this study or in other studies using Peptide5 (Davidson et al., 2012a, Danesh-Meyer et al., 2012). Further, there were no statistically significant differences between Peptide5 and SP-treated sham animals in all the molecular, cellular and behavioural analyses. It is suggested that Peptide5 rarely travels to the uninjured tissue, nor should it act globally on gap junctions in other organs at the low concentration used in the current study. Certainly, higher doses may prove deleterious, and this has been shown to be the case in a foetal model of ischaemia in sheep (Davidson et al., 2013b). Future studies must determine the long-term effects of Peptide5 treatment on the injured spinal cord and

other uninjured tissue. Additionally, the systemic effects of Peptide5 have not been reported in any *in vivo* models when delivered locally (Chen et al., 2015, Chen et al., 2014b, Danesh-Meyer et al., 2012, O'Carroll et al., 2013, Davidson et al., 2015, Davidson et al., 2013a, Davidson et al., 2013b, Davidson et al., 2014). Similarly, Hawat et al. (2012) intravenously injected another Connexin43 mimetic peptide, Gap26, into rats with myocardial infarction, and did not report any systemic or adverse events.

Over the past 25 years, there have been more than 14 different types of animal models to replicate SCI in humans as closely as possible. With various strengths and weakness, no one model can encompass all aspects of injury due to the complexity of human SCI (Cheriyan et al., 2014). A number of factors are taken into account for selecting the most appropriated model for SCI study, such as focus of study, animal species and methods of behavioural assessment. The transection models are easy to produce consistent and reliable injury for axonal regeneration studies, but they do not mimic the common clinical SCI type (Cheriyan et al., 2014). Despite of the relatively imprecise duration of impaction, the contusion models have been widely used to produce validated SCI for studying tissue and behavioural improvements (Cheriyan et al., 2014). However, this rat model of SCI does not mimic the multisystem trauma often experienced after motor vehicle accidents. Clearly, this is a very important factor that would need to be considered carefully in the clinical setting. The systemic delivery of Peptide5 to regulate Connexin43 hemichannels is more likely to be beneficial after a traumatic event to multiple systems, especially the brain and heart. Connexin43 mimetic peptides, including Peptide5, have been reported to regulate Connexin43 hemichannels, and leading to the restriction of lesions in cardiovascular injury (Hawat et al., 2010, Hawat et al., 2012, Ongstad et al., 2013, Wang et al., 2013). Connexin43 mimetic peptides have been shown to be neuroprotective in a few models of ischaemic injury (Glass et al.,

2015, Chen et al., 2015, Danesh-Meyer et al., 2012, Davidson et al., 2013a). It is believed that Peptide5 would also function in the same way in SCI to reduce the secondary injury of brain tissue, although the application of Connexin43 mimetic peptides has barely been explored in traumatic brain injury. It is less likely that Peptide5 has any effect on other major organs such as the lung, kidney, liver, spleen and pancreas, as currently there is no evidence of the expression of Connexin43 in these organs. It is clear that the acute systemic administration of Peptide5 is less likely to incur deleterious effects on a non-injured spinal cord, other major organs and systemic inflammatory responses, and thus is more likely to be a safe treatment option for traumatic SCI.

Chapter 5

General Discussion

5.1 Project summary

Within hours after traumatic SCI, it is commonly accepted that Connexin43 hemichannels are implicated in ATP release, lesion spread, neuronal cell loss and inflammation, with subsequent astrogliosis formation limiting functional recovery and developing chronic pain. Therefore, modulation of the Connexin43 hemichannels becomes an attractive therapeutic approach for SCI. In an effort to halt the pathological opening of Connexin43 hemichannels, different agents or molecules that target various recognition sites, such as AS-ODN and mimetic peptides, have been developed and validated in the regulation of Connexin43 gap junctional communication. As one of the most promising candidates, Peptide5 has been designed to mimic the sequences in the extracellular loop of Connexin43 protein, and has shown striking efficacy in modulating gap junction-mediated intercellular communication in SCI animal models (O'Carroll et al., 2013, O'Carroll et al., 2008) and several nerve injury models (Danesh-Meyer et al., 2012, Davidson et al., 2013a, Davidson et al., 2012a, Chen et al., 2015, Chen et al., 2014b, Davidson et al., 2014). Especially following a traumatic SCI, Peptide5 via local delivery has resoundingly demonstrated its ability in limiting lesion spread, astrogliosis formation, inflammatory responses and neuronal cell loss, as well as improving functional recovery, as shown in previous studies (O'Carroll et al., 2013). Despite success in neuroprotection by interfering with the Connexin43 upregulation and the pathological opening of hemichannels following SCI, the administration route of Peptide5 is still of major concern for researchers and clinicians. Local administration requires a highly invasive surgical procedure immediately following a trauma. This would significantly delay the application of Peptide5 and thus miss the window of opportunity for modulating the pathological opening of Connexin43 hemichannels within hours of injury. Peptide5 has the potential to be delivered systemically to reach

the lesion area, particularly to the sites where the capillary bed has been compromised, as in the injured spinal cord (Cronin et al., 2008, Mautes et al., 2000a). Accordingly, the current research project was conducted to demonstrate that the systemic administration of Peptide5 is a feasible, neuroprotective and safe treatment option for SCI using a rat model of contusion SCI.

To justify this hypothesis, the first study was performed to optimise the systemic administration protocol of Peptide5 for traumatic SCI (Chapter 2). The electrophoresis experiments demonstrated the gradual degradation of Peptide5 in normal rat and human sera to reveal the *in vitro* half-life of Peptide5 as 2 and 4 hours in rats and humans respectively. From this, the dosing regimen for the Peptide5 systemic administration was determined as the initial dose at 10 mg/kg immediately following SCI (pre-established by collaborators at the University of Auckland), the second dose at 5 mg/kg 2 hours after injury and the third dose at 2.5 mg/kg 4 hours after injury. Using the first animal cohort of SCI, the *in vivo* dosing responses at 24 hours after injury confirmed that triple injections of Peptide5 emerged as the most effective dosing regimen in supressing Connexin43 upregulation and maintaining Connexin43 phosphorylation (closed hemichannels), compared with single and double injections. The second animal cohort of contusion injury was utilised to demonstrate that Peptide5, via systemic administration, was able to reach the lesion area for regulating the Connexin43 expression and its hemichannel opening at 8 hours following SCI. Therefore, three doses of Peptide5 systemic administration were utilised to investigate its efficacy in SCI animals.

The third animal cohort of contusion SCI was used to explore the cellular and functional improvements from the Peptide5 acute systemic administration, compared with the SP control treatment (Chapter 3) (Mao et al., 2017). The lesion size was significantly

reduced by Peptide5 at 24 hours, 2 and 6 weeks post-injury. At the early time point (24 hours), the Peptide5 treatment has been demonstrated to restrict the Connexin43 upregulation and maintain the Connexin43 phosphorylation (hemichannel closure). At the later time points (2 and 6 weeks), astrogliosis formation, activated macrophage and/or microglial response and neuronal cell loss were all decreased in the injured animals treated with Peptide5. More importantly, Peptide5 treated rats showed significant improvements in hind limb locomotor function between 3 and 6 weeks post-injury, and reductions in at-level pain at 1 and 6 weeks post-injury. In line with the previous study employing local delivery (O'Carroll et al., 2013), these findings provided strong *in vivo* data supporting the benefits of systemic delivery of Peptide5 in reducing secondary injury and improving functional recovery.

An additional study was conducted to complete the safety profile of the acute systemic administration of Pepticde5 (Chapter 4). In the fourth animal cohort of contusion SCI, a fluorescence label was used to locate the *in vivo* distribution of Peptide5, and there was no evidence to suggest Peptide5, via systemic delivery, entered the heart, liver, brain or uninjured spinal cord. As Connexin43 is also found on cardiomyocytes (Hawat et al., 2010, Hawat et al., 2012, Ishikawa et al., 2012, Clarke et al., 2009), the Connexin43 protein and phosphorylation levels were examined, and it was determined that Peptide5 delivered systemically did not regulate Connexin43 or its hemichannels in uninjured heart tissue. Additionally, no significant changes were observed in other major connexins expressed in the spinal cord, including Connexin30 on astrocytes, Connexin36 on neurons and Connexin47 on oligodendrocytes. These findings indicate that the acute systemic administration of Peptide5 did not cause any systemic effects in control and SCI animals.

The current research sheds new light on the beneficial role of systemic administration of Peptide5, a Connexin43 mimetic peptide, for SCI. To our knowledge, this is the first study demonstrating that Peptide5 can be delivered systemically to the lesion area for reducing the secondary injury, without causing marked adverse effects in other uninjured tissue following SCI. This strategy itself is not thought to promote neural repair and regeneration. If the injury can be limited by Peptide5 in the early stages, this will lead to a reduction of functional deficits, and provide a more suitable microenvironment for later neuroregenerative intervention. This pre-clinical research has successfully determined the administration protocol, therapeutic efficacy and safety profile of Peptide5 in a rat SCI model, thus providing support for the translation to human clinical trials. Therefore, the acute systemic administration of Peptide5 is a potentially novel therapy for reducing secondary damage and improving functional recovery for traumatic SCI.

5.2 Future directions

The current research raises several questions and opens new avenues of research in the laboratory. There are a number of avenues of research that could yet be explored including:

1) Mechanism of action. Future studies are required to investigate the mechanism of action of Peptide5 in modulating the Connexin43 gap junctional communication. This necessitates one of the following approaches or an integration of them: direct biomedical methods, genetic interaction and genomic methods, and computational inference methods (Schenone et al., 2013, Gaulton et al., 2012, Gregori-Puigjané et al., 2012). By knowing how

Peptide5 exerts its pharmacological functions in Connexin43 gap junctional communications, these insights can help fully characterise on-target effects in order to complete the application of Peptide5 for not only SCI but also other pathological conditions.

2) Detailed analysis. A few molecules such as ATP, glutamate and ROS could be measured directly to evaluate the closure of Connexin43 hemichannels by Peptide5 in the spinal cord tissue. The inflammatory cytokines such as TNFα and IL-1β, could also be quantified to assess the downstream effects of closed hemichannels by using enzyme-linked immunosorbent assay.

3) Pharmacokinetics. Although the systemic administration of Peptide5 has shown to be neuroprotective in an animal model of SCI, several pharmacokinetic issues should be addressed before translating into human clinical trials. *In vivo* and *in vitro* degradation and metabolism information is required to be precisely acquired to further optimise the dosing regimen as well as the administration route and timing as a relevant treatment option for human SCI patients.

4) Toxicity. It is also necessary to establish the toxicity profile of Peptide5, particularly to examine any adverse effects in the immune system. Connexin43 is also expressed by human peripheral blood lymphocytes (Bermudez-Fajardo et al., 2007, Oviedo‐orta et al., 2000). T cell proliferation and cytokine assays would be useful to evaluate the influence of Peptide5 on these cells.

5) Combined therapies. Secondary treatments such as manipulation of endogenous neural progenitor cells and inflammatory responses could be

applied in parallel to the Peptide5 systemic treatment. The combined therapies might potentially provide synergetic impact on functional improvements.

6) Chronic administration. It is worth investigating the efficacy of chronic administration of Peptide5, as the reactive astrocytes and inflammatory responses persist for a long time after SCI (Li and Raisman, 1995, Beck et al., 2010, Donnelly and Popovich, 2008). If Peptide5 could still close Connexin43 hemichannels at the later phase, there would be less efflux of neurotoxic molecules such as ATP, glutamate and ROS into extracellular space and adjacent cells, and thus the ongoing cycle of Connexin43 hemichannel dysfunction, inflammation and secondary damage could possibly be interrupted. Therefore, Peptide5 may be able to contribute to functional benefits, even at the chronic stage of SCI.

7) Statistical analysis of the BBB scale. Whilst the BBB rating scale is non-parametric (Basso et al., 1996) there is much controversy over the use of statistical analysis for it. This sensitive rating scale was initially developed by Basso et al. (1995) to differentiate hind limb locomotor skills over a wide range of injury severities, using a two-way ANOVA with a Tukey's *post-hoc* test. The factors were treatment groups and time with repeated measures on the second factor. However, Scheff et al. (2002) recommended to use a mixed factorial ANOVA for the effect of treatment group and time, or one-way ANOVA with a Bonferroni *post-hoc* test for the simple effect (using the omnibus error term in the calculation of F). There should be further investigation to define the appropriate statistical analysis of BBB rating scale,

in order to provide a common methodology for the correct interpretation of SCI behavioural data.

8) Experimental design of controls. There are a number of controls that could feasibly be included in this study for completeness. In accordance with the 3Rs (Replacement, Reduction and Refinement) in the Code of Practice for the care and use of animals for scientific purposes, only the sham animals with SP or Peptide5 treatment and the SCI animals treated with SP were included in order to reduce the number of animals used in the current study. The control groups selected for inclusion were considered as sufficient as the purpose of the current study, and the data of controls were similar to previously used "vehicle only" controls (O'Carroll et al., 2013). A total of 288 control additional animals in 36 groups (normal, sham or SCI with no injection, vehicle injection, SP or Peptide5 at three time points) could have been included completed to provide rigorous data in the current study.

5.3 Conclusion

The studies presented in this thesis have shown that regulating the Connexin43 hemichannels at the lesion area, by acute systemic administration of Peptide5 is a feasible, neuroprotective and safe treatment option for reducing secondary damage and improving functional recovery in a contusive SCI model of rats. The results suggest that that systemic administration of Peptide5 might be a novel avenue for future medical intervention, and may also offer a platform to boost the efficacy of other treatments following traumatic SCI.

Bibliography

ABDELAZIZ, R. R., ELKASHEF, W. F. & SAID, E. 2016. Tadalafil reduces airway hyperactivity and protects against lung and respiratory airways dysfunction in a rat model of silicosis. *International Immunopharmacology,* 40**,** 530-541.

ABUDARA, V., BECHBERGER, J., FREITAS-ANDRADE, M., DE BOCK, M., WANG, N., BULTYNCK, G., NAUS, C. C., LEYBAERT, L. & GIAUME, C. 2014. The connexin43 mimetic peptide Gap19 inhibits hemichannels without altering gap junctional communication in astrocytes. *Frontiers in Cellular Neuroscience,* 8**,** 306.

AGRAWAL, S. K. & FEHLINGS, M. G. 1997. Role of NMDA and non-NMDA ionotropic glutamate receptors in traumatic spinal cord axonal injury. *The Journal of Neuroscience,* 17**,** 1055-1063.

AJAMI, B., BENNETT, J. L., KRIEGER, C., MCNAGNY, K. M. & ROSSI, F. M. 2011. Infiltrating monocytes trigger EAE progression, but do not contribute to the resident microglia pool. *Nature Neuroscience,* 14**,** 1142-1149.

AMAT, J. A., ISHIGURO, H., NAKAMURA, K. & NORTON, W. T. 1996. Phenotypic diversity and kinetics of proliferating microglia and astrocytes following cortical stab wounds. *Glia,* 16**,** 368-382.

AMORINI, M., ROMEO, P., BRUNO, R., GALLETTI, F., DI BELLA, C., LONGO, P., BRIUGLIA, S., SALPIETRO, C. & RIGOLI, L. 2015. Prevalence of Deafness‐Associated Connexin‐26 (GJB2) and Connexin‐30 (GJB6) Pathogenic Alleles in a Large Patient Cohort from Eastern Sicily. *Annals of Human Genetics,* 79**,** 341-349.

ANDERSON, K. D. 2004. Targeting recovery: priorities of the spinal cord-injured population. *Journal of Neurotrauma,* 21**,** 1371-1383.

ANDJELKOVIC, A., NIKOLIC, B., PACHTER, J. & ZECEVIC, N. 1998. Macrophages/microglial cells in human central nervous system during development: an immunohistochemical study. *Brain Research,* 814**,** 13-25.

ANKARCRONA, M., DYPBUKT, J. M., BONFOCO, E., ZHIVOTOVSKY, B., ORRENIUS, S., LIPTON, S. A. & NICOTERA, P. 1995. Glutamate-induced neuronal death: a succession of necrosis or apoptosis depending on mitochondrial function. *Neuron,* 15**,** 961-973.

APUZZO, M. L. 2002. Pharmacological therapy after acute cervical spinal cord injury. *Neurosurgery,* 50**,** S63-72.

ARAKI, E., FORSTER, C., DUBINSKY, J. M., ROSS, M. E. & IADECOLA, C. 2001. Cyclooxygenase-2 inhibitor ns-398 protects neuronal cultures from lipopolysaccharide-induced neurotoxicity. *Stroke,* 32**,** 2370-2375.

ARBOLEDA, D., FOROSTYAK, S., JENDELOVA, P., MAREKOVA, D., AMEMORI, T., PIVONKOVA, H., MASINOVA, K. & SYKOVA, E. 2011. Transplantation of predifferentiated adipose-derived stromal cells for the treatment of spinal cord injury. *Cellular and Molecular Neurobiology,* 31**,** 1113-1122.

AUBERT, N., AMELLER, T. & LEGRAND, J.-J. 2012. Systemic exposure to parabens: pharmacokinetics, tissue distribution, excretion balance and plasma metabolites of [14 C]-methyl-, propyl-and butylparaben in rats after oral, topical or subcutaneous administration. *Food and Chemical Toxicology,* 50**,** 445-454.

AZBILL, R. D., MU, X., BRUCE-KELLER, A. J., MATTSON, M. P. & SPRINGER, J. E. 1997. Impaired mitochondrial function, oxidative stress and altered

antioxidant enzyme activities following traumatic spinal cord injury. *Brain Research,* 765**,** 283-290.

BAASTRUP, C., MAERSK-MOLLER, C. C., NYENGAARD, J. R., JENSEN, T. S. & FINNERUP, N. B. 2010. Spinal-, brainstem-and cerebrally mediated responses at-and below-level of a spinal cord contusion in rats: evaluation of pain-like behavior. *Pain,* 151**,** 670-679.

BAEK, M., CHUNG, H.-E., YU, J., LEE, J.-A., KIM, T.-H., OH, J.-M., LEE, W.-J., PAEK, S.-M., LEE, J. K. & JEONG, J. 2012. Pharmacokinetics, tissue distribution, and excretion of zinc oxide nanoparticles. *International Journal of Nanomedicine,* 7**,** 3081-3097.

BAINS, M. & HALL, E. D. 2012. Antioxidant therapies in traumatic brain and spinal cord injury. *Biochimica et Biophysica Acta - Molecular Basis of Disease,* 1822**,** 675-684.

BAO, F., DEKABAN, G. A. & WEAVER, L. C. 2005. Anti‐CD11d antibody treatment reduces free radical formation and cell death in the injured spinal cord of rats. *Journal of Neurochemistry,* 94**,** 1361-1373.

BAPTISTE, D. C. & FEHLINGS, M. G. 2007. Update on the treatment of spinal cord injury. *Progress in Brain Research,* 161**,** 217-233.

BARKHO, B. Z., SONG, H., AIMONE, J. B., SMRT, R. D., KUWABARA, T., NAKASHIMA, K., GAGE, F. H. & ZHAO, X. 2006. Identification of astrocyte-expressed factors that modulate neural stem/progenitor cell differentiation. *Stem Cells and Development,* 15**,** 407-421.

BARNABE-HEIDER, F., GORITZ, C., SABELSTROM, H., TAKEBAYASHI, H., PFRIEGER, F. W., MELETIS, K. & FRISEN, J. 2010. Origin of new glial cells in intact and injured adult spinal cord. *Cell Stem Cell,* 7**,** 470-482.

BARTHOLDI, D. & SCHWAB, M. E. 1997. Expression of pro‐inflammatory cytokine and chemokine mRNA upon experimental spinal cord injury in mouse: An in situ hybridization study. *European Journal of Neuroscience,* 9**,** 1422-1438.

BASSO, D. M., BEATTIE, M. S. & BRESNAHAN, J. C. 1995. A sensitive and reliable locomotor rating scale for open field testing in rats. *Journal of Neurotrauma,* 12**,** 1-21.

BASSO, D. M., BEATTIE, M. S. & BRESNAHAN, J. C. 1996. Graded histological and locomotor outcomes after spinal cord contusion using the NYU weight-drop device versus transection. *Experimental Neurology,* 139**,** 244-256.

BASU, S., HELLBERG, A., ULUS, A., WESTMAN, J. & KARACAGIL, S. 2001. Biomarkers of free radical injury during spinal cord ischemia. *FEBS Letters,* 508**,** 36-38.

BATTISTUZZO, C. R., ARMSTRONG, A., CLARK, J., WORLEY, L., SHARWOOD, L., LIN, P., ROOKE, G., SKEERS, P., NOLAN, S., GERAGHTY, T., NUNN, A., BROWN, D. J., HILL, S., ALEXANDER, J., MILLARD, M., COX, S. F., RAO, S., WATTS, A., GOODS, L., ALLISON, G. T., AGOSTINELLO, J., CAMERON, P. A., MOSLEY, I., LIEW, S. M., GEDDES, T., MIDDLETON, J., BUCHANAN, J., ROSENFELD, J. V., BERNARD, S., ATRESH, S., PATEL, A., SCHOUTEN, R., FREEMAN, B. J. C., DUNLOP, S. A. & BATCHELOR, P. E. 2016. Early decompression following cervical spinal cord injury: examining the process of care from accident scene to surgery. *Journal of Neurotrauma,* 33**,** 1161-1169.

BAUTISTA, W., MCCREA, D. & NAGY, J. 2014. Connexin36 identified at morphologically mixed chemical/electrical synapses on trigeminal motoneurons

and at primary afferent terminals on spinal cord neurons in adult mouse and rat. *Neuroscience,* 263**,** 159-180.

BEATTIE, E. C., STELLWAGEN, D., MORISHITA, W., BRESNAHAN, J. C., HA, B. K., VON ZASTROW, M., BEATTIE, M. S. & MALENKA, R. C. 2002. Control of synaptic strength by glial TNFα. *Science,* 295**,** 2282-2285.

BECK, K. D., NGUYEN, H. X., GALVAN, M. D., SALAZAR, D. L., WOODRUFF, T. M. & ANDERSON, A. J. 2010. Quantitative analysis of cellular inflammation after traumatic spinal cord injury: evidence for a multiphasic inflammatory response in the acute to chronic environment. *Brain,* 133**,** 433-447.

BECKER, D., SADOWSKY, C. L. & MCDONALD, J. W. 2003. Restoring function after spinal cord injury. *The Neurologist,* 9**,** 1-15.

BECKER, D. L., THRASIVOULOU, C. & PHILLIPS, A. R. 2012. Connexins in wound healing; perspectives in diabetic patients. *Biochimica et Biophysica Acta (BBA)-Biomembranes,* 1818**,** 2068-2075.

BENNETT, M. V., GARRÉ, J. M., ORELLANA, J. A., BUKAUSKAS, F. F., NEDERGAARD, M., GIAUME, C. & SÁEZ, J. C. 2012. Connexin and pannexin hemichannels in inflammatory responses of glia and neurons. *Brain Research,* 1487**,** 3-15.

BERMUDEZ-FAJARDO, A., YLIHÄRSILÄ, M., EVANS, W. H., NEWBY, A. C. & OVIEDO-ORTA, E. 2007. CD4+ T lymphocyte subsets express connexin 43 and establish gap junction channel communication with macrophages in vitro. *Journal of Leukocyte Biology,* 82**,** 608-612.

BERNARDS, C. & AKERS, T. 2006. Effect of postinjury intravenous or intrathecal methylprednisolone on spinal cord excitatory amino-acid release, nitric oxide generation, PGE2 synthesis, and myeloperoxidase content in a pig model of acute spinal cord injury. *Spinal Cord,* 44**,** 594-604.

BERNEY, S., BRAGGE, P., GRANGER, C., OPDAM, H. & DENEHY, L. 2011. The acute respiratory management of cervical spinal cord injury in the first 6 weeks after injury: a systematic review. *Spinal Cord,* 49**,** 17-29.

BERTHOUD, V. M., BEYER, E. C. & SEUL, K. H. 2000. Peptide inhibitors of intercellular communication. *American Journal of Physiology-Lung Cellular and Molecular Physiology,* 279**,** L619-L622.

BESANCON, E., GUO, S., LOK, J., TYMIANSKI, M. & LO, E. H. 2008. Beyond NMDA and AMPA glutamate receptors: emerging mechanisms for ionic imbalance and cell death in stroke. *Trends in Pharmacological Sciences,* 29**,** 268-275.

BETAGERI, G. & ROGERS, J. 1987. Thermodynamics of partitioning of β-blockers in the n-octanol-buffer and liposome systems. *International Journal of Pharmaceutics,* 36**,** 165-173.

BILGEN, M., DOGAN, B. & NARAYANA, P. A. 2002. In vivo assessment of blood-spinal cord barrier permeability: serial dynamic contrast enhanced MRI of spinal cord injury. *Magnetic Resonance Imaging,* 20**,** 337-341.

BLIGHT, A. R. 1994. Effects of silica on the outcome from experimental spinal cord injury: implication of macrophages in secondary tissue damage. *Neuroscience,* 60**,** 263-273.

BOITANO, S. & EVANS, W. H. 2000. Connexin mimetic peptides reversibly inhibit Ca2+ signaling through gap junctions in airway cells. *American Journal of Physiology-Lung Cellular and Molecular Physiology,* 279**,** L623-L630.

BRACKEN, M. B., COLLINS, W. F., FREEMAN, D. F., SHEPARD, M. J., WAGNER, F. W., SILTEN, R. M., HELLENBRAND, K. G., RANSOHOFF, J., HUNT, W.

E. & PEROT JR, P. L. 1984. Efficacy of methylprednisolone in acute spinal cord injury. *The Journal of the American Medical Association,* 251**,** 45-52.

BRACKEN, M. B. & HOLFORD, T. R. 1993. Effects of timing of methylprednisolone or naloxone administration on recovery of segmental and long-tract neurological function in NASCIS 2. *Journal of Neurosurgery,* 79**,** 500-507.

BRACKEN, M. B., SHEPARD, M. J., COLLINS, W. F., HOLFORD, T. R., YOUNG, W., BASKIN, D. S., EISENBERG, H. M., FLAMM, E., LEO-SUMMERS, L. & MAROON, J. 1990. A randomized, controlled trial of methylprednisolone or naloxone in the treatment of acute spinal-cord injury. *New England Journal of Medicine,* 322**,** 1405-1411.

BRACKEN, M. B., SHEPARD, M. J., HOLFORD, T. R., LEO-SUMMERS, L., ALDRICH, E. F., FAZL, M., FEHLINGS, M., HERR, D. L., HITCHON, P. W. & MARSHALL, L. F. 1997. Administration of methylprednisolone for 24 or 48 hours or tirilazad mesylate for 48 hours in the treatment of acute spinal cord InjuryResults of the third national acute spinal cord injury randomized controlled trial. *The Journal of the American Medical Association,* 277**,** 1597-1604.

BRACKEN, M. B., SHEPARD, M. J., HOLFORD, T. R., LEO-SUMMERS, L., ALDRICH, E. F., FAZL, M., FEHLINGS, M. G., HERR, D. L., HITCHON, P. W. & MARSHALL, L. F. 1998. Methylprednisolone or tirilazad mesylate administration after acute spinal cord injury: 1-year follow up. *Journal of Neurosurgery,* 89**,** 699-706.

BRAMBILLA, R., BRACCHI-RICARD, V., HU, W.-H., FRYDEL, B., BRAMWELL, A., KARMALLY, S., GREEN, E. J. & BETHEA, J. R. 2005. Inhibition of astroglial nuclear factor κB reduces inflammation and improves functional recovery after spinal cord injury. *The Journal of Experimental Medicine,* 202**,** 145-156.

BRAUGHLER, J. M. & HALL, E. D. 1984. Effects of multi-dose methylprednisolone sodium succinate administration on injured cat spinal cord neurofilament degradation and energy metabolism. *Journal of Neurosurgery,* 61**,** 290-295.

BUDD, S. L. & LIPTON, S. A. 1998. Calcium tsunamis: do astrocytes transmit cell death messages via gap junctions during ischemia? *Nature Neuroscience,* 1**,** 431-432.

BUTOVSKY, O., HAUBEN, E. & SCHWARTZ, M. 2001. Morphological aspects of spinal cord autoimmune neuroprotection: colocalization of T cells with B7–2 (CD86) and prevention of cyst formation. *The FASEB Journal,* 15**,** 1065-1067.

CACCAMO, D., CAMPISI, A., CURRO, M., VOLTI, G. L., VANELLA, A. & IENTILE, R. 2004. Excitotoxic and post-ischemic neurodegeneration: involvement of transglutaminases. *Amino Acids,* 27**,** 373-379.

CAGNEY, G. & EMILI, A. 2002. De novo peptide sequencing and quantitative profiling of complex protein mixtures using mass-coded abundance tagging. *Nature Biotechnology,* 20**,** 163-170.

CAMPBELL, S. J., WILCOCKSON, D. C., BUTCHART, A. G., PERRY, V. H. & ANTHONY, D. C. 2002. Altered chemokine expression in the spinal cord and brain contributes to differential interleukin‐1β‐induced neutrophil recruitment. *Journal of Neurochemistry,* 83**,** 432-441.

CARLSON, G. D., MIINATO, Y., OKADA, A., GORDEN, C. D., WARDEN, K. E., BARBEAU, J. M., BIRO, C. L., BAHNUIK, E., BOHLMAN, H. H. & C, L. J. 1997. Early time-dependent decompression for spinal cord injury: vascular mechanisms of recovery. *Journal of Neurotrauma,* 14**,** 951-962.

CAWSEY, T., DUFLOU, J., SHANNON-WEIKERT, C. & GORRIE, C. A. 2015. Nestin positive ependymal cells are increased in the human spinal cord after traumatic CNS injury. *Journal of Neurotrauma,* 32**,** 1-10.

CESTA, M. F. 2006. Normal structure, function, and histology of the spleen. *Toxicologic Pathology,* 34**,** 455-465.

CHAN, C. 2008. Inflammation: beneficial or detrimental after spinal cord injury? *Recent Patents on CNS Drug Discovery,* 3**,** 189-199.

CHANG, H.-M., CHENG, J.-C. & LEUNG, P. C. 2013. Theca-derived BMP4 and BMP7 down-regulate connexin43 expression and decrease gap junction intercellular communication activity in immortalized human granulosa cells. *The Journal of Clinical Endocrinology and Metabolism,* 98**,** E437-E445.

CHANG, Y.-C., CHANG, H.-Y., HAHN, R., LEE, E., SVOBODA, K., GORDON, M. & GERECKE, D. 2015. Connexin 43 antisense therapy modulates connexin expression and wound repair in nitrogen mustard injured mouse skin. *The FASEB Journal,* 29**,** 876-3.

CHAPLAN, S., BACH, F., POGREL, J., CHUNG, J. & YAKSH, T. 1994. Quantitative assessment of tactile allodynia in the rat paw. *Journal of Neuroscience Methods,* 53**,** 55-63.

CHAYTOR, A., EVANS, W., GRIFFITH, T. & THORNBURY, K. 1997. Peptides homologous to extracellular loop motifs of connexin 43 reversibly abolish rhythmic contractile activity in rabbit arteries. *The Journal of Physiology,* 503**,** 99-110.

CHEN, G., PARK, C. K., XIE, R. G., BERTA, T., NEDERGAARD, M. & JI, R. R. 2014a. Connexin-43 induces chemokine release from spinal cord astrocytes to maintain late-phase neuropathic pain in mice. *Brain,* 137.

CHEN, V. M., AHAMED, J., VERSTEEG, H. H., BERNDT, M. C., RUF, W. & HOGG, P. J. 2006. Evidence for activation of tissue factor by an allosteric disulfide bond. *Biochemistry,* 45**,** 12020-12028.

CHEN, Y. S., GREEN, C. R., TEAGUE, R., PERRETT, J., DANESH-MEYER, H. V., TOTH, I. & RUPENTHAL, I. D. 2015. Intravitreal injection of lipoamino acid-modified connexin43 mimetic peptide enhances neuroprotection after retinal ischemia. *Drug Delivery and Translational Tesearch,* 5**,** 480-488.

CHEN, Y. S., GREEN, C. R., WANG, K., DANESH-MEYER, H. V. & RUPENTHAL, I. D. 2014b. Sustained intravitreal delivery of connexin43 mimetic peptide by poly (d, l-lactide-co-glycolide) acid micro-and nanoparticles–Closing the gap in retinal ischaemia. *European Journal of Pharmaceutics and Biopharmaceutics*.

CHERIYAN, T., RYAN, D. J., WEINREB, J. H., CHERIYAN, J., PAUL, J. C., LAFAGE, V., KIRSCH, T. & ERRICO, T. J. 2014. Spinal cord injury models: a review. *Spinal Cord,* 52**,** 588-95.

CHEVALLIER, D., CARETTE, D., SEGRETAIN, D., GILLERON, J. & POINTIS, G. 2013. Connexin 43 a check-point component of cell proliferation implicated in a wide range of human testis diseases. *Cellular and Molecular Life Sciences,* 70**,** 1207-1220.

CHIU, I. M., MORIMOTO, E. T., GOODARZI, H., LIAO, J. T., O'KEEFFE, S., PHATNANI, H. P., MURATET, M., CARROLL, M. C., LEVY, S. & TAVAZOIE, S. 2013. A neurodegeneration-specific gene-expression signature of acutely isolated microglia from an amyotrophic lateral sclerosis mouse model. *Cell Reports,* 4**,** 385-401.

CHO, W.-S., KANG, B.-C., LEE, J. K., JEONG, J., CHE, J.-H. & SEOK, S. H. 2013. Comparative absorption, distribution, and excretion of titanium dioxide and zinc

oxide nanoparticles after repeated oral administration. *Particle and Fibre Toxicology,* 10**,** 1.

CHOI, D. W. 1994. Glutamate receptors and the induction of excitotoxic neuronal death. *Progress in Brain Research,* 100**,** 47-52.

CHONG, K. F., NING, K., LEONG, H. W. & PEVZNER, P. 2006. Modeling and characterization of multi-charge mass spectra for peptide sequencing. *Journal of Bioinformatics and Computational Biology,* 4**,** 1329-1352.

CIGLIOLA, V., CHELLAKUDAM, V., ARABIETER, W. & MEDA, P. 2013. Connexins and β-cell functions. *Diabetes Research and Clinical Practice,* 99**,** 250-259.

CIGLIOLA, V., POPULAIRE, C., PIERRI, C. L., DEUTSCH, S., HAEFLIGER, J.-A., FADISTA, J., LYSSENKO, V., GROOP, L., RUEEDI, R. & THOREL, F. 2016. A variant of GJD2, encoding for Connexin 36, alters the function of insulin producing β-cells. *PloS one,* 11**,** e0150880.

CIZKOVA, D., NAGYOVA, M., SLOVINSKA, L., NOVOTNA, I., RADONAK, J., CIZEK, M., MECHIROVA, E., TOMORI, Z., HLUCILOVA, J., MOTLIK, J., SULLA, I., JR. & VANICKY, I. 2009. Response of ependymal progenitors to spinal cord injury or enhanced physical activity in adult rat. *Cellular and Molecular Neurobiology,* 29**,** 999-1013.

ČÍŽKOVÁ, D., ROSOCHA, J., VANICKÝ, I., JERGOVÁ, S. & ČÍŽEK, M. 2006. Transplants of human mesenchymal stem cells improve functional recovery after spinal cord injury in the rat. *Cellular and Molecular Neurobiology,* 26**,** 1165-1178.

CLARKE, T. C., WILLIAMS, O. J., MARTIN, P. E. & EVANS, W. H. 2009. ATP release by cardiac myocytes in a simulated ischaemia model: inhibition by a connexin mimetic and enhancement by an antiarrhythmic peptide. *European Journal of Pharmacology,* 605**,** 9-14.

CLEVELAND, D. W., FISCHER, S. G., KIRSCHNER, M. W. & LAEMMLI, U. K. 1977. Peptide mapping by limited proteolysis in sodium dodecyl sulfate and analysis by gel electrophoresis. *Journal of Biological Chemistry,* 252**,** 1102-1106.

COLEMAN, W. P., BENZEL, E., CAHILL, D. W., DUCKER, T., GEISLER, F., GREEN, B., GROPPER, M. R., GOFFIN, J., MADSEN III, P. W. & MAIMAN, D. J. 2000. A critical appraisal of the reporting of the National Acute Spinal Cord Injury Studies (II and III) of methylprednisolone in acute spinal cord injury. *Journal of Spinal Disorders and Techniques,* 13**,** 185-199.

CONNORS, B. W. 2012. Tales of a dirty drug: carbenoxolone, gap junctions, and seizures. *Epilepsy Currents,* 12**,** 66-68.

CONTRERAS, J. E., SÁNCHEZ, H. A., EUGENÍN, E. A., SPEIDEL, D., THEIS, M., WILLECKE, K., BUKAUSKAS, F. F., BENNETT, M. V. & SÁEZ, J. C. 2002. Metabolic inhibition induces opening of unapposed connexin 43 gap junction hemichannels and reduces gap junctional communication in cortical astrocytes in culture. *Proceedings of the National Academy of Sciences,* 99**,** 495-500.

CONTRERAS, J. E., SÁNCHEZ, H. A., VÉLIZ, L. P., BUKAUSKAS, F. F., BENNETT, M. V. & SÁEZ, J. C. 2004. Role of connexin-based gap junction channels and hemichannels in ischemia-induced cell death in nervous tissue. *Brain Research Reviews,* 47**,** 290-303.

COOK, K. M. & HOGG, P. J. 2013. Post-translational control of protein function by disulfide bond cleavage. *Antioxidants and Redox Signaling,* 18**,** 1987-2015.

COTRINA, M. L., LIN, J. H.-C., ALVES-RODRIGUES, A., LIU, S., LI, J., AZMI-GHADIMI, H., KANG, J., NAUS, C. C. & NEDERGAARD, M. 1998. Connexins regulate calcium signaling by controlling ATP release. *Proceedings of the National Academy of Sciences,* 95**,** 15735-15740.

COUTINHO, P., QIU, C., FRANK, S., TAMBER, K. & BECKER, D. 2003. Dynamic changes in connexin expression correlate with key events in the wound healing process. *Cell Biology International,* 27**,** 525-541.

COUTINHO, P., QIU, C., FRANK, S., WANG, C., BROWN, T., GREEN, C. & BECKER, D. 2005. Limiting burn extension by transient inhibition of Connexin43 expression at the site of injury. *British Journal of Plastic Surgery,* 58**,** 658-667.

COX, A., VARMA, A., BARRY, J., VERTEGEL, A. & BANIK, N. 2015. Nanoparticle estrogen in rat spinal cord injury elicits rapid anti-inflammatory effects in plasma, cerebrospinal fluid, and tissue. *Journal of Neurotrauma,* 32**,** 1413-1421.

CRIPPS, R. A., LEE, B. B., WING, P., WEERTS, E., MACKAY, J. & BROWN, D. 2011. A global map for traumatic spinal cord injury epidemiology: towards a living data repository for injury prevention. *Spinal Cord,* 49**,** 493-501.

CROCKER, S. J., WHITMIRE, J. K., FRAUSTO, R. F., CHERTBOONMUANG, P., SOLOWAY, P. D., WHITTON, J. L. & CAMPBELL, I. L. 2006. Persistent macrophage/microglial activation and myelin disruption after experimental autoimmune encephalomyelitis in tissue inhibitor of metalloproteinase-1-deficient mice. *The American Journal of Pathology,* 169**,** 2104-2116.

CRONIN, M., ANDERSON, P. N., COOK, J. E., GREEN, C. R. & BECKER, D. L. 2008. Blocking connexin43 expression reduces inflammation and improves functional recovery after spinal cord injury. *Molecular and Cellular Neuroscience,* 39**,** 152-160.

CRONIN, M., ANDERSON, P. N., GREEN, C. R. & BECKER, D. L. 2006. Antisense delivery and protein knockdown within the intact central nervous system. *Frontiers in Bioscience,* 11**,** 2967-2975.

CURSIEFEN, C., BOCK, F., HORN, F. K., KRUSE, F. E., SEITZ, B., BORDERIE, V., FRÜH, B., THIEL, M. A., WILHELM, F. & GEUDELIN, B. 2009. GS-101 antisense oligonucleotide eye drops inhibit corneal neovascularization: interim results of a randomized phase II trial. *Ophthalmology,* 116**,** 1630-1637.

DANESH-MEYER, H. V., KERR, N. M., ZHANG, J., EADY, E. K., O'CARROLL, S. J., NICHOLSON, L. F., JOHNSON, C. S. & GREEN, C. R. 2012. Connexin43 mimetic peptide reduces vascular leak and retinal ganglion cell death following retinal ischaemia. *Brain,* 135**,** 506-520.

DAVID, S. & KRONER, A. 2011. Repertoire of microglial and macrophage responses after spinal cord injury. *Nature Reviews Neuroscience,* 12**,** 388-399.

DAVIDSON, J., GREEN, C., BENNET, L. & GUNN, A. 2015. Battle of the hemichannels–connexins and pannexins in ischemic brain injury. *International Journal of Developmental Neuroscience,* 45**,** 66-74.

DAVIDSON, J., GREEN, C., NICHOLSON, L., BENNET, L. & GUNN, A. 2013a. Connexin hemichannel blockade is neuroprotective after, but not during, global cerebral ischemia in near-term fetal sheep. *Experimental Neurology,* 248**,** 301-308.

DAVIDSON, J., R GREEN, C., BENNET, L., FB NICHOLSON, L., DANESH-MEYER, H., J O'CARROLL, S. & J GUNN, A. 2013b. A key role for connexin hemichannels in spreading ischemic brain injury. *Current Drug Targets,* 14**,** 36-46.

DAVIDSON, J. O., DRURY, P. P., GREEN, C. R., NICHOLSON, L. F., BENNET, L. & GUNN, A. J. 2014. Connexin hemichannel blockade is neuroprotective after asphyxia in preterm fetal sheep. *PLoS One,* 9**,** e96558.

DAVIDSON, J. O., GREEN, C. R., NICHOLSON, B., LOUISE, F., O'CARROLL, S. J., FRASER, M., BENNET, L. & JAN GUNN, A. 2012a. Connexin hemichannel blockade improves outcomes in a model of fetal ischemia. *Annals of Neurology,* 71**,** 121-132.

DAVIDSON, J. O., GREEN, C. R., NICHOLSON, L. F., BENNET, L. & GUNN, A. J. 2012b. Deleterious effects of high dose connexin 43 mimetic peptide infusion after cerebral ischaemia in near-term fetal sheep. *International Journal of Molecular Sciences,* 13**,** 6303-6319.

DE MAIO, A., VEGA, V. L. & CONTRERAS, J. E. 2002. Gap junctions, homeostasis, and injury. *Journal of Cellular Physiology,* 191**,** 269-282.

DE RIVERO VACCARI, J. P., BASTIEN, D., YURCISIN, G., PINEAU, I., DIETRICH, W. D., DE KONINCK, Y., KEANE, R. W. & LACROIX, S. 2012. P2X4 receptors influence inflammasome activation after spinal cord injury. *The Journal of Neuroscience,* 32**,** 3058-3066.

DE VUYST, E., DECROCK, E., DE BOCK, M., YAMASAKI, H., NAUS, C. C., EVANS, W. H. & LEYBAERT, L. 2007. Connexin hemichannels and gap junction channels are differentially influenced by lipopolysaccharide and basic fibroblast growth factor. *Molecular Biology of the Cell,* 18**,** 34-46.

DECROCK, E., DE BOCK, M., WANG, N., BULTYNCK, G., GIAUME, C., NAUS, C. C., GREEN, C. R. & LEYBAERT, L. 2015. Connexin and pannexin signaling pathways, an architectural blueprint for CNS physiology and pathology? *Cellular and Molecular Life Sciences,* 72**,** 2823-2851.

DEL CASTILLO, I., VILLAMAR, M., MORENO-PELAYO, M. A., DEL CASTILLO, F. J., ÁLVAREZ, A., TELLERÍA, D., MENÉNDEZ, I. & MORENO, F. 2002. A deletion involving the connexin 30 gene in nonsyndromic hearing impairment. *New England Journal of Medicine,* 346**,** 243-249.

DENG, Z.-H., LIAO, J., ZHANG, J.-Y., LIANG, C., SONG, C.-H., HAN, M., WANG, L.-H., XUE, H., ZHANG, K. & ZABEAU, L. 2014. Inhibition of the connexin 43 elevation may be involved in the neuroprotective activity of leptin against brain ischemic injury. *Cellular and Molecular Neurobiology,* 34**,** 871-879.

DENNIS, M. S., ZHANG, M., MENG, Y. G., KADKHODAYAN, M., KIRCHHOFER, D., COMBS, D. & DAMICO, L. A. 2002. Albumin binding as a general strategy for improving the pharmacokinetics of proteins. *Journal of Biological Chemistry,* 277**,** 35035-35043.

DETLOFF, M. R., FISHER, L. C., MCGAUGHY, V., LONGBRAKE, E. E., POPOVICH, P. G. & BASSO, D. M. 2008. Remote activation of microglia and pro-inflammatory cytokines predict the onset and severity of below-level neuropathic pain after spinal cord injury in rats. *Experimental Neurology,* 212**,** 337-347.

DEVIVO, M. 2007. Sir Ludwig Guttmann Lecture: Trends in spinal cord injury rehabilitation outcomes from model systems in the United States: 1973–2006. *Spinal Cord,* 45**,** 713-721.

DEVIVO, M. J., KARTUS, P. L., STOVER, S. L., RUTT, R. D. & FINE, P. R. 1987. Seven-year survival following spinal cord injury. *Archives of Neurology,* 44**,** 872.

DI, W.-L., RUGG, E. L., LEIGH, I. M. & KELSELL, D. P. 2001. Multiple epidermal connexins are expressed in different keratinocyte subpopulations including connexin 31. *Journal of Investigative Dermatology,* 117**,** 958-964.

DIBAJ, P., NADRIGNY, F., STEFFENS, H., SCHELLER, A., HIRRLINGER, J., SCHOMBURG, E. D., NEUSCH, C. & KIRCHHOFF, F. 2010. NO mediates microglial response to acute spinal cord injury under ATP control in vivo. *Glia,* 58**,** 1133-1144.

DIEKMANN, S., HENNEKE, M., BURCKHARDT, B. C. & GÄRTNER, J. 2010. Pelizaeus–Merzbacher-like disease is caused not only by a loss of connexin47 function but also by a hemichannel dysfunction. *European Journal of Human Genetics,* 18**,** 985-992.

DIMAR, J. R., GLASSMAN, S. D., RAQUE, G. H., ZHANG, Y. P. & SHIELDS, C. B. 1999. The influence of spinal canal narrowing and timing of decompression on neurologic recovery after spinal cord contusion in a rat model. *Spine,* 24**,** 1623.

DITOR, D., HAMILTON, S., TARNOPOLSKY, M., GREEN, H., CRAVEN, B., PARISE, G. & HICKS, A. 2004. Na+, K+ - ATPase concentration and fiber type distribution after spinal cord injury. *Muscle and Nerve,* 29**,** 38-45.

DOBKIN, B., APPLE, D., BARBEAU, H., BASSO, M., BEHRMAN, A., DEFORGE, D., DITUNNO, J., DUDLEY, G., ELASHOFF, R. & FUGATE, L. 2006. Weight-supported treadmill vs over-ground training for walking after acute incomplete SCI. *Neurology,* 66**,** 484-493.

DOLL, R., HILL, I. & HUTTON, C. 1965. Treatment of gastric ulcer with carbenoxolone sodium and oestrogens. *Gut,* 6**,** 19-24.

DONNELLY, D. J. & POPOVICH, P. G. 2008. Inflammation and its role in neuroprotection, axonal regeneration and functional recovery after spinal cord injury. *Experimental Neurology,* 209**,** 378-388.

DORSHKIND, K., GREEN, L., GODWIN, A. & FLETCHER, W. 1993. Connexin-43-type gap junctions mediate communication between bone marrow stromal cells. *Blood,* 82**,** 38-45.

DOUGHERTY, K. D., DREYFUS, C. F. & BLACK, I. B. 2000. Brain-derived neurotrophic factor in astrocytes, oligodendrocytes, and microglia/macrophages after spinal cord injury. *Neurobiology of Disease,* 7**,** 574-585.

DUGAN, L., SENSI, S., CANZONIERO, L., HANDRAN, S., ROTHMAN, S., LIN, T.-S., GOLDBERG, M. & CHOI, D. 1995. Mitochondrial production of reactive oxygen species in cortical neurons following exposure to N-methyl-D-aspartate. *The Journal of Neuroscience,* 15**,** 6377-6388.

DUMONT, R. J., VERMA, S., OKONKWO, D. O., HURLBERT, R. J., BOULOS, P. T., ELLEGALA, D. B. & DUMONT, A. S. 2001. Acute spinal cord injury, part II: contemporary pharmacotherapy. *Clinical Neuropharmacology,* 24**,** 265-279.

DÜRIG, J., ROSENTHAL, C., HALFMEYER, K., WIEMANN, M., NOVOTNY, J., BINGMANN, D., DÜHRSEN, U. & SCHIRRMACHER, K. 2000. Intercellular communication between bone marrow stromal cells and CD34+ haematopoietic progenitor cells is mediated by connexin 43 - type gap junctions. *British Journal of Haematology,* 111**,** 416-425.

ELORANTA, M. & ALM, G. 1999. Splenic Marginal Metallophilic Macrophages and Marginal Zone Macrophages are the Major Interferon- / Producers in Mice upon Intravenous Challenge with Herpes Simplex Virus. *Scandinavian Journal of Immunology,* 49**,** 391-394.

EUGENÍN, E. A., ECKARDT, D., THEIS, M., WILLECKE, K., BENNETT, M. V. & SÁEZ, J. C. 2001. Microglia at brain stab wounds express connexin 43 and in vitro form functional gap junctions after treatment with interferon-γ and tumor necrosis factor-α. *Proceedings of the National Academy of Sciences,* 98**,** 4190-4195.

EVANIEW, N., BELLEY-CÔTÉ, E. P., FALLAH, N., NOONAN, V. K., RIVERS, C. S. & DVORAK, M. F. 2016. Methylprednisolone for the treatment of patients with acute spinal cord injuries: A systematic review and meta-analysis. *Journal of Neurotrauma,* 33**,** 468-481.

EVANIEW, N., NOONAN, V. K., FALLAH, N., KWON, B. K., RIVERS, C. S., AHN, H., BAILEY, C. S., CHRISTIE, S. D., FOURNEY, D. R. & HURLBERT, R. J. 2015. Methylprednisolone for the treatment of patients with acute spinal cord injuries: a propensity score-matched cohort study from a Canadian multi-center spinal cord injury registry. *Journal of Neurotrauma,* 32**,** 1674-1683.

FAIGLE, M., SEESSLE, J., ZUG, S., EL KASMI, K. C. & ELTZSCHIG, H. K. 2008. ATP release from vascular endothelia occurs across Cx43 hemichannels and is attenuated during hypoxia. *PLoS One,* 3**,** e2801.

FARLEY, R., TRAN, C., CARILLI, C., HAWKE, D. & SHIVELY, J. 1984. The amino acid sequence of a fluorescein-labeled peptide from the active site of (Na, K)-ATPase. *Journal of Biological Chemistry,* 259**,** 9532-9535.

FARRAH, T., DEUTSCH, E. W., OMENN, G. S., CAMPBELL, D. S., SUN, Z., BLETZ, J. A., MALLICK, P., KATZ, J. E., MALMSTRÖM, J. & OSSOLA, R. 2011. A high-confidence human plasma proteome reference set with estimated concentrations in PeptideAtlas. *Molecular and Cellular Proteomics,* 10**,** M110. 006353.

FAULKNER, J. R., HERRMANN, J. E., WOO, M. J., TANSEY, K. E., DOAN, N. B. & SOFRONIEW, M. V. 2004. Reactive astrocytes protect tissue and preserve function after spinal cord injury. *The Journal of Neuroscience,* 24**,** 2143-2155.

FAWCETT, J., CURT, A., STEEVES, J., COLEMAN, W., TUSZYNSKI, M., LAMMERTSE, D., BARTLETT, P., BLIGHT, A., DIETZ, V. & DITUNNO, J. 2007. Guidelines for the conduct of clinical trials for spinal cord injury as developed by the ICCP panel: spontaneous recovery after spinal cord injury and statistical power needed for therapeutic clinical trials. *Spinal Cord,* 45**,** 190-205.

FAWCETT, J. W. 2006. The glial response to injury and its role in the inhibition of CNS repair. *Advances in Experimental Medicine and Biology,* 557**,** 11-24.

FEE, D., CRUMBAUGH, A., JACQUES, T., HERDRICH, B., SEWELL, D., AUERBACH, D., PIASKOWSKI, S., HART, M. N., SANDOR, M. & FABRY, Z. 2003. Activated/effector CD4+ T cells exacerbate acute damage in the central nervous system following traumatic injury. *Journal of Neuroimmunology,* 136**,** 54-66.

FEHLINGS, M. G., VACCARO, A., WILSON, J. R., SINGH, A., CADOTTE, D. W., HARROP, J. S., AARABI, B., SHAFFREY, C., DVORAK, M. & FISHER, C. 2012. Early versus delayed decompression for traumatic cervical spinal cord injury: results of the Surgical Timing in Acute Spinal Cord Injury Study (STASCIS). *PloS One,* 7**,** 1-8.

FENN, A. M., HALL, J. C., GENSEL, J. C., POPOVICH, P. G. & GODBOUT, J. P. 2014. IL-4 signaling drives a unique arginase+/IL-1β+ microglia phenotype and recruits macrophages to the inflammatory CNS: consequences of age-related deficits in IL-4Rα after traumatic spinal cord injury. *The Journal of Neuroscience,* 34**,** 8904-8917.

FERGUSON, A. R., CHRISTENSEN, R. N., GENSEL, J. C., MILLER, B. A., SUN, F., BEATTIE, E. C., BRESNAHAN, J. C. & BEATTIE, M. S. 2008. Cell death after spinal cord injury is exacerbated by rapid TNFα-induced trafficking of GluR2-lacking AMPARs to the plasma membrane. *The Journal of Neuroscience,* 28**,** 11391-11400.

FÉRON, F., PERRY, C., COCHRANE, J., LICINA, P., NOWITZKE, A., URQUHART, S., GERAGHTY, T. & MACKAY-SIM, A. 2005. Autologous olfactory ensheathing cell transplantation in human spinal cord injury. *Brain,* 128**,** 2951-2960.

FIALKOW, L., WANG, Y. & DOWNEY, G. P. 2007. Reactive oxygen and nitrogen species as signaling molecules regulating neutrophil function. *Free Radical Biology and Medicine,* 42**,** 153-164.

FIGIEL, M., ALLRITZ, C., LEHMANN, C. & ENGELE, J. 2007. Gap junctional control of glial glutamate transporter expression. *Molecular and Cellular Neuroscience,* 35**,** 130-137.

FIGLEY, S. A., KHOSRAVI, R., LEGASTO, J. M., TSENG, Y.-F. & FEHLINGS, M. G. 2014. Characterization of vascular disruption and blood–spinal cord barrier permeability following traumatic spinal cord injury. *Journal of Neurotrauma,* 31**,** 541-552.

FITCH, M. T., DOLLER, C., COMBS, C. K., LANDRETH, G. E. & SILVER, J. 1999. Cellular and molecular mechanisms of glial scarring and progressive cavitation: in vivo and in vitroanalysis of inflammation-induced secondary injury after CNS trauma. *The Journal of Neuroscience,* 19**,** 8182-8198.

FITCH, M. T. & SILVER, J. 2008. CNS injury, glial scars, and inflammation: Inhibitory extracellular matrices and regeneration failure. *Experimental Neurology,* 209**,** 294-301.

FLARIS, N. A., DENSMORE, T. L., MOLLESTON, M. C. & HICKEY, W. F. 1993. Characterization of microglia and macrophages in the central nervous system of rats: definition of the differential expression of molecules using standard and novel monoclonal antibodies in normal CNS and in four models of parenchymal reaction. *Glia,* 7**,** 34-40.

FLEMING, J. C., NORENBERG, M. D., RAMSAY, D. A., DEKABAN, G. A., MARCILLO, A. E., SAENZ, A. D., PASQUALE-STYLES, M., DIETRICH, W. D. & WEAVER, L. C. 2006. The cellular inflammatory response in human spinal cords after injury. *Brain,* 129**,** 3249-3269.

FLING, S. P. & GREGERSON, D. S. 1986. Peptide and protein molecular weight determination by electrophoresis using a high-molarity tris buffer system without urea. *Analytical Biochemistry,* 155**,** 83-88.

FRANKEL, H., COLL, J., CHARLIFUE, S., WHITENECK, G., GARDNER, B., JAMOUS, M., KRISHNAN, K., NUSEIBEH, I., SAVIC, G. & SETT, P. 1998. Long-term survival in spinal cord injury: a fifty year investigation. *Spinal Cord,* 36**,** 266-274.

FRANTSEVA, M. V., KOKAROVTSEVA, L., NAUS, C. G., CARLEN, P. L., MACFABE, D. & VELAZQUEZ, J. L. P. 2002a. Specific gap junctions enhance the neuronal vulnerability to brain traumatic injury. *The Journal of Neuroscience,* 22**,** 644-653.

FRANTSEVA, M. V., KOKAROVTSEVA, L. & VELAZQUEZ, J. L. P. 2002b. Ischemia-induced brain damage depends on specific gap-junctional coupling. *Journal of Cerebral Blood Flow and Metabolism,* 22**,** 453-462.

FREUND, P., WANNIER, T., SCHMIDLIN, E., BLOCH, J., MIR, A., SCHWAB, M. E. & ROUILLER, E. M. 2007. Anti‐Nogo‐A antibody treatment enhances sprouting of corticospinal axons rostral to a unilateral cervical spinal cord lesion in adult macaque monkey. *Journal of Comparative Neurology,* 502**,** 644-659.

FRIEDMANN, I., HAUBEN, E., YOLES, E., KARDASH, L. & SCHWARTZ, M. 2001. T cell-mediated neuroprotection involves antithrombin activity. *Journal of Neuroimmunology,* 121**,** 12-21.

FRISÉN, J., JOHANSSON, C. B., TÖRÖK, C., RISLING, M. & LENDAHL, U. 1995. Rapid, widespread, and longlasting induction of nestin contributes to the generation of glial scar tissue after CNS injury. *The Journal of Cell Biology,* 131**,** 453-464.

FURLAN, J. C. & FEHLINGS, M. G. 2008. Cardiovascular complications after acute spinal cord injury: pathophysiology, diagnosis, and management. *Neurosurgical Focus,* 25**,** E13.

FURLAN, J. C., NOONAN, V., CADOTTE, D. W. & FEHLINGS, M. G. 2011. Timing of decompressive surgery of spinal cord after traumatic spinal cord injury: an evidence-based examination of pre-clinical and clinical studies. *Journal of Neurotrauma,* 28**,** 1371-1399.

GAO, M., LU, P., BEDNARK, B., LYNAM, D., CONNER, J. M., SAKAMOTO, J. & TUSZYNSKI, M. H. 2013. Templated agarose scaffolds for the support of motor axon regeneration into sites of complete spinal cord transection. *Biomaterials,* 34**,** 1529-1536.

GAULTON, A., BELLIS, L. J., BENTO, A. P., CHAMBERS, J., DAVIES, M., HERSEY, A., LIGHT, Y., MCGLINCHEY, S., MICHALOVICH, D. & AL-LAZIKANI, B. 2012. ChEMBL: a large-scale bioactivity database for drug discovery. *Nucleic Acids Research,* 40**,** D1100-D1107.

GAUTER-FLECKENSTEIN, B., REBOUCAS, J. S., FLECKENSTEIN, K., TOVMASYAN, A., OWZAR, K., JIANG, C., BATINIC-HABERLE, I. & VUJASKOVIC, Z. 2014. Robust rat pulmonary radioprotection by a lipophilic Mn N-alkylpyridylporphyrin, MnTnHex-2-PyP 5+. *Redox Biology,* 2**,** 400-410.

GAVIRIA, M., PRIVAT, A., D'ARBIGNY, P., KAMENKA, J.-M., HATON, H. & OHANNA, F. 2000. Neuroprotective effects of a novel NMDA antagonist, Gacyclidine, after experimental contusive spinal cord injury in adult rats. *Brain Research,* 874**,** 200-209.

GEHRMANN, J., MATSUMOTO, Y. & KREUTZBERG, G. W. 1995. Microglia: intrinsic immuneffector cell of the brain. *Brain Research Reviews,* 20**,** 269-287.

GIBSON, J. R., BEIERLEIN, M. & CONNORS, B. W. 2005. Functional properties of electrical synapses between inhibitory interneurons of neocortical layer 4. *Journal of Neurophysiology,* 93**,** 467-480.

GIGOUT, S., LOUVEL, J., KAWASAKI, H., D'ANTUONO, M., ARMAND, V., KURCEWICZ, I., OLIVIER, A., LASCHET, J., TURAK, B. & DEVAUX, B. 2006. Effects of gap junction blockers on human neocortical synchronization. *Neurobiology of Disease,* 22**,** 496-508.

GLASS, B. J., HU, R. G., PHILLIPS, A. R. & BECKER, D. L. 2015. The action of mimetic peptides on connexins protects fibroblasts from the negative effects of ischemia reperfusion. *Biology Open,* 4**,** 1473-1480.

GOODENOUGH, D. A., GOLIGER, J. A. & PAUL, D. L. 1996. Connexins, connexons, and intercellular communication. *Annual Review of Biochemistry,* 65**,** 475-502.

GORDH, T., CHU, H. & SHARMA, H. S. 2006. Spinal nerve lesion alters blood–spinal cord barrier function and activates astrocytes in the rat. *Pain,* 124**,** 211-221.

GORRIE, C. A., HAYWARD, I., CAMERON, N., KAILAINATHAN, G., NANDAPALAN, N., SUTHARSAN, R., WANG, J., MACKAY-SIM, A. & WAITE, P. 2010. Effects of human OEC-derived cell transplants in rodent spinal cord contusion injury. *Brain Research,* 1337**,** 8-20.

GOURDIE, R. G., SEVERS, N. J., GREEN, C. R., ROTHERY, S., GERMROTH, P. & THOMPSON, R. P. 1993. The spatial distribution and relative abundance of gap-junctional connexin40 and connexin43 correlate to functional properties of components of the cardiac atrioventricular conduction system. *Journal of Cell Science,* 105**,** 985-991.

GRABITZ, K., FREYE, E., PRIOR, R., KOLVENBACH, R. & SANDMANN, W. 1990. The role of superoxide dismutase (SOD) in preventing postischemic spinal cord injury. *Advances in Experimental Medicine and Biology***,** 13-16.

GRANAT, M., FERGUSON, A., ANDREWS, B. & DELARGY, M. 1993. The role of functional electrical stimulation in the rehabilitation of patients with incomplete spinal cord injury-observed benefits during gait studies. *Spinal Cord,* 31**,** 207-215.

GRANSEE, H. M., ZHAN, W.-Z., SIECK, G. C. & MANTILLA, C. B. 2015. Localized delivery of brain-derived neurotrophic factor-expressing mesenchymal stem cells enhances functional recovery following cervical spinal cord injury. *Journal of Neurotrauma,* 32**,** 185-193.

GREEN, C. R., YONG LAW, L., LIN, J. S. & BECKER, D. L. 2001. Spatiotemporal depletion of connexins using antisense oligonucleotides. *In:* BRUZZONE, R. & GIAUME, C. (eds.) *Connexin Methods and Protocols*. Totowa, New Jersey: Humana Press.

GREGORI-PUIGJANÉ, E., SETOLA, V., HERT, J., CREWS, B. A., IRWIN, J. J., LOUNKINE, E., MARNETT, L., ROTH, B. L. & SHOICHET, B. K. 2012. Identifying mechanism-of-action targets for drugs and probes. *Proceedings of the National Academy of Sciences,* 109**,** 11178-11183.

GROSSMAN, R. G., FEHLINGS, M. G., FRANKOWSKI, R. F., BURAU, K. D., CHOW, D. S., TATOR, C., TENG, A., TOUPS, E. G., HARROP, J. S. & AARABI, B. 2014. A prospective, multicenter, phase I matched-comparison group trial of safety, pharmacokinetics, and preliminary efficacy of riluzole in patients with traumatic spinal cord injury. *Journal of Neurotrauma,* 31**,** 239-255.

GRUPCHEVA, C. N., LAUX, W. T., RUPENTHAL, I. D., MCGHEE, J., MCGHEE, C. N. & GREEN, C. R. 2012. Improved corneal wound healing through modulation of gap junction communication using connexin43-specific antisense oligodeoxynucleotides. *Investigative Ophthalmology and Visual Science,* 53**,** 1130-1138.

GU, Y., WU, G., WANG, X., WANG, X., WANG, Y. & HUANG, C. 2014. Artemisinin prevents electric remodeling following myocardial infarction possibly by upregulating the expression of connexin 43. *Molecular Medicine Reports,* 10**,** 1851-1856.

GUERRERO, A. R., UCHIDA, K., NAKAJIMA, H., WATANABE, S., NAKAMURA, M., JOHNSON, W. & BABA, H. 2012. Blockade of interleukin-6 signaling inhibits the classic pathway and promotes an alternative pathway of macrophage activation after spinal cord injury in mice. *Journal of Neuroinflammation,* 9**,** 40.

GUO, H., ACEVEDO, P., PARSA, F. D. & BERTRAM, J. S. 1992. Gap-junctional protein connexin 43 is expressed in dermis and epidermis of human skin: differential modulation by retinoids. *Journal of Investigative Dermatology,* 99**,** 460-467.

GWAK, Y. S., KANG, J., UNABIA, G. C. & HULSEBOSCH, C. E. 2012. Spatial and temporal activation of spinal glial cells: role of gliopathy in central neuropathic pain following spinal cord injury in rats. *Experimental Neurology,* 234**,** 362-372.

HABGOOD, M., BYE, N., DZIEGIELEWSKA, K., EK, C., LANE, M., POTTER, A., MORGANTI‐KOSSMANN, C. & SAUNDERS, N. 2007. Changes in blood‐brain barrier permeability to large and small molecules following traumatic brain injury in mice. *European Journal of Neuroscience,* 25**,** 231-238.

HADLEY, M. N., WALTERS, B. C., GRABB, P. A., OYESIKU, N. M., PRZYBYLSKI, G. J., RESNICK, D. K. & RYKEN, T. C. 2010. Guidelines for the management of acute cervical spine and spinal cord injuries. Section on Disorders of the Spine and Peripheral Nerves of the American Association of Neurological Surgeons and the Congress of Neurological Surgeons.

HAGG, T. & OUDEGA, M. 2006. Degenerative and spontaneous regenerative processes after spinal cord injury. *Journal of Neurotrauma,* 23**,** 263-280.

HAINS, B. C. & WAXMAN, S. G. 2006. Activated microglia contribute to the maintenance of chronic pain after spinal cord injury. *The Journal of Neuroscience,* 26**,** 4308-4317.

HALL, E. D. & BRAUGHLER, J. M. 1981. Acute effects of intravenous glucocorticoid pretreatment on the in vitro peroxidation of cat spinal cord tissue. *Experimental Neurology,* 73**,** 321-324.

HAN, S., ARNOLD, S. A., SITHU, S. D., MAHONEY, E. T., GERALDS, J. T., TRAN, P., BENTON, R. L., MADDIE, M. A., D'SOUZA, S. E. & WHITTEMORE, S. R. 2010. Rescuing vasculature with intravenous angiopoietin-1 and αvβ3 integrin peptide is protective after spinal cord injury. *Brain,* 133**,** 1026-1042.

HANIGAN, W. C. & ANDERSON, R. J. 1992. Commentary on NASCIS-2. *Journal of Spinal Disorders and Techniques,* 5**,** 125-131.

HASHIMOTO, M., NITTA, A., FUKUMITSU, H., NOMOTO, H., SHEN, L. & FURUKAWA, S. 2005. Involvement of glial cell line‐derived neurotrophic factor in activation processes of rodent macrophages. *Journal of Neuroscience Research,* 79**,** 476-487.

HAUBEN, E., NEVO, U., YOLES, E., MOALEM, G., AGRANOV, E., MOR, F., AKSELROD, S., NEEMAN, M., COHEN, I. & SCHWARTZ, M. 2000. Autoimmune T cells as potential neuroprotective therapy for spinal cord injury. *The Lancet,* 355**,** 286-287.

HAUPT, C., WITTE, O. W. & FRAHM, C. 2007. Up-regulation of Connexin43 in the glial scar following photothrombotic ischemic injury. *Molecular and Cellular Neuroscience,* 35**,** 89-99.

HAUSMANN, O. N. 2003. Post-traumatic inflammation following spinal cord injury. *Spinal Cord,* 41**,** 369-378.

HAWAT, G., BENDERDOUR, M., ROUSSEAU, G. & BAROUDI, G. 2010. Connexin 43 mimetic peptide Gap26 confers protection to intact heart against myocardial ischemia injury. *Pflügers Archiv-European Journal of Physiology,* 460**,** 583-592.

HAWAT, G., HÉLIE, P. & BAROUDI, G. 2012. Single intravenous low-dose injections of connexin 43 mimetic peptides protect ischemic heart in vivo against myocardial infarction. *Journal of Molecular and Cellular Cardiology,* 53**,** 559-566.

HAYATDAVOUDI, G., CRAPO, J. D., MILLER, F. J. & O'NEIL, J. J. 1980. Factors determining degree of inflation in intratracheally fixed rat lungs. *Journal of Applied Physiology,* 48**,** 389-393.

HERMANN, G. E., ROGERS, R. C., BRESNAHAN, J. C. & BEATTIE, M. S. 2001. Tumor necrosis factor-α induces cFOS and strongly potentiates glutamate-mediated cell death in the rat spinal cord. *Neurobiology of Disease,* 8**,** 590-599.

HERRERA, J. J., NESIC, O. & NARAYANA, P. A. 2009. Reduced vascular endothelial growth factor expression in contusive spinal cord injury. *Journal of Neurotrauma,* 26**,** 995-1003.

HESKETH, G. G., SHAH, M. H., HALPERIN, V. L., COOKE, C. A., AKAR, F. G., YEN, T. E., KASS, D. A., MACHAMER, C. E., VAN EYK, J. E. & TOMASELLI, G. F. 2010. Ultrastructure and regulation of lateralized connexin43 in the failing heart. *Circulation Research,* 106**,** 1153-1163.

HILL, M. 2013. *Cell Junctions* [Online]. Sydney, Australia: University of New South Wales. Available: http://php.med.unsw.edu.au/cellbiology/index.php?title=Cell_Junctions [Accessed 22 April, 2014].

HINKEROHE, D., SMIKALLA, D., HAGHIKIA, A., HEUPEL, K., HAASE, C. G., DERMIETZEL, R. & FAUSTMANN, P. M. 2005. Effects of cytokines on microglial phenotypes and astroglial coupling in an inflammatory coculture model. *Glia,* 52**,** 85-97.

HOLMGREN, A., JOHANSSON, C., BERNDT, C., LÖNN, M., HUDEMANN, C. & LILLIG, C. 2005. Thiol redox control via thioredoxin and glutaredoxin systems. *Biochemical Society Transactions,* 33**,** 1375-1377.

HONEGGER, C. G., KRENGER, W. & LANGEMANN, H. 1989. Measurement of free radical scavengers in the spinal cord of rats with experimental autoimmune encephalomyelitis. *Neuroscience Letters,* 98**,** 327-332.

HONG, F. D. & CLAYMAN, G. L. 2000. Isolation of a peptide for targeted drug delivery into human head and neck solid tumors. *Cancer Research,* 60**,** 6551-6556.

HONG, T., WANG, H., WANG, Y. & WANG, H. 2009. Effects of gap junctional blockers on cerebral vasospasm after subarachnoid hemorrhage in rabbits. *Neurological Research,* 31**,** 238-244.

HOOPMANN, M. R. & MORITZ, R. L. 2013. Current algorithmic solutions for peptide-based proteomics data generation and identification. *Current Opinion in Biotechnology,* 24**,** 31-38.

HORKY, L. L., GALIMI, F., GAGE, F. H. & HORNER, P. J. 2006. Fate of endogenous stem/progenitor cells following spinal cord injury. *Journal of Comparative Neurology,* 498**,** 525-538.

HORMUZDI, S. G., FILIPPOV, M. A., MITROPOULOU, G., MONYER, H. & BRUZZONE, R. 2004. Electrical synapses: a dynamic signaling system that shapes the activity of neuronal networks. *Biochimica et Biophysica Acta (BBA)-Biomembranes,* 1662**,** 113-137.

HORNER, P. J., POWER, A. E., KEMPERMANN, G., KUHN, H. G., PALMER, T. D., WINKLER, J., THAL, L. J. & GAGE, F. H. 2000. Proliferation and differentiation of progenitor cells throughout the intact adult rat spinal cord. *The Journal of Neuroscience,* 20**,** 2218-2228.

HU, R., ZHOU, J., LUO, C., LIN, J., WANG, X., LI, X., BIAN, X., LI, Y., WAN, Q. & YU, Y. 2010. Glial scar and neuroregeneration: histological, functional, and magnetic resonance imaging analysis in chronic spinal cord injury: Laboratory investigation. *Journal of Neurosurgery: Spine,* 13**,** 169-180.

HUANG, C., HAN, X., LI, X., LAM, E., PENG, W., LOU, N., TORRES, A., YANG, M., GARRE, J. M. & TIAN, G.-F. 2012. Critical role of connexin 43 in secondary expansion of traumatic spinal cord injury. *The Journal of Neuroscience,* 32**,** 3333-3338.

HURLBERT, R. J. 2000. Methylprednisolone for acute spinal cord injury: an inappropriate standard of care. *Journal of Neurosurgery,* 93**,** 1-7.

HURLBERT, R. J., HADLEY, M. N., WALTERS, B. C., AARABI, B., DHALL, S. S., GELB, D. E., ROZZELLE, C. J., RYKEN, T. C. & THEODORE, N. 2013. Pharmacological therapy for acute spinal cord injury. *Neurosurgery,* 72**,** 93-105.

IKEDA, H. & MURASE, K. 2004. Glial nitric oxide-mediated long-term presynaptic facilitation revealed by optical imaging in rat spinal dorsal horn. *The Journal of Neuroscience,* 24**,** 9888-9896.

ILVESARO, J., TAVI, P. & TUUKKANEN, J. 2001. Connexin-mimetic peptide Gap 27 decreases osteoclastic activity. *BMC Musculoskeletal Disorders,* 2**,** 10.

ISHII, H., JIN, X., UENO, M., TANABE, S., KUBO, T., SERADA, S., NAKA, T. & YAMASHITA, T. 2012. Adoptive transfer of Th1-conditioned lymphocytes promotes axonal remodeling and functional recovery after spinal cord injury. *Cell Death and Disease,* 3**,** e363.

ISHIKAWA, S., KUNO, A., TANNO, M., MIKI, T., KOUZU, H., ITOH, T., SATO, T., SUNAGA, D., MURASE, H. & MIURA, T. 2012. Role of connexin-43 in protective PI3K-Akt-GSK-3β signaling in cardiomyocytes. *American Journal of Physiology-Heart and Circulatory Physiology,* 302**,** H2536-H2544.

IZUMI, B., NAKASA, T., TANAKA, N., NAKANISHI, K., KAMEI, N., YAMAMOTO, R., NAKAMAE, T., OHTA, R., FUJIOKA, Y. & YAMASAKI, K. 2011. MicroRNA-223 expression in neutrophils in the early phase of secondary damage after spinal cord injury. *Neuroscience Letters,* 492**,** 114-118.

JASIM, D. A., MÉNARD-MOYON, C., BÉGIN, D., BIANCO, A. & KOSTARELOS, K. 2015. Tissue distribution and urinary excretion of intravenously administered chemically functionalized graphene oxide sheets. *Chemical Science,* 6**,** 3952-3964.

JIA, Z., ZHU, H., LI, J., WANG, X., MISRA, H. & LI, Y. 2012. Oxidative stress in spinal cord injury and antioxidant-based intervention. *Spinal Cord,* 50**,** 264-274.

JIANG, M. H., CHUNG, E., CHI, G. F., AHN, W., LIM, J. E., HONG, H. S., KIM, D. W., CHOI, H., KIM, J. & SON, Y. 2012. Substance P induces M2-type macrophages after spinal cord injury. *Neuroreport,* 23**,** 786-792.

JIN, Y., BOUYER, J., SHUMSKY, J., HAAS, C. & FISCHER, I. 2016. Transplantation of neural progenitor cells in chronic spinal cord injury. *Neuroscience,* 320**,** 69-82.

JONES, D., ANDERSON, E. & GALVIN, K. 2003a. Spinal cord regeneration: moving tentatively towards new perspectives. *NeuroRehabilitation,* 18**,** 339-351.

JONES, L. L., MARGOLIS, R. U. & TUSZYNSKI, M. H. 2003b. The chondroitin sulfate proteoglycans neurocan, brevican, phosphacan, and versican are differentially regulated following spinal cord injury. *Experimental Neurology,* 182**,** 399-411.

JONES, S. A. 2005. Directing transition from innate to acquired immunity: defining a role for IL-6. *The Journal of Immunology,* 175**,** 3463-3468.

JONES, T., MCDANIEL, E. & POPOVICH, P. 2005. Inflammatory-mediated injury and repair in the traumatically injured spinal cord. *Current Pharmaceutical Design,* 11**,** 1223-1236.

JONES, T. B., BASSO, D. M., SODHI, A., PAN, J. Z., HART, R. P., MACCALLUM, R. C., LEE, S., WHITACRE, C. C. & POPOVICH, P. G. 2002. Pathological CNS autoimmune disease triggered by traumatic spinal cord injury: implications for autoimmune vaccine therapy. *The Journal of Neuroscience,* 22**,** 2690-2700.

KAMASAWA, N., SIK, A., MORITA, M., YASUMURA, T., DAVIDSON, K., NAGY, J. & RASH, J. 2005. Connexin-47 and connexin-32 in gap junctions of oligodendrocyte somata, myelin sheaths, paranodal loops and Schmidt-Lanterman incisures: implications for ionic homeostasis and potassium siphoning. *Neuroscience,* 136**,** 65-86.

KAMIYA, N., ABE, H., GOTO, M., TSUJI, Y. & JIKUYA, H. 2009. Fluorescent substrates for covalent protein labeling catalyzed by microbial transglutaminase. *Organic and Biomolecular Chemistry,* 7**,** 3407-3412.

KANG, J., KANG, N., LOVATT, D., TORRES, A., ZHAO, Z., LIN, J. & NEDERGAARD, M. 2008. Connexin 43 hemichannels are permeable to ATP. *The Journal of Neuroscience,* 28**,** 4702-4711.

KANNO, H., OZAWA, H., SEKIGUCHI, A., YAMAYA, S. & ITOI, E. 2011. Induction of autophagy and autophagic cell death in damaged neural tissue after acute spinal cord injury in mice. *Spine,* 36**,** E1427-E1434.

KARIMI-ABDOLREZAEE, S. & BILLAKANTI, R. 2012. Reactive astrogliosis after spinal cord injury - beneficial and detrimental effects. *Molecular Neurobiology,* 46**,** 251-264.

KARIMI-ABDOLREZAEE, S., EFTEKHARPOUR, E., WANG, J., MORSHEAD, C. M. & FEHLINGS, M. G. 2006. Delayed transplantation of adult neural precursor cells promotes remyelination and functional neurological recovery after spinal cord injury. *The Journal of Neuroscience,* 26**,** 3377-3389.

KE, Y., CHI, L., XU, R., LUO, C., GOZAL, D. & LIU, R. 2006. Early response of endogenous adult neural progenitor cells to acute spinal cord injury in mice. *Stem Cells,* 24**,** 1011-1019.

KERR, N. M., JOHNSON, C. S., DE SOUZA, C. F., CHEE, K.-S., GOOD, W. R., GREEN, C. R. & DANESH-MEYER, H. V. 2010. Immunolocalization of gap junction protein connexin43 (GJA1) in the human retina and optic nerve. *Investigative Ophthalmology and Visual science,* 51**,** 4028-4034.

KIGERL, K. A., GENSEL, J. C., ANKENY, D. P., ALEXANDER, J. K., DONNELLY, D. J. & POPOVICH, P. G. 2009. Identification of two distinct macrophage subsets with divergent effects causing either neurotoxicity or regeneration in the injured mouse spinal cord. *The Journal of Neuroscience,* 29**,** 13435-13444.

KIGERL, K. A., MCGAUGHY, V. M. & POPOVICH, P. G. 2006. Comparative analysis of lesion development and intraspinal inflammation in four strains of mice following spinal contusion injury. *Journal of Comparative Neurology,* 494**,** 578-594.

KIM, S., GUPTA, N., BANDEIRA, N. & PEVZNER, P. A. 2009. Spectral dictionaries integrating de novo peptide sequencing with database search of tandem mass spectra. *Molecular and Cellular Proteomics,* 8**,** 53-69.

KIM, Y., GRIFFIN, J. M., HARRIS, P. W., CHAN, S. H. C., NICHOLSON, L. F., BRIMBLE, M. A., O'CARROLL, S. J. & GREEN, C. R. 2017. Characterizing the mode of action of extracellular Connexin43 channel blocking mimetic peptides in an in vitro ischemia injury model. *Biochimica et Biophysica Acta - General Subjects,* 1861**,** 68-78.

KIPNIS, J., YOLES, E., SCHORI, H., HAUBEN, E., SHAKED, I. & SCHWARTZ, M. 2001. Neuronal survival after CNS insult is determined by a genetically encoded autoimmune response. *The Journal of Neuroscience,* 21**,** 4564-4571.

KIRSHBLUM, S., GONZALEZ, P., CUCCURULLO, S. & LUCIANO, L. 2004. *Physical Medicine and Rehabilitation Board Review,* New York, Demos Medical Publishing.

KIRSHBLUM, S. C., PRIEBE, M. M., HO, C. H., SCELZA, W. M., CHIODO, A. E. & WUERMSER, L. A. 2007. Spinal cord injury medicine. 3. Rehabilitation phase after acute spinal cord injury. *Archives of Physical Medicine and Rehabilitation,* 88**,** 62-70.

KLEOPA, K. A., ORTHMANN, J. L., ENRIQUEZ, A., PAUL, D. L. & SCHERER, S. S. 2004. Unique distributions of the gap junction proteins connexin29, connexin32, and connexin47 in oligodendrocytes. *Glia,* 47**,** 346-357.

KLUSMAN, I. & SCHWAB, M. E. 1997. Effects of pro-inflammatory cytokines in experimental spinal cord injury. *Brain Research,* 762**,** 173-184.

KOSUGE, M., TAKEUCHI, T., NAKASE, I., JONES, A. T. & FUTAKI, S. 2008. Cellular internalization and distribution of arginine-rich peptides as a function of extracellular peptide concentration, serum, and plasma membrane associated proteoglycans. *Bioconjugate Chemistry,* 19**,** 656-664.

KOULAKOFF, A., EZAN, P. & GIAUME, C. 2008. Neurons control the expression of connexin 30 and connexin 43 in mouse cortical astrocytes. *Glia,* 56**,** 1299-1311.

KOZLOV, G., MÄÄTTÄNEN, P., THOMAS, D. Y. & GEHRING, K. 2010. A structural overview of the PDI family of proteins. *The FEBS Journal,* 277**,** 3924-3936.

KOZLOVA, E. N. 2003. Differentiation and migration of astrocytes in the spinal cord following dorsal root injury in the adult rat. *European Journal of Neuroscience,* 17**,** 782-790.

KRATZ, F. 2008. Albumin as a drug carrier: design of prodrugs, drug conjugates and nanoparticles. *Journal of Controlled Release,* 132**,** 171-183.

KREUTZBERG, G. W. 1996. Microglia: a sensor for pathological events in the CNS. *Trends in Neurosciences,* 19**,** 312-318.

KRUSE, D., O'LEARY, P., BERKOWITZ, M. & HARVEY, C. 1998. *Spinal cord injury: An analysis of medical and social costs,* New York, Demos Medical Publishing.

KUBINOVÁ, Š., HORÁK, D., HEJČL, A., PLICHTA, Z., KOTEK, J., PROKS, V., FOROSTYAK, S. & SYKOVÁ, E. 2015. SIKVAV‐modified highly superporous PHEMA scaffolds with oriented pores for spinal cord injury repair. *Journal of Tissue Engineering and Regenerative Medicine,* 9**,** 1298-1309.

KUBOTA, K., SAIWAI, H., KUMAMARU, H., MAEDA, T., OHKAWA, Y., ARATANI, Y., NAGANO, T., IWAMOTO, Y. & OKADA, S. 2012. Myeloperoxidase exacerbates secondary injury by generating highly reactive oxygen species and mediating neutrophil recruitment in experimental spinal cord injury. *Spine,* 37**,** 1363-1369.

KUHLMANN, M. T., KIRCHHOF, P., KLOCKE, R., HASIB, L., STYPMANN, J., FABRITZ, L., STELLJES, M., TIAN, W., ZWIENER, M. & MUELLER, M. 2006. G-CSF/SCF reduces inducible arrhythmias in the infarcted heart potentially via increased connexin43 expression and arteriogenesis. *The Journal of Experimental Medicine,* 203**,** 87-97.

KWAK, B. R., PEPPER, M. S., GROS, D. B. & MEDA, P. 2001. Inhibition of endothelial wound repair by dominant negative connexin inhibitors. *Molecular Biology of the Cell,* 12**,** 831-845.

KWON, B. K., TETZLAFF, W., GRAUER, J. N., BEINER, J. & VACCARO, A. R. 2004. Pathophysiology and pharmacologic treatment of acute spinal cord injury. *The Spine Journal,* 4**,** 451-464.

KWON, K. J., JUNG, Y. S., LEE, S. H., MOON, C. H. & BAIK, E. J. 2005. Arachidonic acid induces neuronal death through lipoxygenase and cytochrome P450 rather than cyclooxygenase. *Journal of Neuroscience Research,* 81**,** 73-84.

LAABS, T., CARULLI, D., GELLER, H. M. & FAWCETT, J. W. 2005. Chondroitin sulfate proteoglycans in neural development and regeneration. *Current Opinion in Neurobiology,* 15**,** 116-120.

LACROIX, S., CHANG, L., ROSE‐JOHN, S. & TUSZYNSKI, M. H. 2002. Delivery of hyper‐interleukin‐6 to the injured spinal cord increases neutrophil and macrophage infiltration and inhibits axonal growth. *Journal of Comparative Neurology,* 454**,** 213-228.

LAMKE, L.-O. & LILJEDAHL, S.-O. 1976. Plasma volume changes after infusion of various plasma expanders. *Resuscitation,* 5**,** 93-101.

LAMPE, P. D., TENBROEK, E. M., BURT, J. M., KURATA, W. E., JOHNSON, R. G. & LAU, A. F. 2000. Phosphorylation of connexin43 on serine368 by protein kinase C regulates gap junctional communication. *The Journal of Cell Biology,* 149**,** 1503-1512.

LANE, M., TRUETTNER, J., BRUNSCHWIG, J. P., GOMEZ, A., BUNGE, M., DIETRICH, W., DZIEGIELEWSKA, K., EK, C., VANDEBERG, J. & SAUNDERS, N. 2007. Age‐related differences in the local cellular and molecular responses to injury in developing spinal cord of the opossum, Monodelphis domestica. *European Journal of Neuroscience,* 25**,** 1725-1742.

LEBRETON, F., PIROG, A., BELOUAH, I., BOSCO, D., BERNEY, T., MEDA, P., BORNAT, Y., CATARGI, B., RENAUD, S. & RAOUX, M. 2015. Slow potentials encode intercellular coupling and insulin demand in pancreatic beta cells. *Diabetologia,* 58**,** 1291-1299.

LEE, I. H., LINDQVIST, E., KIEHN, O., WIDENFALK, J. & OLSON, L. 2005. Glial and neuronal connexin expression patterns in the rat spinal cord during development and following injury. *Journal of Comparative Neurology,* 489**,** 1-10.

LEE-KUBLI, C. A., INGVES, M., HENRY, K. W., SHIAO, R., COLLYER, E., TUSZYNSKI, M. H. & CAMPANA, W. M. 2016. Analysis of the behavioral, cellular and molecular characteristics of pain in severe rodent spinal cord injury. *Experimental Neurology,* 278**,** 91-104.

LEEM, J. W., KIM, H. K., HULSEBOSCH, C. E. & GWAK, Y. S. 2010. Ionotropic glutamate receptors contribute to maintained neuronal hyperexcitability following spinal cord injury in rats. *Experimental Neurology,* 224**,** 321-324.

LEPORE, A. C., O'DONNELL, J., BONNER, J. F., PAUL, C., MILLER, M. E., RAUCK, B., KUSHNER, R. A., ROTHSTEIN, J. D., FISCHER, I. & MARAGAKIS, N. J. 2011. Spatial and temporal changes in promoter activity of the astrocyte glutamate transporter GLT1 following traumatic spinal cord injury. *Journal of Neuroscience Research,* 89**,** 1001-1017.

LEWEN, A., MATZ, P. & CHAN, P. H. 2000. Free radical pathways in CNS injury. *Journal of Neurotrauma,* 17**,** 871-890.

LEYBAERT, L., BRAET, K., VANDAMME, W., CABOOTER, L., MARTIN, P. E. & EVANS, W. H. 2003. Connexin channels, connexin mimetic peptides and ATP release. *Cell Communication and Adhesion,* 10**,** 251-257.

LI, F., SUGISHITA, K., SU, Z., UEDA, I. & BARRY, W. H. 2001. Activation of connexin-43 hemichannels can elevate [Ca 2+] i and [Na+] i in rabbit ventricular myocytes during metabolic inhibition. *Journal of Molecular and Cellular Cardiology,* 33**,** 2145-2155.

LI, M. W., MRUK, D. D., LEE, W. M. & CHENG, C. Y. 2010. Connexin 43 is critical to maintain the homeostasis of the blood–testis barrier via its effects on tight junction reassembly. *Proceedings of the National Academy of Sciences,* 107**,** 17998-18003.

LI, S. & STYS, P. 2001. Na+–K+-ATPase inhibition and depolarization induce glutamate release via reverse Na+-dependent transport in spinal cord white matter. *Neuroscience,* 107**,** 675-683.

LI, X., IONESCU, A., LYNN, B., LU, S., KAMASAWA, N., MORITA, M., DAVIDSON, K., YASUMURA, T., RASH, J. & NAGY, J. 2004. Connexin47, connexin29 and connexin32 co-expression in oligodendrocytes and Cx47 association with zonula occludens-1 (ZO-1) in mouse brain. *Neuroscience,* 126**,** 611-630.

LI, Y. & RAISMAN, G. 1995. Sprouts from cut corticospinal axons persist in the presence of astrocytic scarring in long-term lesions of the adult rat spinal cord. *Experimental Neurology,* 134**,** 102-111.

LI, Z.-W., TANG, R.-H., ZHANG, J.-P., TANG, Z.-P., QU, W.-S., ZHU, W.-H., LI, J.-J., XIE, M.-J., TIAN, D.-S. & WANG, W. 2011. Inhibiting epidermal growth factor receptor attenuates reactive astrogliosis and improves functional outcome after spinal cord injury in rats. *Neurochemistry International,* 58**,** 812-819.

LIANG, L., LIU, X., WANG, Q., CHENG, S., ZHANG, S. & ZHANG, M. 2013. Pharmacokinetics, tissue distribution and excretion study of resveratrol and its prodrug 3, 5, 4′ -tri-O-acetylresveratrol in rats. *Phytomedicine,* 20**,** 558-563.

LIAO, Y. & DULING, B. R. 2000. Blockade of connexin 43 expression by stable transfection of antisense cDNA in cultured vascular smooth muscle cells. *Antisense and Nucleic Acid Drug Development,* 10**,** 275-281.

LIN, J. H., WEIGEL, H., COTRINA, M. L., LIU, S., BUENO, E., HANSEN, A. J., HANSEN, T. W., GOLDMAN, S. & NEDERGAARD, M. 1998. Gap-junction-mediated propagation and amplification of cell injury. *Nature Neuroscience,* 1**,** 494-500.

LIU, C., SHI, Z., FAN, L., ZHANG, C., WANG, K. & WANG, B. 2011. Resveratrol improves neuron protection and functional recovery in rat model of spinal cord injury. *Brain Besearch,* 1374**,** 100-109.

LIU, D., XU, G.-Y., PAN, E. & MCADOO, D. 1999. Neurotoxicity of glutamate at the concentration released upon spinal cord injury. *Neuroscience,* 93**,** 1383-1389.

LIU, N. K., ZHANG, Y. P., TITSWORTH, W. L., JIANG, X., HAN, S., LU, P. H., SHIELDS, C. B. & XU, X. M. 2006. A novel role of phospholipase A2 in mediating spinal cord secondary injury. *Annals of Neurology,* 59**,** 606-619.

LIU, Y., YE, H., SATKUNENDRARAJAH, K., YAO, G. S., BAYON, Y. & FEHLINGS, M. G. 2013. A self-assembling peptide reduces glial scarring, attenuates post-traumatic inflammation and promotes neurological recovery following spinal cord injury. *Acta Biomaterialia,* 9**,** 8075-8088.

LOANE, D. J. & BYRNES, K. R. 2010. Role of microglia in neurotrauma. *Neurotherapeutics,* 7**,** 366-377.

LOPES‐CARVALHO, T. & KEARNEY, J. F. 2004. Development and selection of marginal zone B cells. *Immunological Reviews,* 197**,** 192-205.

LUND, U., RIPPE, A., VENTUROLI, D., TENSTAD, O., GRUBB, A. & RIPPE, B. 2003. Glomerular filtration rate dependence of sieving of albumin and some neutral proteins in rat kidneys. *American Journal of Physiology-Renal Physiology,* 284**,** F1226-F1234.

LUO, J., BORGENS, R. & SHI, R. 2002. Polyethylene glycol immediately repairs neuronal membranes and inhibits free radical production after acute spinal cord injury. *Journal of Neurochemistry,* 83**,** 471-480.

LYNCH, C. L. & POPOVIC, M. R. 2008. Functional electrical stimulation. *Control Systems,* 28**,** 40-50.

MABON, P. J., WEAVER, L. C. & DEKABAN, G. A. 2000. Inhibition of monocyte/macrophage migration to a spinal cord injury site by an antibody to the integrin alphaD: a potential new anti-inflammatory treatment. *Experimental Neurology,* 166**,** 52-64.

MACKINTOSH, J. A., CHOI, H. Y., BAE, S. H., VEAL, D. A., BELL, P. J., FERRARI, B. C., VAN DYK, D. D., VERRILLS, N. M., PAIK, Y. K. & KARUSO, P. 2003. A fluorescent natural product for ultra sensitive detection of proteins in one‐dimensional and two‐dimensional gel electrophoresis. *Proteomics,* 3**,** 2273-2288.

MAIER, I. C. & SCHWAB, M. E. 2006. Sprouting, regeneration and circuit formation in the injured spinal cord: factors and activity. *Philosophical Transactions of the Royal Society B: Biological Sciences,* 361**,** 1611-1634.

MAIKOS, J. T. & SHREIBER, D. I. 2007. Immediate damage to the blood-spinal cord barrier due to mechanical trauma. *Journal of Neurotrauma,* 24**,** 492-507.

MANABE, Y., ANRATHER, J., KAWANO, T., NIWA, K., ZHOU, P., ROSS, M. E. & IADECOLA, C. 2004. Prostanoids, not reactive oxygen species, mediate COX‐2‐dependent neurotoxicity. *Annals of Neurology,* 55**,** 668-675.

MANTOVANI, A., SICA, A. & LOCATI, M. 2007. New vistas on macrophage differentiation and activation. *European Journal of Immunology,* 37**,** 14-16.

MANTOVANI, A., SICA, A., SOZZANI, S., ALLAVENA, P., VECCHI, A. & LOCATI, M. 2004. The chemokine system in diverse forms of macrophage activation and polarization. *Trends in Immunology,* 25**,** 677-686.

MAO, Y., MATHEWS, K. & GORRIE, C. A. 2016. Temporal response of endogenous neural progenitor cells following injury to the adult rat spinal cord. *Frontiers in Cellular Neuroscience,* 10.

MAO, Y., TONKIN, R. S., NGUYEN, T., O'CARROLL, S. J., NICHOLSON, L. F., GREEN, C. R., MOALEM-TAYLOR, G. & GORRIE, C. A. 2017. Systemic administration of Connexin43 mimetic peptide improves functional recovery after traumatic spinal cord Injury in adult Rats. *Journal of Neurotrauma,* 33**,** 707-719.

MÁRQUEZ-ROSADO, L., SOLAN, J. L., DUNN, C. A., NORRIS, R. P. & LAMPE, P. D. 2012. Connexin43 phosphorylation in brain, cardiac, endothelial and epithelial tissues. *Biochimica et Biophysica Acta (BBA)-Biomembranes,* 1818**,** 1985-1992.

MARRACCI, G. H., JONES, R. E., MCKEON, G. P. & BOURDETTE, D. N. 2002. Alpha lipoic acid inhibits T cell migration into the spinal cord and suppresses and treats experimental autoimmune encephalomyelitis. *Journal of Neuroimmunology,* 131**,** 104-114.

MARTIN, P. E., WALL, C. & GRIFFITH, T. M. 2005. Effects of connexin‐mimetic peptides on gap junction functionality and connexin expression in cultured vascular cells. *British Journal of Pharmacology,* 144**,** 617-627.

MARX, H., LEMEER, S., SCHLIEP, J. E., MATHERON, L., MOHAMMED, S., COX, J., MANN, M., HECK, A. J. & KUSTER, B. 2013. A large synthetic peptide and phosphopeptide reference library for mass spectrometry-based proteomics. *Nature Biotechnology,* 31**,** 557-564.

MASAKI, K., SUZUKI, S. O., MATSUSHITA, T., YONEKAWA, T., MATSUOKA, T., ISOBE, N., MOTOMURA, K., WU, X.-M., TABIRA, T. & IWAKI, T. 2012. Extensive loss of connexins in Baló's disease: evidence for an auto-antibody-independent astrocytopathy via impaired astrocyte–oligodendrocyte/myelin interaction. *Acta Neuropathologica,* 123**,** 887-900.

MATSUE, H., YAO, J., MATSUE, K., NAGASAKA, A., SUGIYAMA, H., AOKI, R., KITAMURA, M. & SHIMADA, S. 2006. Gap junction-mediated intercellular communication between dendritic cells (DCs) is required for effective activation of DCs. *The Journal of Immunology,* 176**,** 181-190.

MATUTE, C., SÁNCHEZ-GÓMEZ, M. V., MARTÍNEZ-MILLÁN, L. & MILEDI, R. 1997. Glutamate receptor-mediated toxicity in optic nerve oligodendrocytes. *Proceedings of the National Academy of Sciences,* 94**,** 8830-8835.

MAUTES, A. E., BERGERON, M., SHARP, F. R., PANTER, S. S., WEINZIERL, M., GUENTHER, K. & NOBLE, L. J. 2000a. Sustained induction of heme oxygenase-1 in the traumatized spinal cord. *Experimental Neurology,* 166**,** 254-265.

MAUTES, A. E., WEINZIERL, M. R., DONOVAN, F. & NOBLE, L. J. 2000b. Vascular events after spinal cord injury: contribution to secondary pathogenesis. *Physical Therapy,* 80**,** 673-687.

MCCREEDY, D., WILEMS, T., XU, H., BUTTS, J., BROWN, C., SMITH, A. & SAKIYAMA-ELBERT, S. 2014. Survival, differentiation, and migration of high-purity mouse embryonic stem cell-derived progenitor motor neurons in fibrin scaffolds after sub-acute spinal cord injury. *Biomaterials Science,* 2**,** 1672-1682.

MCDONALD, J. W., LIU, X.-Z., QU, Y., LIU, S., MICKEY, S. K., TURETSKY, D., GOTTLIEB, D. I. & CHOI, D. W. 1999. Transplanted embryonic stem cells survive, differentiate and promote recovery in injured rat spinal cord. *Nature Medicine,* 5**,** 1410-1412.

MCDONALD, J. W. & SADOWSKY, C. 2002. Spinal-cord injury. *The Lancet,* 359**,** 417-425.

MCKINLEY, W., MEADE, M. A., KIRSHBLUM, S. & BARNARD, B. 2004. Outcomes of early surgical management versus late or no surgical intervention after acute spinal cord injury. *Archives of Physical Medicine and Rehabilitation,* 85**,** 1818-1825.

MEBIUS, R. E. & KRAAL, G. 2005. Structure and function of the spleen. *Nature Reviews Immunology,* 5**,** 606-616.

METZ, G. A. & WHISHAW, I. Q. 2002. Cortical and subcortical lesions impair skilled walking in the ladder rung walking test: a new task to evaluate fore-and hindlimb stepping, placing, and co-ordination. *Journal of Neuroscience Methods,* 115**,** 169-179.

MEYER, A., HILGEN, G., DORGAU, B., SAMMLER, E. M., WEILER, R., MONYER, H., DEDEK, K. & HORMUZDI, S. G. 2014. All amacrine cells discriminate between heterocellular and homocellular locations when assembling connexin36-containing gap junctions. *Journal of Cell Science,* 127**,** 1190-1202.

MEYER, E., KURIAN, M., MORGAN, N., MCNEILL, A., PASHA, S., TEE, L., YOUNIS, R., NORMAN, A., VAN DER KNAAP, M. & WASSMER, E. 2011. Promoter mutation is a common variant in GJC2-associated Pelizaeus–Merzbacher-like disease. *Molecular Genetics and Metabolism,* 104**,** 637-643.

MIZUNO, H., WARITA, H., AOKI, M. & ITOYAMA, Y. 2008. Accumulation of chondroitin sulfate proteoglycans in the microenvironment of spinal motor neurons in amyotrophic lateral sclerosis transgenic rats. *Journal of Neuroscience Research,* 86**,** 2512-2523.

MOLINA, H., HORN, D. M., TANG, N., MATHIVANAN, S. & PANDEY, A. 2007. Global proteomic profiling of phosphopeptides using electron transfer dissociation tandem mass spectrometry. *Proceedings of the National Academy of Sciences,* 104**,** 2199-2204.

MOORE, L. K. & BURT, J. M. 1994. Selective block of gap junction channel expression with connexin-specific antisense oligodeoxynucleotides. *American Physiological Society,* 267**,** 1371-1380.

MORENO, A. P. 2005. Connexin phosphorylation as a regulatory event linked to channel gating. *Biochimica et Biophysica Acta -Biomembranes,* 1711**,** 164-171.

MORI, R., POWER, K. T., WANG, C. M., MARTIN, P. & BECKER, D. L. 2006. Acute downregulation of connexin43 at wound sites leads to a reduced inflammatory response, enhanced keratinocyte proliferation and wound fibroblast migration. *Journal of Cell Science,* 119**,** 5193-5203.

MORITA, M., SARUTA, C., KOZUKA, N., OKUBO, Y., ITAKURA, M., TAKAHASHI, M. & KUDO, Y. 2007. Dual regulation of astrocyte gap junction hemichannels by growth factors and a pro‐inflammatory cytokine via the mitogen‐activated protein kinase cascade. *Glia,* 55**,** 508-515.

MOTHE, A. & TATOR, C. 2005. Proliferation, migration, and differentiation of endogenous ependymal region stem/progenitor cells following minimal spinal cord injury in the adult rat. *Neuroscience,* 131**,** 177-187.

MOTHE, A. J., TAM, R. Y., ZAHIR, T., TATOR, C. H. & SHOICHET, M. S. 2013. Repair of the injured spinal cord by transplantation of neural stem cells in a hyaluronan-based hydrogel. *Biomaterials,* 34**,** 3775-3783.

MU, X., AZBILL, R. D. & SPRINGER, J. E. 2000. Riluzole and methylprednisolone combined treatment improves functional recovery in traumatic spinal cord injury. *Journal of Neurotrauma,* 17**,** 773-780.

MUKAINO, M., NAKAMURA, M., YAMADA, O., OKADA, S., MORIKAWA, S., RENAULT-MIHARA, F., IWANAMI, A., IKEGAMI, T., OHSUGI, Y. & TSUJI, O. 2010. Anti-IL-6-receptor antibody promotes repair of spinal cord injury by inducing microglia-dominant inflammation. *Experimental Neurology,* 224**,** 403-414.

MULDOON, L. L., ALVAREZ, J. I., BEGLEY, D. J., BOADO, R. J., DEL ZOPPO, G. J., DOOLITTLE, N. D., ENGELHARDT, B., HALLENBECK, J. M., LONSER, R. R. & OHLFEST, J. R. 2013. Immunologic privilege in the central nervous system and the blood–brain barrier. *Journal of Cerebral Blood Flow and Metabolism,* 33**,** 13-21.

MUSKAL, S. M., HOLBROOK, S. R. & KIM, S.-H. 1990. Prediction of the disulfide-bonding state of cysteine in proteins. *Protein Engineering,* 3**,** 667-672.

NAGAMATSU, S., SAWA, H., KAMADA, K., NAKAMICHI, Y., YOSHIMOTO, K. & HOSHINO, T. 1993. Neuron-specific glucose transporter (NSGT): CNS distribution of GLUT3 rat glucose transporter (RGT3) in rat central neurons. *FEBS Letters,* 334**,** 289-295.

NAGY, J. I., PATEL, D., OCHALSKI, P. A. & STELMACK, G. L. 1999. Connexin30 in rodent, cat and human brain: selective expression in gray matter astrocytes, co-localization with connexin43 at gap junctions and late developmental appearance. *Neuroscience,* 88**,** 447-68.

NAGY, J. I. & RASH, J. E. 2003. Astrocyte and oligodendrocyte connexins of the glial syncytium in relation to astrocyte anatomical domains and spatial buffering. *Cell Communication and Adhesion,* 10**,** 401-406.

NAHRENDORF, M., SWIRSKI, F. K., AIKAWA, E., STANGENBERG, L., WURDINGER, T., FIGUEIREDO, J.-L., LIBBY, P., WEISSLEDER, R. & PITTET, M. J. 2007. The healing myocardium sequentially mobilizes two monocyte subsets with divergent and complementary functions. *The Journal of Experimental Medicine,* 204**,** 3037-3047.

NAIK, S. H., METCALF, D., VAN NIEUWENHUIJZE, A., WICKS, I., WU, L., O'KEEFFE, M. & SHORTMAN, K. 2006. Intrasplenic steady-state dendritic cell precursors that are distinct from monocytes. *Nature Immunology,* 7**,** 663-671.

NAKAJIMA, H., UCHIDA, K., GUERRERO, A. R., WATANABE, S., SUGITA, D., TAKEURA, N., YOSHIDA, A., LONG, G., WRIGHT, K. T. & JOHNSON, W. E. 2012. Transplantation of mesenchymal stem cells promotes an alternative pathway of macrophage activation and functional recovery after spinal cord injury. *Journal of Neurotrauma,* 29**,** 1614-1625.

NAKAJIMA, H., UCHIDA, K., YAYAMA, T., HONJOH, K., SAKAMOTO, T. & BABA, H. 2014. Targeted retrograde gene delivery into the injured spinal cord using recombinant adenovirus vector carrying neurotrophic factor gene. *Neuroprotection and Regeneration of the Spinal Cord.* Springer.

NAKASE, T., SÖHL, G., THEIS, M., WILLECKE, K. & NAUS, C. C. 2004. Increased apoptosis and inflammation after focal brain ischemia in mice lacking connexin43 in astrocytes. *The American Journal of Pathology,* 164**,** 2067-2075.

NASHOLD, B. 1991. Paraplegia and pain. *Advances in Pain Research and Therapy,* 19**,** 301-319.

NESIC, O., SUNDBERG, L. M., HERRERA, J. J., MOKKAPATI, V. U., LEE, J. & NARAYANA, P. A. 2010. Vascular endothelial growth factor and spinal cord injury pain. *Journal of Neurotrauma,* 27**,** 1793-1803.

NGUYEN, V. & MCQUILLEN, P. S. 2010. AMPA and metabotropic excitoxicity explain subplate neuron vulnerability. *Neurobiology of Disease,* 37**,** 195-207.

NING, K., CHONG, K. F. & LEONG, H. W. De novo peptide sequencing for mass spectra based on multi-charge strong tags. Asia Pacific Bioinformatics Conference, 2007. 287-296.

NLEND, R. N., AÏT-LOUNIS, A., ALLAGNAT, F., CIGLIOLA, V., CHAROLLAIS, A., REITH, W., HAEFLIGER, J.-A. & MEDA, P. 2012. Cx36 is a target of Beta2/NeuroD1, which associates with prenatal differentiation of insulin-producing β cells. *The Journal of Membrane Biology,* 245**,** 263-273.

NORENBERG, M. D., SMITH, J. & MARCILLO, A. 2004. The pathology of human spinal cord injury: defining the problems. *Journal of Neurotrauma,* 21**,** 429-440.

NORTON, L. 2010. Spinal Cord Injury, Australia, 2007-08. Australian Institute of Health and Welfare, Australian Government.

O'CARROLL, S. J., ALKADHI, M., NICHOLSON, L. F. & GREEN, C. R. 2008. Connexin43 mimetic peptides reduce swelling, astrogliosis, and neuronal cell death after spinal cord injury. *Cell Communication and Adhesion,* 15**,** 27-42.

O'CARROLL, S. J., GORRIE, C. A., VELAMOOR, S., GREEN, C. R. & NICHOLSON, L. F. 2013. Connexin43 mimetic peptide is neuroprotective and improves function following spinal cord injury. *Neuroscience Research,* 75**,** 256-267.

O'CONNOR, P., MCCORMACK, O., GAVIN, C., DUNGAN, R., KIRKE, C., MCCORMACK, D., O'BYRNE, J., STEPHENS, M., MCMANUS, F. &

WALSH, M. 2003. Methylprednisolone in acute spinal cord injuries. *Irish Journal of Medical Science,* 172**,** 24-26.

OHSUMI, A., NAWASHIRO, H., OTANI, N., OOIGAWA, H., TOYOOKA, T., YANO, A., NOMURA, N. & SHIMA, K. 2006. Alteration of gap junction proteins (connexins) following lateral fluid percussion injury in rats. *Brain Edema XIII.* Springer.

OKADA, S., NAKAMURA, M., MIKAMI, Y., SHIMAZAKI, T., MIHARA, M., OHSUGI, Y., IWAMOTO, Y., YOSHIZAKI, K., KISHIMOTO, T. & TOYAMA, Y. 2004. Blockade of interleukin‐6 receptor suppresses reactive astrogliosis and ameliorates functional recovery in experimental spinal cord injury. *Journal of Neuroscience Research,* 76**,** 265-276.

OKANO, H., OGAWA, Y., NAKAMURA, M., KANEKO, S., IWANAMI, A. & TOYAMA, Y. 2003. Transplantation of neural stem cells into the spinal cord after injury. *Seminars in Cell and Developmental Biology,* 14**,** 191-198.

ONGSTAD, E. L., O'QUINN, M. P., GHATNEKAR, G. S., YOST, M. J. & GOURDIE, R. G. 2013. A connexin43 mimetic peptide promotes regenerative healing and improves mechanical properties in skin and heart. *Advances in Wound Care,* 2**,** 55-62.

OPERATION MANUAL 1993. *Impactor: NYU Spinal Cord Contusion System,* New Jersey, USA, New York University.

ORELLANA, J. A., FROGER, N., EZAN, P., JIANG, J. X., BENNETT, M. V., NAUS, C. C., GIAUME, C. & SÁEZ, J. C. 2011a. ATP and glutamate released via astroglial connexin 43 hemichannels mediate neuronal death through activation of pannexin 1 hemichannels. *Journal of Neurochemistry,* 118**,** 826-840.

ORELLANA, J. A., HERNÁNDEZ, D. E., EZAN, P., VELARDE, V., BENNETT, M. V., GIAUME, C. & SÁEZ, J. C. 2010. Hypoxia in high glucose followed by reoxygenation in normal glucose reduces the viability of cortical astrocytes through increased permeability of connexin 43 hemichannels. *Glia,* 58**,** 329-343.

ORELLANA, J. A., SÁEZ, P. J., SHOJI, K. F., SCHALPER, K. A., PALACIOS–PRADO, N., VELARDE, V., GIAUME, C., BENNETT, M. V. & SÁEZ, J. C. 2009. Modulation of brain hemichannels and gap junction channels by pro-inflammatory agents and their possible role in neurodegeneration. *Antioxidants and Redox Signaling,* 11**,** 369-399.

ORELLANA, J. A., SHOJI, K. F., ABUDARA, V., EZAN, P., AMIGOU, E., SÁEZ, P. J., JIANG, J. X., NAUS, C. C., SÁEZ, J. C. & GIAUME, C. 2011b. Amyloid β-induced death in neurons involves glial and neuronal hemichannels. *The Journal of Neuroscience,* 31**,** 4962-4977.

ORMONDE, S., CHOU, C.-Y., GOOLD, L., PETSOGLOU, C., AL-TAIE, R., SHERWIN, T., MCGHEE, C. N. & GREEN, C. R. 2012. Regulation of connexin43 gap junction protein triggers vascular recovery and healing in human ocular persistent epithelial defect wounds. *The Journal of Membrane Biology,* 245**,** 381-388.

ORTHMANN-MURPHY, J. L., ABRAMS, C. K. & SCHERER, S. S. 2008. Gap junctions couple astrocytes and oligodendrocytes. *Journal of Molecular Neuroscience,* 35**,** 101-116.

OVIEDO-ORTA, E., ERRINGTON, R. J. & EVANS, W. H. 2002. Gap junction intercellular communication during lymphocyte transendothelial migration. *Cell Biology International,* 26**,** 253-263.

OVIEDO‐ORTA, E., HOY, T. & EVANS, W. H. 2000. Intercellular communication in the immune system: differential expression of connexin40 and 43, and

perturbation of gap junction channel functions in peripheral blood and tonsil human lymphocyte subpopulations. *Immunology,* 99**,** 578-590.

PANDEY, N., XAVIER, D. F., CHATTERJEE, A., MANI, R. S., HIREMAGALORE, R., THARAKAN, A., RAJASHEKHAR, B. & ANAND, A. 2016. Functional Analysis of a Novel Connexin30 Mutation in a Large Family with Hearing Loss, Pesplanus, Ichthyosis, Cutaneous Nodules, and Keratoderma. *Annals of Human Genetics,* 80**,** 11-19.

PANDYA, K. A., WEANT, K. A. & COOK, A. M. 2010. High-Dose Methyiprednisolone in Acute Spinal Cord Injuries: Proceed With Caution. *Orthopedics,* 33**,** 327-331.

PARK, E., VELUMIAN, A. A. & FEHLINGS, M. G. 2004. The role of excitotoxicity in secondary mechanisms of spinal cord injury: a review with an emphasis on the implications for white matter degeneration. *Journal of Neurotrauma,* 21**,** 754-774.

PARPURA, V., SCEMES, E. & SPRAY, D. C. 2004. Mechanisms of glutamate release from astrocytes: gap junction "hemichannels", purinergic receptors and exocytotic release. *Neurochemistry International,* 45**,** 259-264.

PELEGRIN, P. & SURPRENANT, A. 2009. Dynamics of macrophage polarization reveal new mechanism to inhibit IL-1β release through pyrophosphates. *The EMBO Journal,* 28**,** 2114-2127.

PEREIRA, J. E., COSTA, L. M., CABRITA, A. M., COUTO, P. A., FILIPE, V. M., MAGALHÃES, L. G., FORNARO, M., DI SCIPIO, F., GEUNA, S. & MAURÍCIO, A. C. 2009. Methylprednisolone fails to improve functional and histological outcome following spinal cord injury in rats. *Experimental Neurology,* 220**,** 71-81.

PEREZ VELAZQUEZ, J. L., KOKAROVTSEVA, L., SARBAZIHA, R., JEYAPALAN, Z. & LESHCHENKO, Y. 2006. Role of gap junctional coupling in astrocytic networks in the determination of global ischaemia‐induced oxidative stress and hippocampal damage. *European Journal of Neuroscience,* 23**,** 1-10.

PETERSEN, C. M., DAVIDSEN, O., MOESTRUP, S., SONNE, O., NYKJAER, A. & MØLLER, B. 1990. Cellular targets and receptors for interleukin‐6 II. Characterization of IL‐6 binding and receptors in peripheral blood cells and macrophages. *European Journal of Clinical Investigation,* 20**,** 377-384.

PETROSYAN, H. A., HUNANYAN, A. S., ALESSI, V., SCHNELL, L., LEVINE, J. & ARVANIAN, V. L. 2013. Neutralization of inhibitory molecule NG2 improves synaptic transmission, retrograde transport, and locomotor function after spinal cord injury in adult rats. *The Journal of Neuroscience,* 33**,** 4032-4043.

PHADKE, C. P., FLYNN, S. M., THOMPSON, F. J., BEHRMAN, A. L., TRIMBLE, M. H. & KUKULKA, C. G. 2009. Comparison of single bout effects of bicycle training versus locomotor training on paired reflex depression of the soleus H-reflex after motor incomplete spinal cord injury. *Archives of Physical Medicine and Rehabilitation,* 90**,** 1218-1228.

PINEAU, I. & LACROIX, S. 2007. Proinflammatory cytokine synthesis in the injured mouse spinal cord: multiphasic expression pattern and identification of the cell types involved. *Journal of Comparative Neurology,* 500**,** 267-285.

PINEAU, I., SUN, L., BASTIEN, D. & LACROIX, S. 2010. Astrocytes initiate inflammation in the injured mouse spinal cord by promoting the entry of neutrophils and inflammatory monocytes in an IL-1 receptor/MyD88-dependent fashion. *Brain, Behavior, and Immunity,* 24**,** 540-553.

PLOTKIN, L. I., MANOLAGAS, S. C. & BELLIDO, T. 2002. Transduction of cell survival signals by connexin-43 hemichannels. *Journal of Biological Chemistry,* 277**,** 8648-8657.

POLLOK, S., PFEIFFER, A. C., LOBMANN, R., WRIGHT, C. S., MOLL, I., MARTIN, P. E. & BRANDNER, J. M. 2011. Connexin 43 mimetic peptide Gap27 reveals potential differences in the role of Cx43 in wound repair between diabetic and non‐diabetic cells. *Journal of Cellular and Molecular Medicine,* 15**,** 861-873.

POPOVICH, P. G. 2000. Immunological regulation of neuronal degeneration and regeneration in the injured spinal cord. *Progress in Brain Research,* 128**,** 43-58.

POPOVICH, P. G., HORNER, P. J., MULLIN, B. B. & STOKES, B. T. 1996. A quantitative spatial analysis of the blood–spinal cord barrier: I. Permeability changes after experimental spinal contusion injury. *Experimental Neurology,* 142**,** 258-275.

POPOVICH, P. G., WEI, P. & STOKES, B. T. 1997. Cellular inflammatory response after spinal cord injury in sprague‐dawley and lewis rats. *Journal of Comparative Neurology,* 377**,** 443-464.

POTAS, J. R., ZHENG, Y., MOUSSA, C., VENN, M., GORRIE, C. A., DENG, C. & WAITE, P. M. 2006. Augmented locomotor recovery after spinal cord injury in the athymic nude rat. *Journal of Neurotrauma,* 23**,** 660-673.

PRIEBE, M. M., CHIODO, A. E., SCELZA, W. M., KIRSHBLUM, S. C., WUERMSER, L. A. & HO, C. H. 2007. Spinal cord injury medicine. 6. Economic and societal issues in spinal cord injury. *Archives of Physical Medicine and Rehabilitation,* 88**,** 84-88.

PRÜSS, H., KOPP, M. A., BROMMER, B., GATZEMEIER, N., LAGINHA, I., DIRNAGL, U. & SCHWAB, J. M. 2011. Non‐resolving aspects of acute inflammation after spinal cord injury (SCI): indices and resolution plateau. *Brain Pathology,* 21**,** 652-660.

QIU, C., COUTINHO, P., FRANK, S., FRANKE, S., LAW, L.-Y., MARTIN, P., GREEN, C. R. & BECKER, D. L. 2003. Targeting connexin43 expression accelerates the rate of wound repair. *Current Biology,* 13**,** 1697-1703.

RABINOWITZ, R. S., ECK, J. C., HARPER JR, C. M., LARSON, D. R., JIMENEZ, M. A., PARISI, J. E., FRIEDMAN, J. A., YASZEMSKI, M. J. & CURRIER, B. L. 2008. Urgent surgical decompression compared to methylprednisolone for the treatment of acute spinal cord injury: a randomized prospective study in beagle dogs. *Spine,* 33**,** 2260-2268.

RAHIMI-MOVAGHAR, V., SAADAT, S., VACCARO, A. R., GHODSI, S. M., SAMADIAN, M., SHEYKHMOZAFFARI, A., SAFDARI, S. M. & KESHMIRIAN, B. 2009. The efficacy of surgical decompression before 24 hours versus 24 to 72 hours in patients with spinal cord injury from T1 to L1–with specific consideration on ethics: a randomized controlled trial. *Trials,* 10**,** 77-83.

RAMACHANDRAN, S., XIE, L.-H., JOHN, S. A., SUBRAMANIAM, S. & LAL, R. 2007. A novel role for connexin hemichannel in oxidative stress and smoking-induced cell injury. *PLoS One,* 2**,** e712.

RAMI, A., VOLKMANN, T. & WINCKLER, J. 2001. Effective reduction of neuronal death by inhibiting gap junctional intercellular communication in a rodent model of global transient cerebral ischemia. *Experimental Neurology,* 170**,** 297-304.

RASH, J., STAINES, W., YASUMURA, T., PATEL, D., FURMAN, C., STELMACK, G. & NAGY, J. 2000. Immunogold evidence that neuronal gap junctions in adult

rat brain and spinal cord contain connexin-36 but not connexin-32 or connexin-43. *Proceedings of the National Academy of Sciences,* 97**,** 7573-7578.

RASH, J., YASUMURA, T., DAVIDSON, K., FURMAN, C., DUDEK, F. & NAGY, J. 2001. Identification of cells expressing Cx43, Cx30, Cx26, Cx32 and Cx36 in gap junctions of rat brain and spinal cord. *Cell Communication and Adhesion,* 8**,** 315-320.

RASH, J. E., YASUMURA, T. & DUDEK, F. 1998. Ultrastructure, histological distribution, and freeze-fracture immunocytochemistry of gap junctions in rat brain and spinal cord. *Cell Biology International,* 22**,** 731-749.

RATKAY-TRAUB, I., HOPP, B., BOR, Z., DUX, L., BECKER, D. & KRENACS, T. 2001. Regeneration of rabbit cornea following excimer laser photorefractive keratectomy: a study on gap junctions, epithelial junctions and epidermal growth factor receptor expression in correlation with cell proliferation. *Experimental Eye Research,* 73**,** 291-302.

REAUME, A. G., DE SOUSA, P. A., KULKARNI, S. & LANGILLE, B. L. 1995. Cardiac malformation in neonatal mice lacking connexin43. *Science,* 267**,** 1831.

RENAULT-MIHARA, F., OKADA, S., SHIBATA, S., NAKAMURA, M., TOYAMA, Y. & OKANO, H. 2008. Spinal cord injury: emerging beneficial role of reactive astrocytes' migration. *The International Journal of Biochemistry and Cell Biology,* 40**,** 1649-1653.

RETAMAL, M. A., CORTÉS, C. J., REUSS, L., BENNETT, M. V. & SÁEZ, J. C. 2006. S-nitrosylation and permeation through connexin 43 hemichannels in astrocytes: induction by oxidant stress and reversal by reducing agents. *PNAS,* 103**,** 4475-4480.

RETAMAL, M. A., FROGER, N., PALACIOS-PRADO, N., EZAN, P., SÁEZ, P. J., SÁEZ, J. C. & GIAUME, C. 2007. Cx43 hemichannels and gap junction channels in astrocytes are regulated oppositely by proinflammatory cytokines released from activated microglia. *The Journal of Neuroscience,* 27**,** 13781-13792.

ROH, D. H., YOON, S. Y., SEO, H. S., KANG, S. Y., HAN, H. J., BEITZ, A. J. & LEE, J. H. 2010. Intrathecal injection of carbenoxolone, a gap junction decoupler, attenuates the induction of below-level neuropathic pain after spinal cord injury in rats. *Experimental Neurology,* 224**,** 123-132.

ROLLS, A., SHECHTER, R. & SCHWARTZ, M. 2009. The bright side of the glial scar in CNS repair. *Nature Reviews Neuroscience,* 10**,** 235-241.

ROTHSTEIN, J. D., DYKES-HOBERG, M., PARDO, C. A., BRISTOL, L. A., JIN, L., KUNCL, R. W., KANAI, Y., HEDIGER, M. A., WANG, Y. & SCHIELKE, J. P. 1996. Knockout of glutamate transporters reveals a major role for astroglial transport in excitotoxicity and clearance of glutamate. *Neuron,* 16**,** 675-686.

ROTTLAENDER, D., BOENGLER, K., WOLNY, M., MICHELS, G., ENDRES-BECKER, J., MOTLOCH, L. J., SCHWAIGER, A., BUECHERT, A., SCHULZ, R. & HEUSCH, G. 2010. Connexin 43 acts as a cytoprotective mediator of signal transduction by stimulating mitochondrial K ATP channels in mouse cardiomyocytes. *The Journal of Clinical Investigation,* 120**,** 1441-1453.

ROWLAND, M. & TOZER, T. N. 2005. *Clinical Pharmacokinetics and Pharmacodynamics: Concepts and Applications,* Philadelphia, USA, Lippincott Williams and Wilkins

ROZENTAL, R., SRINIVAS, M. & SPRAY, D. C. 2001. How to close a gap junction channel. *Methods in Molecular Biology,* 154**,** 447-476.

RYU, H.-H., LIM, J.-H., BYEON, Y.-E., PARK, J.-R., SEO, M.-S., LEE, Y.-W., KIM, W. H., KANG, K.-S. & KWEON, O.-K. 2009. Functional recovery and neural differentiation after transplantation of allogenic adipose-derived stem cells in a canine model of acute spinal cord injury. *Journal of Veterinary Science,* 10**,** 273-284.

SABELSTRÖM, H., STENUDD, M., RÉU, P., DIAS, D. O., ELFINEH, M., ZDUNEK, S., DAMBERG, P., GÖRITZ, C. & FRISÉN, J. 2013. Resident neural stem cells restrict tissue damage and neuronal loss after spinal cord injury in mice. *Science,* 342**,** 637-640.

SAIWAI, H., OHKAWA, Y., YAMADA, H., KUMAMARU, H., HARADA, A., OKANO, H., YOKOMIZO, T., IWAMOTO, Y. & OKADA, S. 2010. The LTB4-BLT1 axis mediates neutrophil infiltration and secondary injury in experimental spinal cord injury. *The American Journal of Pathology,* 176**,** 2352-2366.

SANDOVAL, R. M., WAGNER, M. C., PATEL, M., CAMPOS-BILDERBACK, S. B., RHODES, G. J., WANG, E., WEAN, S. E., CLENDENON, S. S. & MOLITORIS, B. A. 2012. Multiple factors influence glomerular albumin permeability in rats. *Journal of the American Society of Nephrology,* 23**,** 447-457.

SATO, A., OHTAKI, H., TSUMURAYA, T., SONG, D., OHARA, K., ASANO, M., IWAKURA, Y., ATSUMI, T. & SHIODA, S. 2012. Interleukin-1 participates in the classical and alternative activation of microglia/macrophages after spinal cord injury. *Journal of Neuroinflammation,* 9**,** 65.

SCEMES, E., SUADICANI, S. O. & SPRAY, D. C. 2000. Intercellular communication in spinal cord astrocytes: fine tuning between gap junctions and P2 nucleotide receptors in calcium wave propagation. *The Journal of Neuroscience,* 20**,** 1435-1445.

SCHACHTRUP, C., LU, P., JONES, L. L., LEE, J. K., LU, J., SACHS, B. D., ZHENG, B. & AKASSOGLOU, K. 2007. Fibrinogen inhibits neurite outgrowth via β3 integrin-mediated phosphorylation of the EGF receptor. *Proceedings of the National Academy of Sciences,* 104**,** 11814-11819.

SCHEFF, S. W., RABCHEVSKY, A. G., FUGACCIA, I., MAIN, J. A. & LUMPP JR, J. E. 2003. Experimental modeling of spinal cord injury: characterization of a force-defined injury device. *Journal of Neurotrauma,* 20**,** 179-193.

SCHEFF, S. W., SAUCIER, D. A. & CAIN, M. E. 2002. A statistical method for analyzing rating scale data: the BBB locomotor score. *Journal of Neurotrauma,* 19**,** 1251-1260.

SCHENONE, M., DANČÍK, V., WAGNER, B. K. & CLEMONS, P. A. 2013. Target identification and mechanism of action in chemical biology and drug discovery. *Nature Chemical Biology,* 9**,** 232-240.

SCHMIDT, C. E. & LEACH, J. B. 2003. Neural tissue engineering: strategies for repair and regeneration. *Annual Review of Biomedical Engineering,* 5**,** 293-347.

SCHNELL, L., FEARN, S., SCHWAB, M., PERRY, V. & ANTHONY, D. 1999. Cytokine-induced acute inflammation in the brain and spinal cord. *Journal of Neuropathology and Experimental Neurology,* 58**,** 245-254.

SCHÜTZ, M., SCIMEMI, P., MAJUMDER, P., DE SIATI, R. D., CRISPINO, G., RODRIGUEZ, L., BORTOLOZZI, M., SANTARELLI, R., SEYDEL, A. & SONNTAG, S. 2010. The human deafness-associated connexin 30 T5M mutation causes mild hearing loss and reduces biochemical coupling among

cochlear non-sensory cells in knock-in mice. *Human Molecular Genetics,* 19**,** 4759-4773.

SCHWARTZ, M. & KIPNIS, J. 2002. Multiple sclerosis as a by-product of the failure to sustain protective autoimmunity: a paradigm shift. *The Neuroscientist,* 8**,** 405-413.

SERRE-BEINIER, V., BOSCO, D., ZULIANELLO, L., CHAROLLAIS, A., CAILLE, D., CHARPANTIER, E., GAUTHIER, B. R., DIAFERIA, G. R., GIEPMANS, B. N. & LUPI, R. 2009. Cx36 makes channels coupling human pancreatic β-cells, and correlates with insulin expression. *Human Molecular Genetics,* 18**,** 428-439.

SHAMASH, S., REICHERT, F. & ROTSHENKER, S. 2002. The cytokine network of Wallerian degeneration: tumor necrosis factor-α, interleukin-1α, and interleukin-1β. *The Journal of Neuroscience,* 22**,** 3052-3060.

SHARMA, H. S. 2011. Early microvascular reactions and blood–spinal cord barrier disruption are instrumental in pathophysiology of spinal cord injury and repair: novel therapeutic strategies including nanowired drug delivery to enhance neuroprotection. *Journal of Neural Transmission,* 118**,** 155-176.

SHARMA, K., SELZER, M. E. & LI, S. 2012. Scar-mediated inhibition and CSPG receptors in the CNS. *Experimental Neurology,* 237**,** 370-378.

SHARP, J., FRAME, J., SIEGENTHALER, M., NISTOR, G. & KEIRSTEAD, H. S. 2010. Human embryonic stem cell ‐ derived oligodendrocyte progenitor cell transplants improve recovery after cervical spinal cord injury. *Stem Cells,* 28**,** 152-163.

SHARP, P. & LAREGINA, M. 1998. *The laboratory Rat. A volume in the laboratory animal pocket reference series,* Boca Raton, FL, CRC.

SHAW, P. J., CHINNERY, R. M., THAGESEN, H., BORTHWICK, G. M. & INCE, P. G. 1997. Immunocytochemical study of the distribution of the free radical scavenging enzymes Cu/Zn superoxide dismutase (SOD1); MN superoxide dismutase (MN SOD) and catalase in the normal human spinal cord and in motor neuron disease. *Journal of the Neurological Sciences,* 147**,** 115-125.

SHECHTER, R., LONDON, A., VAROL, C., RAPOSO, C., CUSIMANO, M., YOVEL, G., ROLLS, A., MACK, M., PLUCHINO, S. & MARTINO, G. 2009. Infiltrating blood-derived macrophages are vital cells playing an anti-inflammatory role in recovery from spinal cord injury in mice. *PLoS Medicine,* 6**,** e1000113.

SHECHTER, R., MILLER, O., YOVEL, G., ROSENZWEIG, N., LONDON, A., RUCKH, J., KIM, K.-W., KLEIN, E., KALCHENKO, V. & BENDEL, P. 2013. Recruitment of beneficial M2 macrophages to injured spinal cord is orchestrated by remote brain choroid plexus. *Immunity,* 38**,** 555-569.

SHIBATA, T., YAMADA, K., WATANABE, M., IKENAKA, K., WADA, K., TANAKA, K. & INOUE, Y. 1997. Glutamate transporter GLAST is expressed in the radial glia–astrocyte lineage of developing mouse spinal cord. *The Journal of Neuroscience,* 17**,** 9212-9219.

SHIELDS, C. B., ZHANG, Y. P., SHIELDS, L. B., HAN, Y., BURKE, D. A. & MAYER, N. W. 2005. The therapeutic window for spinal cord decompression in a rat spinal cord injury model. *Journal of Neurosurgery: Spine,* 3**,** 302-307.

SHORT, D., EL MASRY, W. & JONES, P. 2000. High dose methylprednisolone in the management of acute spinal cord injury–a systematic review from a clinical perspective. *Spinal Cord,* 38.

SIDDALL, P. J., MCCLELLAND, J. M., RUTKOWSKI, S. B. & COUSINS, M. J. 2003. A longitudinal study of the prevalence and characteristics of pain in the first 5 years following spinal cord injury. *Pain,* 103**,** 249-257.

SIUSHANSIAN, R., BECHBERGER, J. F., CECHETTO, D. F., HACHINSKI, V. C. & NAUS, C. C. 2001. Connexin43 null mutation increases infarct size after stroke. *Journal of Comparative Neurology,* 440**,** 387-394.

SOFRONIEW, M. V. 2009. Molecular dissection of reactive astrogliosis and glial scar formation. *Trends in Neurosciences,* 32**,** 638-647.

SOFRONIEW, M. V. & VINTERS, H. V. 2010. Astrocytes: biology and pathology. *Acta Nuropathologica,* 119**,** 7-35.

SOLAN, J. L. & LAMPE, P. D. 2005. Connexin phosphorylation as a regulatory event linked to gap junction channel assembly. *Biochimica et Biophysica Acta - Biomembranes,* 1711**,** 154-163.

SOMERS, M. F. 2001. *Spinal cord injury: functional rehabilitation,* New Jersey, Prentice Hall.

SOUBEYRAND, M., BADNER, A., VAWDA, R., CHUNG, Y. S. & FEHLINGS, M. G. 2014. Very high resolution ultrasound imaging for real-time quantitative visualization of vascular disruption after spinal cord injury. *Journal of Neurotrauma,* 31**,** 1767-1775.

SOUDY, R., GILL, A., SPRULES, T., LAVASANIFAR, A. & KAUR, K. 2011. Proteolytically stable cancer targeting peptides with high affinity for breast cancer cells. *Journal of Medicinal Chemistry,* 54**,** 7523-7534.

SROGA, J. M., JONES, T., KIGERL, K. A., MCGAUGHY, V. M. & POPOVICH, P. G. 2003. Rats and mice exhibit distinct inflammatory reactions after spinal cord injury. *Journal of Comparative Neurology,* 462**,** 223-240.

STEEVES, J., LAMMERTSE, D., CURT, A., FAWCETT, J., TUSZYNSKI, M., DITUNNO, J., ELLAWAY, P., FEHLINGS, M., GUEST, J. & KLEITMAN, N. 2006. Guidelines for the conduct of clinical trials for spinal cord injury (SCI) as developed by the ICCP panel: clinical trial outcome measures. *Spinal Cord,* 45**,** 206-221.

STEGER, K., TETENS, F. & BERGMANN, M. 1999. Expression of connexin 43 in human testis. *Histochemistry and Cell Biology,* 112**,** 215-220.

STEHBERG, J., MORAGA-AMARO, R., SALAZAR, C., BECERRA, A., ECHEVERRÍA, C., ORELLANA, J. A., BULTYNCK, G., PONSAERTS, R., LEYBAERT, L. & SIMON, F. 2012. Release of gliotransmitters through astroglial connexin 43 hemichannels is necessary for fear memory consolidation in the basolateral amygdala. *The FASEB Journal,* 26**,** 3649-3657.

STEIN, D. M., MENAKER, J., MCQUILLAN, K., HANDLEY, C., AARABI, B. & SCALEA, T. M. 2010. Risk factors for organ dysfunction and failure in patients with acute traumatic cervical spinal cord injury. *Neurocritical Care,* 13**,** 29-39.

STELLWAGEN, D., BEATTIE, E. C., SEO, J. Y. & MALENKA, R. C. 2005. Differential regulation of AMPA receptor and GABA receptor trafficking by tumor necrosis factor-α. *The Journal of Neuroscience,* 25**,** 3219-3228.

STIRLING, D. P., CUMMINS, K., MISHRA, M., TEO, W., YONG, V. W. & STYS, P. 2013. Toll-like receptor 2-mediated alternative activation of microglia is protective after spinal cord injury. *Brain,* 137**,** 707-723.

STOKOLS, S. & TUSZYNSKI, M. H. 2006. Freeze-dried agarose scaffolds with uniaxial channels stimulate and guide linear axonal growth following spinal cord injury. *Biomaterials,* 27**,** 443-451.

STOUT, C. E., COSTANTIN, J. L., NAUS, C. C. & CHARLES, A. C. 2002. Intercellular calcium signaling in astrocytes via ATP release through connexin hemichannels. *Journal of Biological Chemistry,* 277**,** 10482-10488.

STREIT, W. J. 2001. Microglia and macrophages in the developing CNS. *Neurotoxicology,* 22**,** 619-624.

STREIT, W. J., SEMPLE-ROWLAND, S. L., HURLEY, S. D., MILLER, R. C., POPOVICH, P. G. & STOKES, B. T. 1998. Cytokine mRNA profiles in contused spinal cord and axotomized facial nucleus suggest a beneficial role for inflammation and gliosis. *Experimental Neurology,* 152**,** 74-87.

SU, Z., CAO, L., ZHU, Y., LIU, X., HUANG, Z., HUANG, A. & HE, C. 2007. Nogo enhances the adhesion of olfactory ensheathing cells and inhibits their migration. *Journal of Cell Science,* 120**,** 1877-1887.

SUN, F., LIN, C. L. G., MCTIGUE, D., SHAN, X., TOVAR, C. A., BRESNAHAN, J. C. & BEATTIE, M. S. 2010. Effects of axon degeneration on oligodendrocyte lineage cells: dorsal rhizotomy evokes a repair response while axon degeneration rostral to spinal contusion induces both repair and apoptosis. *Glia,* 58**,** 1304-1319.

TABAKOW, P., JARMUNDOWICZ, W., CZAPIGA, B., FORTUNA, W., MIEDZYBRODZKI, R., CZYZ, M., HUBER, J., SZAREK, D., OKUROWSKI, S. & SZEWCZYK, P. 2013. Transplantation of autologous olfactory ensheathing cells in complete human spinal cord injury. *Cell Transplantation,* 22**,** 1591-1612.

TADA, J. & HASHIMOTO, K. 1997. Ultrastructural localization of gap junction protein connexin 43 in normal human skin, basal cell carcinoma, and squamous cell carcinoma. *Journal of Cutaneous Pathology,* 24**,** 628-635.

TAKAHASHI, D., VARGAS, J. & WILCOX, K. 2010. Increased coupling and altered glutamate transport currents in astrocytes following kainic-acid-induced status epilepticus. *Neurobiology of Disease,* 40**,** 573-585.

TAKEUCHI, H., JIN, S., WANG, J., ZHANG, G., KAWANOKUCHI, J., KUNO, R., SONOBE, Y., MIZUNO, T. & SUZUMURA, A. 2006. Tumor necrosis factor-α induces neurotoxicity via glutamate release from hemichannels of activated microglia in an autocrine manner. *Journal of Biological Chemistry,* 281**,** 21362-21368.

TAOKA, Y., OKAJIMA, K., UCHIBA, M. & JOHNO, M. 2001. Methylprednisolone reduces spinal cord injury in rats without affecting tumor necrosis factor-α production. *Journal of Neurotrauma,* 18**,** 533-543.

TAOKA, Y., OKAJIMA, K., UCHIBA, M., MURAKAMI, K., KUSHIMOTO, S., JOHNO, M., NARUO, M., OKABE, H. & TAKATSUKI, K. 1997. Role of neutrophils in spinal cord injury in the rat. *Neuroscience,* 79**,** 1177-1182.

TATOR, C. H. 1995. Update on the pathophysiology and pathology of acute spinal cord injury. *Brain Pathology,* 5**,** 407-413.

TATOR, C. H. 1998. Biology of neurological recovery and functional restoration after spinal cord injury. *Neurosurgery,* 42**,** 696-707.

TATOR, C. H. & KOYANAGI, I. 1997. Vascular mechanisms in the pathophysiology of human spinal cord injury. *Journal of Neurosurgery,* 86**,** 483-492.

TENG, Y. D., CHOI, H., ONARIO, R. C., ZHU, S., DESILETS, F. C., LAN, S., WOODARD, E. J., SNYDER, E. Y., EICHLER, M. E. & FRIEDLANDER, R. M. 2004. Minocycline inhibits contusion-triggered mitochondrial cytochrome c release and mitigates functional deficits after spinal cord injury. *PNAS,* 101**,** 3071-3076.

TENG, Y. D., LAVIK, E. B., QU, X., PARK, K. I., OUREDNIK, J., ZURAKOWSKI, D., LANGER, R. & SNYDER, E. Y. 2002. Functional recovery following traumatic spinal cord injury mediated by a unique polymer scaffold seeded with neural stem cells. *PNAS,* 99**,** 3024-3029.

TETZLAFF, W., OKON, E. B., KARIMI-ABDOLREZAEE, S., HILL, C. E., SPARLING, J. S., PLEMEL, J. R., PLUNET, W. T., TSAI, E. C., BAPTISTE, D. & SMITHSON, L. J. 2011. A systematic review of cellular transplantation therapies for spinal cord injury. *Journal of Neurotrauma,* 28**,** 1611-1682.

TEUBNER, B., MICHEL, V., PESCH, J., LAUTERMANN, J., COHEN-SALMON, M., SÖHL, G., JAHNKE, K., WINTERHAGER, E., HERBERHOLD, C. & HARDELIN, J.-P. 2003. Connexin30 (Gjb6)-deficiency causes severe hearing impairment and lack of endocochlear potential. *Human Molecular Genetics,* 12**,** 13-21.

THERIAULT, E., FRANKENSTEIN, U., HERTZBERG, E. & NAGY, J. 1997. Connexin43 and astrocytic gap junctions in the rat spinal cord after acute compression injury. *Journal of Comparative Neurology,* 382**,** 199-214.

THOMPSON, R. J., ZHOU, N. & MACVICAR, B. A. 2006. Ischemia opens neuronal gap junction hemichannels. *Science,* 312**,** 924-927.

THURET, S., MOON, L. D. & GAGE, F. H. 2006. Therapeutic interventions after spinal cord injury. *Nature Reviews Neuroscience,* 7**,** 628-643.

THURMAN, D. J. 1995. *Guidelines for Surveillance of Central Nervous System Injury*, U.S. Department of Health and Human Services, Public Health Service, National Center for Injury Prevention Control.

TJOA, T., STRAUSBAUGH, H. J., MAIDA, N., DAZIN, P. F., ROSEN, S. D. & NOBLE-HAEUSSLEIN, L. J. 2003. The use of flow cytometry to assess neutrophil infiltration in the injured murine spinal cord. *Journal of Neuroscience Methods,* 129**,** 49-59.

TOM, V. J., SANDROW-FEINBERG, H. R., MILLER, K., DOMITROVICH, C., BOUYER, J., ZHUKAREVA, V., KLAW, M. C., LEMAY, M. A. & HOULÉ, J. D. 2013. Exogenous BDNF enhances the integration of chronically injured axons that regenerate through a peripheral nerve grafted into a chondroitinase-treated spinal cord injury site. *Experimental Neurology,* 239**,** 91-100.

TONKIN, R. S., MAO, Y., O'CARROLL, S. J., NICHOLSON, L. F., GREEN, C. R., GORRIE, C. A. & MOALEM-TAYLOR, G. 2015. Gap junction proteins and their role in spinal cord injury. *Frontiers in Molecular Neuroscience,* 7.

TRIVEDI, A., OLIVAS, A. D. & NOBLE-HAEUSSLEIN, L. J. 2006. Inflammation and spinal cord injury: infiltrating leukocytes as determinants of injury and repair processes. *Clinical Neuroscience Research,* 6**,** 283-292.

TYSSELING-MATTIACE, V. M., SAHNI, V., NIECE, K. L., BIRCH, D., CZEISLER, C., FEHLINGS, M. G., STUPP, S. I. & KESSLER, J. A. 2008. Self-assembling nanofibers inhibit glial scar formation and promote axon elongation after spinal cord injury. *The Journal of Neuroscience,* 28**,** 3814-3823.

UBERTI, D., MELI, E. & MEMO, M. 2002. Expression of cell-cycle-related proteins and excitoxicity. *Amino Acids,* 23**,** 27-30.

VAN DEN BRULE, S., BECKERS, E., CHAURAND, P., LIU, W., IBOURAADATEN, S., PALMAI-PALLAG, M., UWAMBAYINEMA, F., YAKOUB, Y., AVELLAN, A. & LEVARD, C. 2014. Nanometer-long Ge-imogolite nanotubes cause sustained lung inflammation and fibrosis in rats. *Particle and Fibre Toxicology,* 11**,** 67.

VAN KEMPEN, M., FROMAGET, C., GROS, D., MOORMAN, A. & LAMERS, W. 1991. Spatial distribution of connexin43, the major cardiac gap junction protein, in the developing and adult rat heart. *Circulation Research,* 68**,** 1638-1651.

VAN ROOIJEN, N. 1990. Antigen processing and presentation in vivo: the microenvironment as a crucial factor. *Immunology Today,* 11**,** 436-439.

VAZIRI, N. D., LEE, Y.-S., LIN, C.-Y., LIN, V. W. & SINDHU, R. K. 2004. NAD (P) H oxidase, superoxide dismutase, catalase, glutathione peroxidase and nitric oxide synthase expression in subacute spinal cord injury. *Brain Research,* 995**,** 76-83.

VENKATACHALAM, M. A. & RENNKE, H. G. 1978. The structural and molecular basis of glomerular filtration. *Circulation Research,* 43**,** 337-347.

WANDELL, N. 2010. The Effect of Social Participation on Adults with Spinal cord Injury. *Mental Health,* 12**,** 1-15.

WANG, C. M., LINCOLN, J., COOK, J. E. & BECKER, D. L. 2007. Abnormal connexin expression underlies delayed wound healing in diabetic skin. *Diabetes,* 56**,** 2809-2817.

WANG, N., DE VUYST, E., PONSAERTS, R., BOENGLER, K., PALACIOS-PRADO, N., WAUMAN, J., LAI, C. P., DE BOCK, M., DECROCK, E. & BOL, M. 2013. Selective inhibition of Cx43 hemichannels by Gap19 and its impact on myocardial ischemia/reperfusion injury. *Basic Research in Cardiology,* 108**,** 1-16.

WANG, X., BAUGHMAN, K. W., BASSO, D. M. & STRITTMATTER, S. M. 2006. Delayed Nogo receptor therapy improves recovery from spinal cord contusion. *Annals of Neurology,* 60**,** 540-549.

WANG, Y., CHENG, X., HE, Q., ZHENG, Y., KIM, D. H., WHITTEMORE, S. R. & CAO, Q. L. 2011. Astrocytes from the contused spinal cord inhibit oligodendrocyte differentiation of adult oligodendrocyte precursor cells by increasing the expression of bone morphogenetic proteins. *The Journal of Neuroscience,* 31**,** 6053-6058.

WATANABE, S., UCHIDA, K., NAKAJIMA, H., MATSUO, H., SUGITA, D., YOSHIDA, A., HONJOH, K., JOHNSON, W. E. & BABA, H. 2015. Early transplantation of mesenchymal stem cells after spinal cord injury relieves pain hypersensitivity through suppression of pain‐related signaling cascades and reduced Inflammatory cell recruitment. *Stem Cells,* 33**,** 1902-1914.

WATANABE, T., YAMAMOTO, T., ABE, Y., SAITO, N., KUMAGAI, T. & KAYAMA, H. 1999. Differential activation of microglia after experimental spinal cord injury. *Journal of Neurotrauma,* 16**,** 255-265.

WEIDEKAMM, E., WALLACH, D. F. & FLÜCKIGER, R. 1973. A new sensitive, rapid fluorescence technique for the determination of proteins in gel electrophoresis and in solution. *Analytical Biochemistry,* 54**,** 102-114.

WELLS, J. E., HURLBERT, R. J., FEHLINGS, M. G. & YONG, V. W. 2003a. Neuroprotection by minocycline facilitates significant recovery from spinal cord injury in mice. *Brain,* 126**,** 1628-1637.

WELLS, J. E., RICE, T. K., NUTTALL, R. K., EDWARDS, D. R., ZEKKI, H., RIVEST, S. & YONG, V. W. 2003b. An adverse role for matrix metalloproteinase 12 after spinal cord injury in mice. *The Journal of Neuroscience,* 23**,** 10107-10115.

WELLS, K., ANDERSON, D., FAROOQUI, A. & HORROCKS, L. 1994. Excitotoxicity of glutamate and four analogs in primary spinal cord cell cultures. *Neurochemistry International,* 25**,** 377-384.

WHITE, R. E., MCTIGUE, D. M. & JAKEMAN, L. B. 2010. Regional heterogeneity in astrocyte responses following contusive spinal cord injury in mice. *Journal of Comparative Neurology,* 518**,** 1370-1390.

WIITA, A. P., AINAVARAPU, S. R. K., HUANG, H. H. & FERNANDEZ, J. M. 2006. Force-dependent chemical kinetics of disulfide bond reduction observed with single-molecule techniques. *Proceedings of the National Academy of Sciences,* 103**,** 7222-7227.

WILEMS, T. S., PARDIECK, J., IYER, N. & SAKIYAMA-ELBERT, S. E. 2015. Combination therapy of stem cell derived neural progenitors and drug delivery of anti-inhibitory molecules for spinal cord injury. *Acta Biomaterialia,* 28**,** 23-32.

WITT, K. A., GILLESPIE, T. J., HUBER, J. D., EGLETON, R. D. & DAVIS, T. P. 2001. Peptide drug modifications to enhance bioavailability and blood-brain barrier permeability. *Peptides,* 22**,** 2329-2343.

WONG, C. W., CHRISTEN, T., ROTH, I., CHADJICHRISTOS, C. E., DEROUETTE, J.-P., FOGLIA, B. F., CHANSON, M., GOODENOUGH, D. A. & KWAK, B. R. 2006. Connexin37 protects against atherosclerosis by regulating monocyte adhesion. *Nature Medicine,* 12**,** 950-954.

WU, B., MATIC, D., DJOGO, N., SZPOTOWICZ, E., SCHACHNER, M. & JAKOVCEVSKI, I. 2012. Improved regeneration after spinal cord injury in mice lacking functional T-and B-lymphocytes. *Experimental Neurology,* 237**,** 274-285.

WU, Z., XU, H., HE, Y., YANG, G., LIAO, C., GAO, W., LIANG, M. & HE, X. 2013. Antisense oligodeoxynucleotides targeting connexin43 reduce cerebral astrocytosis and edema in a rat model of traumatic brain injury. *Neurological Research,* 35**,** 255-262.

WYNDAELE, M. & WYNDAELE, J. J. 2006. Incidence, prevalence and epidemiology of spinal cord injury: what learns a worldwide literature survey? *Spinal Cord,* 44**,** 523-529.

XU, G.-Y., HUGHES, M. G., YE, Z., HULSEBOSCH, C. E. & MCADOO, D. J. 2004. Concentrations of glutamate released following spinal cord injury kill oligodendrocytes in the spinal cord. *Experimental Neurology,* 187**,** 329-336.

YAMAMOTO, T., OCHALSKI, A., HERTZBERG, E. & NAGY, J. 1990. LM and EM immunolocalization of the gap junctional protein connexin 43 in rat brain. *Brain Besearch,* 508**,** 313-319.

YAN, P., LI, Q., KIM, G.-M., XU, J., HSU, C. Y. & XU, X. M. 2001. Cellular localization of tumor necrosis factor-α following acute spinal cord injury in adult rats. *Journal of Neurotrauma,* 18**,** 563-568.

YANG, L., BLUMBERGS, P. C., JONES, N. R., MANAVIS, J., SARVESTANI, G. T. & GHABRIEL, M. N. 2004a. Early expression and cellular localization of proinflammatory cytokines interleukin-1β, interleukin-6, and tumor necrosis factor-α in human traumatic spinal cord injury. *Spine,* 29**,** 966-971.

YANG, L., JONES, N. R., BLUMBERGS, P. C., VAN DEN HEUVEL, C., MOORE, E. J., MANAVIS, J., SARVESTANI, G. T. & GHABRIEL, M. N. 2005. Severity-dependent expression of pro-inflammatory cytokines in traumatic spinal cord injury in the rat. *Journal of Clinical Neuroscience,* 12**,** 276-284.

YANG, Y. H., MORAND, E. F., GETTING, S. J., PAUL‐CLARK, M., LIU, D. L., YONA, S., HANNON, R., BUCKINGHAM, J. C., PERRETTI, M. & FLOWER, R. J. 2004b. Modulation of inflammation and response to dexamethasone by Annexin 1 in antigen‐induced arthritis. *Arthritis & Rheumatism,* 50**,** 976-984.

YASUI, K., KADA, K., HOJO, M., LEE, J.-K., KAMIYA, K., TOYAMA, J., OPTHOF, T. & KODAMA, I. 2000. Cell-to-cell interaction prevents cell death in cultured neonatal rat ventricular myocytes. *Cardiovascular Research,* 48**,** 68-76.

YATES, C., CHARLESWORTH, A., ALLEN, S., REESE, N., SKINNER, R. & GARCIA-RILL, E. 2008. The onset of hyperreflexia in the rat following complete spinal cord transection. *Spinal Cord,* 46**,** 798-803.

YATES, C., GARRISON, K., REESE, N., CHARLESWORTH, A. & GARCIA-RILL, E. 2011. Novel mechanism for hyper-reflexia and spasticity. *Progress in Brain Research,* 188**,** 167.

YE, Z. C., WYETH, M. S., BALTAN-TEKKOK, S. & RANSOM, B. R. 2003. Functional hemichannels in astrocytes: a novel mechanism of glutamate release. *The Journal of Neuroscience,* 23**,** 3588-3596.

YEH, H. I., LAI, Y. J., CHANG, H. M., KO, Y. S., SEVERS, N. J. & TSAI, C. H. 2000. Multiple connexin expression in regenerating arterial endothelial gap junctions. *Arteriosclerosis, Thrombosis and Vascular Biology,* 20**,** 1753-1762.

YEH, H. I., LUPU, F., DUPONT, E. & SEVERS, N. J. 1997. Upregulation of connexin43 gap junctions between smooth muscle cells after balloon catheter injury in the rat carotid artery. *Arteriosclerosis, Thrombosis and Vascular Biology,* 17**,** 3174-3184.

YEO, J. D., WALSH, J., RUTKOWSKI, S., SODEN, R., CRAVEN, M. & MIDDLETON, J. 1998. Mortality following spinal cord injury. *Spinal Cord,* 36**,** 329-336.

YONG, V. W., POWER, C., FORSYTH, P. & EDWARDS, D. R. 2001. Metalloproteinases in biology and pathology of the nervous system. *Nature Reviews Neuroscience,* 2**,** 502-511.

YOON, J. J., GREEN, C. R., O'CARROLL, S. J. & NICHOLSON, L. F. 2010. Dose-dependent protective effect of connexin43 mimetic peptide against neurodegeneration in an ex vivo model of epileptiform lesion. *Epilepsy Research,* 92**,** 153-162.

ZENG, X., ZENG, Y.-S., MA, Y.-H., LU, L.-Y., DU, B.-L., ZHANG, W., LI, Y. & CHAN, W. Y. 2011. Bone marrow mesenchymal stem cells in a three-dimensional gelatin sponge scaffold attenuate inflammation, promote angiogenesis, and reduce cavity formation in experimental spinal cord injury. *Cell Transplantation,* 20**,** 1881-1899.

ZHANG, C., LI, Y., CHEN, J., GAO, Q., ZACHAREK, A., KAPKE, A. & CHOPP, M. 2006. Bone marrow stromal cells upregulate expression of bone morphogenetic proteins 2 and 4, gap junction protein connexin-43 and synaptophysin after stroke in rats. *Neuroscience,* 141**,** 687-695.

ZHANG, G., ANNAN, R. S., CARR, S. A. & NEUBERT, T. A. 2014. Overview of peptide and protein analysis by mass spectrometry. *Current Protocols in Molecular Biology***,** 10-21.

ZHANG, H. Y., ZHANG, X., WANG, Z. G., SHI, H. X., WU, F. Z., LIN, B. B., XU, X. L., WANG, X. J., FU, X. B. & LI, Z. Y. 2013. Exogenous basic fibroblast growth factor inhibits ER stress–induced apoptosis and improves recovery from spinal cord injury. *CNS Neuroscience and Therapeutics,* 19**,** 20-29.

ZHAO, R. R., ANDREWS, M. R., WANG, D., WARREN, P., GULLO, M., SCHNELL, L., SCHWAB, M. E. & FAWCETT, J. W. 2013. Combination treatment with anti‐Nogo‐A and chondroitinase ABC is more effective than single treatments at enhancing functional recovery after spinal cord injury. *European Journal of Neuroscience,* 38**,** 2946-2961.

Appendix – Reagent Specifications

Reagent	Brand	Catalogue Number
Acetonitrile	Sigma-Aldrich	126349-100G
Bio-Plex Pro rat cytokine 23-plex assay	Bio-Rad	L8001V11S5
Bupivacaine	Hospira	38-515-DK
Cephalozin sodium	WG Critical Care	44567-707-25
DPX mountant	Sigma-Aldrich	44581
Eosin alcoholic 1%	Fronine	II016
Ethanol	Sigma-Aldrich	24102-1L-R
Fluorescein isothiocyanate conjugated Peptide5	Auspep	BB30666
Fluorescent mounting medium	Dako	GM304
Formalin	Sigma-Aldrich	HT501128-4L
Formic acid	Sigma-Aldrich	633321-4X4L
Gelatine	Sigma-Aldrich	G9391
Glycerol	Sigma-Aldrich	G5516-500ML
Goat anti-mouse Alexa Fluor 488	Thermo Fisher	A-11001
Goat anti-mouse Alexa Fluor 568	Thermo Fisher	A-11004
Goat anti-rabbit Alexa Fluor 488	Thermo Fisher	A-11008
Goat anti-rabbit Alexa Fluor 568	Thermo Fisher	A-11011
Hartman's replacement solution	Baxter	AHB2324
Heparin	B. BRAUN	126/318476/0212
HEPES lysis buffer	Thermo Fisher	15630080
Hoechst	Thermo Fisher	H3570
Horseradish peroxidase-conjugated goat anti-rabbit IgG	Thermo Fisher	A16096
Isoflurane	VCA	IPN-49
Lethabarb	Virbac	47815
Lumi-Light chemiluminescence substrate	Sigma-Aldrich	1205200001
Matsunami Platinum PLC-14	Matsunami	PRO-14
Mayer's Haematoxylin	Fronine	II009
Mouse anti-ED1	AbD Serotec	MCA341R
Mouse anti-neuronal nuclei	Millipore	MAB377
Nitrocellulose membrane	Thermo Fisher	LC2009
Normal goat serum	Sigma-Aldrich	G9023-10ML
Normal rat serum	Abcam	ab7488

NuPAGE® 4-12% Bis-Tris gels	Thermo Fisher	NP0321BOX
NuPAGE® MES SDS running buffer	Thermo Fisher	NP0002
OCT compound	Tissue-Tek	IA018
Paraffin	Leica	39601006
Paraformaldehyde	Sigma-Aldrich	158127-500G
Peptide5	Mimotopes	2492001
Phosphate buffer	Sigma-Aldrich	P3619-1GA
Phosphate buffer	Sigma-Aldrich	P3619-1GA
Phosphate buffered saline	Sigma-Aldrich	P4417-100TAB
Protease inhibitor cocktail	Roche	11836153001
Protein assay kit	Bio-Rad	5000002
Rabbit anti-Connexin30	Thermo Fisher	71-2200
Rabbit anti-Connexin36	Thermo Fisher	51-6200
Rabbit anti-Connexin43	Sigma-Aldrich	C6219
Rabbit anti-Connexin47	Thermo Fisher	PA5-39184
Rabbit anti-glial fibrillary acidic protein	Dako	Z0334
Rabbit anti-ionised calcium-binding adapter molecule 1	Abcam	ab108539
Rabbit anti-phosphorylated Connexin43	Santa Cruz	sc-101660
Scott's Blue	Fronine	II019
Scrambled peptide	Mimotopes	2492002
SDS-polyacrylamide gels	Thermo Fisher	EC6265BOX
Skim milk	Coles	7910660P
Sodium azide	Sigma-Aldrich	S2002-100G
Sodium chloride	Sigma-Aldrich	S9888-25KG
Sodium dodecyl sulphate	Sigma-Aldrich	436143-100G
Sucrose	Sigma-Aldrich	S0389-5KG
Temgesic	Reckitt Benckiser	R15394
Trifluoroacetic acid	Sigma-Aldrich	299537-100G
Tris-buffered saline	Bio-Rad	1706435
Tris-hydrochloride	Sigma-Aldrich	10812846001
Triton X-100	Sigma-Aldrich	X100-500ML
Tween-20	Sigma-Aldrich	P1379-500ML
Xylene	Fronine	JJ028/5